

University of Wollongong - Research Online

Thesis Collection

Title: Attempts to find the correct structure of uniflorine A

Author: Andrew Stewart Davis

Year: 2008

Repository DOI:

Copyright Warning

You may print or download ONE copy of this document for the purpose of your own research or study. The University does not authorise you to copy, communicate or otherwise make available electronically to any other person any copyright material contained on this site.

You are reminded of the following: This work is copyright. Apart from any use permitted under the Copyright Act 1968, no part of this work may be reproduced by any process, nor may any other exclusive right be exercised, without the permission of the author. Copyright owners are entitled to take legal action against persons who infringe their copyright. A reproduction of material that is protected by copyright may be a copyright infringement. A court may impose penalties and award damages in relation to offences and infringements relating to copyright material.

Higher penalties may apply, and higher damages may be awarded, for offences and infringements involving the conversion of material into digital or electronic form.

Unless otherwise indicated, the views expressed in this thesis are those of the author and do not necessarily represent the views of the University of Wollongong.

Research Online is the open access repository for the University of Wollongong. For further information contact the UOW Library: research-pubs@uow.edu.au

University of Wollongong Theses Collection

University of Wollongong Theses Collection

University of Wollongong

Year 2008

Attempts to find the correct structure of uniflorine A

Andrew Stewart Davis
University of Wollongong

Davis, Andrew S, Attempts to find the correct structure of uniflorine A, PhD thesis, School of Chemistry, University of Wollongong, 2008. <http://ro.uow.edu.au/theses/143>

This paper is posted at Research Online.
<http://ro.uow.edu.au/theses/143>

NOTE

This online version of the thesis may have different page formatting and pagination from the paper copy held in the University of Wollongong Library.

UNIVERSITY OF WOLLONGONG

COPYRIGHT WARNING

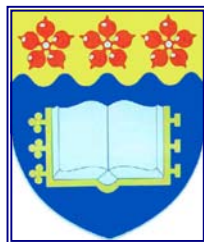
You may print or download ONE copy of this document for the purpose of your own research or study. The University does not authorise you to copy, communicate or otherwise make available electronically to any other person any copyright material contained on this site. You are reminded of the following:

Copyright owners are entitled to take legal action against persons who infringe their copyright. A reproduction of material that is protected by copyright may be a copyright infringement. A court may impose penalties and award damages in relation to offences and infringements relating to copyright material. Higher penalties may apply, and higher damages may be awarded, for offences and infringements involving the conversion of material into digital or electronic form.

Attempts to find the correct structure of uniflorine A

A thesis submitted in fulfilment of the requirements
for the award of the degree of

Doctor of Philosophy
from
University of Wollongong



Andrew Stewart Davis

B. Sc (Hons)

School of Chemistry

May, 2008

Declaration

I, Andrew Stewart Davis, declare that this thesis, submitted in fulfilment of the requirements for the award of Doctor of Philosophy, in the Department of Chemistry, University of Wollongong, is wholly my own work unless due reference is provided. This document has not been submitted for qualifications at any other academic institution.

Andrew Stewart Davis

May, 2008

TABLE OF CONTENTS

Declaration.....	ii
Table of Contents.....	iii
List of Figures.....	vi
List of Schemes.....	ix
List of Tables.....	xii
List of Abbreviations.....	xiv
ABSTRACT	xvi
Acknowledgements.....	xvii
Publications arising from this thesis.....	xviii
 CHAPTER 1: Introduction	 1
1.1. Alkaloids.....	1
1.2. Definition of alkaloids.....	2
1.3. Occurrence and distribution of alkaloids.....	3
1.4. Alkaloids in folkloric medicine.....	4
1.5. Initial project plan.....	6
1.6. Polyhydroxylated alkaloids.....	7
1.7. Occurance of polyhydroxylated alkaloids.....	9
1.8. Biological activities of polyhydroxylated alkaloids.....	12
1.9. The value of total synthesis in natural product structure determination.....	14
1.10. Retrosynthetic analysis of the proposed structure of uniflorine A.....	16
 CHAPTER 2. 1-Deoxy-castanospermine – a model study	 21
2.1. Petasis reaction.....	21
2.2. Ring-closing metathesis.....	24
2.3. Hydrogenation.....	25
2.4. De-acetylation.....	26
2.5. Mitsunobu cyclization.....	26
 CHAPTER 3. Synthesis of 1, the proposed structure of uniflorine A	 30
3.1. Petasis reaction.....	31
3.2. Ion-exchange chromatography.....	32
3.3. <i>N</i> -Boc protection.....	34
3.4. <i>O</i> -Tr protection.....	35
3.5. <i>O</i> -Bn protection.....	37
3.6. Ring-closing metathesis.....	42
3.7. Dihydroxylation.....	44

3.8. <i>O</i> -Benzylation.....	44
3.9. <i>O</i> -Tr and <i>N</i> -Boc deprotection.....	45
3.10. Appel cyclization.....	52
3.11. <i>O</i> -Bn deprotection	53
3.12. Acetylation	56
3.13. Synthesis of the correct enantiomer of putative uniflorine A.....	59
CHAPTER 4. Attempted syntheses of 1-<i>epi</i>- and 2-<i>epi</i>-1	63
4.1. Preparation of substrate 80	64
4.2. Synthetic strategies for 1- <i>epi</i> -1.....	65
4.3. Synthetic strategies for 2- <i>epi</i> -1.....	67
4.4. Choosing a synthesis from several options.....	69
4.5. Formation of cyclic sulfate.....	70
4.6. Ring-opening of cyclic sulfate.....	72
4.7. Epoxidation.....	73
4.8. Attempted epoxide ring-opening.....	74
CHAPTER 5. Synthesis of putative 1,2-di-<i>epi</i>-1	79
5.1. RCM of oxazolidinone 122	81
5.2. RCM of oxazinanone 114	83
5.3. Differences in Grubbs' I and II catalyst activities	84
5.3.1. Back-bonding	85
5.4. Methods for improving access to oxazinone 115	88
5.4.1. Triphosgene method	88
5.4.2. The ' <i>N</i> -Troc' method.....	93
5.4.3. Comparison of the different methods for accessing 123 and 115	95
5.5. Dihydroxylation of oxazinone 115	95
5.6. Dihydroxylation of oxazolone 123	96
5.7. <i>O</i> -Benzylation and <i>O</i> -Tr deprotection.....	98
5.8. Hydrolysis of oxazinanone 144	99
5.9. Elaboration to the target	100
CHAPTER 6. Glycosidase inhibitor testing.....	102
CHAPTER 7. Determining the correct structures of uniflorine A and B.....	106
CONCLUSIONS.....	115
EXPERIMENTAL	117

REFERENCES.....	155
------------------------	------------

List of Figures

Figure 1.1. Chemical structures of theophylline and caffeine	1
Figure 1.2. Chemical structures of morphine, codeine and heroin	1
Figure 1.3. Examples of simple and complex alkaloid structures	2
Figure 1.4. Chemical structures of berberine, senecionine <i>N</i> -oxide and taxol	3
Figure 1.5. Bitter-tasting alkaloid coccinelline is emitted from <i>Coccinella septempunctata</i>	3
Figure 1.6. <i>Atta Texana</i> communicate using trail pheromones comprised of alkaloids	3
Figure 1.7. Highly lethal alkaloid Batrachotoxin; found in the skin of <i>Phyllobates terribilis</i>	4
Figure 1.8. <i>Eugenia uniflora</i> , source of Nangapiri	5
Figure 1.9. Proposed chemical structures for the alkaloids isolated from a water-soluble extract of <i>E. uniflora</i>	6
Figure 1.10. Some analogous compounds of uniflorine A, synthesized by Pyne <i>et al</i>	6
Figure 1.11. Norjirimycin, the first polyhydroxylated alkaloid isolated	7
Figure 1.12. Selected piperidine, pyrrolidine, pyrrolizidine, indolizidine and nortropane alkaloids.....	8
Figure 1.13. (a) <i>Omphalea diandra</i> (Euphorbiaceae) in Panama, a source of DMJ.....	9
(b) <i>Angylocalyx</i> sp. (Leguminosae) in Kenya, a source of DMJ and D-AB1.....	9
Figure 1.14. <i>Castanospermum australe</i> (Leguminosae) in Australia, a source of castanospermine and fagomine	10
Figure 1.15. <i>Alexa canaracunensis</i> (Leguminosae) in Brazil, a source of alexins	11
Figure 1.16. <i>Hyacinthoides non-scripta</i> in the UK (Hyacinthaceae), a source of hyacinthacines.....	11
Figure 1.17. Comparison of DNJ and DMDP with the carboxonium ion transition state.....	13
Figure 1.18. Mechanism of retaining (a) and inverting (b) glycoside hydrolysis.....	13
Figure 1.19. Miglitol, a clinical treatment for non-insulin-dependent diabetes.....	14
Figure 1.20. Progression of natural product synthesis.....	15
Figure 1.21. Comparison of 1 and similar synthesized compounds	16
Figure 1.22. Anti-1,2-amino alcohol functionality within the structure of 1	19
Figure 2.1. ¹ H NMR spectrum (300 MHz, CDCl ₃) of acetylated Petasis product 39	21
Figure 2.2. ¹ H NMR spectrum (300 MHz, CDCl ₃) of 40	24
Figure 2.3. Single crystal X-ray structure of 40	24
Figure 2.4. Single crystal X-ray structure of 41	25
Figure 2.5. C-3 and C-5 ¹³ C NMR (CDCl ₃) chemical shifts (ppm) for a C-6,7 acetonide of <i>ent</i> -1-deoxycastanospermine and stereoisomers	27
Figure 2.6. DEPT NMR spectrum (CDCl ₃) of 44	28

Figure 2.7. ^1H NMR spectrum (300 MHz, CDCl_3) of 44	29
Figure 3.1. ^1H NMR spectrum (300 MHz, CD_3OD) of 38	32
Figure 3.2. ^1H NMR spectrum (300 MHz, CDCl_3) of 47 , showing peak-broadening	35
Figure 3.3. TLC analyses of the <i>O</i> -benzylation of 48 at 6 h and 24 h	37
Figure 3.4. ^1H NMR spectrum (300 MHz, CDCl_3) of oxazolidinone 41	41
Figure 3.5. ^1H NMR spectrum (300 MHz, CDCl_3) of oxazinanone 57	41
Figure 3.6. TLC analysis of the TFA mediated deprotection of <i>N</i> -Boc and <i>O</i> -Tr groups	46
Figure 3.7. ^1H NMR spectrum (300 MHz, CDCl_3) of 61	46
Figure 3.8. ^1H NMR spectrum (300 MHz, CDCl_3) of 62	47
Figure 3.9. ^1H NMR spectrum (300 MHz, CDCl_3) of mono-protected <i>O</i> -Tr derivative 63	48
Figure 3.10. ^{13}C NMR spectrum (75 MHz, CDCl_3) of mono-protected <i>O</i> -Tr derivative 63	48
Figure 3.11. ^1H NMR spectrum (500 MHz, D_2O) of <i>ent</i> - 1 and ^1H NMR data of uniflorine A.....	53
Figure 3.12. C-3,5 ^{13}C NMR chemical shifts (D_2O , ppm) for several 2-hydroxycastanospermines synthesized by Fleet <i>et al</i>	54
Figure 3.13. ^{13}C NMR spectrum (75 MHz, D_2O) of 54	54
Figure 3.14. Fully assigned ^1H NMR spectrum (500 MHz, D_2O) of <i>ent</i> - 1	55
Figure 3.15. Selected nOe correlations observed in the NOSEY spectrum of <i>ent</i> - 1	55
Figure 3.16. Single crystal X-ray structure of 64	56
Figure 3.17. Comparison of assigned ^1H NMR chemical shifts between uniflorine A, <i>ent</i> - 1 , and three analogous pentahydroxyindolizidines, 65 , 66 , 67	57
Figure 3.18. Selected ^1H NMR <i>J</i> values for uniflorine A, <i>ent</i> - 1 , 66 and 69	58
Figure 3.19. Our proposed structure for uniflorine A	58
Figure 3.20. Single crystal X-ray structure of 80	62
Figure 4.1. Synthetic targets 1- <i>epi</i> - 1 and 2- <i>epi</i> - 1	63
Figure 4.2. (a) AM1 representation of oxazolone 85 (b) 6-31G* representation of the HOMO of oxazolone 85	66
Figure 4.3. TLC analysis of reaction to produce cyclic sulfite 97	71
Figure 4.4. ^1H NMR (500 MHz, CD_3OD) spectrum of the major product	75
Figure 4.5. ^{13}C NMR (125 MHz, CD_3OD) spectrum of the major product	76
Figure 4.6. ^{13}C NMR chemical shifts (CDCl_3 , 75 MHz) of C-3 and C-4 carbinol carbons in the previously synthesized diols 91 and 75	76
Figure 4.7. Possible structures for the major product of the epoxide ring-opening reaction	76
Figure 4.8. ^1H NMR comparison of product 107 and an analogous literature compound 109	78
Figure 4.9. Assigned ^{13}C NMR spectrum (75 MHz, CDCl_3) of the major product	78

Figure 5.1. ^1H NMR spectrum of the oxazolone 123 (300 MHz, CDCl_3)	81
Figure 5.2. Desired oxazolidinone 125 and three other candidates for the two side-products ..	89
Figure 5.3. ^1H NMR spectra (500 MHz, CDCl_3) of diastereomers 141 and 142	97
Figure 5.4. ^1H NMR spectrum (500 MHz, CDCl_3) of 1,2-di- <i>epi</i> - 1	101
Figure 6.1. Determination of the extinction coefficient of <i>p</i> -nitrophenolate	103
Figure 7.1. Casuarine diastereomers that have appeared in the literature	106
Figure 7.2. (a) Casuarine glycoside isolated from <i>Casuarina equisetifolia</i> , and <i>Eugenia jambolana</i> ; (b) Natural products isolated from <i>Eugenia uniflora</i>	107
Figure 7.3. Overlap of 1 with 152 and 154	109
Figure 7.4. ^1H NMR spectra of D_2O at 30 °C of (a) casuarine 150 , pH 8.3, and (b) 3- <i>epi</i> -casuarine 151 , pH 9.3. Spectra taken from Fleet <i>et al</i>	110
Figure 7.5. nOe Analysis of the proposed conformation of putative uniflorine A; comparison to 6- <i>epi</i> -casuarine	113

List of Schemes

Scheme 1.1. Synthesis of 2 <i>S</i> -2-hydroxycastanospermine 8 by Fleet <i>et al</i>	17
Scheme 1.2. Cornerstone of Denmark's synthesis of 1- <i>epi</i> -castanospermine	17
Scheme 1.3. Synthesis of dipolarophile 25	18
Scheme 1.4. Remainder of the synthesis of 1- <i>epi</i> -castanospermine by Denmark <i>et al</i>	18
Scheme 1.5. Retrosynthetic analysis for uniflorine A	20
Scheme 2.1. Model study synthesis of <i>ent</i> -1-deoxy-castanospermine 37	21
Scheme 2.2. Results of the Petasis reaction and subsequent <i>O</i> -acetylation	22
Scheme 2.3. Proposed mechanism explaining stereoselectivity in the Petasis reaction.....	23
Scheme 2.4. Results of the RCM of 39 and hydrogenation of 40	25
Scheme 2.5. Result of the deacetylation of 41	26
Scheme 2.6. Potential mechanisms of reacting 42 under Mitsunobu conditions	28
Scheme 3.1. Proposed synthesis of <i>ent</i> - 1	31
Scheme 3.2. Mechanism of acidic ion-exchange chromatography	33
Scheme 3.3. Selected literature procedures for <i>N</i> - Boc protection.....	34
Scheme 3.4. Synthesis of <i>N</i> -Boc product 47	35
Scheme 3.5. Selected literature procedures for <i>O</i> -Tr protection	36
Scheme 3.6. Selected literature procedures for <i>O</i> -Bn protection	37
Scheme 3.7. Characterization of side-products 1 and 2 by LRMS.....	39
Scheme 3.8. Possible reaction pathways for the <i>O</i> -benzylation of 48	40
Scheme 3.9. Revised synthetic route to <i>ent</i> - 1	42
Scheme 3.10. Further revised synthetic route to <i>ent</i> - 1	43
Scheme 3.11. Possible mechanism for the cyclization of 60	49
Scheme 3.12. Prof. Anthony Barrett's proposed mechanism for the cyclization of 60	49
Scheme 3.13. β -Hydride abstraction by trityl cation in selected organometallics.....	50
Scheme 3.14. Example of <i>O</i> -Bn deprotection by Ph_3C^+ and subsequent cyclization.....	50
Scheme 3.15. Mechanism of de- <i>O</i> -benzylation by Ph_3C^+	51
Scheme 3.16. A method for validating Prof. Anthony Barrett's proposed mechanism.....	51
Scheme 3.17. Appel cyclization and <i>O</i> -Bn deprotection reactions by Naruse <i>et al</i>	52
Scheme 3.18. The synthetic route for 1	59
Scheme 4.1. Synthetic plan for 1- <i>epi</i> - 1 and 2- <i>epi</i> - 1 , based on the previous synthesis of 1	63
Scheme 4.2. Synthesis of substrate 82	64
Scheme 4.3. Alternative synthesis of substrate 82	64
Scheme 4.4. Summary of the two syntheses of 82	64
Scheme 4.5. A potential way of accessing <i>trans</i> -(3 β ,4 α)-diol 84 using the Prevost reaction....	65

Scheme 4.6. Dihydroxylation of substituted 2,5-dihydropyrroles; comparison of diastereoselectivity according to nitrogen protection	65
Scheme 4.7. Synthetic plan for 1- <i>epi</i> - 1 using cyclic sulfate methodology	67
Scheme 4.8. Synthetic plan for 1- <i>epi</i> - 1 using epoxide methodology	67
Scheme 4.9. Synthetic plan for 2- <i>epi</i> - 1 using cyclic sulfonation or epoxidation methodologies	68
Scheme 4.10. Mechanism of the Mattocks reaction when applied to diol 91	68
Scheme 4.11. Application of Prevost chemistry to the α -bromoacetate 94	69
Scheme 4.12. Strategies available for the synthesis of 1- <i>epi</i> - 1 and 2- <i>epi</i> - 1	69
Scheme 4.13. Example of using cyclic sulfate chemistry to convert a diol moiety from <i>cis</i> to <i>trans</i>	70
Scheme 4.14. Synthesis of cyclic sulfonation starting material 93	70
Scheme 4.15. Results of the formation of cyclic sulfate 98 from diol 93	71
Scheme 4.16. Direct cyclic sulfonation using 1,1'-sulfonyldiimidazole	72
Scheme 4.17. Results of the ring-opening of cyclic sulfate 100	72
Scheme 4.18. Mechanism of Oxone mediated epoxidation of an olefin	73
Scheme 4.19. Literature example of the synthesis of a <i>trans</i> diol from a 2,5-dihydropyrrole ..	74
Scheme 4.20. Proposed synthetic pathway from epoxide 90 to final product 2- <i>epi</i> - 1	75
Scheme 4.21. Alternate mechanisms of the epoxide ring-opening reaction	77
Scheme 5.1. Strategy for the synthesis of 1,2-di- <i>epi</i> - 1 from oxazolone 88	79
Scheme 5.2. A strategy for the synthesis of 1,2-di- <i>epi</i> - 1 via an oxazinone 116 intermediate ..	80
Scheme 5.4. Plan for the synthesis of 1,2-di- <i>epi</i> - 1 using the Woodward reaction	80
Scheme 5.5. Results for the RCM of oxazolidinone 122 with Grubbs' I catalyst	81
Scheme 5.6. Literature example of RCM of an oxazolidinone with Grubbs' I catalyst	82
Scheme 5.7. Result for the RCM of 114 with Grubbs' I catalyst	83
Scheme 5.8. Mechanism of the RCM reaction of a diene with either Grubbs' I or II catalyst ..	85
Scheme 5.9. Formation of a σ -bond between a metal and ligand	86
Scheme 5.10. Types of bonding involved in Grubbs' I and II catalysts	86
Scheme 5.11. Decomposition pathway for Grubbs' I catalyst	86
Scheme 5.12. Decomposition pathway for Grubbs' II catalyst	87
Scheme 5.13. Results for the synthesis of 123 and 115 using <i>N</i> -Boc methodology	88
Scheme 5.14. Using triphosgene to form an oxazolidinone by Lindsay <i>et al</i>	88
Scheme 5.15. Proposed synthesis of 125 and 126 from 70 using triphosgene	89
Scheme 5.16. Results for the synthesis of oxazolidinone 125 from Petasis product 70	90
Scheme 5.17. Results for the <i>O</i> -Tritylation of 125 and RCM of 130	91
Scheme 5.18. Results for the di- <i>O</i> -benzylation of 131	92

Scheme 5.19. Proposed mechanism for the formation of oxazinone 115 from oxazolone 123	92
Scheme 5.20. Results for the <i>N</i> -Troc protection of 70 and <i>O</i> -Tr protection of 135	94
Scheme 5.21. Results of the <i>O</i> -Benzylation of 136 , and subsequent RCM of an isolated mixture of 122 and 114	94
Scheme 5.22. Results of the RCM of 136 and subsequent <i>O</i> -Benzylation of 138	95
Scheme 5.23. Result of the <i>cis</i> -dihydroxylation of 115	96
Scheme 5.24. Result of the <i>cis</i> -dihydroxylation of 123	97
Scheme 5.25. Revised synthetic plan from oxazinone 146 to 1,2-di- <i>epi</i> - 1	98
Scheme 5.26. Results of the <i>O</i> -Bn protection of 116 and <i>O</i> -Tr deprotection of 143	99
Scheme 5.27. Base hydrolysis of an oxazolone under microwave conditions	99
Scheme 5.28. Result of the microwave-assisted hydrolysis of 141	99
Scheme 5.29. Result of the microwave-assisted hydrolysis of 144	100
Scheme 5.30. Results of the Appel cyclization of 145 and <i>O</i> -Bn deprotection of 146	100
Scheme 6.1. Mechanism of the glycosidase inhibitory activity assay	103

List of Tables

Table 1.1. Inhibition of α -glucosidases by uniflorine A, uniflorine B and 3	6
Table 1.2. Selected results from Petasis <i>et al.</i>	19
Table 3.1. Results of the <i>O</i> -Tr protection of 47	36
Table 3.2. Comparison of carbonyl ^{13}C NMR chemical shifts between benzylation side-products and starting materials (CDCl_3 , 75 MHz).....	38
Table 3.3. NMR chemical shifts for benzylic units in side-products 1 and 2.....	39
Table 3.4. Results of the RCM reaction of 48	43
Table 3.5. NMR chemical shifts (CDCl_3) of hydrocarbon units α to the nitrogen in 48 and 58	43
Table 3.6. Results of the dihydroxylation of 58	44
Table 3.7. Results of the <i>O</i> -benzylation of 59	44
Table 3.8. Results of TFA mediated deprotection of <i>N</i> -Boc and <i>O</i> -Tr groups in 60	47
Table 3.9. Comparison of the results for the synthesis of <i>ent</i> - 1 and 1	60
Table 3.9 cont'd. Comparison of the results for the synthesis of <i>ent</i> - 1 and 1	61
Table 3.10. Rotation and melting point data for uniflorine A and 1	62
Table 3.11. Overall yields for the synthesis of <i>ent</i> - 1 and 1	62
Table 4.1. Results of the epoxidation of 82	74
Table 5.1. ^1H NMR chemical shifts of corresponding protons in 122 and 123	82
Table 5.2. Results for the RCM of 122 with Grubbs' II catalyst.....	83
Table 5.3. NMR chemical shifts for selected corresponding nuclei in 125 , 127 and 129	91
Table 5.4. Overall yields for 123 and 115 from 70 via different methodologies.....	95
Table 5.5. Selected NMR chemical shifts for corresponding nuclei in 115 and 116	96
Table 5.6. Selected ^1H and ^{13}C NMR chemical shifts of corresponding nuclei in 141 and 142	98
Table 5.7. Comparison of the NMR data for 1,2-di- <i>epi</i> - 1 and corresponding literature data.	101
Table 6.1. Types of buffer, substrate and temperature for each enzymatic assay.....	102
Table 6.2. IC_{50} values of <i>ent</i> - 1 , 1 , and castanospermine.....	104
Table 6.3. Components in the α -D-mannosidase assay of putative 1,2-di- <i>epi</i> - 1	104
Table 6.4. IC_{50} of 1,2-di- <i>epi</i> - 1 and swainsonine.....	105
Table 7.1. Literature sources of casuarine diastereomers and related data.....	106
Table 7.2. NMR and optical rotation data for casuarine and uniflorine B.....	108

Table 7.3. Corresponding carbon nuclei in overlapping pyrrolizidine and indolizidine structures	109
Table 7.4. The ^1H NMR chemical shifts for 152 , 154 and uniflorine A	109
Table 7.5. $^3J_{\text{HH}}$ values for the A-ring protons of 152 , 154 and uniflorine A	110
Table 7.6. A-ring $^3J_{\text{HH}}$ values for casuarine diastereomers that are epimeric at C-3	111
Table 7.7. B-ring $^3J_{\text{HH}}$ values for 152 , 154 and uniflorine A.....	111
Table 7.8. ^{13}C NMR chemical shifts for 152 , 154 and uniflorine A.....	112
Table 7.9. Optical rotation data for 152 , 154 , and uniflorine A	112

List of Abbreviations

[α] _D	specific rotation
Ac	acetyl
Ar	aromatic
ax	axial
Bn	benzyl
Boc	<i>tert</i> -butyloxycarbonyl
br	broad
Bz	benzoyl
CI	chemical ionisation
Cy	cyclohexyl
d	doublet
δ	NMR chemical shift
DCM	dichloromethane
DEAD	diethylazodicarboxylate
DEPT	Distortionless Enhancement by Polarisation Transfer
DMAP	<i>N,N</i> -Dimethyl-4-aminopyridine
DMF	dimethylformamide
EI	Electron impact Ionisation
eq	equatorial
ESI+	electrospray ionisation (positive ion mode)
FCC	flash column chromatography
gCOSY	gradient Correlated Spectroscopy
gHSQC	gradient Heteronuclear Single Quantum Correlation
gHMBC	gradient Heteronuclear Multiple Bond Correlation
HR	high resolution
Hz	Hertz
LR	low resolution
MS	mass spectrometry
m	multiplet
m.p.	melting point
[M ⁺]	molecular ion
<i>m/z</i>	mass/charge ratio
NMR	nuclear magnetic resonance
NMO	<i>N</i> -methylmorpholine- <i>N</i> -oxide
petrol	petroleum spirit bp 40-60 °C

ppm	parts per million
pyr	pyridine
q	quartet
R_f	relative mobility
rt	room temperature
s	singlet
t	triplet
TFA	trifluoroacetic acid
THF	tetrahydrofuran
Tr	trityl, triphenylmethyl
Troc	(2,2,2-trichloroethoxy)carbonyl

ABSTRACT

The alkaloid uniflorine A was isolated in 2000 from the leaves of the tree *Eugenia uniflora* L, together with two other water soluble alkaloids, uniflorine B and the known alkaloid (+)-(3 α ,4 α ,5 β)-1-methylpiperidine-3,4,5-triol piperidine. Uniflorine A was found to be an inhibitor of the α -glucosidases, rat intestinal maltase and sucrase, with IC₅₀ values of 12 and 3.1 μ M, respectively, and its structure was deduced from NMR analysis to be structure **1**. Uniflorine B was also found to be an inhibitor of the above α -glucosidases and its structure was determined from NMR analysis to be structure **2**.

The initial goal of this study was to complete the total synthesis of **1** and determine the validity of its proposed structure. In the event, an efficient 9-step diastereoselective synthesis of **1** was achieved by using the Petasis borono-Mannich reaction, ring-closing metathesis and stereoselective *cis*-dihydroxylation as key steps. The structure of our synthetic **1** was unequivocally established by a single-crystal X-ray crystallographic study of its pentaacetate derivative. However, the ¹H and ¹³C NMR data for synthetic **1** did not match with those reported for uniflorine A; the latter showed many more downfield peaks in the ¹H NMR, perhaps consistent with the amine salt. The ¹H NMR of the hydrochloride salt of synthetic **1**, however, did not match the literature spectroscopic data either. We therefore concluded that the structure assigned to uniflorine A was not correct. We also found that the coupling constant *J*_{1,8a} of 4.5 Hz for uniflorine A, was more consistent with the relative *syn*-H-8a, H-1 configuration, suggesting that uniflorine A, if it was an indolizidine alkaloid, had the same H-1 configuration as castanospermine. Our attempts to prepare 2-*epi*-**1** and 1,2-di-*epi*-**1** were unsuccessful due to unexpected competing side-reactions.

In addition, the diastereoselective synthesis of the C-1, C-2 di-epimer of **1** was achieved. This synthesis employed a novel pyrrolo[1,2-*c*]oxazin-1-one precursor to allow for the reversal of π -facial diastereoselectivity in an osmium(VIII)-catalysed *syn*-dihydroxylation (DH) reaction. The NMR spectroscopic data of this epimeric compound and that of related isomers did not match that of the natural product. From a comparison of the NMR data of uniflorine A and uniflorine B with that of casuarine and the known synthetic 1,2,6,7-tetrahydroxy-3-hydroxymethylpyrrolizidine isomers we concluded unequivocally that uniflorine B is the known alkaloid casuarine. Although we cannot unequivocally prove the structure of uniflorine A, without access to the original material and data, the published data suggest that the natural product is also a 1,2,6,7-tetrahydroxy-3-hydroxymethylpyrrolizidine with the same relative C-7-C-7a-C-1-C-2-C-3 configuration as casuarine. We thus suggest that uniflorine A is 6-*epi*-casuarine.

Acknowledgments

First and foremost, I would like to extend a very sincere thankyou to Prof. Stephen Pyne for his expert supervision of this project. Steve has always been engaged with the project, giving direction and help with problem solving. His strong work ethic is always motivating and his response time for thesis editing cannot be surpassed.

Next I would like to acknowledge my family for their support. To my parents, Ken and Wendy, thankyou for giving me the financial support to undertake university studies, particularly at undergraduate level but also during the final stages of this PhD project. Your investment in my education has rewarded me in so many untold ways. Together with my sisters Katrina and Megan, you have taught me to appreciate the journey of life rather than be unnecessarily focussed on getting to some 'better' place. Such perspective has sustained me with the patience to endure 9 years of university study.

Throughout this project I have been richly blessed with some amazing friendships. For your support, encouragement and humour, thankyou Paul, Min and baby Ruby Sanders, Dan and Marg Nichols, De-Arne Brampton, Chris and Liza Hawley, Simon Barritt, Marty and Ali Barritt, Bill Hawkins, Dave Brennan, Steve Taylor, Tien Pham, Minyan Tang, Joseph Hartley, Jane Faragalla, Soli, David Ruffels, Bree and Michael, David and Pha and my ANSTO car-pool buddies Naomi, Guita and Honqin.

To the members of the Pyne Group that I have worked with, this project has been made easier by the diligence, sense of fun and camaraderie that you have brought to the laboratory. I would like to particularly acknowledge Thunwadee for her willingness to engage, learn and provide assistance in the latter stages of this project. I would also like to thank Ian Morgan for some helpful discussions on chemistry and for sparking my interest in computational chemistry, and Leena Burgess for graciously testing the biological activities of some of my compounds. Other School of Chemistry members I would like to thank are Wilford Lie for assistance with NMR spectroscopy, Karin Maxwell, Roger Kanitz and the late Larry Hick for the running of high-resolution mass spectra, and to John Korth, Peter Pavlik, Peter Sara and Steve Cooper for their own expert assistance.

Finally, I would like to state my gratitude to the sovereign Lord God for the majestic natural world He has created and the freedom He has given us to explore it with intellectual endeavour. The challenge of synthesizing a complex natural product in the laboratory, in contrast to the effortless way that nature does it, has certainly increased my appreciation of the greatness of God. To the members of St Marks Anglican Church, West Wollongong, thankyou for your reliable Christian fellowship and support during my PhD study.

Publications arising from this thesis

1. Davis, Andrew S.; Ritthiwigrom, Thunwadee; Pyne, Stephen G. Synthetic and spectroscopic studies on the structures of uniflorines A and B: structural revision to 1,2,6,7-tetrahydroxy-3-hydroxymethylpyrrolizidine alkaloids. *Tetrahedron*. **2008**, 64(21), 4868-4879.
2. Pyne, Stephen G.; Au, Christopher W. G.; Davis, Andrew S.; Morgan, Ian R.; Ritthiwigrom, Thunwadee; Yazici, Arife. Exploiting the borono-Mannich reaction in bioactive alkaloid synthesis. *Pure Appl. Chem.* **2008**, 80(4), 751-762.
3. Machan, Theeraphan; Davis, Andrew S.; Liawruangrath, Boonsom; Pyne, Stephen G. Synthesis of castanospermine. *Tetrahedron*. **2008**, 64(12), 2725-2732.
4. Pyne, Stephen G.; Davis, Andrew S.; Gates, Nicole J.; Hartley, Joseph P.; Lindsay, Karl B.; Machan, Theeraphan; Tang, Minyan. Asymmetric synthesis of polyfunctionalized pyrrolidines and related alkaloids. *Synlett*. **2004**, 15, 2670-2680.
5. Davis, Andrew S.; Pyne, Stephen G.; Skelton, Brian W.; White, Allan H. Synthesis of Putative Uniflorine A. *J. Org. Chem.* **2004**, 69(9), 3139-3143.
6. Davis, Andrew S.; Gates, Nicole J.; Lindsay, Karl B.; Tang, Minyan; Pyne, Stephen G. A new strategy for the diastereoselective synthesis of polyfunctionalized pyrrolidines. *Synlett*. **2004**, 1, 49-52.

Chapter 1: Introduction

1.1. Alkaloids

The morning ritual of waking-up to a breakfast that includes either a cup of tea or coffee is a common experience for many people. These ubiquitous beverages contain two examples of alkaloids, theophylline and caffeine (Figure 1.1.).

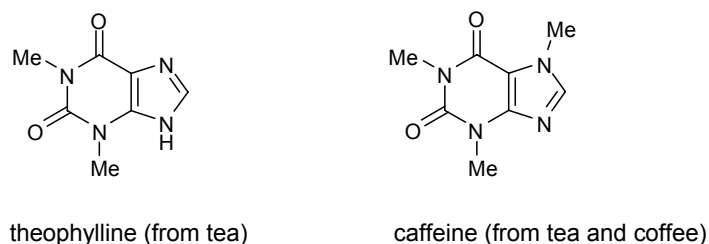


Figure 1.1. Chemical structures of theophylline and caffeine.

Another well-known alkaloid is morphine, which is isolated from the opium poppy (*Papaver somniferum*), and to which codeine and heroin are derived (Figure 1.2). Some alkaloids like nicotine have relatively simple structures, while others like vinblastine have complex structures (Figure 1.3). With these examples alone, one gains an insight into the rich diversity of chemical entities that comprise the family of alkaloids.

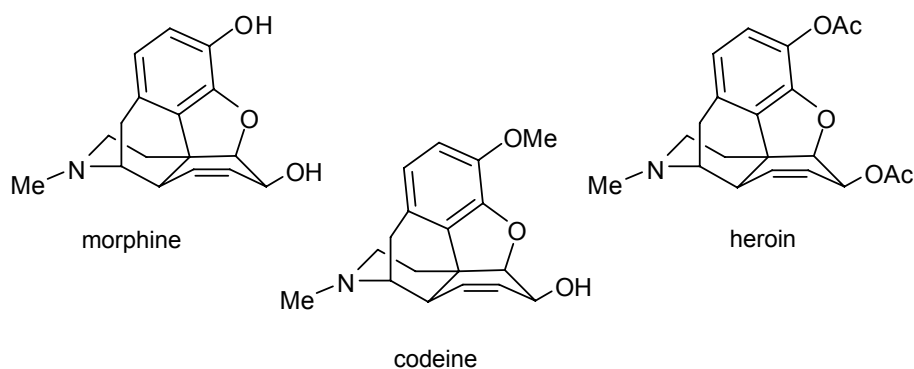


Figure 1.2. Chemical structures of morphine, codeine and heroin.

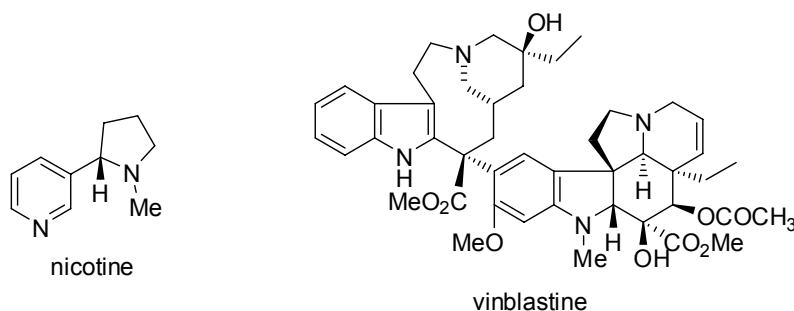


Figure 1.3. Examples of simple and complex alkaloid structures.

1.2. Definition of alkaloids

The German apothecary Carl Meissner coined the term ‘alkaloid’ in 1819, to broadly classify the alkaline nitrogen containing compounds that were beginning to be isolated and crystallized from plants.¹ Previously, it was believed that plant-derived substances were principally acids, including those contained within plant extracts that were known to produce pronounced pharmacological effects.¹ It was the German pharmacist, Scheele (1742-1786) who isolated ingredients from plants in crystalline form including tartaric acid, citric acid, oxalic acid and tannins.¹ However, in 1817 Sertürner reported the isolation and crystallization of a compound from opium, which had alkaline properties.² In the same paper, he reported its pharmacological properties that he had studied on stray dogs and himself. He found that his pure crystals carried the sleep generating properties of opium and he named this substance morphine, after Morpheus, the god of sleep and the creator of dreams.² This discovery set off a huge international search for basic plant-derived compounds.¹

Winterstein and Trier gave a more rigorous definition for alkaloid in 1910,³ and although still relevant today, some caveats remain. It states: alkaloids are compounds with heterocyclic bound nitrogen atoms, with more or less basic character, with pronounced physiological action, of complex molecular structure and are found in plants (and animals).¹

The last part of this definition contains no exceptions; a chemical substance that is not a natural product cannot be classified as an alkaloid, no matter how analogous it is to known alkaloids. The reference to an alkaloid having a complex structure is open to opinion, as the structure of nicotine is relatively simple compared to the chemical structure of vinblastine (Figure 1.3). It is true that most alkaloids exhibit basic character but prominent exceptions to this are berberine and senecionine *N*-oxide (Figure 1.4), which have quaternary nitrogen atoms. Finally, the part of the definition pertaining to the heterocyclic bound nitrogen atom can easily be overlooked for nitrogeneous compounds like taxol (Figure 1.4). Taxol is a natural product and exhibits pronounced physiological action through its high cytotoxicity, yet it cannot strictly be classified as an alkaloid because it does not contain a heterocyclic bound nitrogen atom. It is sometimes referred to as a pseudo-alkaloid.

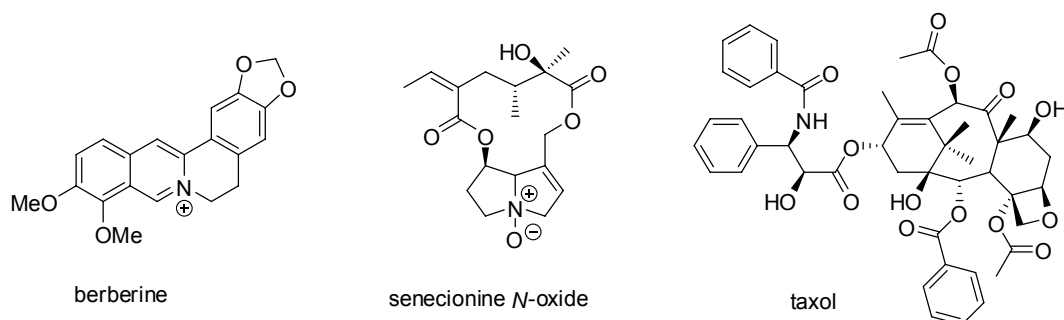
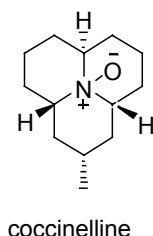


Figure 1.4. Chemical structures of berberine, senecionine *N*-oxide and taxol.

1.3. Occurrence and distribution of alkaloids

Historically, the major source of alkaloids has been flowering plants (Angiospermae), where approximately 20 % contain alkaloids.⁴ Increasingly though, alkaloids have been isolated from animals, insects, marine organisms, microorganisms, and lower plants.⁴

When threatened, certain species of ladybird beetles emit hemolymph droplets at their joints. These droplets contain bitter-tasting alkaloids, such as coccinelline, which is produced from *Coccinella septempunctata* (Figure 1.5).⁵

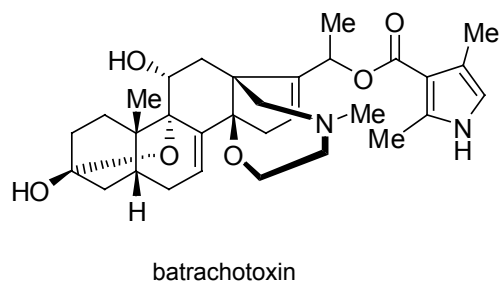


Please see print
copy for Figure
1.5

Coccinella septempunctata
(picture taken from Wikipedia⁶)

Figure 1.5. Bitter-tasting alkaloid coccinelline is emitted from *Coccinella septempunctata*.

The batrachotoxins are highly toxic steroidal alkaloids that have been isolated from the skin exudates of five species of *Phyllobates* (Figure 1.7). Remarkably, batrachotoxin is five times more toxic than tetrodotoxin, yet its mechanism of action is reversed in that it activates Na^+ channels and leaves them open.⁴ Highlighting its activity, batrachotoxin has an LD_{50} of 0.002 mg / kg for subcutaneous injection in mice.⁴ In South America, natives relied on this toxin for hunting purposes and the secretion of one frog was enough to provide adequate poison for fifty arrows.⁴



Please see print copy for
Figure 1.7

Phyllobates terribilis
(picture taken from Wikipedia⁷)

Figure 1.7. Highly lethal alkaloid Batrachotoxin; found in the skin of *Phyllobates terribilis*.

1.4. Alkaloids in folkloric medicine

The same South American natives that relied on alkaloidic arrow toxins for their hunting, also used alkaloids as natural medicines in times of sickness. One such natural medicine comes from the leaves of *Eugenia uniflora*, a tree widely distributed in South American countries including Argentina, Brazil, Uruguay and Paraguay (Figure 1.8).⁸ Locally, it is known as ‘nangapiri’ or ‘pitanga’ and was introduced into folkloric medicine by the ‘Guaranies’ in the 15th century.⁹ Its fresh or dried leaves are now popularly used at an enthotherapeutic dose of 0.7 - 1.5 g dried leaves per litre of boiling water and taken for a day (0.4 - 0.8 mg/kg/h).⁹ Infusions or hot water extracts are used as an antihypertensive^{10,11} and diuretic,¹¹ as well as for the treatment of digestive disorders,^{12,13} fever,^{14,10} hypocholesterolemia,¹⁰ gout,¹⁰ rheumatism,^{14,10} cough,¹⁰ sore throat,¹⁰ amygdalitis,¹⁰ hemorrhoids,¹⁰ obesity¹⁵ and diabetes.¹⁵ The leaves are also used in Madeira for the treatment of bronchitis, influenza and intestinal troubles,¹⁶ as well as in the Seychelles for agitation,¹⁷ and in Nigeria as a febrifuge.¹⁸

Please see print copy for Figure 1.8

Figure 1.8. *Eugenia uniflora*, source of Nangapiri.
(Photo © Gerald D. Carr, University of Hawaii Botany Department)¹⁹

Studies that have probed the pharmacological basis for Nangapiri's popular use, have demonstrated it to have diuretic and antiinflammatory properties²⁰ and xantine-oxidase inhibitory activity,^{21,10} as well as *in vivo* inhibition of gastrointestinal transit and an increase in pentobarbital sleeping time in mice.²⁰ Moreover, treatment of hypertensive patients with *E. uniflora* extracts has resulted in the reduction of blood pressure, together with decreased plasma cholesterol and triglyceride levels.²²

In 2000, Matsumura and co-workers published an investigation into the purported anti-diabetic effect of Nangapiri, together with the isolation and structural elucidation of its bioactive constituents.²³ The water-soluble extract (WSE) from chopped dry leaves of *E. uniflora*, inhibited the increase of plasma glucose levels in a sucrose tolerance test (STT) with mice, at a single oral dose of 100 mg / kg. Conversely, the WSE was not found to inhibit the increase of plasma glucose levels in a glucose tolerance test, in the same mice, which demonstrated that the WSE contained glucosidase inhibitors. Three active compounds in the WSE were isolated, uniflorine A and uniflorine B with proposed structures **1** and **2**, respectively, and the known alkaloid, (+)-(3 α ,4 α ,5 β)-1-methylpiperidine-3,4,5-triol (**3**) (Figure 1.9). Mass spectrometric and NMR spectroscopic analyses facilitated the structural elucidation of these compounds. Uniflorine A and uniflorine B displayed moderate activity in inhibiting maltase and sucrase while compound **3** showed weak activity for these α -glucosidases (Table 1.1).

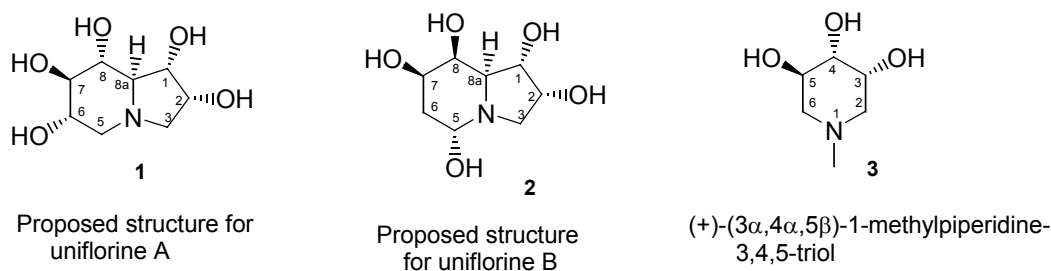


Figure 1.9. Proposed chemical structures for the alkaloids isolated from a water-soluble extract of *E. uniflora*.

Table 1.1. Inhibition of α -glucosidases by uniflorine A, uniflorine B and **3**.

	IC ₅₀	
	maltase	sucrase
uniflorine A	12.0 μ M	3.1 μ M
uniflorine B	4.0 μ M	1.8 μ M
compound 3	500 μ M	270 μ M

1.5. Initial project plan

When this project commenced, there was no reported synthesis of the structure of **1** in the literature. As a synthetic target, structure **1** is analogous to other polyhydroxylated alkaloids synthesized in our research group, namely, swainsonine²⁴ (**4**) and the australine diastereomers^{25,26} (**5-7**) depicted in Figure 1.10. Given that the structure of uniflorine A was proposed on the basis of NMR spectroscopy studies and not by single-crystal X-ray diffraction, the synthesis of structure **1** would allow the verification of its structure. Thus, the initial goal of this project was to complete the total synthesis of structure **1**. However, it would be helpful to further contextualise this structure within the family of polyhydroxylated alkaloids, before discussing the plan for its synthesis.

Please see print copy for Figure 1.10

Figure 1.10. Some analogous compounds of uniflorine A, synthesized by Pyne *et al.*²⁴⁻²⁶

1.6. Polyhydroxylated alkaloids

The practice of obtaining natural products as potential medicinal agents using organic solvent extraction (MeOH, CHCl₃, hexane) has been widespread. Yet, the knowledge of folkloric medicines as water-soluble extracts has been known for millennia. It is now apparent that water-soluble fractions of plants and microbial cultures contain many potentially therapeutic chemical entities, including carbohydrate analogues. These analogues include a rapidly growing number of polyhydroxylated alkaloids with molecular weights below 250 Da.

The first polyhydroxylated alkaloid discovered was the piperidine alkaloid norjirimycin, which was isolated in 1966 by Inouye *et al.* (Figure 1.11).²⁷ In excess of one hundred more polyhydroxylated alkaloids have been reported so far in the literature, although most have been discovered since 1983. Looking at its structure, norjirimycin mimics glucose, with a nitrogen atom substituted for the ring oxygen atom. Norjirimycin was first described as an antibiotic produced by *Streptomyces roseochromogenes* R-468 and *S. lavendulae* SF-425, and was demonstrated from various sources, to be a potent inhibitor of α - and β -glucosidases.²⁸

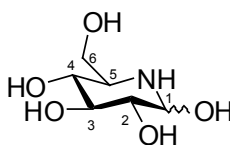
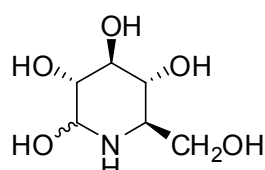
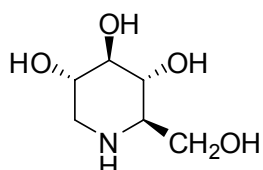


Figure 1.11. Norjirimycin, the first polyhydroxylated alkaloid isolated.

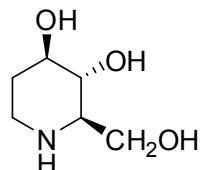
The family of polyhydroxylated alkaloids is subdivided into five structural groups, pyrrolidine, piperidine, pyrrolizidine (fused pyrrolidines with *N* at the bridgehead), indolizidine (fused piperidine and pyrrolidine) and nortropane. Several examples of each group are depicted in Figure 1.12.

Piperidines

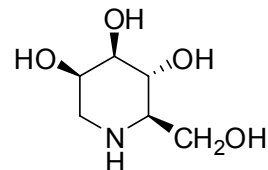
nojirimycin



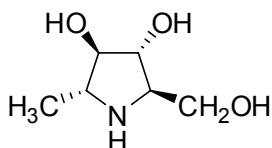
1-deoxynojirimycin (DNJ)



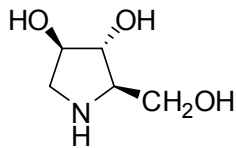
fagomine



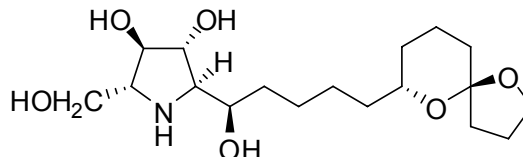
1-deoxymannojojirimycin (DMJ)

Pyrrolidines

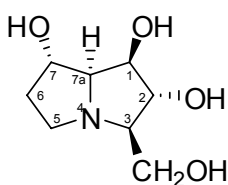
2,5-dihydroxymethyl-3,4-dihydroxypyrrolidine (DMDP)



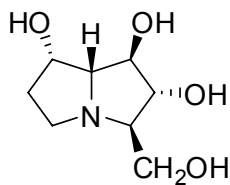
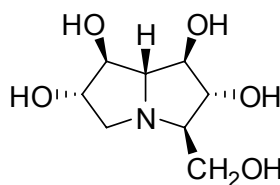
1,4-dideoxy-1,4-imino-D-arabinitol (D-AB1)



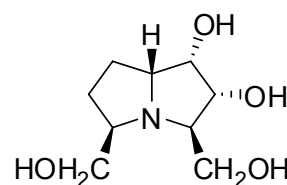
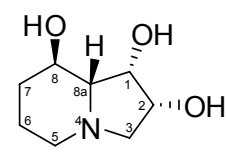
broussetine G

Pyrrolizidines

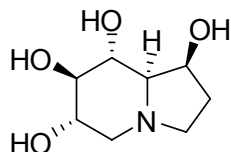
alexine

7a-epi-alexine
(australine)

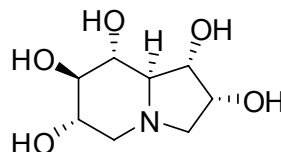
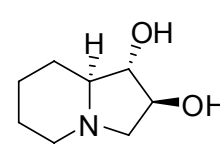
casuarine

hyacinthacine B₁**Indolizidines**

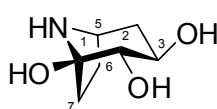
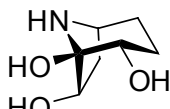
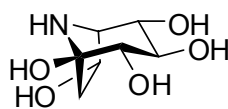
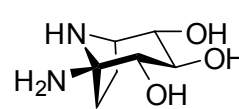
swainsonine



castanospermine

uniflorine A
(proposed structure)

lentiginosine

Nortropenescalystegine A₃calystegine A₆calystegine C₁calystegine N₁**Figure 1.12.** Selected piperidine, pyrrolidine, pyrrolizidine, indolizidine and nortropane alkaloids.

1.7. Occurance of polyhydroxylated alkaloids

1-Deoxynorjirimycin (DNJ) was first prepared synthetically from L-sorbofuranose²⁹ and by the reduction of norjirimycin.³⁰ It was isolated later from the roots of Mulberry trees, and is produced by many strains of *Bacillus* and *Streptomyces*. 1-Deoxymannojirimycin (DMJ) was first isolated from the seeds of *Lonchocarpus sericeus*, a legume native to the West Indies and tropical America.³¹ It was later isolated from the neotropical liana *Omphalea diandra*³² (Figure 1.13a) and the legume *Angylocalyx pynaertii*³³ (Figure 1.13b) from tropical Africa. DMJ was also isolated from the culture broth of *Streptomyces lavendulae* GC-148,³⁴ a strain of *Streptomyces* that produces DNJ in high yield.³⁵

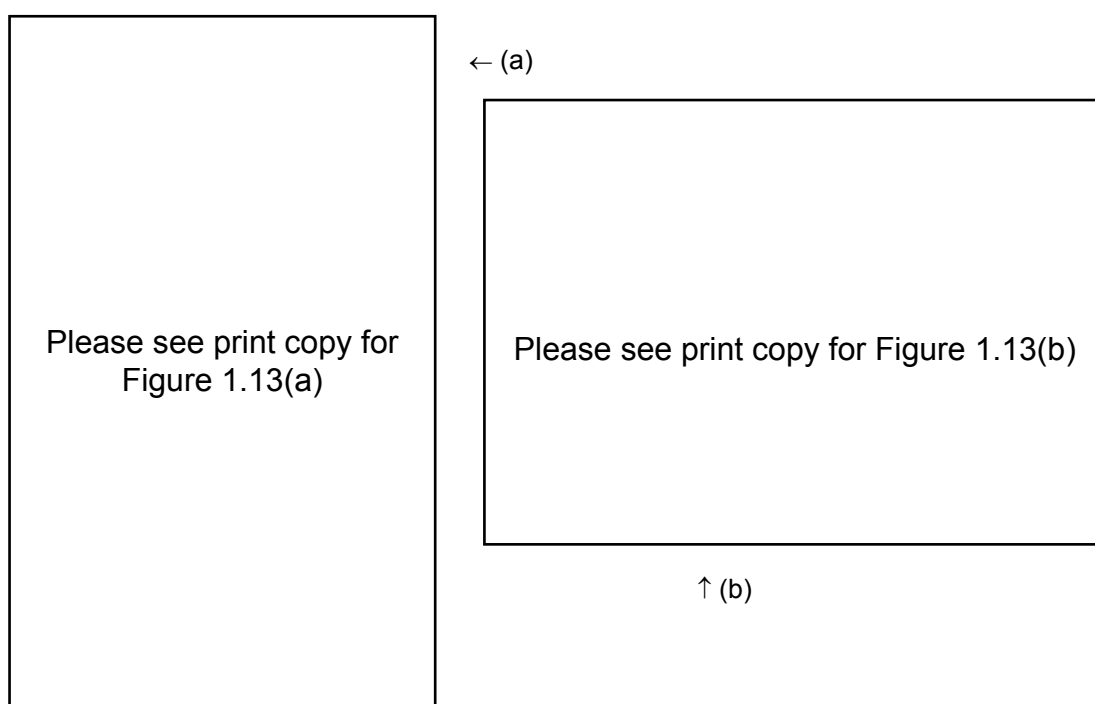
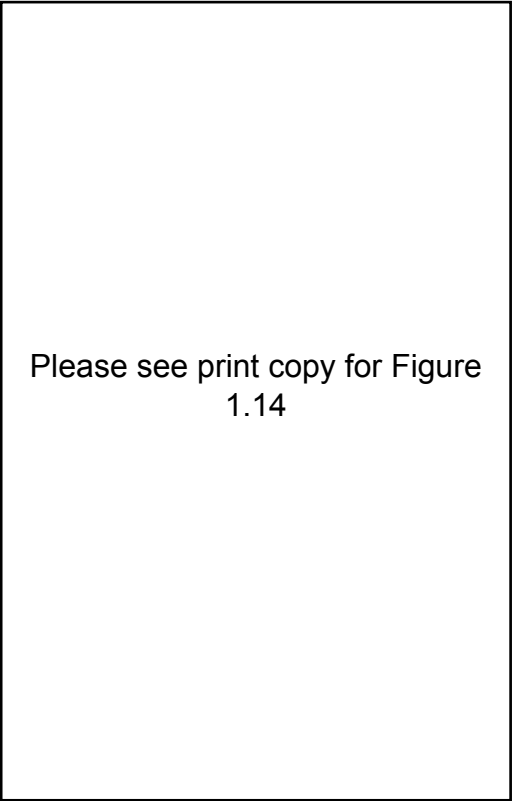


Figure 1.13. (a) *Omphalea diandra* (Euphorbiaceae) in Panama, a source of DMJ.;
 (b) *Angylocalyx* sp. (Leguminosae) in Kenya, a source of DMJ and D-AB1.
 (Both photographs taken from Asano *et al.*²⁸)

Fagomine was isolated from the seeds of *Fagopyrum esculentum*,³⁶ otherwise known as Japanese buckwheat, and from the Moreton Bay chestnut (black bean), *Castanospermum australe* (Figure 1.14).³⁷ It has also been isolated from the leaves and roots of *Xanthocercis zambesiaca*³⁸ and in the roots of *Lycium chinense*.³⁹



Please see print copy for Figure
1.14

Figure 1.14. *Castanospermum australe* (Leguminosae) in Australia, a source of castanospermine and fagomine (photograph taken from Asano *et al.*²⁸).

DMDP (Figure 1.12) was first isolated from the leaves of *Derris eliptica*⁴⁰ and was later discovered in many unrelated species of plants and microorganisms.⁴¹ Similarly, D-AB1 (Figure 1.12) has also been found in many different species of plants and microorganisms, although it was first discovered in *Angylocalyx boutiqueanus* (Figure 1.13b).⁴²

The polyhydroxylated pyrrolizidine alkaloids appeared to be restricted to the Leguminosae, with alexine and australine (Figure 1.12) being isolated at about the same time from *Alexa* sp.⁴³ (Figure 1.15) and seeds of *Castanospermum australe*,³⁷ respectively. Later, casuarine⁴⁴ (Figure 1.12) and its 6-*O*- α -D-glucoside were isolated from the bark of *Casuarina equisetifolia* (Casuarinaceae) and from the leaves of *Eugenia jambolana* (Myrtaceae).⁴⁵ More recently, a whole host of pyrrolizidines have been isolated from members of the Hyacinthaceae (Figure 1.16), including hyacinthacine B1 (Figure 1.12).⁴⁶



Please see print copy for Figure 1.15

Figure 1.15. *Alexa canaracunensis* (Leguminosae) in Brazil, a source of alexines (photograph taken from Asano *et al.*²⁸)



Please see print copy for Figure 1.16

Figure 1.16. *Hyacinthoides non-scripta* in the UK (Hyacinthaceae), a source of hyacinthacines (photograph taken from Asano *et al.*²⁸)

Swainsonine and castanospermine (Figure 1.12) were first isolated from the legumes *Swainsona canescens*⁴⁷ and *Castanospermum australe*,⁴⁸ respectively. Swainsonine is also present in locoweeds *Astragalus* and *Oxytropis* sp.,⁴⁹ while castanospermine has also been isolated from the seeds of *C. australe* and from the dried pods of *Alexa leiopetala*.⁵⁰ Lentiginosine (Figure 1.12) was isolated from the leaves of *Astragalus lentiginosus*.⁵¹

Finally, the nortropane alkaloids appear to be predominately found in the closely related families Solanaceae and Convolvulaceae, where they co-occur with tropane alkaloids.⁵² In particular, calystegines are profuse in the sub-soil organs and root exudates of *Calystegia sepium*, *Convolvulus arvensis* (both Convolvulaceae) and *Atropa belladonna* (Solanaceae).²⁸ Calystegine A₃ (Figure 1.12) was isolated from *C. sepium*.⁵³ Calystegines A₆ and N₁ (Figure 1.12) were isolated from *Hyoscyamus niger*⁵⁴ (Solanaceae) while calystegine C₁ (Figure 1.12) has been found in *Scolopia japonica*⁵⁴ and *Duboisia leichhardtii*⁵⁵ (both Solonaceae). Recently, calystegine C₁ was isolated from a different family, the Moraceae, in which two species have contained this alkaloid.^{56,57} Interestingly, calystegines have been detected among edible fruits and vegetables in the Convolvulaceae, Solanaceae and Moraceae: sweet and chilli peppers, potatoes, eggplants, tomatoes, *Physalis* fruits, sweet potatoes and mulberries.⁵⁸

1.8. Biological activities of polyhydroxylated alkaloids

It is perhaps not surprising that many of the polyhydroxylated alkaloids isolated have displayed activity as inhibitors of glycosidases, given their structural imitation of well-known glycosides like glucose and mannose. Glycosidases participate in a diverse array of biological processes, including intestinal digestion, post-translational modification of glycoproteins and the lysosomal catabolism of glycoconjugates. Hence, there is a realisation that sugar-mimicking polyhydroxylated alkaloids could have significant therapeutic potential in many diseases such as viral infection, cancer and diabetes.

Studies of glycosidases originate from the 1840's when Liebig *et al.* made their first contributions to this emerging area.⁵⁹ These enzymes are well understood today, from the pioneering work of Legler,⁶⁰ Sinnot⁶¹ and Withers *et al.*,⁶² among others. Glycosidases are enzymes that catalyse the hydrolysis of the glycosidic bonds in complex carbohydrates and glycoconjugates. Polyhydroxylated alkaloids can inhibit these enzymes by adopting a similar conformation to that for the pyranosyl or furanosyl moiety of the natural substrate, within the transition-state of the substrate-enzyme complex (Figure 1.17). These alkaloids are protonated at physiological pH and mimic the charge and conformation of the oxocarbenium ions formed in the enzyme active site, upon glycoside hydrolysis (Figure 1.17). The manner in which this occurs is competitive and reversible for the vast majority of sugar-mimicking alkaloids.^{63,60}

Please see print copy for Figure 1.17

Figure 1.17. Comparison of DNJ and DMDP with the carboxonium ion transition state (taken from Wrodnigg⁶⁴).

The mechanism of the glycoside hydrolysis depends upon whether the enzyme is a retaining glycosidase or an inverting glycosidase (Figure 1.18). Both types of glycosidases contain two carboxylic acids in the active site that facilitate catalysis. In the case of retaining glycosidases, the catalysis is believed to occur by protonation of the anomeric hydroxyl group by one of the active sites' carboxylic acids (the general catalytic acid). The resulting cation, an oxocarbenium ion intermediate, reacts with the other active site carboxylate group (the catalytic nucleophile), to form an intermediate ester. Subsequently, this ester is displaced by a molecule of water with general base catalysis, to form the product hemiacetal with retention of configuration (Figure 1.18a). In the case of inverting glycosidases, the general acid has the same initial catalytic function. However, instead of a cation (oxocarbenium ion) being discretely formed, the general base acts by directing a water molecule to attack the anomeric carbon. The product is then obtained with inversion of configuration (Figure 1.18b).

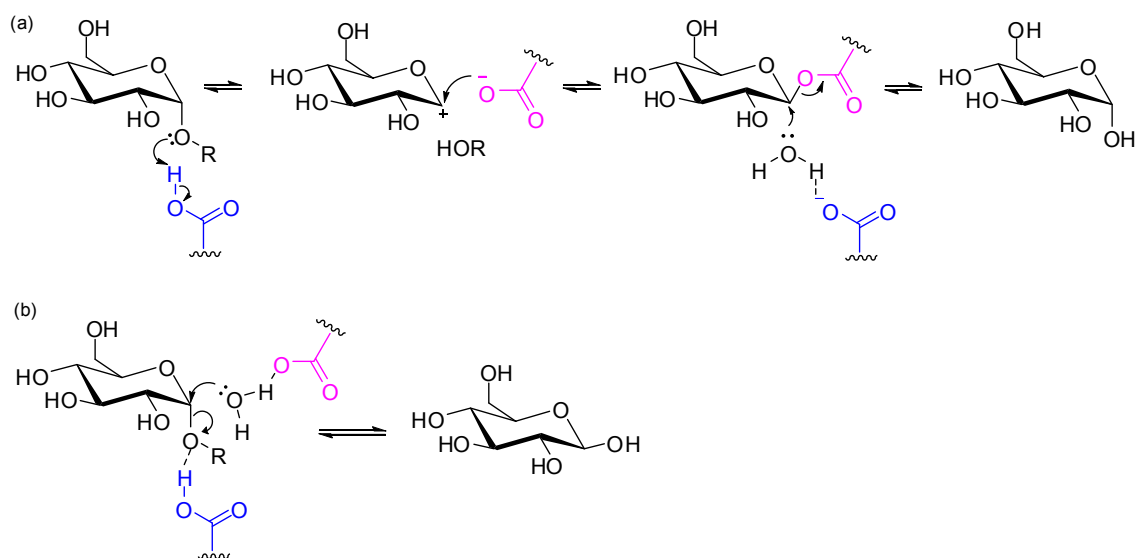


Figure 1.18. Mechanism of retaining (a) and inverting (b) glycoside hydrolysis.

Recent estimates indicate that genes responsible for regulating *N*- and *O*-glycosylation of glycoproteins constitute 1–2 % of the human genome.⁶⁵ For *N*-linked oligosaccharides, there are more than 30 glycosyltransferases and glycosidases, located in the cytosol, endoplasmic reticulum and the golgi apparatus, that are required to generate, attach and process the oligosaccharides.⁶⁵

The impact of targeting glycosylation as a therapeutic approach has been demonstrated with Miglitol achieving clinical approval for the treatment of non-insulin-dependent diabetes (Figure 1.19).⁶⁵ Miglitol (*N*-hydroxy-DNJ), a modified polyhydroxylated alkaloid, partially inhibits intestinal disaccharidases to reduce the level of postprandial glucose.⁶⁶

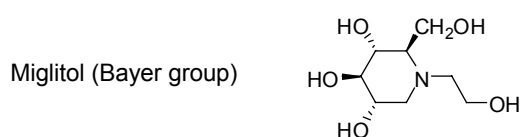


Figure 1.19. Miglitol, a clinical treatment for non-insulin-dependent diabetes.

1.9. The value of total synthesis in natural product structure determination

A simple broad definition of total synthesis is the chemical synthesis of a molecule from relatively simple and readily available starting materials. This is to differentiate from the concept of partial synthesis, which refers to the synthesis of a molecule from a relatively advanced precursor. In terms of natural product total synthesis, the first molecule to be synthesized this way was urea in 1828 by Wöhler.⁶⁷ Today, practically any class of natural product can be reached by synthesis; one of the most spectacular examples to date being Kishi and co-workers synthesis of palytoxin (Figure 1.20).⁶⁸⁻⁷²

From the early days of urea synthesis to the middle of the twentieth century, total synthesis played an important role in the structural determination of natural products. It was used to provide conclusive proof of structure, thus complementing chemical degradation and other analytical tools of the time. With the advent of high-field NMR and routine X-ray crystallography in the late 1960's, the requirement for total synthesis to prove a structure became less compelling.⁷³ However, one should not overlook its value in this role. There are plenty of examples of the limitations and fallibility of spectroscopic methodology in establishing natural product structures. Recent notable cases include the mischaracterization of cylindrospermopsin,⁷⁴ the sclerophytins,^{75,76} batzelladine,⁷⁷ and even the diazonamides^{78,79} – where there was an X-ray structure reported. In all of these instances, the correct structures were ultimately determined by total synthesis. In the scope of this thesis, the story of 7-*epi*-australine (Figure 1.10) is a particularly relevant example.

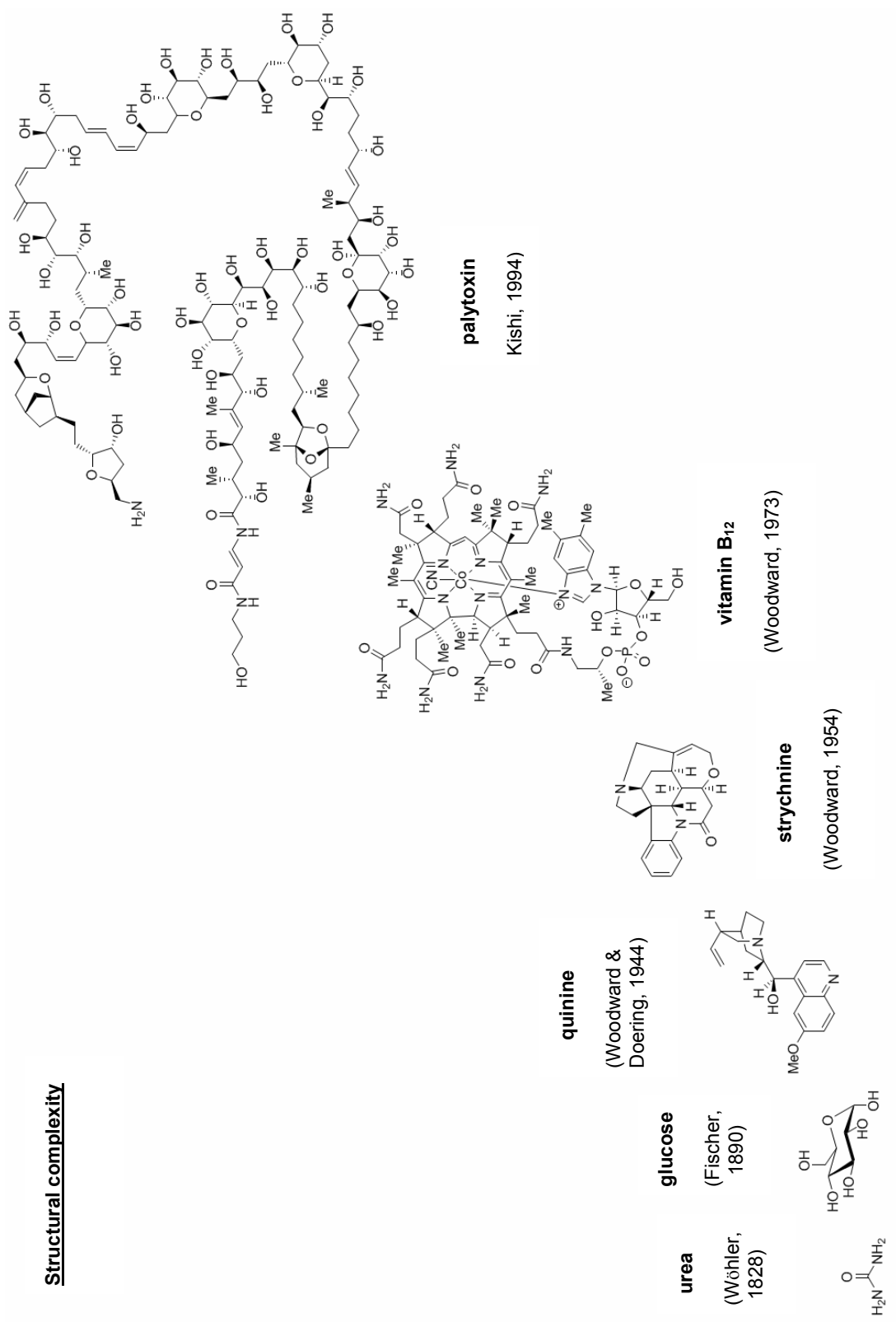


Figure 1.20. Progression of natural product synthesis.

7-*epi*-Australine **5** (Figure 1.10) was isolated along with another stereoisomer from extracts of *Castanospermum australe*, and its structure was assigned by spectroscopic methods and by analogy to crystallographically defined natural epimers.⁸⁰ Eight years later, Denmark *et al.* published the total synthesis of 7-*epi*-australine, which included a single-crystal X-ray analysis of the synthetic product.⁸¹ The crystallographic data proved the successful synthesis of the targeted structure **5**, however the spectroscopic data and physical characteristics of the synthetic material did not match the natural product. Most significantly, the natural product was reported as a levorotatory oil ($[\alpha]_D^{23} - 13.0^\circ$ (c 0.55, H_2O))⁸⁰ while the synthetic product was described as a highly crystalline (mp 193 – 194 °C) dextrorotatory material ($[\alpha]_D^{23} + 11.6^\circ$ (c 0.37, H_2O)).⁸¹ Thus, the assignment of the natural product first reported as 7-*epi*-australine (**5**) was proved incorrect, and has led to a complete re-evaluation of all the published data on naturally occurring australines.⁸²

1.10. Retrosynthetic analysis of the proposed structure of uniflorine A.

The proposed structure for uniflorine A represented a challenging synthetic target. Although relatively small (MW 205 Da), its eight-carbon skeleton contains six contiguous stereocentres. The synthesis of polyhydroxylated indolizidine compounds has many precedents and two of the closest structural relatives of **1** that have been synthesized are 2*S*-hydroxycastanospermine **8**⁸³ and 1-*epi*-castanospermine **9**⁸⁴ (Figure 1.21).

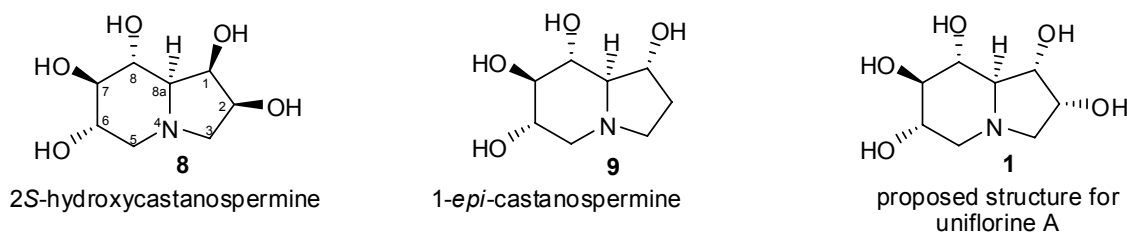


Figure 1.21. Comparison of **1** and similar synthesized compounds.

One might suspect that the synthesis of polyhydroxylated alkaloids like **8** and **9** would include a sugar synthon or some derivative thereof, towards the start of their syntheses. While the synthesis of 2*S*-hydroxycastanospermine **8** by Fleet *et al.*⁸³ does include such a strategy, the synthesis of 1-*epi*-castanospermine **9** by Denmark *et al.*⁸⁴ does not.

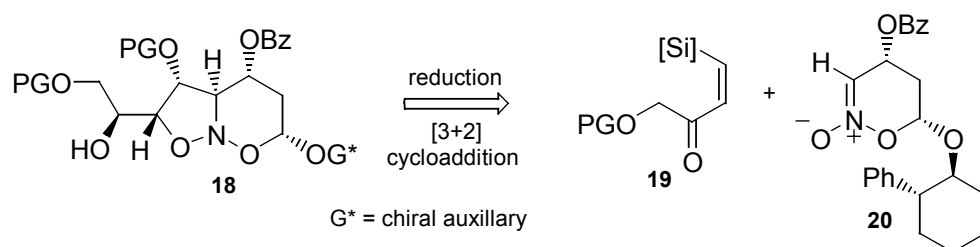
Fleet's strategy for the construction of **8** hinged around the joining of C-1, C-4 and C-8 through nitrogen, in a reductive cyclization of the azido mesylate **15** (Scheme 1.1). The

nitrogen atom was initially introduced at C-8, so that piperidine ring formation would precede completion of the bicyclic system. Starting from the triacetone **10**, selective acid hydrolysis was followed by selective silylation and esterification of the resulting primary and secondary carbinol functionalities, to give the silyltriflate **11**. Removal of the silyl protecting group in **11** produced epoxide **12**, which was subsequently ring-opened with sodium azide. The free hydroxyl group at C-7 was converted to a TBS-ether to give the fully protected azidolactone **13**. Reduction of the lactone ring was followed by activation of the liberated hydroxyl groups, which set-up a subsequent tandem ring-closure. Thus, reduction of azide **15** promoted an attack of the excipient primary amine onto the activated secondary carbon to give a piperidine ring. In cascade style, reaction of the resulting cyclic secondary amine onto the primary mesylate generated the indolizidine system **16**, and subsequent deprotection gave the desired product **8**.

Please see print copy for Scheme 1.1

Scheme 1.1. Synthesis of 2*S*-hydroxycastanospermine **8** by Fleet *et al.*⁸³

In stark contrast, the cornerstone of Denmark's synthesis of 1-*epi*-castanospermine was a [3+2]-cycloaddition methodology, in which a nitronate **20** and dipolarophile **19** react to form a nitroso acetal **18** (Scheme 1.2).



Scheme 1.2. Cornerstone of Denmark's synthesis of 1-*epi*-castanospermine.

Synthesis of the dipolarophile **25** followed the synthetic route outlined in Scheme 1.3. Addition of the bromomagnesium derivative of silyl acetylene **21** to aldehyde **22** produced the propargyl alcohol **23**, which was semi-hydrogenated with 2 equiv. of dicyclohexylborane, followed by the addition of acetic acid. This resulted in the clean conversion to the *cis*-alkene **24** with no other olefinic material present. Swern oxidation of this alkene completed the synthesis of the dipolarophile **25** in good overall yield.

Please see print copy for Scheme 1.3

Scheme 1.3. Synthesis of dipolarophile **25**.⁸⁴

The thermal [3+2]-cycloaddition between the chiral nitronate **20** and dipolarophile **25** gave the desired nitroso acetal **26** with complete *exo* selectivity, albeit in a 26/1 ratio of regioisomers (Scheme 1.4). The *exo* selectivity was rationalised on the basis of the C-4 (OBz) substituent controlling the approach of the dipolarophile. After the reduction of the ketone moiety the TDS group was removed from the primary alcohol and replaced with an activating tosyl group. Hydrogenolysis of the tosylate **29** gave the indolizidine **30** together with a small quantity of the pyrrolizidine **31**. Tamao-Fleming oxidation of the silane **30**, followed by deprotection gave 1-*epi*-castanospermine **9** in good yield.

Please see print copy for Scheme 1.4

Scheme 1.4. Remainder of the synthesis of 1-*epi*-castanospermine by Denmark *et al.*⁸⁴

In planning a synthesis of **1**, we were not constrained by the preselection of a specific methodology, like in the above synthesis of 1-*epi*-castanospermine. Instead, in desiring an efficient synthesis, we were naturally attracted towards using sugars, as a means of expeditiously and stereospecifically installing contiguous carbinol functionalities. Fleet and co-workers' synthesis of 2*S*-2-hydroxycastanospermine **8** was a good model for this type of approach. In the end, we did include a sugar in our synthetic plan but in a radically different approach to Fleet. Providing the genesis for our synthetic plan was a relatively new reaction that surfaced in the literature, one that would theoretically allow us to use a hexose in the first step of our synthesis.

In 1998 Petasis *et al.* reported the synthesis of *anti*-1,2-amino alcohols using a borono-variation of the Mannich reaction.⁸⁶ In this process, the combination of an amine, an α -hydroxyaldehyde and an organoboronic acid in a one-pot reaction, produced *anti*-1,2-amino alcohols in a highly diastereoselective manner (Table 1.2). A close examination of the proposed structure for uniflorine A revealed an *anti* configuration between the C-8a – N bond and the C-8 carbinol (Figure 1.22), thus making the Petasis reaction amenable to our synthetic strategy.

Table 1.2. Selected results from Petasis *et al.*⁸⁶

Please see print copy for Table 1.2

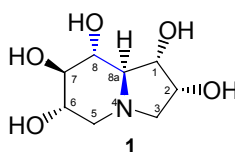
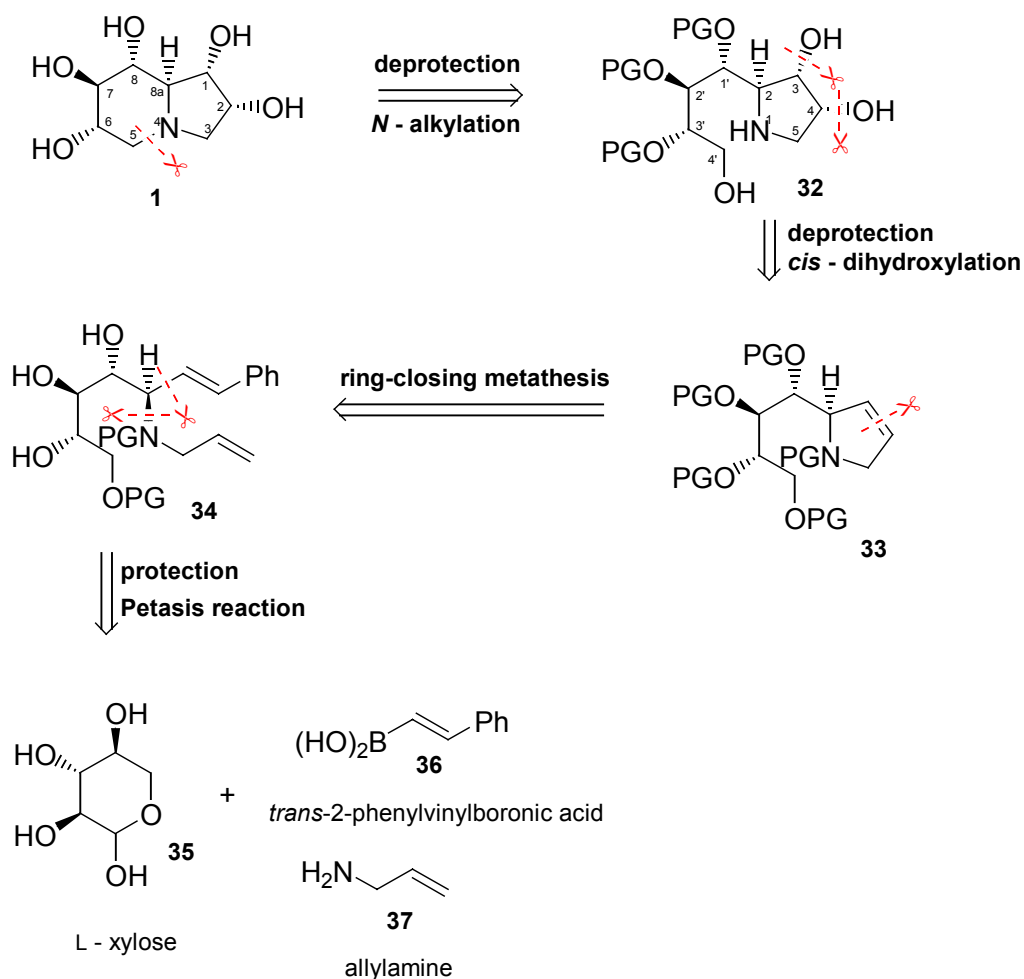


Figure 1.22. *Anti*-1,2-amino alcohol functionality within the structure of **1**.

Our retrosynthetic analysis of **1** began with a disconnection of the C-5 and N-4 bond (Scheme 1.5). This bond, we envisaged, would be constructed by *N*-alkylation employing a typical Mitsunobu⁸⁷ or Appel⁸⁸ process. Diol **32** would be generated by a *cis*-dihydroxylation reaction on the 2,5-dihydropyrrole **33**. It was envisaged that the C-2 side-chain would control the diastereofacial selectivity of the dihydroxylation reaction, within the parameters of an UpJohn⁸⁹ (potassium osmate / NMO) process. In the event of poor selectivity, a Sharpless⁹⁰ asymmetric dihydroxylation reaction would be tried. We were particularly confident that a ring-closing metathesis approach using Grubbs' catalyst would deliver the 2,5-dihydropyrrole **33** from the diene precursor **34**. Aside from some protecting group manipulations, the amino alcohol **34** would be provided by the above-mentioned Petasis reaction, from commercially sourced L-xylose **35**, *trans*-2-phenylvinylboronic acid **36** and allylamine **37**.

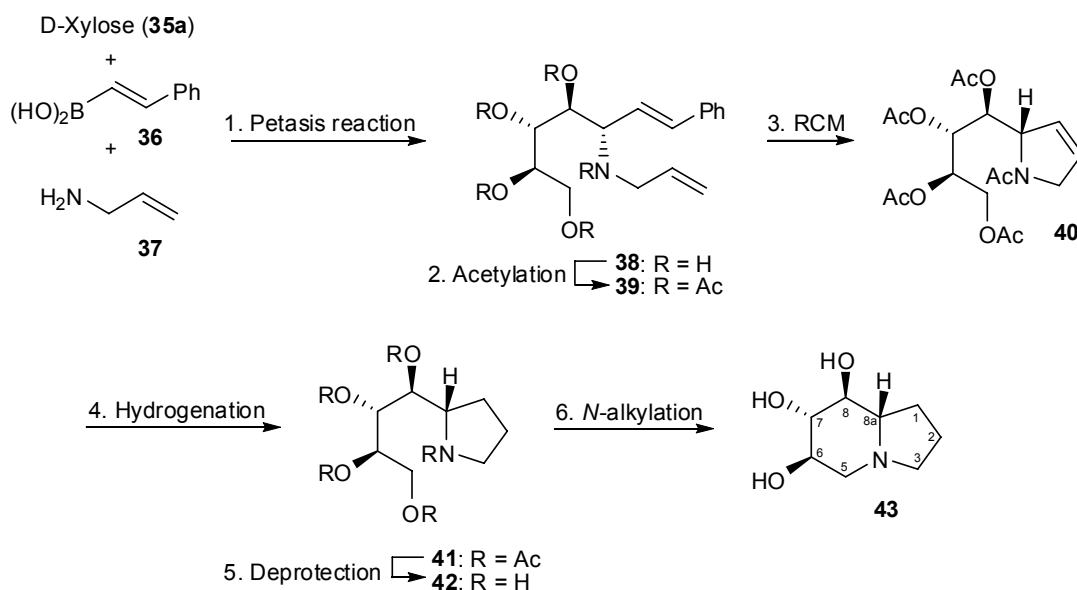


Scheme 1.5. Retrosynthetic analysis for compound **1**.

Chapter 2. 1-Deoxy-castanospermine – a model study

The purpose of this model study was to synthesize the relatively simple tri-hydroxy indolizidine **43**, which is the enantiomer of the known compound 1-deoxy-castanospermine. Several key reactions planned for use in the synthesis of **1** would be tested (Scheme 2.1). In particular, we wanted to observe whether the Petasis reaction would facilitate a stereoselective entry into the *anti*-1,2 amino alcohol **38**, and whether this molecule would undergo RCM, to give the corresponding 2,5-dihydropyrrole **40**. If successful, hydrogenation of **40** would be followed by the removal of protecting groups to give the amino alcohol **42**, which we anticipated would undergo cyclization to form the final product **43**. Originally, L-xylose **35**, *trans*-2-phenylvinylboronic acid **36** and allylamine **37** were the planned starting materials for the Petasis reaction in Scheme 2.1. However, D-xylose **35a** was substituted for L-xylose **35** after learning that L-xylose was much more expensive to purchase.

Confirmation of compound **43** would be made by comparing its spectroscopic data to that reported for its enantiomer in the literature.⁹¹⁻⁹⁹

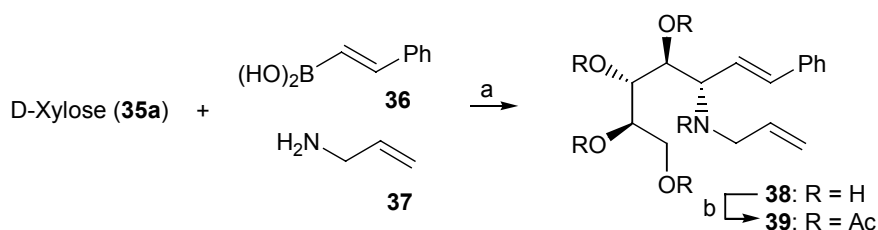


Scheme 2.1. Model study synthesis of *ent*-1-deoxy-castanospermine **43**.

2.1. Petasis reaction

Following Petasis's literature report, the reaction between **35a**, **36** and **37** was carried out using equimolar equivalents of the three components in EtOH at rt for 24 h (Scheme 2.2).⁸⁶ Analysing the reaction by TLC was very difficult, as the starting materials and product were

highly polar. ¹H NMR analysis of the crude product was complex and unhelpful. Purification of the product using flash column chromatography (FCC) seemed unrealistic, given the previously mentioned polarity issues. The next logical step was to decrease the polarity of the product by protecting the nitrogen and hydroxyl groups, thereby enabling purification on silica gel. To this end, the crude product was per-acetylated using a large excess of Ac₂O and pyridine (45 equiv).^{100,101} Gratifyingly, the crude product was purified by FCC without incident, and gave compound **39** in 76 % yield over two steps.



Reagents and conditions: (a) EtOH, rt, 18 h; (b) Ac₂O, dry pyr. rt, 18 h, 76 % over 2 steps.

Scheme 2.2. Results of the Petasis reaction and subsequent *O*-acetylation.

The ^1H NMR spectrum of **39** displayed five aromatic, five olefinic and five acetyl methyl resonances (Figure 2.1). The remainder of the peaks integrated correctly to 8 protons. Further 2D NMR and MS analysis completed the characterization of **39**. According to TLC analysis, one diastereomer was obtained from this reaction, and was assumed to be the desired *anti*-1,2-amino alcohol, given the literature precedence. A NOESY NMR experiment was not performed on the acetylated product. However, the *anti* configuration was confirmed in the next step following single crystal X-ray analysis of its product (Section 2.2).

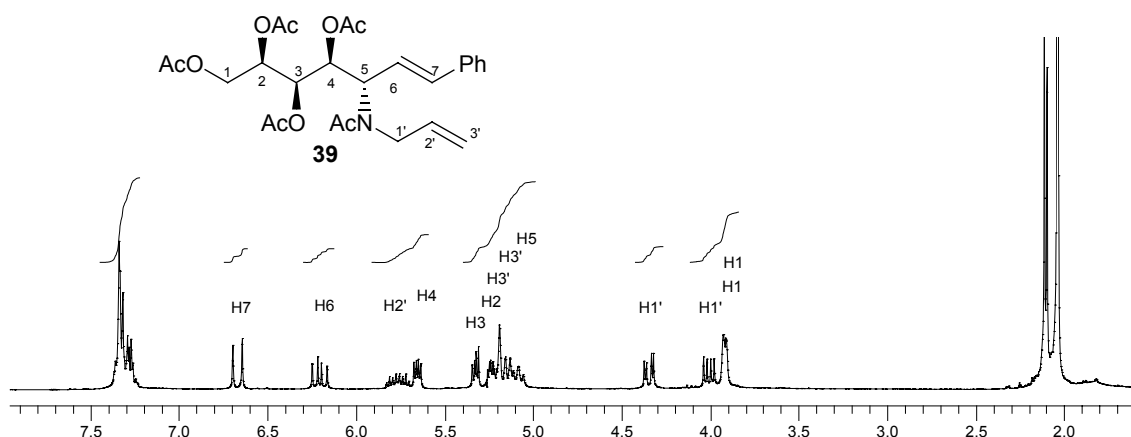
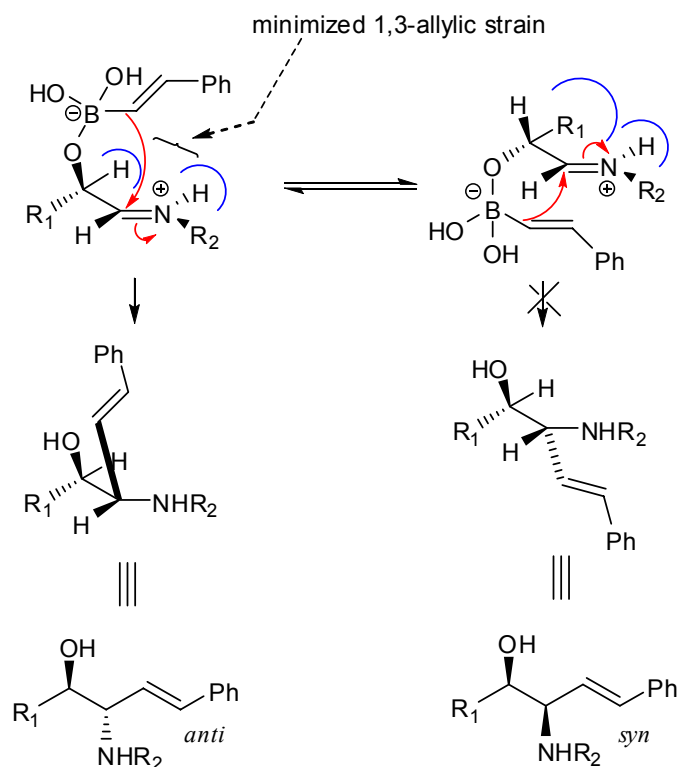


Figure 2.1. ^1H NMR spectrum (300 MHz, CDCl_3) of acetylated Petasis product **39**.

The full mechanism of the Petasis reaction is unknown. Initially, one can assume that the aldehyde reacts with the amine to form an iminium ion, in the classic sense of a Mannich reaction. From here, the mechanism is ambiguous, particularly in how the boron reagent is stereoselectively delivered to the imine. One of the pre-requisites in the Petasis reaction is an α -hydroxyl group in the aldehyde. Pyne *et al.* speculated that this hydroxyl group controls the stereoselectivity of the boron reagents delivery (Scheme 2.3).¹⁰² In particular, a lone pair of electrons of the α -hydroxyl oxygen atom is transferred to the vacant p orbital of the boron atom, to give a boronate complex. This complex then adopts the conformation shown in Scheme 2.3, to minimize 1,3-allylic strain,^{103,104} before delivery of the boron reagent on the β -face of the iminium ion. Minimized 1,3-allylic strain refers to the lowest energy conformation of an acyclic alkene containing an allylic chiral centre. In such a system, the smallest α -substituent (in our case a hydrogen atom) on the stereogenic carbon will be eclipsed by the iminium double bond. This results in the lowest steric interaction between the allylic substituents with the NH hydrogen, thus giving rise to the lowest energy conformation. While the other hydroxyl groups in the side chain of the iminium ion intermediate can also form boronate complexes with the boronic acid in a reversible reaction, these boronate complexes are less likely to lead to products because of their more remote distance to the iminium ion.



Scheme 2.3. Proposed mechanism explaining stereoselectivity in the Petasis reaction.

2.2. Ring-closing metathesis

With an ample quantity of the diene **39** in hand, attention turned to reacting it with Grubbs'I catalyst to produce the cyclized product **40**. TLC analysis of the reaction mixture showed the product spot being far more polar than anticipated. Reaction times ranged from 16 h to 24 h, with a fixed catalyst loading of 10 mol %, producing yields that ranged from 76 % to 94 %. All reactions were performed at high dilution (6.7 mM, DCM), to mitigate the formation of cross-metathesis products.

^1H NMR analysis of the product confirmed that successful ring closure had occurred, by the absence of aromatic resonances, and by a reduction in the number of olefinic protons, from five to two (Figure 2.2).

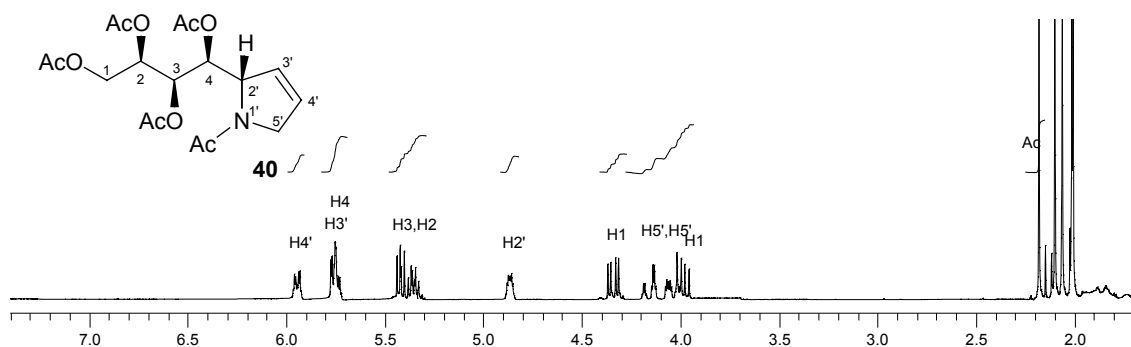


Figure 2.2. ^1H NMR spectrum (300 MHz, CDCl_3) of **40**.

An attempt was made to produce a crystal of **40** for X-ray analysis after the discovery of precipitate in a product-containing fraction from FCC. This was successful using a slow-evaporation method (from EtOAc) resulting in suitable single crystals. X-ray analysis confirmed the structure of the ring-closed product (Figure 2.3). It also confirmed the *anti*-1,2 amino alcohol configuration of the product from the earlier Petasis reaction.

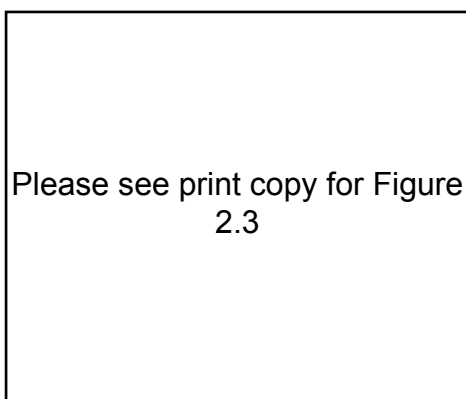


Figure 2.3. Single crystal X-ray structure of **40** (viewed as a CIF file in CCDC Mercury¹⁰⁵).

2.3. Hydrogenation

Hydrogenation of olefin **40** using Pd/C and H₂ was consistently high yielding, recording a minimum 95 % yield of **41**. The reaction went smoothly at rt over 16 h (un-optimized), and the work-up provided product **41** that by ¹H NMR analysis required no further purification. Crystallization of the product was successful, using the same method described above, giving suitable crystals for X-ray analysis (Figure 2.4).

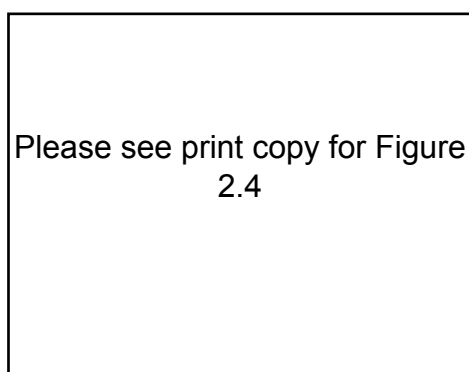
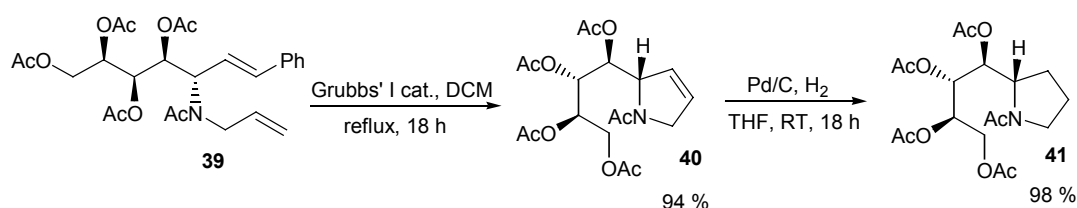


Figure 2.4. Single crystal X-ray structure of **41** (viewed as a CIF file in CCDC Mercury¹⁰⁵).

The synthesis of *ent*-1-deoxycastanospermine **43** had so far been relatively uneventful. Two of the major reactions that required testing, the Petasis reaction and the RCM, proved highly successful on their respective substrates. Our final test in this model study was to observe whether cyclization of **42** would occur as planned in Scheme 2.1. However, prior to discussing this, a summary of the previous two reactions is shown below (Scheme 2.4).



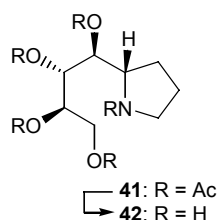
Scheme 2.4. Results of the RCM of **39** and hydrogenation of **40**.

2.4. De-acetylation

Before final construction of the indolizidine ring could occur, removal of the *N* and *O*-Ac protecting groups from **41** was required. This procedure is well established in the literature and we selected a HCl catalysed hydrolysis¹⁰⁶ from various others. The reaction of **41** in Et₂O with 50 eq of 10 % v/v HCl gave complete removal of the acetate groups after 16 h at 110 °C in

a sealed tube reaction. As a HCl salt, the product was incompatible with Mitsunobu cyclization and was too polar to attempt purification by FCC. Instead, given its water solubility, efforts were made to purify this compound using ion-exchange chromatography.

Purification by this method produced two necessary outcomes in the one procedure. Apart from actually purify the product by removing any water-soluble impurities, this method gave the product in the free-base form. In the event, the crude hydrolysis product was dissolved in a minimum volume of 1M HCl and loaded onto a prepared ion-exchange column, followed by half a column-bed aliquot of H₂O. Following washings with water, the product was eluted with aqueous ammonia (28 %) and was shown to be pure by ¹H NMR analysis. The resulting yield of **42** after purification was 86 % (Scheme 2.5).



Reagents and conditions: 10 % v/v HCl, Et₂O, 16 h, 110 °C, 86 %

Scheme 2.5. Result of the deacetylation of **41**.

2.5. Mitsunobu cyclization

The Mitsunobu cyclization of **42** was tried once on a 275 mg scale. Like the earlier Petasis reaction (Section 2.1), the starting material and product were highly polar and susceptible to streaking on a TLC plate. Monitoring the reaction by TLC analysis was therefore very difficult, and after 4 h the reaction was stopped even though full consumption of the starting material was inconclusive. ¹H NMR analysis of the worked-up material showed at least two products. Due to its highly polar nature, the crude material was subjected to *O*-acetylation without purification.

The crude product was *O*-acetylated under the same conditions as used for the Petasis product. TLC analysis of the reaction mixture showed multiple products, each having a similar *R_f*. This led to repeated purifications by FCC, and even semi-preparative TLC to separate the products. Eventually, the major product **45** was isolated and gave a CIMS (*M* + 1⁺) peak of *m/z* 300, indicating the desired net loss of water from the starting material. The yield of this product over the cyclization and *O*-acetylation steps was 18 %.

¹³C DEPT NMR analysis confirmed the requisite number of four methylene, four methine and five methyl groups. However, the starting material had the same composition of

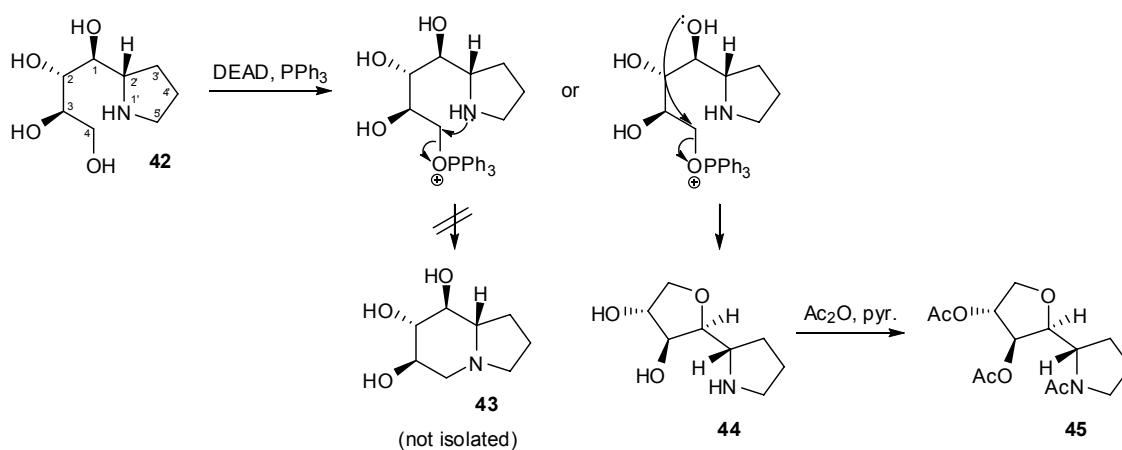
hydrocarbon groups. Notwithstanding, the chemical shifts of these units did change, but to unexpected ones. St. Denis and Chan demonstrated that in the C-6,7 acetonide of *ent*-1-deoxycastanospermine, and in several of its stereoisomers, the C-3 methylene ^{13}C NMR chemical shifts ranged from 51.1 to 52.6 ppm, while the corresponding C-5 methylene ^{13}C NMR chemical shifts ranged from 52.8 and 54.4 ppm (Figure 2.5).⁹⁸ Our ^{13}C DEPT NMR analysis of the major product showed no evidence of methylene resonances in either of these ranges. Unexpectedly, there was a relatively downfield methylene resonance at 71.8 ppm.

Please see print copy for Figure 2.5

Figure 2.5. C-3 and C-5 ^{13}C NMR (CDCl_3) chemical shifts (ppm) for a C-6,7 acetonide of *ent*-1-deoxycastanospermine and stereoisomers.⁹⁸

Clearly our data was not consistent with the literature and made us question whether we had actually made an indolizidine. A study of the mechanism of the Mitsunobu reaction was undertaken, which provided some explanation for the unexpected major product (Scheme 2.6). It was anticipated that the reaction of **42** would proceed via an attack of the pyrrolidine nitrogen onto C-4, liberating triphenylphosphine oxide, and giving the desired indolizidine **43**. It appeared that, without protecting groups on the hydroxyl groups attached to C-2, C-3 and C-4 of **42**, there was the availability for these groups to independently act as nucleophiles. Of these possibilities, the C-3 OH group was thought less likely to react, as this would result in a comparatively unfavourable epoxide. The same is true for the C-2 OH, as attack by this group would result in a four-membered cyclic ether. It is most likely that the C-1 OH would react at C-4 to give the tetrahydrofuran **44**.

Closer inspection of the NMR data of **45**, the major acetylated product indicated that **44** represented a valid structure. The unusually downfield methylene carbon (71.9 ppm) of **45** could be representative of C-5, due to it being directly bonded to an oxygen atom (Figure 2.6). The methylene resonance at 47.9 ppm would then be attributed to C-5' (Figure 2.6), which is relatively upfield compared to the corresponding C-3 resonances in Figure 2.6.



Scheme 2.6. Potential mechanisms of reacting **42** under Mitsunobu conditions.

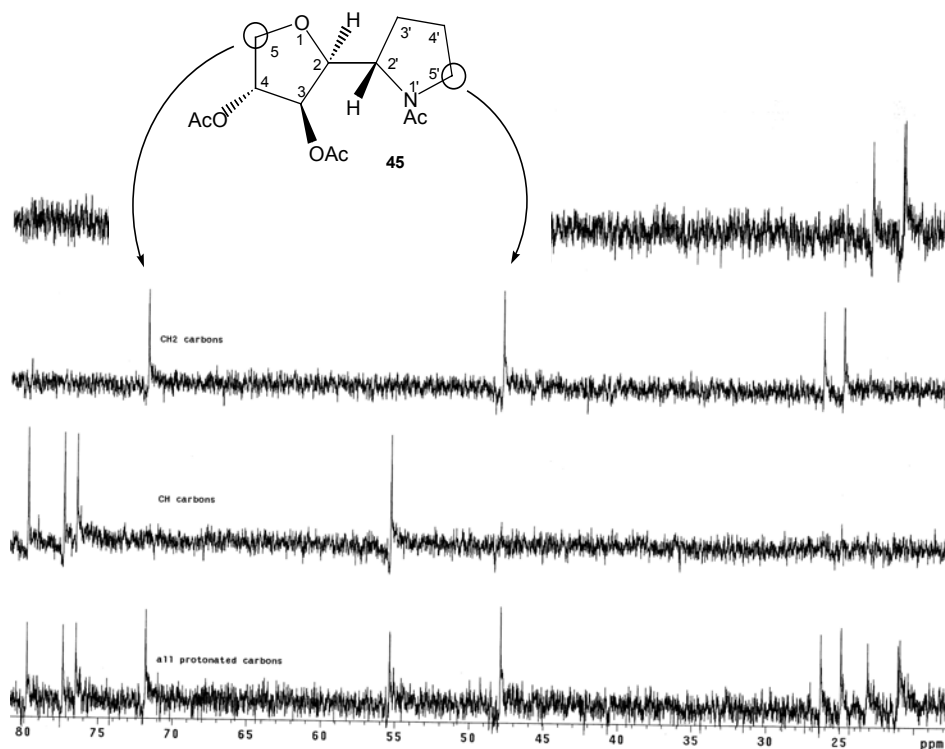


Figure 2.6. DEPT NMR spectrum (CDCl₃) of **45**.

The HSQC spectrum of **45** showed that the C-5 methylene protons resonated at 4.23 and 3.66 ppm, respectively, in the ¹H NMR spectrum. These had ‘dd’ multiplicity, and the gCOSY spectrum showed that they correlated to a methine proton with ‘ddd’ multiplicity at 5.04 ppm. H-4 was the obvious candidate for this proton and it correlated to another methine proton at 4.35 ppm, which was attributed to H-3. H-2 was then identified at 5.30 ppm by 1) its correlation to H-3; 2) the absence of a cross-peak with H-4; 3) its ‘dd’ multiplicity and 4) its

chemical shift, being the most downfield proton. The remainder of the ^1H NMR spectrum was assigned in a straightforward manner, and is shown in Figure 2.7.

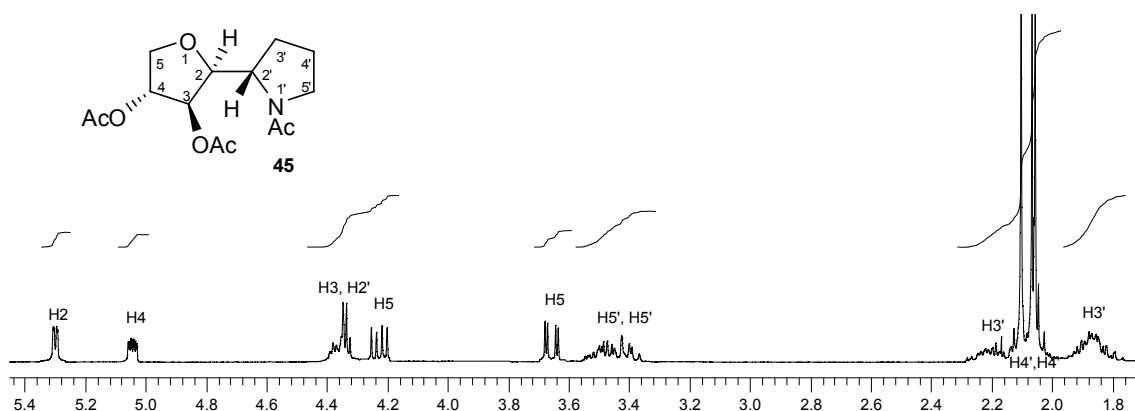


Figure 2.7. ^1H NMR spectrum (300 MHz, CDCl_3) of **45**.

The confirmation of **45** as the major product, demonstrated the problem of having unprotected secondary hydroxyl groups in the starting material. This is something that needed to be addressed in the subsequent attempt to synthesize **1** (see Chapter 3). However this model study served us well in several regards. Firstly, the Petasis reaction provided stereoselective access to the *anti*-1,2-amino alcohol **38**. Secondly, the subsequent RCM proved facile and high yielding. Thirdly, there were lessons learned about the highly polar characteristics of some of the products, particularly in regards to their purification.

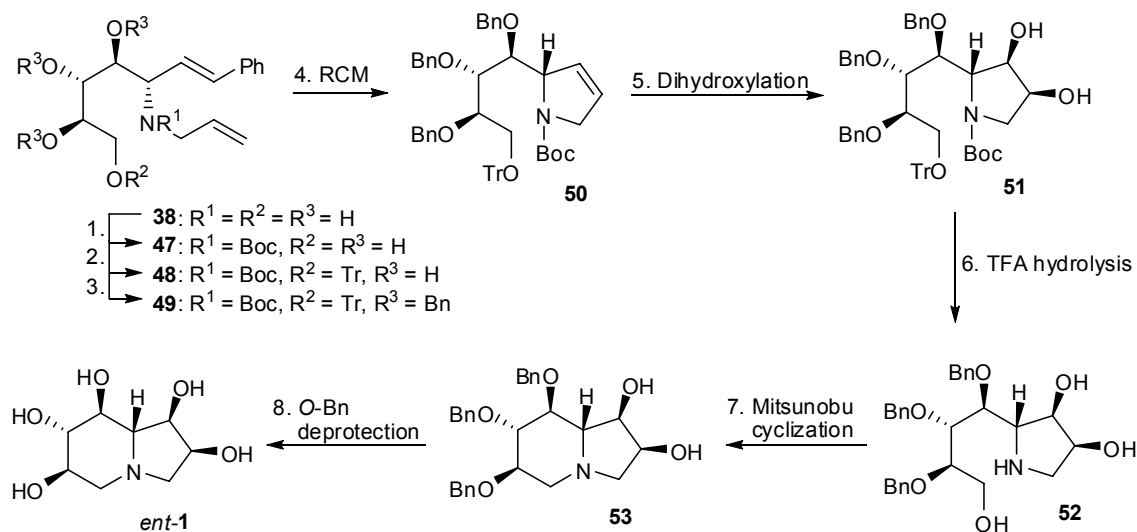
CHAPTER 3. Synthesis of **1**, the proposed structure of uniflorine A

Chapter 2 demonstrated that our planned synthesis of **1** as described in Scheme 1.5 required minor revision. In particular, a carefully considered protecting group strategy was needed; one that ensured that the protecting groups could be selectively introduced and removed. In particular, the secondary hydroxyl groups in Petasis product **38** required protecting (Scheme 3.1). These protecting groups would have to be stable to the same conditions that remove the nitrogen and primary alcohol protecting groups. Upon removal of these latter protecting groups, the resulting amino alcohol would be cyclized under Mitsunobu conditions. Hence, the problem encountered in Section 2.5 of a free secondary hydroxyl group participating in the Mitsunobu reaction would be avoided. Finally, all protecting groups in this synthesis would have to be stable to RCM and *cis*-dihydroxylation reactions, and the secondary hydroxyl protecting groups would have to be stable to Mitsunobu cyclization.

To fulfil this protecting groups strategy, we began by choosing the protecting groups for the nitrogen and primary hydroxyl (R^1 and R^2 respectively in Scheme 3.1). It was preferable to have both these groups labile to the same conditions, in the one-pot reaction. With this in mind, we chose a Boc protecting group for the nitrogen and a triphenylmethyl (trityl or Tr) for the primary hydroxyl. Both of these groups are normally cleaved under acidic conditions such as TFA hydrolysis, with the *O*-Tr group normally being more sensitive to acid than the *N*-Boc group.

Protecting the nitrogen was the logical first step, as it was the most nucleophilic functionality in **38**. The secondary amine in **38** was expected to react with di-*tert*-butyldicarbonate to give the carbamate **47**. However, there was also the possibility of the primary hydroxyl group in **38** also reacting with di-*tert*-butyldicarbonate to give a di-Boc protected product.

Next, the primary hydroxyl in **47** would be protected under basic conditions, using trityl chloride and pyridine. By imparting its low polarity onto the rest of the protected molecule, the trityl group would provide a clear benefit to the purification of all subsequent products that include it. Although, the trityl group has a drawback in that it adds a lot of redundant mass to the synthesis, thereby reducing atom efficiency. In terms of forming a trityl ether, the risk of the secondary hydroxyls in the Petasis product **38** reacting with trityl chloride was low, as the literature has demonstrated numerous times that trityl chloride is selective for primary hydroxyls over secondary ones.¹⁰⁷⁻¹¹³

Scheme 3.1. Proposed synthesis of *ent*-1.

This left us to decide upon the group to protect the secondary hydroxyl groups. It had to be stable to acid and go on under basic conditions. It also had to possess a relatively low degree of steric bulk, as there were three contiguous hydroxyls to protect, and be relatively non-polar, again making the product easier to purify. Taking these requirements into account, we chose the benzyl protecting group, which is installed under basic conditions and has the versatility of being stable to strong acid and base. Furthermore, its removal is typically achieved in a selective manner, by hydrogenolysis over a palladium catalyst.

This attempted synthesis of **1** would, like the model study, use D-xylose in the first step. The reason for this was cost concerns and that the protecting group and *cis*-dihydroxylation methodologies had not been tested. This would result in the final product being *ent*-1. However, as stated in Chapter 2, NMR spectroscopic data would not change between enantiomers. Confirmation of the final product would be made by comparing its spectroscopic data to that of the natural product, as reported by Matsumura *et al.*²³

3.1. Petasis reaction

The Petasis reaction was carried out using D-xylose **35a**, *trans*-2-phenylvinylboronic acid **36** and allylamine **37** as described previously in Section 2.1. The major departure from the earlier study was that the product had to be purified before *N*-protection. The option of simply per-acetylating the product, followed by subsequent purification, was not available. Ion-exchange chromatography provided a solution to this problem and an efficient purification of **38** was achieved. The best yield for the purified product was 94 %. A very clean ¹H NMR

spectrum of **38** was obtained (Figure 3.1). It clearly showed the requisite five aromatic and five olefinic protons downfield of 5.0 ppm, while the remaining eight protons were located between 3.0 and 4.0 ppm.

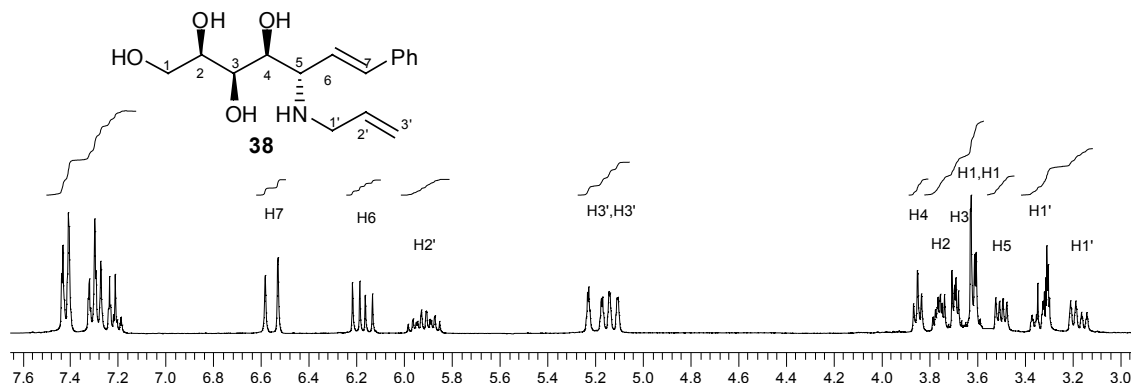


Figure 3.1. ^1H NMR spectrum (300 MHz, CD_3OD) of **38**.

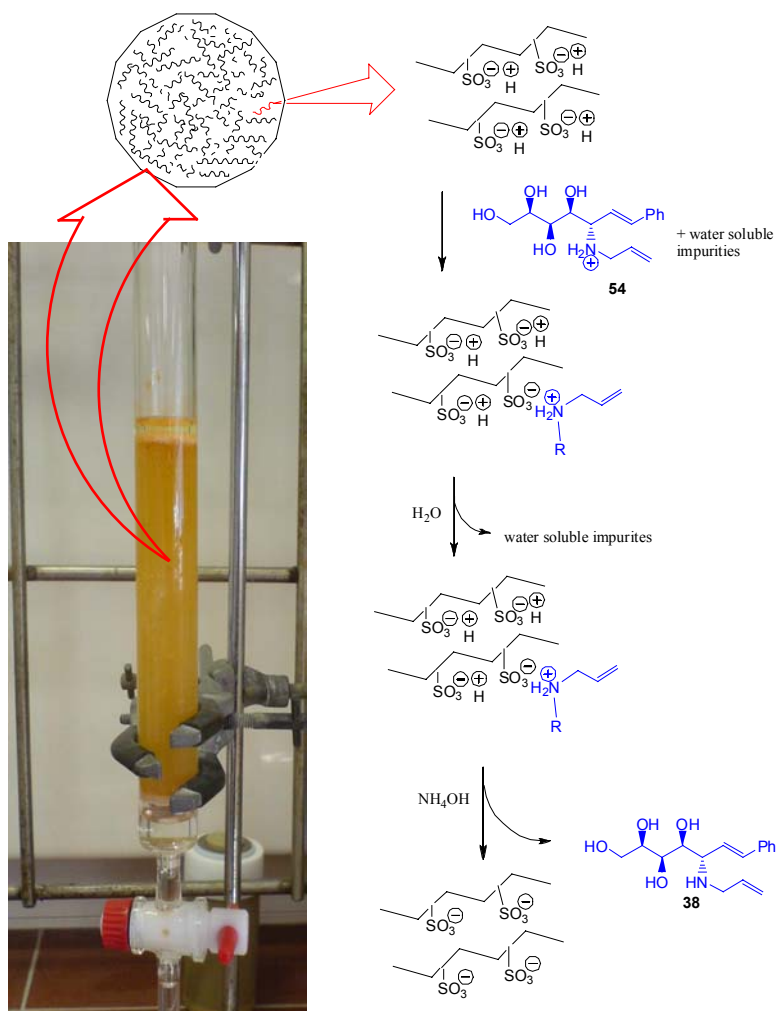
3.2. Ion-exchange chromatography

It might be helpful to divert a little and explain some of the principles behind ion-exchange chromatography. This explanation will give some reasons for the partial-binding of samples that was encountered several times in this project.

Ion-exchange resins are classified on the basis of their exchangeable counter-ion (cation exchanger or anion exchanger) and the ionic strength of the attached ion (strong exchanger or weak exchanger). The type of resin used in this part of the project was DOWEX 50WX4-50, a strong cation exchanger. Its constituent beads have a dense internal structure, with no discrete pores, and are referred to as a microporous resin. The beads are made from styrene and 4% of a cross-linking agent divinyl benzene, which controls porosity.¹¹⁴

Loading of the resin works by the solute ions diffusing through the bead particle to bind with exchange sites. Scheme 3.2 shows what that might look like in the case of purifying **38**. The manufacturer of DOWEX[®] (Dow Chemical Company) claimed that the 50W strongly acidic resin has a binding capacity of 4.2 meq / gram of resin.¹¹⁴ This means that for a mono-cationic species of **38** (**54**, Scheme 3.2), the mass of resin required for purification in grams, is equal to the number of millimoles of the sample divided by 4.2. The manufacturer also claimed that a resin bed is only 65 % efficient, therefore the answer above needs to be divided by 0.65 to get the quantity of resin required for purification. This formula was employed for all subsequent purifications of Petasis products. However it was not the only factor in preventing partial binding of sample.

After loading the sample, eluting an aliquot of water equal to three quarters of the resin-bed volume, following by resting the column for 20 min, resulted in the prevention of sample passing straight through. This is believed to facilitate a more even and widespread distribution of sample, giving more sample molecules the opportunity to interact with vacant binding sites.



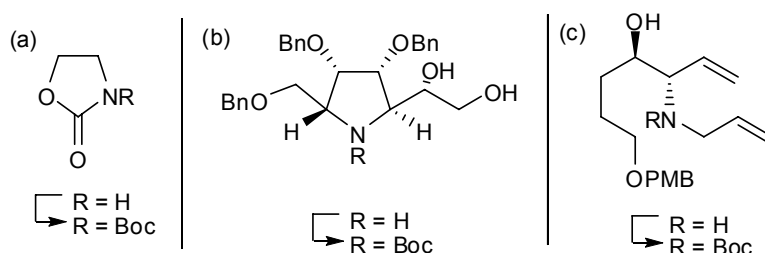
Scheme 3.2. Mechanism of acidic ion-exchange chromatography.

A similar strategy was used for eluting the product. Enough aqueous ammonia solution was applied to the column to render the whole resin basic ($\text{pH} > 14$). After resting the column for 10 min, to ensure that all of the bound amine was converted to its neutral form, the product was eluted off with more aqueous ammonia solution.

Cleaning the resin was achieved by washing with methanol, and reactivation by washing with 1M HCl. It was then decanted into a flask for storage, ensuring that the resin was completely immersed in acid. This cleaning and regeneration procedure allowed for repeated usages of the one quantity of resin, an important factor given its relative high cost.

3.3. *N*-Boc protection

With clean amino alcohol **38** in hand, the next step was to protect the nitrogen with a Boc protecting group. A literature search provided several procedures. Ishizuka *et al.*¹¹⁵ protected an oxazolidinone nitrogen with a Boc group using Boc₂O, Et₃N and catalytic DMAP (Scheme 3.3a). Saotome *et al.*¹¹⁶ published another example, more closely aligned with our project. Their substrate was a pyrrolidine with a C-2 side chain containing a primary and a secondary hydroxyl group, and the protection of the pyrrolidine nitrogen was carried out using Boc₂O and Et₃N, with dichloromethane (DCM) as the solvent, giving a 72 % yield (Scheme 3.3b). No mention was made about the primary hydroxyl group reacting with Boc₂O. Perhaps the most analogous example of *N*-Boc protection came from our own laboratory, with PhD student Karl Lindsay protecting a 1,2-*N*-allylamino alcohol, using Boc₂O and Et₃N in THF (Scheme 3.3c).²⁴

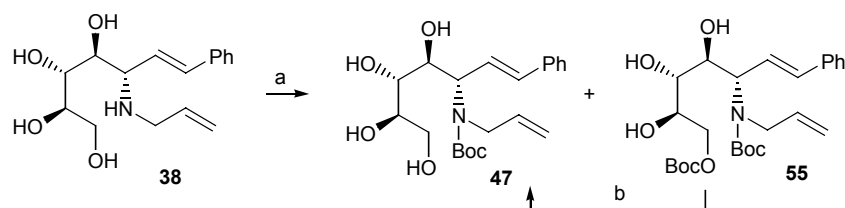


Reagents and conditions: (a) Boc₂O, Et₃N, DMAP; THF, rt, 3 h, 97 %;¹¹⁵
 (b) Boc₂O, Et₃N, DCM, rt, o/n, 72 %;¹¹⁶ (c) Boc₂O, Et₃N, THF, rt, 24 h, 98 %.²⁴

Scheme 3.3. Selected literature procedures for *N*-Boc protection.

Taking these literature examples into consideration, we initially selected 1.1 equiv. of Boc₂O and 1.1 equiv. of Et₃N for the *N*-Boc protection of **38**. DMAP was omitted, in the belief that activating the acylating reagent would increase its reactivity towards the primary hydroxyl group. Initially, dry CH₃CN was used as solvent, as it was assumed that DCM and THF would not dissolve the highly polar starting material. While CH₃CN quickly dissolved the reagent and base, a large volume was required to dissolve the starting material. Adding a small volume of dry DMF remedied this problem.

The best yield for this reaction was 67 %, using 9:1 ratio of CH₃CN to DMF, and 1.75 equiv. of both the reagent and base. This was an exception though, as most yields were between 50 and 60 %. The moderate yields can be attributed to a significant amount of di-Boc protected **55** being formed (Scheme 3.4). Fortunately, the di-Boc compound was easily converted to **47** by base hydrolysis giving a 77 % yield over two steps.



Reagents and conditions: (a) (Boc)₂O, Et₃N, MeCN, DMF, rt, 24 h, **47** (67 %) and **55** (18 %);
(b) K₂CO₃, MeOH, rt, 3 d, 58 %.

Scheme 3.4. Synthesis of *N*-Boc product **47**.

The ¹H NMR analysis of **47** displayed significant peak broadening, presumably caused by restricted rotation about the *CO-N* bond of the carbamate group (Figure 3.2). Intriguingly, peak broadening was not observed with the *N*-acetylated Petasis product **40** (Figure 2.1), suggesting that the energy barrier for rotation about the *CO-N* bond might be less in *N*-Ac protected **40** than the more sterically demanding *N*-Boc protected **47**.

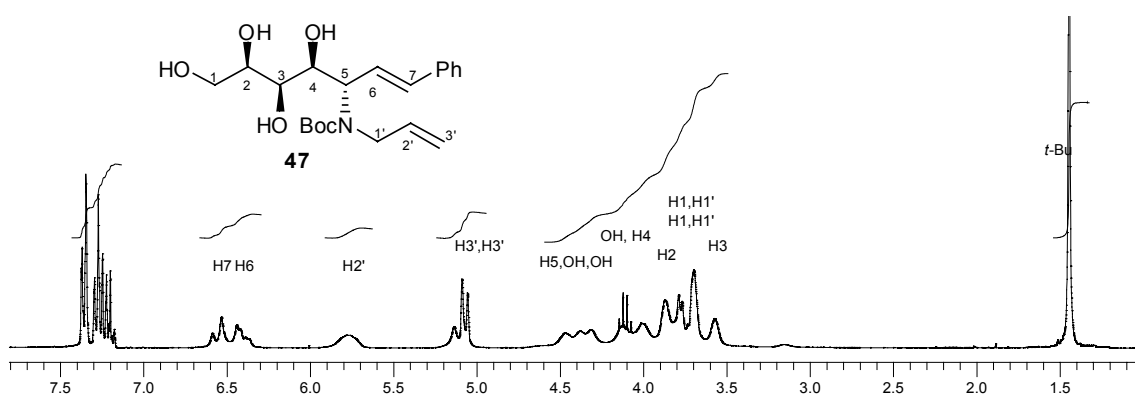
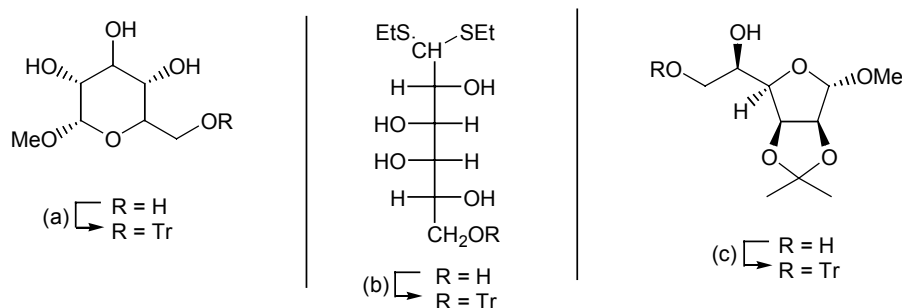


Figure 3.2. ¹H NMR spectrum (300 MHz, CDCl₃) of **47**, showing peak-broadening.

3.4. *O*-Tr protection

The next step in Scheme 3.1 was to protect the primary hydroxyl in **47** with a trityl group. Chaudhary *et al.* converted an α -methylglucoside to its corresponding mono-trityl ether (Scheme 3.5a).¹¹⁰ In the same paper it was demonstrated that trityl protection of the secondary alcohol, 4-*tert*-butyl-cyclohexanol, occurred only after heating it at reflux in DCM. However, this phenomenon was not observed by Barton's group when they selectively *O*-Tr protected a D-galactose dithioacetal at 70 °C over 4 h, using pyridine as both base and solvent (Scheme 3.5b).¹⁰⁸ Similarly, but without heating and the addition of DMAP, Berges *et al.* selectively *O*-Tr protected a mannofuranose derivative in good yield (Scheme 3.5c).¹⁰⁹



Reagents and conditions: (a) TrCl, Et₃N, DMAP, DMF, rt, 12 h, 88 %;¹¹⁰
 (b) TrCl, C₅H₅N, DMAP, 70 °C, 4 h, 84 %;¹⁰⁸ (c) TrCl, C₅H₅N, rt, 12 h, 83 %.¹⁰⁹

Scheme 3.5. Selected literature procedures for *O*-Tr protection.

The method we used initially for the *O*-Tr protection of **47** was based on Barton's, using pyridine as both solvent and base, with a substantial excess of TrCl, and catalytic DMAP (Table 3.1). This best yield of **48** using this method was 84 %. The reaction was also tried using the above conditions but at rt, and the yield dropped off sharply (entry 2, Table 3.1). Other experiments were tried at rt but without DMAP, giving good yields (entries 3-4, Table 3.1). Reaction times were not optimized, but in each reaction TLC analysis indicated the complete consumption of starting material.

Table 3.1. Results of the *O*-Tr protection of **47**.

entry	TrCl (equiv.)	DMAP (equiv.)	temp.	time	yield (%)
1	2.2	0.1	70 °C	3 d	84
2	2.0	0.1	rt	1 d	55
3	2.0	0.0	rt	1 d	81
4	2.0	0.0	rt	18 h	72

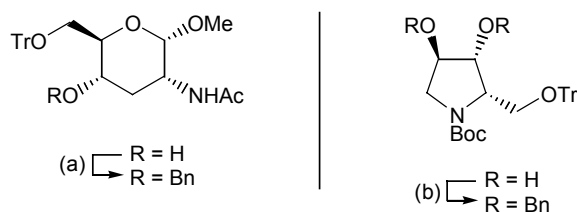
$\begin{cases} \text{47: } R = H \\ \text{48: } R = Tr \end{cases}$

Note: all reactions were performed in dry pyridine

¹H NMR analysis of the product showed only slight differences from the starting material, except for an increase in the integration of aromatic resonances. The C-1 methylene protons shifted slightly upfield, from 3.78-3.69 ppm (m) in **47** to 3.37 ppm (dd) and 3.19 ppm (dd) in **48**. A more obvious difference was found in the ¹³C NMR spectrum, with the quaternary aliphatic carbon of the trityl group resonating at 86.9 ppm. This would become a distinct marker of all subsequent *O*-Tr protected compounds.

3.5. *O*-Bn protection

O-Bn protection of **48** was based on literature procedures by Kanai *et al.*¹¹⁷ and Ikota¹¹⁸ (Scheme 3.6). Both of these procedures included starting materials that contained *O*-Tr protected primary alcohols, with Ikota's substrate also containing a *N*-Boc protected pyrrolidine ring, making it a reasonably close analogue of our starting material.



Reagents and conditions: (a) NaH, BnBr, *n*Bu₄NI, DMF, 99 %;¹¹⁷ (b) NaH, BnBr, THF, DMF, 80 %.¹¹⁸

Scheme 3.6. Selected literature procedures for *O*-Bn protection.

The conditions we selected included BnBr, catalytic *n*Bu₄NI (10 mol %), NaH and dry THF. In the event, NaH (60 % dispersion in mineral oil) was initially added to a solution of **48** in dry THF at 0 °C. After waiting for the cessation of H₂ gas evolution (ca. 5-10 min), BnBr was added, together with *n*Bu₄NI, and the reaction was left to stir at rt. After 6 h, TLC analysis of the reaction showed that the starting material was completely consumed. However, it also showed three new spots of lower polarity. The least polar spot we assumed to be the desired tri-*O*-benzylated product **49**. The other two spots were of similar *R_f* and only slightly less polar than the starting material. We assumed these to be mono- and di-*O*-benzylated products and we therefore left the reaction to stir overnight, hoping that it would be complete by morning. However TLC analysis in the morning showed the same distribution of spots. We were sure that the amount of reagents in the reaction was of sufficient excess to warrant complete reaction, even if there was a trace of water present.

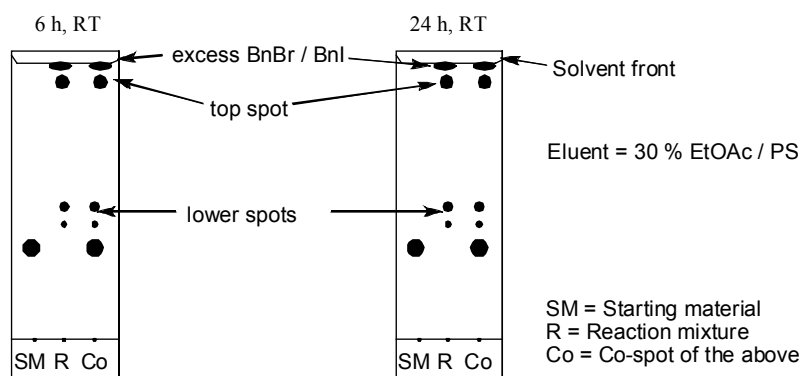


Figure 3.3. TLC analyses of the *O*-benzylation of **48** at 6 h and 24 h.

Therefore, the reaction was worked-up, followed by FCC of the crude product, which separated the three components. NMR and MS analyses of the top spot confirmed it to be the desired product **49**. However, the yield of **49** was only 34 % while the combined mass of the side-products was greater than the mass of the desired product.

Several pieces of evidence led to the identification of the two side-products. Herein, the side-product with the higher R_f shall be referred to as side-product 1 and the other one, side-product 2. The first clue was that the ^1H NMR spectra for each of these compounds were unexpectedly sharp. Intuitively, the elimination of peak broadening could be explained by the loss of the Boc group. Indeed, there were no methyl resonances representative of the *tert*-butyl group in the upfield region of the ^1H NMR spectra of either side-product. However, a carbonyl resonance was present in each of the ^{13}C NMR spectra. These carbonyl peaks had different chemical shifts to the carbonyl resonance of the starting material. In fact, all previously synthesized compounds with a *N*-Boc group had a consistent carbonyl chemical shift of 156.4 ± 0.1 ppm (Table 3.2) including the desired product **47** and over-protected product **55** from the *N*-Boc protection reaction of Petasis product **38**, and the *O*-Tr protected derivative of **47**, compound **48**. The ^{13}C NMR carbonyl chemical shifts of side-product 1 and side-product 2 were 157.2 ppm and 152.8 ppm, respectively. Clearly the carbonyl moiety present in both side-products was not the same as the one present in the *N*-Boc group of the abovementioned precursors.

Table 3.2. Comparison of carbonyl ^{13}C NMR chemical shifts between benzylation side-products and starting materials (CDCl_3 , 75 MHz).

compound	$\delta^{13}\text{C}$ for C=O in <i>N</i> -Boc moiety (ppm)
47	156.4
55	156.5
48	156.4
side-product 1	157.2
side-product 2	152.8

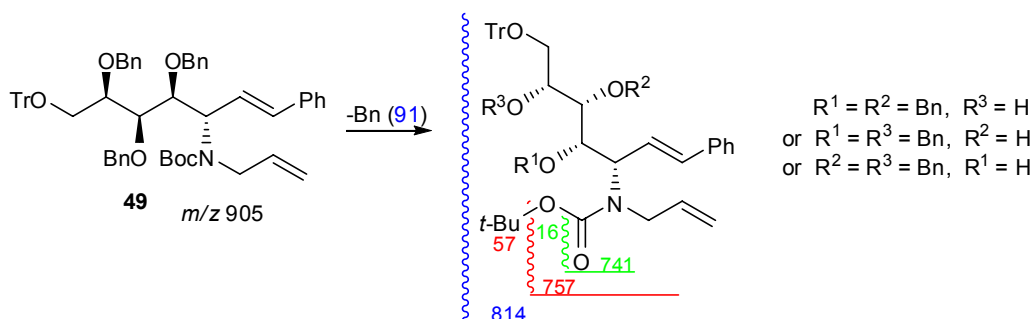
To reiterate, the side-products were thought to be mono and di-*O*-benzylated products. According to 1D and 2D NMR analyses, both side-products were in fact di-*O*-benzylated. Two of the benzylic ^{13}C NMR chemical shifts were similar between the products (71.1 ppm for side-product 1 and 71.2 ppm for side-product 2) but their associated methylene protons had quite different ^1H NMR chemical shifts (Table 3.3). Perhaps more remarkable was that one of the benzylic protons in side-product 2 had a ^1H NMR chemical shift of 3.56 ppm, which was relatively upfield for benzylic protons to resonate.

Table 3.3. NMR chemical shifts for benzylic units in side-products 1 and 2.

side-product	¹³ C (ppm) NMR chemical shift	¹ H (ppm) NMR chemical shifts
1	74.7	4.82, 4.63, <i>J</i> = 11.1 Hz
	71.1	4.64, 4.17, <i>J</i> = 12.2 Hz
2	73.6	4.84, 4.70, <i>J</i> = 11.4 Hz
	71.2	4.24, 3.56, <i>J</i> = 11.0 Hz

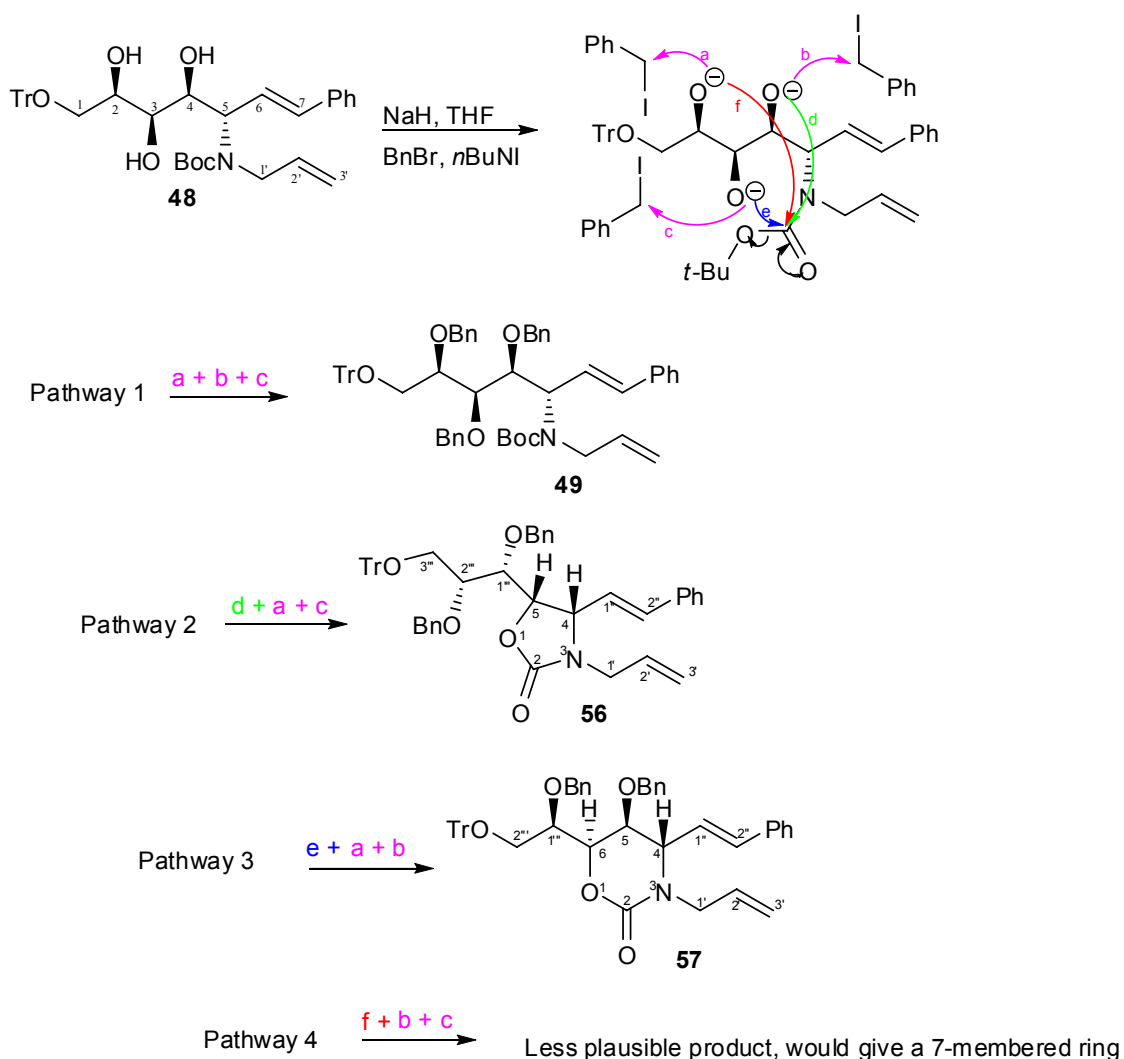
¹³C NMR (CDCl₃, 75 MHz); ¹H NMR (CDCl₃, 300 MHz)

LRMS analysis of the side-products showed that both had a molecular weight of 741, which allowed the yields of side-products 1 and 2 to be calculated as 23 % and 15 %, respectively. The desired product had a mass of 905. Loss of one benzyl group (91 Da) from 905 Da equals 814 Da, and loss of a *tert*-butyl cation (as evidenced by ^1H NMR analysis) reduced the theoretical mass to 757 Da. This left a difference of ^{16}O from the molecular weight of the side-products. Thus, the molecular weight of the side-products (741 Da) indicated that during the benzylation, only two benzyl groups had attached and there had been a loss of a *tert*-butoxide group (Scheme 3.7).



Scheme 3.7. Characterization of side-products 1 and 2 by LRMS.

Two products that fulfilled the NMR and MS data were the oxazolidinone **56** and oxazinanone **57** (Scheme 3.8). The analogous 7-membered ring derivative involving cyclization of the C-2 hydroxyl, would seem less likely due to a larger entropy of cyclisation. Mechanisms of the formation of **49**, **56**, and **57** are shown in Scheme 3.8.



Scheme 3.8. Possible reaction pathways for the *O*-benzylation of **48**.

Upon examination of the oxazolidinone and oxazinanone structures, it was clear that the most downfield non-aromatic proton would be the one α to the ring oxygen (H-5 in oxazolidinone **56** and H-6 in oxazinanone **57**). In the course of characterising these compounds this proton became the ‘anchor’ proton, one that could provide a reference point for subsequent proton assignments. This proton should couple to H-4 and H-1''' in **56** (to give a dd) and to H-5 and H-1''' in **57** (to give a dd). Therefore, identifying each side-product on the basis of their anchor proton multiplicity was not possible. Nonetheless, it was obvious where H-1''' was in each spectrum, the second most downfield non-aromatic proton, with ‘dd’ multiplicity. From the gCOSY spectrum, it was a straightforward process to assign H-4 in each compound, based on its strong coupling to H-1'''.

Due to the vicinal relationship of H-4 and the anchor proton in the oxazolidinone, it became clear that if there were a strong coupling between these two protons in the gCOSY

spectrum, the parent compound would be an oxazolidinone. Alternatively, the oxazinanone does not have a vicinal arrangement between H-4 and its anchor proton; therefore a lack of coupling between these two protons in the gCOSY spectrum would confirm its structure. This logic held true and the remaining characterization of each side-product was swiftly achieved. Side-product 1 was assigned as oxazolidinone **56** (Figure 3.4), while the slightly more polar side-product 2 was assigned as oxazinanone **57** (Figure 3.5).

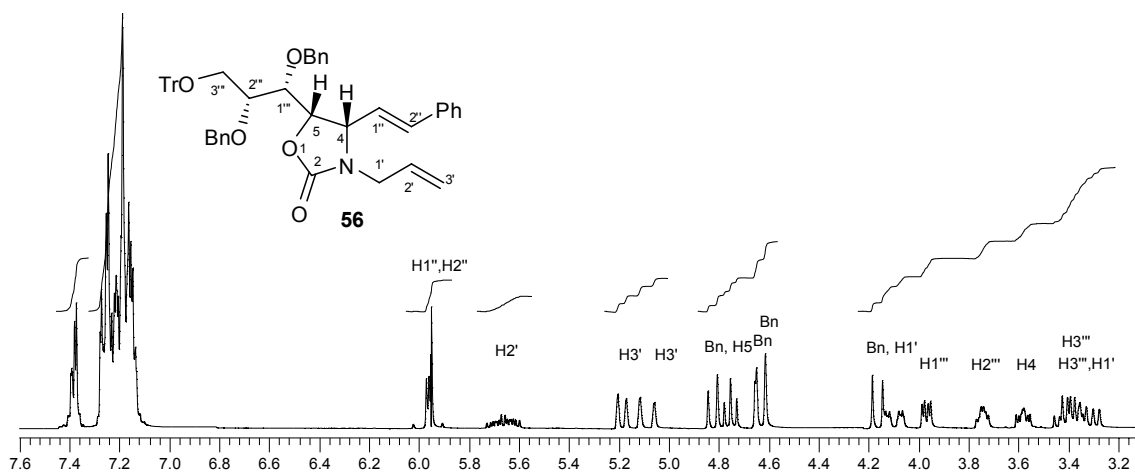


Figure 3.4. ^1H NMR spectrum (300 MHz, CDCl_3) of oxazolidinone **56**.

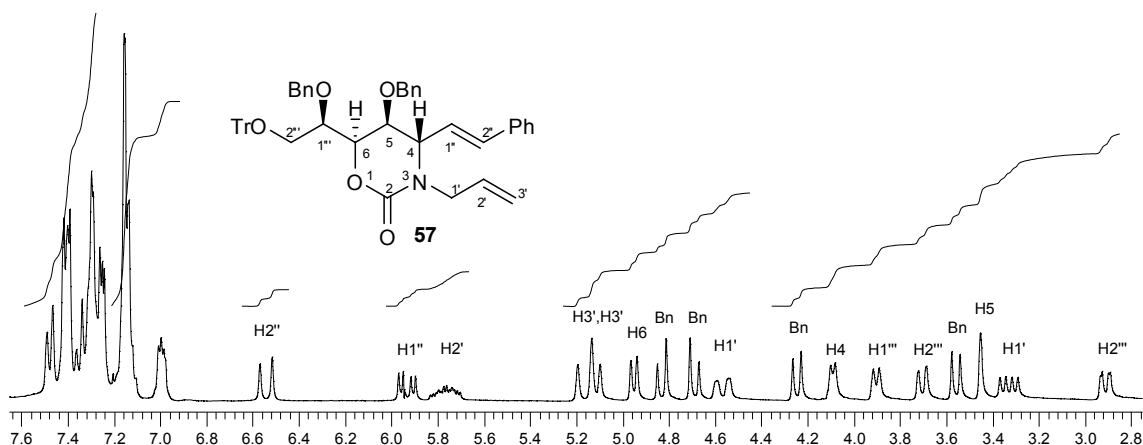
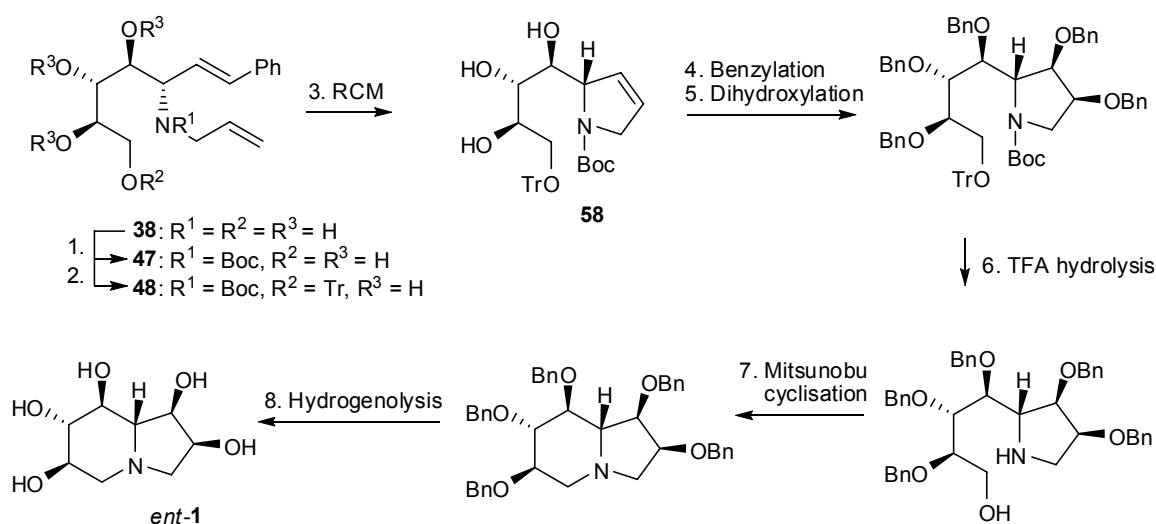


Figure 3.5. ^1H NMR spectrum (300 MHz, CDCl_3) of oxazinanone **57**.

The benzylation of **48** yielded 34 % of the desired tri-*O*-benzylated product **49**, 23 % oxazolidinone **56** and 15 % oxazinanone **57**. Such a low yield of the desired material meant that a review of the synthetic plan for the synthesis of **1** in Scheme 3.1 was necessary. As novel and interesting as they were, compounds **56** and **57** were put aside. Their usefulness would become apparent later in this project.

The next step (Scheme 3.1) was a RCM reaction to form a pyrrolidine ring. There was no specific reason for putting this step after the *O*-benzylation of **48**. While the secondary

hydroxyl groups had to be protected at some stage before the final ring-closure, there was some degree of flexibility in what synthetic stage that could take place. Therefore we changed the order of synthesis to include the RCM step before *O*-benzylation. We speculated that having the *N*-Boc as part of a pyrrolidine ring would reduce the likelihood of further ring formation in the *O*-benzylation reaction, since the resulting bicyclic products would be more highly ring strained. The revised synthetic scheme is shown below (Scheme 3.9).

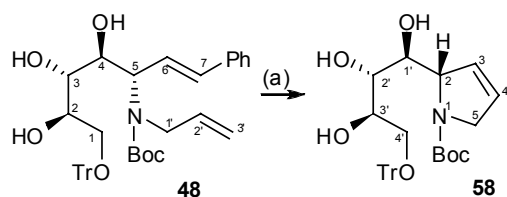


Scheme 3.9. Revised synthetic route to *ent*-1.

3.6. Ring-closing metathesis

The RCM reaction was consistently high yielding in the model study, albeit with a substrate that had all its functional groups protected. The difference now with substrate **48** was the lack of protection afforded to the secondary hydroxyl groups. We did not envisage a problem with unprotected oxygen moieties as the literature contains many examples of RCM reactions performed on such substrates.¹¹⁹⁻¹²⁵

There were two constants in all of the experiments, heating at reflux and catalyst loading (10 mol %) (Table 3.4). The average yield of **58** was 82 % and the highest was 96 %. Reactions were not optimized, although TLC analyses showed that the reactions took at least 8 h to complete. The reactions summarised in entries 3 and 4 of Table 3.4 did not take any longer to complete, they were left longer before having the opportunity to work them up. Due to an insufficient availability of dry DCM, a much more concentrated reaction mixture was used in entry 4, yet the yield did not suffer in comparison to the average and there were no cross-metathesis products detected.



(a) 10 mol % Grubbs' I cat. DCM, reflux

Table 3.4. Results of the RCM of reaction of **48**.

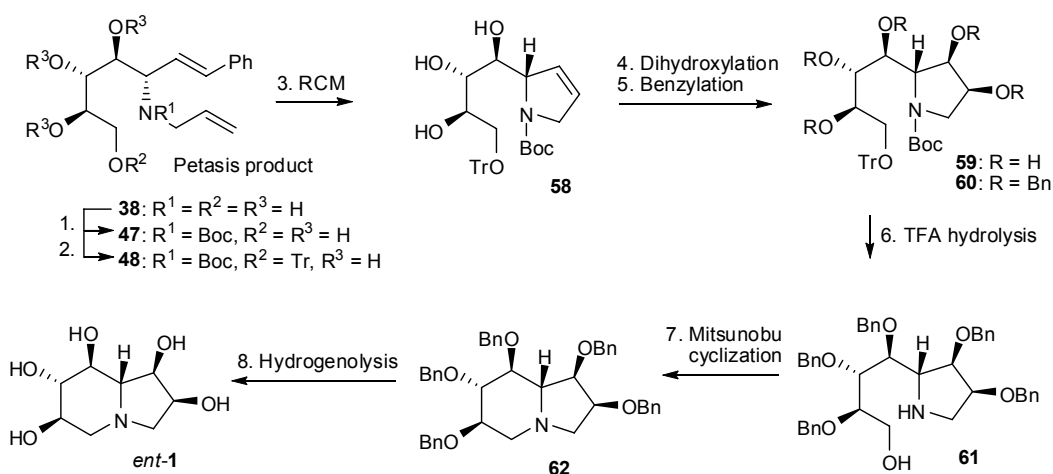
entry	time	conc. (mM)	yield (%)
1	24 h	7	81
2	24 h	8	96
3	3 d	7	82
4	2 d	13	82

As in the model study, the success of this reaction was indicated from ^1H NMR analysis by reduction in the number of olefinic protons from five to two. The effect of ring-closure was also to shift downfield the ^1H and ^{13}C NMR chemical shifts of the methylene and methine hydrocarbon units, α to the nitrogen atom (Table 3.5).

Table 3.5. NMR chemical shifts (CDCl_3) of hydrocarbon units α to the nitrogen in **48** and **58**.

	48	58	48	58
δ ^1H (ppm)	H-5 4.42	H-2 4.67	H-1' 3.78-3.69	H-5 4.22, 3.98
δ ^{13}C (ppm)	C-5 54.3	C-2 67.2	C-1' 48.9	C-5 60.2

At this point, we decided not to proceed with the *O*-benzylation of **58** as outlined in Scheme 3.9, instead preferring to dihydroxylate this compound first, followed by per-*O*-benzylation of the resulting pentaol. The advantage of this change was that after TFA cleavage of the *N*-Boc and *O*-Tr protecting groups, a penta-*O*-benzylated amino alcohol would be produced, instead of the more polar tri-*O*-benzylated amino triol. Hence, another revised synthetic scheme was drawn up (Scheme 3.10).

**Scheme 3.10.** Further revised synthetic route to *ent*-1.

3.7. Dihydroxylation

The method chosen for the *cis*-dihydroxylation of **58** was a standard Upjohn⁸⁹ process. From this reaction we required a product that had a newly installed diol moiety *anti* with respect to the C-2 polyhydroxylated butyl side chain. In the event, *cis*-dihydroxylation of **58** was consistently high yielding but slow, taking at least 2 d to finish (Table 3.6).

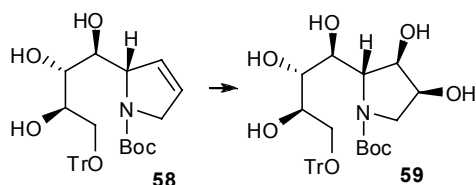


Table 3.6. Results of the dihydroxylation of **58**.

entry	time	yield	d.r.
1	3 d	79 %	100:0
2	2 d	75 %	100:0

Reagents and conditions: 5 mol % $K_2OsO_4 \cdot 2H_2O$, 2.1 equiv. NMO, 1:1 acetone / water, RT.

Remarkably, all dihydroxylation experiments were 100 % diastereoselective. The 1H NMR spectrum of pure **59** was poorly resolved, again due to the influence of the *N*-Boc group. Peaks were very broad and there were several overlapping proton resonances. Thus, using NOSEY NMR to determine the relative stereochemistry of the diol was impractical. We assumed at the time that selectively was in favour of the desired 2,3-*anti*-configuration.

There are reports that the addition of ligands such as pyridine, accelerate the rate of the osmylation of olefins.¹²⁶⁻¹²⁸ However, when our fellow co-worker Karl Lindsay tried adding pyridine to a slow dihydroxylation of a relatively similar substrate, it decreased the diastereoselectivity and actually increased the reaction time.²⁴ Not wanting to risk a reduction in diastereoselectivity, we forwent any attempt to accelerate the dihydroxylation reaction of **58**.

3.8. *O*-Benzylation

O-Benzylation of **59** was carried out using the same conditions that produced oxazolidinone **56** and oxazinanone **57** (Table 3.7).

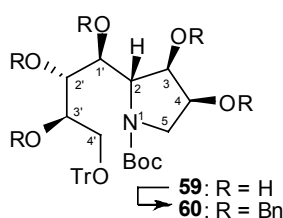


Table 3.7 Results of the *O*-benzylation of **59**.

entry	time	temp.	yield
1	3 d	rt	80 %
2	18 h	60 °C	81 %

Reagents: NaH (60 %, 5.5 eq), BnBr (10 eq), nBu_4NI (10 mol %), THF (0.16 M).

Gratifyingly, the reaction gave excellent yields of the penta-*O*-benzylated product **60**, with no oxazolidinone or oxazinanone detected. The first experiment was left for 3 d at rt, giving complete conversion of the starting material by TLC analysis, and only one product spot. When the reaction was heated to 60 °C, the reaction was complete after 18 h.

A problem with this reaction was that the product gave an exceptionally poor ¹H NMR spectrum. Not only were the peaks broad, there were also two rotameric sets of resonances present. As expected, there was an increase in the ratio of aromatic to non-aromatic protons, as indicated by the integration. However, given the presence of rotamers, it was too difficult to obtain a precise number for the aromatic protons. In fact, the spectrum was so poor that the non-aromatic protons were assigned in regions of multiplets. The ¹³C NMR spectrum also illustrated two rotamers. However, in conjunction with a DEPT spectrum, the resolution was good enough to confirm the requisite numbers of carbon units for **60**. Mass spectrometry also helped to confirm the product by producing a *m/z* peak of 1016 (ESI +ve), equal to the molecular ion (M + H⁺).

Thankfully, our strategy of locking the *N*-Boc moiety into a pyrrolidine ring worked. As a bonus, it exceeded our expectations by not just reducing the formation of oxazolidinone and oxazinanone products, but by preventing their formation altogether.

3.9. *O*-Tr and *N*-Boc deprotection

It was anticipated that the *N*-Boc and *O*-Tr protecting groups would be cleaved together in a one-pot reaction, under acidic conditions. TFA was selected as the acid, in DCM, with anisole added to capture the liberated trityl cation.

In the event, something unexpected happened. After 2 h of stirring at rt, the reaction was checked by TLC analysis. It showed complete consumption of the starting material but there were three new spots (Figure 3.6). There was a much more polar spot, which was assumed to be the desired amino alcohol product **61**. A spot at the solvent front, very non-polar and intensely UV active, was assumed to be a trityl-anisole adduct. However there was another spot, slightly more polar than the starting material, which from herein will be referred to as the side-product.

FCC readily separated all three products, and NMR analysis of the least polar spot confirmed it to be a trityl-anisole adduct. Similarly, NMR and MS analysis of the most polar spot confirmed it to be the desired amino alcohol. However the yield was only 44 %. The yield of the side-product by mass was two thirds of the desired product, which compelled its structural elucidation.

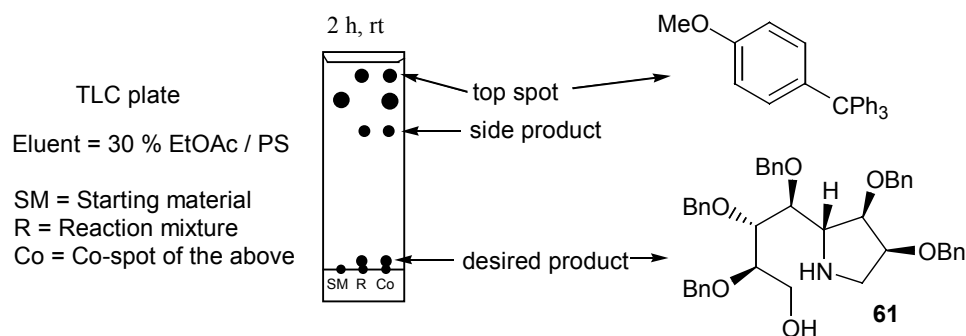


Figure 3.6. TLC analysis of the TFA mediated deprotection of *N*-Boc and *O*-Tr groups.

Comparison of the NMR data between the side-product and the desired product yielded some clues. Both products had similar NMR data. In particular, 2D NMR analysis of the side-product showed that it had the same number of hydrocarbon units as the desired product, including 5 benzyl groups, 2 methylene groups and 6 methine groups. However it did not have a broad singlet at 2.66 ppm, integrating for two protons, which was assigned to NH and OH protons in **61**. This was a telltale sign, as the obvious reason for the absence of these heteroatom protons is due to cyclization of the amino alcohol, resulting in the net loss of water. The $M + 1^+$ (CI +ve) ion for the amino alcohol **61** had a m/z of 674, while the same ($M + 1^+$) ion for the side-product had a m/z of 656, thus giving a difference of 18 Da, equal to water. Therefore, it was concluded that the side-product of this reaction was the indolizidine **62** of the next planned reaction in Scheme 3.9. The fully assigned ^1H NMR spectra for the amino alcohol **61** and for the cyclized product **62** are shown in Figures 3.7 and 3.8, respectively.

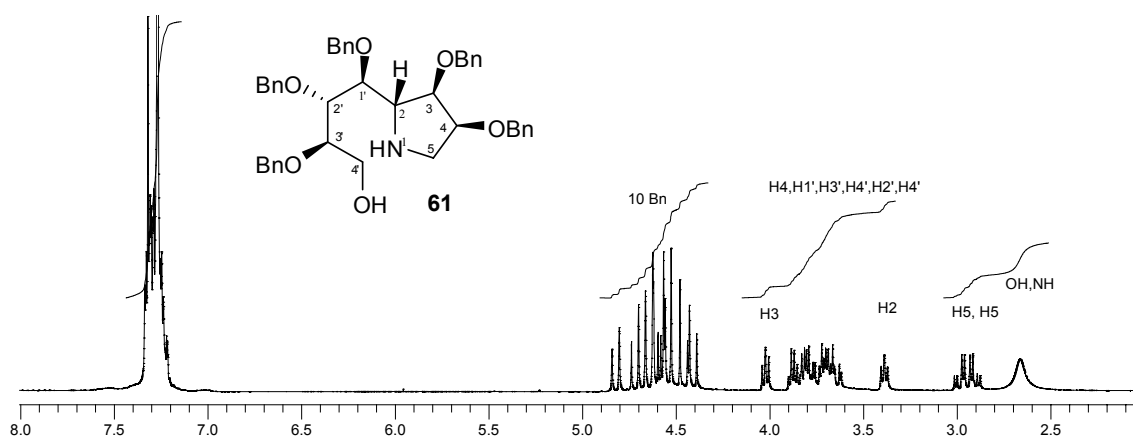


Figure 3.7. ^1H NMR spectrum (300 MHz, CDCl_3) of **61**.

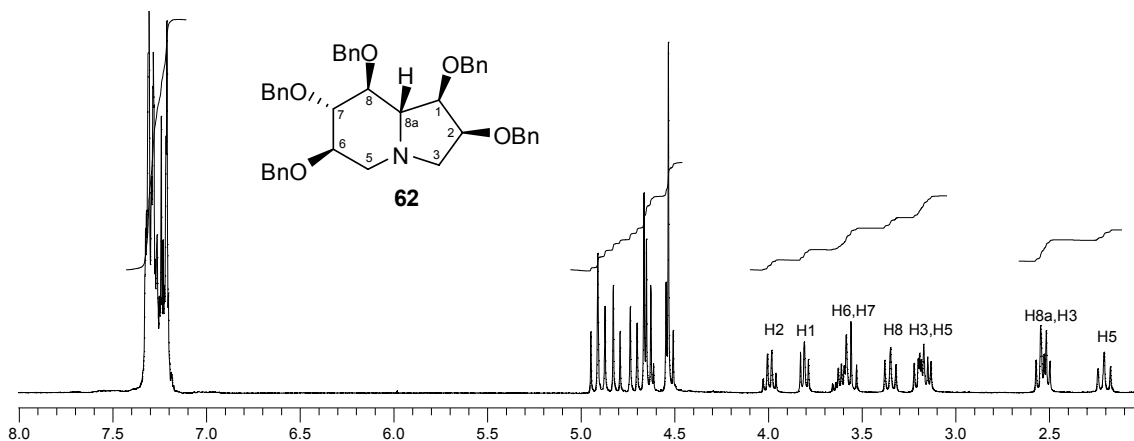
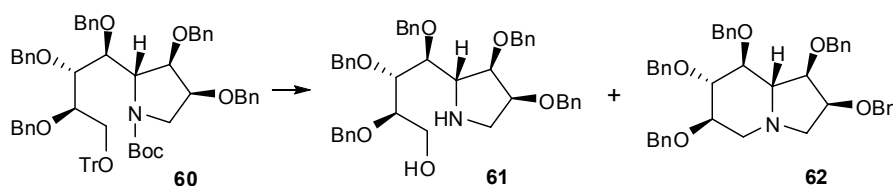


Figure 3.8. ^1H NMR spectrum (300 MHz, CDCl_3) of **62**.

In the end, this first reaction yielded 44 % of **61** and 34 % of **62** (Table 3.8). When the reaction was repeated at a larger scale (0.333 mmol of **60**) a similar result occurred, although the ratio of **61** to **62** increased to 1.6:1. Interestingly, when the reaction was tried without anisole the ratio increased even further to 2:1, although the combined yield decreased.

The reaction was also conducted at 0 °C for 1 h, in which TLC analysis indicated yet another side-product. Once isolated, it was identified as the mono-deprotected *O*-Tr derivative **63** (Figures 3.9 and 3.10). Obtaining such a product would seem to indicate that the *N*-Boc group was removed first under TFA conditions, a rather counter-intuitive proposition given the highly labile nature of *O*-Tr ethers under acidic conditions. Furthermore, it was unlikely that liberated trityl cation would reattach to the primary alcohol, given the excess of anisole present.

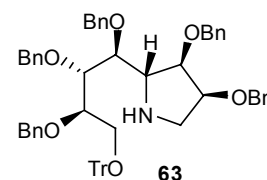
Table 3.8. Results of TFA mediated deprotection of *N*-Boc and *O*-Tr groups in **60**.



Reagents: TFA (115 eq), DCM (0.15 M); other reagents and conditions, see below.

entry	scale (g, mmol)	PhOMe (equiv.)	temp.	time	yield 61	yield 62	61:62
1	0.075, 0.074	10	rt	2 h	44 %	34 %	1.3:1
2	0.338, 0.333	10	rt	2 h	55 %	35 %	1.6:1
3	0.220, 0.221	0	rt	2 h	40 %	20 %	2.0:1
*4	1.500, 1.478	10	0 °C	1 h	37 %	9 %	4.1:1

* 19 % of the mono-deprotected material **63** was also isolated. →
(see Figures 3.9 and 3.10.)



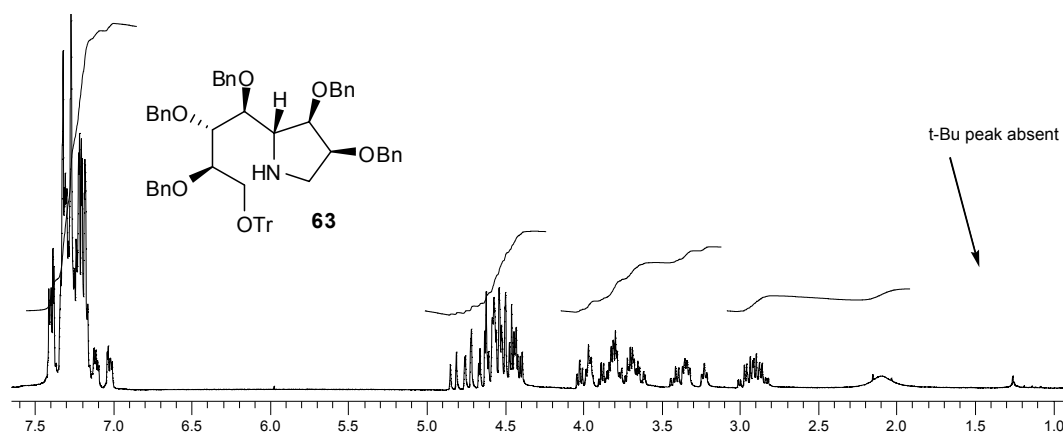


Figure 3.9. ^1H NMR spectrum (300 MHz, CDCl_3) of mono-protected *O*-Tr derivative **63**.

When the mono-deprotected *O*-Tr derivative **63** or the fully deprotected amino alcohol **61** was re-treated with TFA and anisole at rt for 2 days, a poor yield of **62** (< 5 % from ^1H NMR analysis) was obtained.

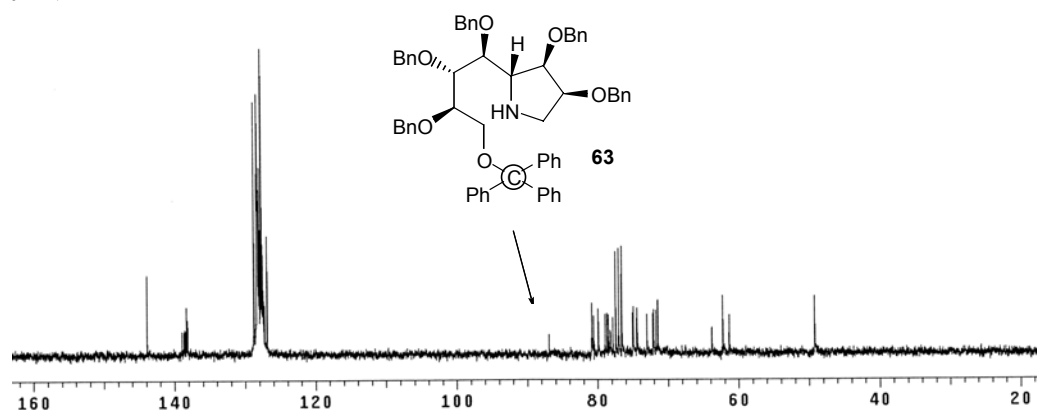
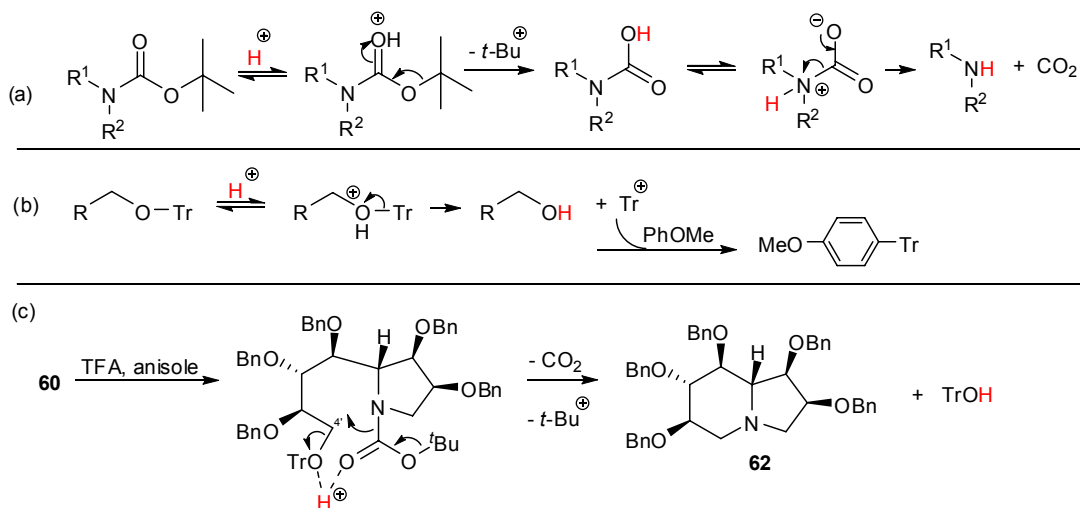


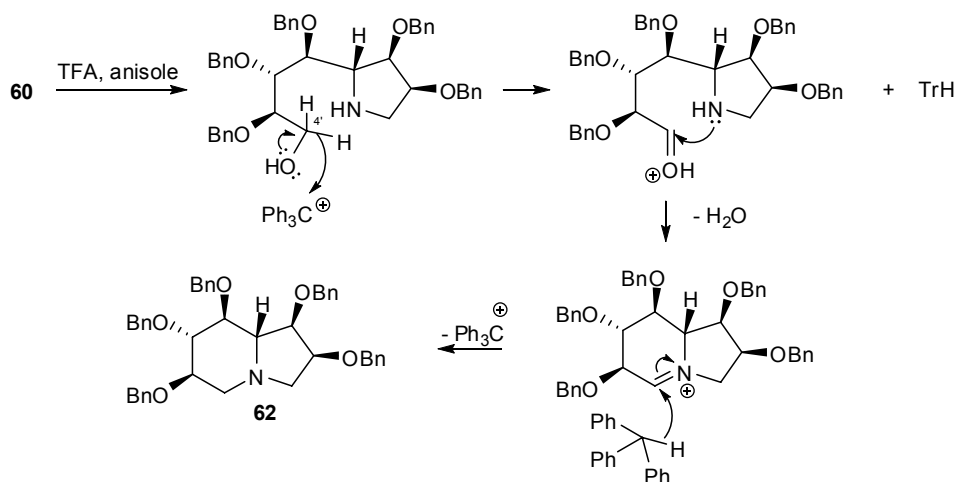
Figure 3.10. ^{13}C NMR spectrum (75 MHz, CDCl_3) of mono-protected *O*-Tr derivative **63**.

A possible mechanism for the unusual cyclization of **60** is described in Scheme 3.11c. We suggest that **62** arises by cyclization of an incipient amide anion, with activation of the *O*-Tr group by protonation with TFA. This assumes that the generated incipient anion reacts with C-4' before any protonation of it by excess TFA. In the normal acid mediated removal of a *N*-Boc group, an oxonium ion is generated by the protonation of the ketyl oxygen, followed by the elimination of *t*-Bu cation. The subsequent carbamic acid can exist in the zwitterion form, which can undergo decarboxylation to give a free amine (Scheme 3.11a). In the normal acid mediated removal of an *O*-Tr group, an oxonium ion is formed and trityl cation is liberated, giving the free alcohol (Scheme 3.11b). Our proposed mechanism merges these two normal deprotections by using only one mole of acid to activate the relevant oxygen atoms, instead of two separate moles of protons. In a sense, the single proton acts as a chelate between the trityl ether oxygen and the Boc carbonyl oxygen.



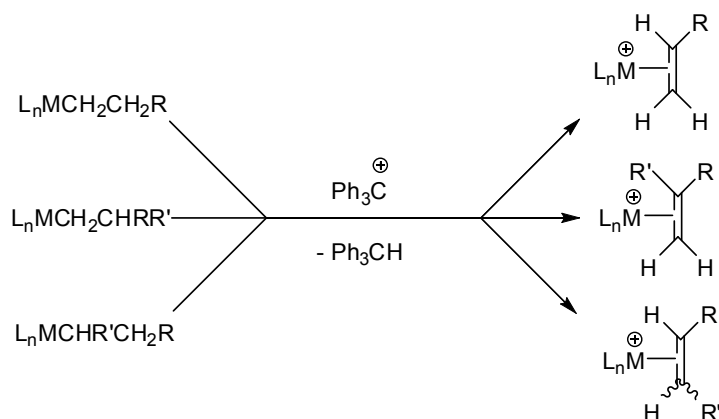
Scheme 3.11. Possible mechanism for the cyclization of **60**.

Prof. Anthony Barrett (Imperial College, London) offered another possible mechanism to us at a Gordon conference in 2006, after a presentation was given about this work. He suggested that both *N*-Boc and *O*-Tr cleavage occurs initially to give an amino alcohol, which subsequently undergoes hydride abstraction at the C-4' position by the liberated trityl cation (Scheme 3.12). The newly formed amino aldehyde then undergoes an intramolecular cyclization to the corresponding iminium ion, which is reduced by triphenylmethane.



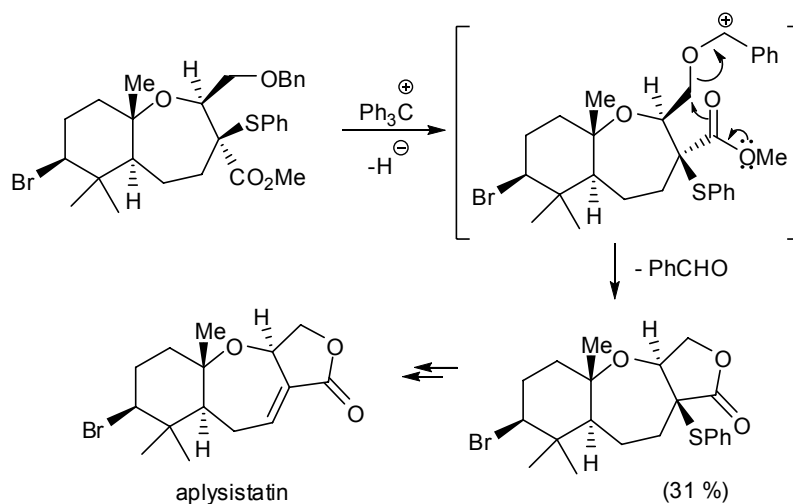
Scheme 3.12. Prof. Anthony Barrett's proposed mechanism for the cyclization of **60**.

The phenomenon of trityl cation (Ph_3C^+) removing hydride is not unprecedented. Many examples of hydride abstraction by Ph_3C^+ have been reported for organometallic compounds.¹²⁹⁻
¹³⁶ For example, transition metal alkene complexes are frequently prepared by β -hydride abstraction from alkyl complexes by Ph_3C^+ (Scheme 3.13).



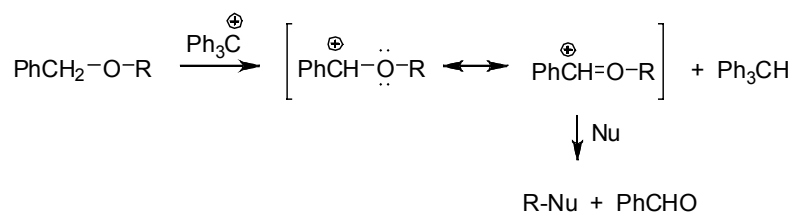
Scheme 3.13. β -Hydride abstraction by trityl cation in selected organometallics.¹³⁰

Hoye *et al.* reported an elegant example of this deprotection method in the synthesis of *dl*-aplysistatin (Scheme 3.14).¹³⁷ They used Ph_3C^+ after earlier attempts at de-*O*-benzylation by hydrogenolysis methods had failed.



Scheme 3.14. Example of *O*-Bn deprotection by Ph_3C^+ and subsequent cyclization.

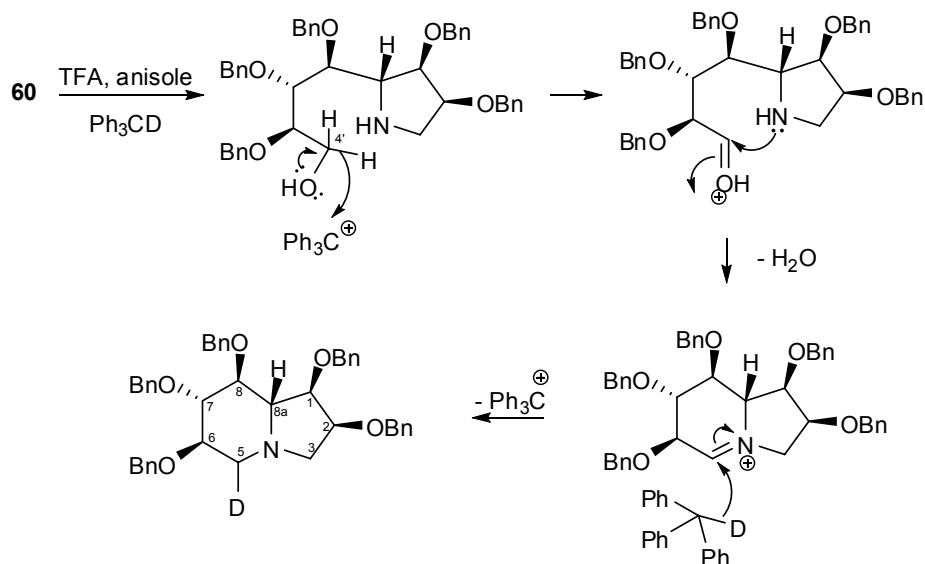
Barton *et al.* first reported the deprotection of benzyl ethers and acetals with Ph_3C^+ .^{138,139} Abstraction of a benzyl hydride by Ph_3C^+ might seem counter-intuitive at first. Benzyl cation has an affinity for hydride of 113 kcal/mol while Ph_3C^+ has a hydride affinity of 99 kcal/mol, which means the abstraction process should be endothermic by 14 kcal/mol. However, the generated carbenium ion is stabilized by the adjacent oxygen lone pair, a process that operates to lower the energy of the hydride transfer step (Scheme 3.15).



Scheme 3.15. Mechanism of de-*O*-benzylation by Ph_3C^+ .

In a similar way, Barretts' proposed mechanism operates with the generated carbenium ion being stabilized by the alcoholic oxygen lone pair, before rapid attack of the amine onto the subsequent activated aldehyde (Scheme 3.12).

Although grateful for Prof. Barrett's contribution, there were nonetheless some contentious aspects to it. Firstly, in all but one of the deprotection reactions we tried, 10 equiv. of anisole was present. Such a large excess of anisole, a good trap for Ph_3C^+ , would surely present a major obstacle for this mechanism. The second issue with this mechanism is the lack of literature precedence for the reduction of an iminium ion with triphenylmethane. In fact, a rigorous literature search proved absolutely fruitless in finding this type of reaction. However one simple way to verify this mechanism would be to add deuterated triphenylmethane to the reaction and observe whether the product becomes deuterated at the C-5 position (Scheme 3.16).



Scheme 3.16. A method for validating Prof. Anthony Barrett's proposed mechanism.

3.10. Appel cyclization

Although we had unexpectedly obtained a cyclized product in the previous step, it was not produced in sufficient quantities to carry it through to the final target. Also, there were substantial quantities of amino alcohol **61** produced from the several TFA deprotection reactions of compound **60**. At this stage in the synthesis of *ent*-**1**, a Mitsunobu cyclization reaction of amino alcohol **61** was scheduled (Scheme 3.10). However, co-workers in our lab had observed that this reaction was capricious when applied to amino alcohols that were reasonably similar to **61**. In these instances, cyclization using the Appel⁸⁸ method was found to be a more reliable reaction. Naruse and co-workers' synthesis of (-)-swainsonine involved a very similar end-stage synthetic pathway to our planned end-stage synthesis of *ent*-**1**.¹⁴⁰ They used Appels' cyclization conditions to construct an indolizidine from an amino alcohol before removing an *O*-Bn protecting group (Scheme 3.17a). Having decided to follow this approach, we revised our end-stage synthetic pathway, which is displayed in Scheme 3.17b. Also included in this Scheme is an additional per-acetylation reaction that was planned to produce the pentaacetate **64**. It was envisaged that this product would probably be more amenable to the production of suitable crystals for X-ray analysis than *ent*-**1**.

Please see print copy for Scheme 3.17

Scheme 3.17. Appel cyclization and *O*-Bn deprotection reactions by Naruse *et al.*¹⁴⁰

The cyclization of **61** was highly anticipated due to its link with the model study findings (Chapter 2) in which the cyclization of amino tetraol **43** under Mitsunobu conditions gave an unwanted regioisomer as the major product, due to the lack of protection afforded to secondary hydroxyl groups. With all the necessary functional groups protected in **61**, it was expected that cyclization would deliver the desired indolizidine **62** exclusively. In addition, a

successful cyclization reaction would confirm the cyclized product observed in the previous TFA reaction of **60**.

In the event, the substantial difference in polarity between **61** and **62** made the purification of **62** by FCC straightforward. Gratifyingly, the ^1H NMR spectrum of **62** was identical to the one for the cyclized side-product in the TFA reaction (Section 3.9). The reaction was tried several times, giving a best yield of 60 %, with no other side-products formed.

3.11. *O*-Bn deprotection

The procedure for the *O*-Bn deprotection of **62** was based on the one used by Naruse¹⁴⁰ in Scheme 3.17a. TLC analysis of the reaction after 18 h showed that the starting material was consumed and that the product was highly polar and unsuitable for purification by FCC.

After filtering the reaction mixture, to remove palladium solids, the organic solvents were evaporated. The residue was dissolved in water and applied to a Amberlyst™ (OH⁻, A - 26 resin) basic ion-exchange column. Unlike the previously described acid ion-exchange chromatography, the sample was loaded onto the resin in water, not acid. The desired product was neutralised by the basic resin and then eluted through with a subsequent water wash, while any anionic impurities remained bound to the resin. Upon evaporation of water, the product appeared as a clear oil, which was crystallized from boiling EtOH and a few drops of H₂O, to give transparent micro-crystals.

The melting point of the crystals was 170-172 °C, a small deviation from the literature value for uniflorine A of 174-178 °C. A cursory inspection of the ^1H NMR spectrum showed there to be only one product present, giving a calculated yield for the reaction of 83 %. However a more detailed analysis of the ^1H NMR data provided very poor conformity in the chemical shifts of *ent*-**1**, when compared to the corresponding chemical shifts for uniflorine A reported by Matsumura *et al.*²³ (Figure 3.11).

Please see print copy for Figure 3.11

Figure 3.11. ^1H NMR spectrum (500 MHz, D₂O) of *ent*-**1** and ^1H NMR data of uniflorine A.²³

The NMR experiments of *ent*-**1** were performed in the same solvent (D₂O) and at the same applied frequency (500 MHz) as for the natural product. The ¹³C NMR spectrum showed the requisite eight carbon peaks but they were also significantly mismatched to those published for uniflorine A. Having consistent melting point and mass spectroscopic data with the literature data was encouraging but without congruous NMR data, the prospect of *ent*-**1** being uniflorine A became obsolete. Nonetheless, *ent*-**1** required full NMR characterization.

The first assignments made were the C-3 and C-5 methylene groups. Recalling Figure 2.6, the ¹³C NMR chemical shifts did not change significantly in the carbon atoms α to the nitrogen atom in *ent*-1-deoxycastanospermine stereoisomers. In those compounds, the C-3 shift was consistently upfield of the C-5 shift, ranging from 0.2 to 3.3 ppm. However, that pattern changes when there are hydroxyl groups attached to C-1 and C-2. Fleet and co-workers synthesized a series of 2-hydroxycastanospermines and found that their C-3 and C-5 carbons consistently obeyed a reverse pattern of ¹³C NMR chemical shifts, with the C-3 chemical shift being consistently downfield from the C-5 shift (Figure 3.12).⁸³

Please see print copy for Figure 3.12

Figure 3.12. C-3,5 ¹³C NMR chemical shifts (D₂O, ppm) for several 2-hydroxycastanospermines synthesized by Fleet *et al.*⁸³

Figure 3.13 shows the ¹³C NMR spectrum of *ent*-**1**, along with the multiplicities of the individual peaks, as determined separately by a DEPT experiment. By extending the pattern that exists for the 2-hydroxycastanospermines above, it followed that the upfield methylene resonance in our product be assigned to C-5, while the downfield one be assigned to C-3.

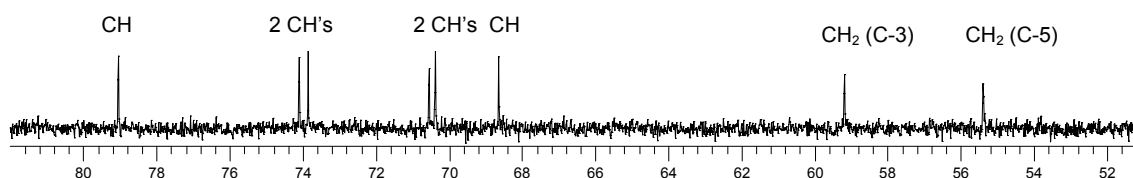


Figure 3.13. ¹³C NMR spectrum (75 MHz, D₂O) of *ent*-**1**.

We could then assign the corresponding protons of C-5 and C-3 in *ent*-**1** by HSQC NMR analysis. Interestingly, both sets of geminal protons were split over a large frequency range. The C-5 protons resonated at 2.09 and 3.01 ppm, respectively, and the C-3 protons

resonated at 2.20 and 3.26 ppm, respectively. The same phenomenon was observed in the 2-hydroxycastanospermines reported by Fleet *et al.*⁸³

Knowing the location of the C-3 and C-5 protons facilitated a straightforward assignment of the remaining methine protons – H-2, H-3, H-6, H-7, H-8 and H-8a, by analysis of the gCOSY spectrum. Figure 3.14 shows the fully assigned ¹H NMR spectrum of *ent*-1.

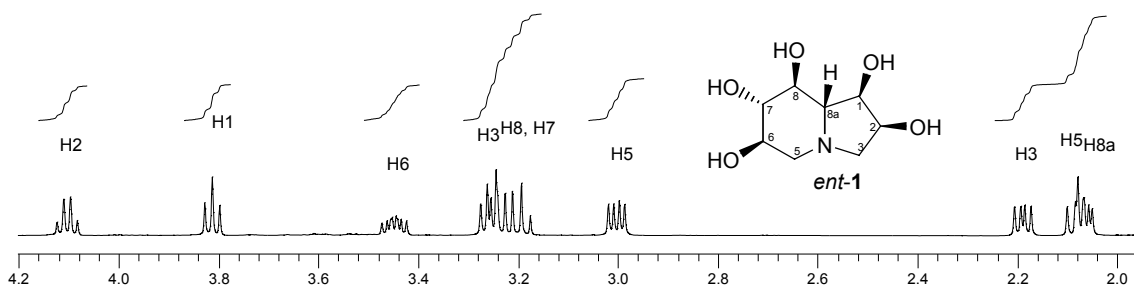


Figure 3.14. Fully assigned ¹H NMR spectrum (500 MHz, D₂O) of *ent*-1.

The stereochemistry of *ent*-1 was verified by a NOESY NMR experiment. We were confident that the stereochemistry of C-6, C-7, C-8 and C-8a was correct, given that it was established in the Petasis reaction of the first step. However, we were yet to verify the stereochemistry of C-1 and C-2 that resulted from the *cis*-dihydroxylation of **58**. Since then, there had been considerable overlap of protons in the ¹H NMR spectra of subsequent products, to effectively utilize a NOESY experiment. Fortunately, in *ent*-1 there was sufficient resolution of proton resonances to allow accurate correlations of individual protons (Figure 3.15).

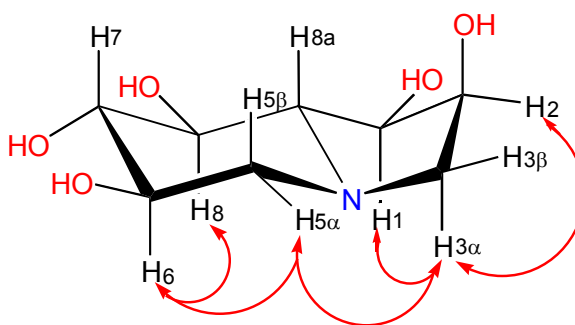


Figure 3.15. Selected NOE correlations observed in the NOESY spectrum of *ent*-1.

To begin with, we looked for correlations with H-6, a discrete proton located at 3.46 ppm. Two cross-peaks were associated with H-6, a strong one with one of the H-5 methylene protons, at 3.01 ppm, and a weak one with H-8, at 3.25 ppm. Thus the proton at 3.01 ppm was identified as H-5α, meaning that its geminal partner, H-5β, was the other H-5 proton located at 2.09 ppm. Tellingly, there was no evidence of a correlation between H-6 and H-5β. H-5α also correlated to a H-3 proton at 3.26 ppm, but not to the other H-3 proton resonating at 2.20 ppm.

Again, this meant that the proton at 3.26 ppm was H-3 α , due to it residing at a significantly closer distance to H-5 α than H-3 β . Identifying H-3 α was pivotal, as its relationship with H-2 and H-1 signified whether the dihydroxylation of **58** occurred *anti* or *syn* with respect to it. The NOESY spectrum clearly showed a cross-peak between H-3 α and H-2, and between H-3 α and H-1, indicating that the dihydroxylation had proceeded *anti* to H-3 α and that the C-1 and C-2 hydroxyl groups were in the correct configuration for structure *ent*-**1**.

Still the problem remained of our mismatched NMR data. As compelling as our NMR data was, it was not unequivocal. An X-ray of a single crystal would be a way to secure the structure of *ent*-**1** but our micro-crystals were unsuitable for X-ray analysis. Therefore the decision was taken to acetylate all five hydroxyl groups in *ent*-**1**, and try to grow more suitable crystals from the pentaacetate derivative.

3.12. Acetylation

Acetylation of *ent*-**1** was carried out using the same conditions described in Section 2.1, giving acetate **64** in a moderate 53 % yield (Scheme 3.). Fortunately, recrystallization of the product gave crystals that were suitable for X-ray analysis (Figure 3.16). Unambiguously, the X-ray structure of **64** verified it to be the pentaacetate derivative of *ent*-**1**. Given that Matsumura *et al.*²³ did not obtain an X-ray for uniflorine A, this result secured unequivocal proof that the structure proposed for uniflorine A was incorrect.

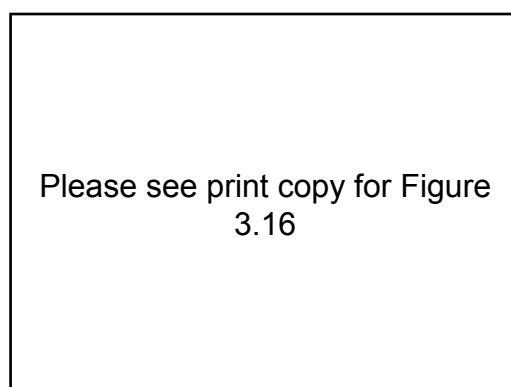


Figure 3.16. Single crystal X-ray structure of **64** (viewed as a CIF file in CCDC Mercury¹⁰⁵).

Such a significant finding changed the scope of this project. Using total synthesis, we invalidated the structure of uniflorine A, which augured our interest into what the real structure was. As a starting point, we undertook a closer examination of the uniflorine A ¹H NMR data and related it to the data for *ent*-**1**. With the inclusion of Fleet and co-workers 2-hydroxycastanospermine derivatives,⁸³ we compared the ¹H NMR chemical shifts for each

proton of the same relative position along the indolizidine skeleton (Figure 3.17), which demonstrated that uniflorine A's pattern of chemical shifts is substantially different to the other pentahydroxyindolizidines. Protons H-2, H-7, H-8a, one of the methylene H-3s, and both methylene H-5s of uniflorine A were significantly downfield of their counterparts in the other compounds. Its H-1 and H-8 protons and the other H-3 proton fell within the same pattern, while H-6 was significantly upfield.

Please see print copy for Figure 3.17

Figure 3.17. Comparison of assigned ^1H NMR chemical shifts between uniflorine A, *ent*-**1**, and three analogous pentahydroxyindolizidines (see Figure 3.12), **65**,⁸³ **66**,⁸³ and **67**.⁸³

With so much downfield disparity between the chemical shifts of uniflorine A and *ent*-**1**, we suspected that NMR data of the natural product might be representative of its amine salt. However, we generated a hydrochloride salt of *ent*-**1** by adding HCl and the subsequent NMR data did not match that for uniflorine A.

After discounting the salt theory, we turned our attention to coupling constant comparisons. One of the coupling constants reported for uniflorine A was highly unusual. Specifically, the coupling between H-8a and H-1 of 4.5 Hz was inconsistent for a *trans*-diaxial configuration of these protons. The $J_{1,8a}$ value of 7.7 Hz for *ent*-**1** was consistent with *trans*-diaxial couplings reported in the literature for fused 5,6-membered rings, including J_{8a-8} (9.5 Hz) for compound **66**, and J_{8a-8} (8.6 Hz) and J_{8a-1} (7.5 Hz) for 1,2-di-*epi*-swainsoine **68**, as shown in Figure 3.18. The low $J_{1,8a}$ (4.5 Hz) value for uniflorine A is more indicative of a *syn* relationship between H-1 and H-8a, like the J_{8a-1} (3.8 Hz) value recorded for **66** (Figure 3.18).⁸³ Hence, we speculated that if uniflorine A was an indolizidine, it could be 2*R*-2-

hydroxycastanospermine **69** (Figure 3.19). With no reported isolation or synthesis of this compound in the literature, it became an attractive synthetic target for us to pursue.

Please see print copy for Figure 3.18

Figure 3.18. Selected ^1H NMR J values for *ent*-**1**, **66**⁸³ and **68**.

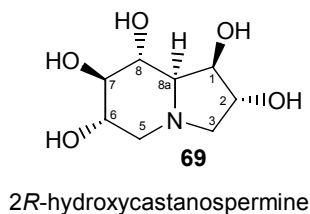
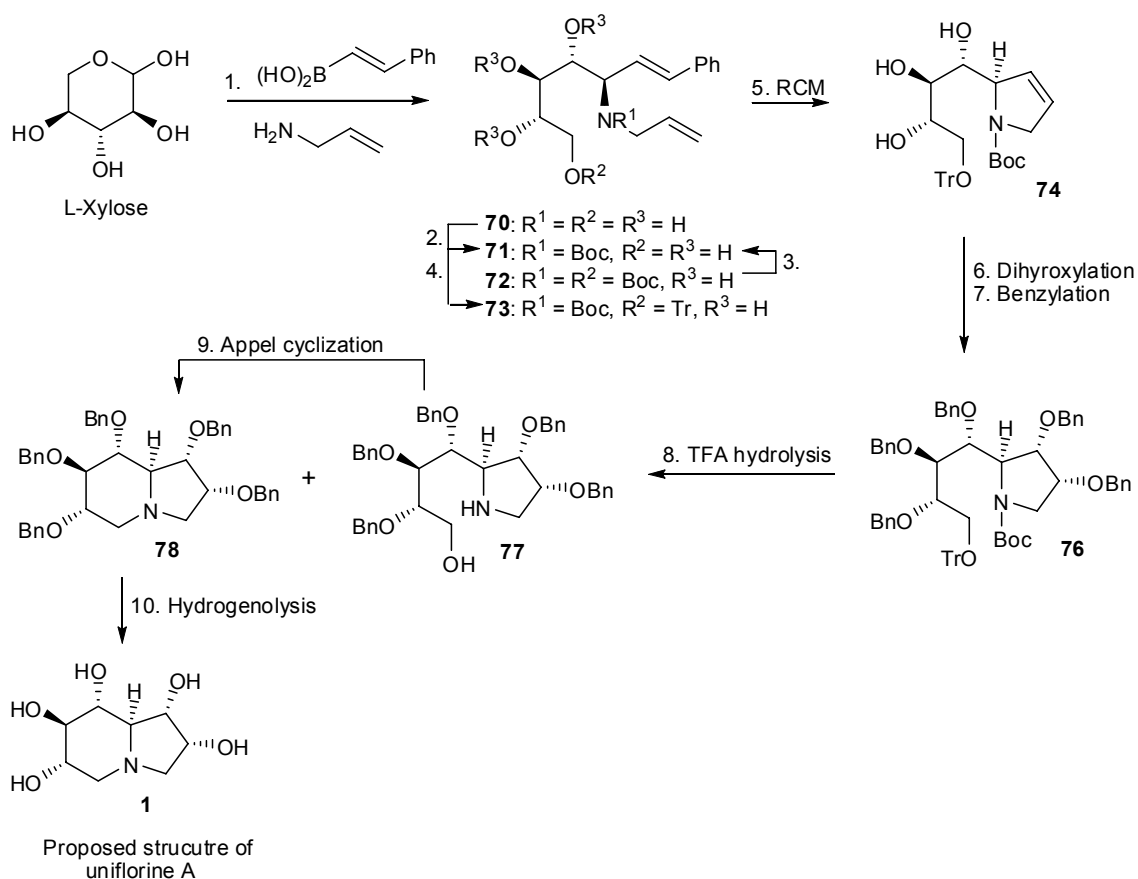


Figure 3.19. Our proposed structure for uniflorine A.

Before embarking on a synthesis for 2*R*-hydroxycastanospermine, we wanted to extend our synthesis of *ent*-**1** to the synthesis of **1** itself.

3.13. Synthesis of the correct enantiomer of putative uniflorine A

By substituting L-xylose for D-xylose in the initial Petasis reaction (Scheme 3.10), we followed the same series of steps to access compound **1**, the ‘putative’ structure of uniflorine A. Scheme 3.18 outlines the steps taken, while Table 3.9 details the yields and other physical properties for each product.

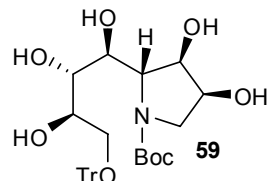
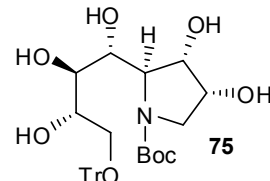
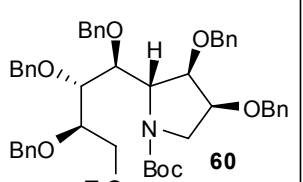
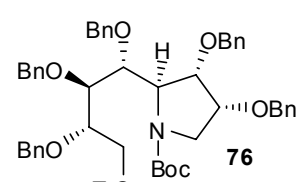
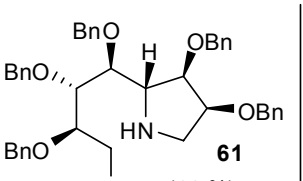
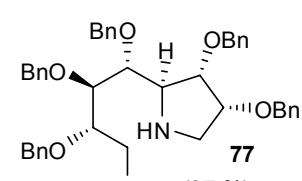
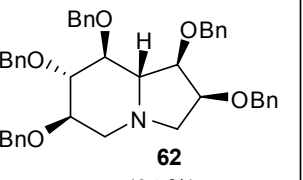
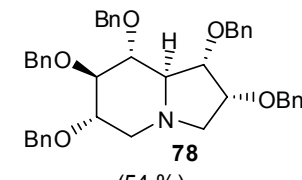
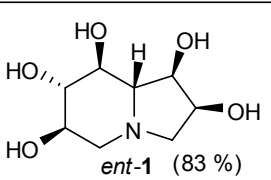
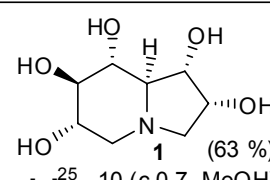
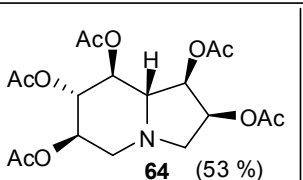
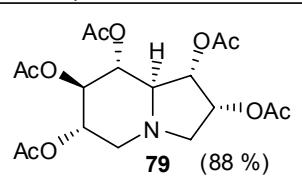


Scheme 3.18. The synthetic route for **1**.

Table 3.9. Comparison of the results for the synthesis of *ent*-**1** and **1**.

Synthetic step	D-Xylose series	L-Xylose series
1. Petasis reaction	 38 (94 %)	 70 (73 %)
	$[\alpha]_D^{25}$ 27 (c 0.06, MeOH)	$[\alpha]_D^{25}$ -17 (c 0.3, MeOH)
2. N-Boc protection	 47 (67 %)	 71 (51 %)
	$[\alpha]_D^{25}$ 29 (c 2.3, CHCl ₃) (77 % over 2 steps)	$[\alpha]_D^{25}$ -50 (c 3.0, CHCl ₃) (64 % over 2 steps)
3. Hydrolysis	 55 (18 %)	 72 (20 %)
	(58 %)	(64 %)
4. O-Tr protection	 48 (84 %)	 73 (68 %)
	$[\alpha]_D^{25}$ 20 (c 1.0, CHCl ₃)	$[\alpha]_D^{24}$ -24 (c 1.5, CHCl ₃)
5. RCM	 58 (96 %)	 74 (86 %)
	$[\alpha]_D^{25}$ -82 (c 5.0, CHCl ₃)	$[\alpha]_D^{25}$ 74 (c 0.7, CHCl ₃)

Table 3.9 cont'd. Comparison of the results for the synthesis of *ent*-1 and 1.

Synthetic step	D-Xylose series	L-Xylose series
6. Dihydroxylation	 <p>59 (79 %) [α]_D²³ -20 (c 9.0, CHCl₃)</p>	 <p>75 (88 %) [α]_D²⁵ 20 (c 4.6, CHCl₃)</p>
7. Benzylation	 <p>60 (81 %) [α]_D²⁷ -12 (c 40.0, CHCl₃)</p>	 <p>76 (76 %) [α]_D²³ 14 (c 3.5, CHCl₃)</p>
8. TFA deprotection	 <p>61 (44 %) [α]_D²⁷ 25 (c 14.0, CHCl₃)</p>	 <p>77 (37 %) [α]_D²² -21 (c 1.3, CHCl₃)</p>
	<p>↓ 9. Appel cyclization (60 %)</p>  <p>62 (34 %) (60 % over 2 steps) [α]_D²⁶ 2 (c 12.2, CHCl₃)</p>	<p>↓ 9. Appel cyclization (84 %)</p>  <p>78 (54 %) (85 % over 2 steps) [α]_D²² -11 (c 0.7, CHCl₃)</p>
10. Debenzylation	 <p><i>ent</i>-1 (83 %) [α]_D²⁴ 4 (c 1.2, MeOH) m.p. 171 - 172 °C</p>	 <p>1 (63 %) [α]_D²⁵ -10 (c 0.7, MeOH) [α]_D²⁵ -6 (c 5.0, H₂O) m.p. 170 - 172 °C</p>
Acetylation	 <p>64 (53 %) [α]_D²⁵ 26 (c 1.5, CHCl₃) m.p. 146 °C</p>	 <p>79 (88 %) [α]_D²¹ -15 (c 1.36, CHCl₃) m.p. 142 °C</p>

In most cases, the yields were very similar between the syntheses. Using L-xylose in the Petasis reaction gave a moderate reduction in yield compared to using D-xylose (73 % vs 94 %). The yields for the RCM and de-*O*-benzylation reactions in the L-xylose series were good, although reduced from the D-series. Remarkably, the magnitudes of the optical rotation values were similar in all but one pair of enantiomers, the *N*-Boc products **47** and **71**. Ironically, the optical rotation for **1** was very close to that reported for the natural product (Table 3.10).

Table 3.10. Rotation and melting point data for uniflorine A and **1**.

	uniflorine A	1
optical rotation	$[\alpha]_{\text{D}} - 4.4$ (<i>c</i> 1.2, H ₂ O)	$[\alpha]_{\text{D}}^{25} - 6$ (<i>c</i> 5.0, H ₂ O)
melting point	174 – 178 °C	170 – 172 °C

For each reaction in the synthesis of **1**, the product was verified by comparing its NMR data to the corresponding data of its enantiomer. Good quality crystals were obtained from the recrystallization of **79**, and its X-ray structure is shown in Figure 3.20.

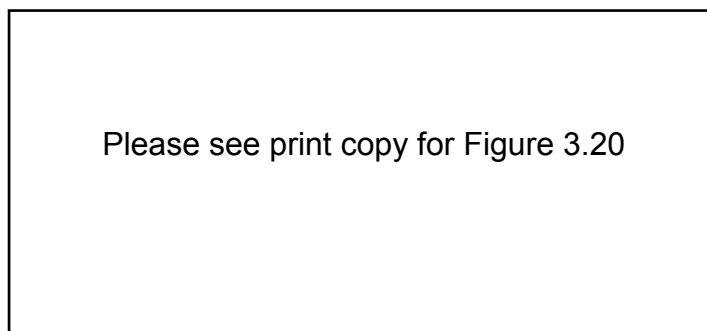


Figure 3.20. Single crystal X-ray structure of **79** (viewed as a CIF file in CCDC Mercury¹⁰⁵).

The synthesis of **1** was very smooth as the chemistry learned in the synthesis of *ent*-**1** substantially reduced the timeframe to produce its antipode. The overall synthetic yields of the enantiomers are shown in Table 3.11.

Table 3.11. Overall yields for the synthesis of *ent*-**1** and **1**.

	<i>ent</i> - 1	1
including all 10 steps	19 %	12 %
excluding steps 3 and 9 (see Table 3.9)	16 %	6 %

CHAPTER 4. Attempted syntheses of 1-*epi*- and 2-*epi*-1

As discussed in Chapter 3, the next synthetic target was 2*R*-hydroxycastanospermine **69**, otherwise referred to as 1-*epi*-1. This target represented a change of the *cis*-(1 α ,2 α)-diol in **1**, to a *trans*-(1 β ,2 α)-diol. Since we planned to synthesize a *trans*-(1 β ,2 α) diol, it was logical to also explore a synthesis of the diastereomeric *trans*-(1 α ,2 β) compound, otherwise referred to as 2-*epi*-1 (Figure 4.1).

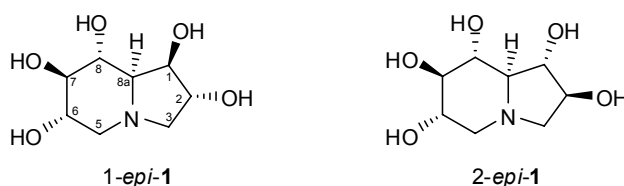
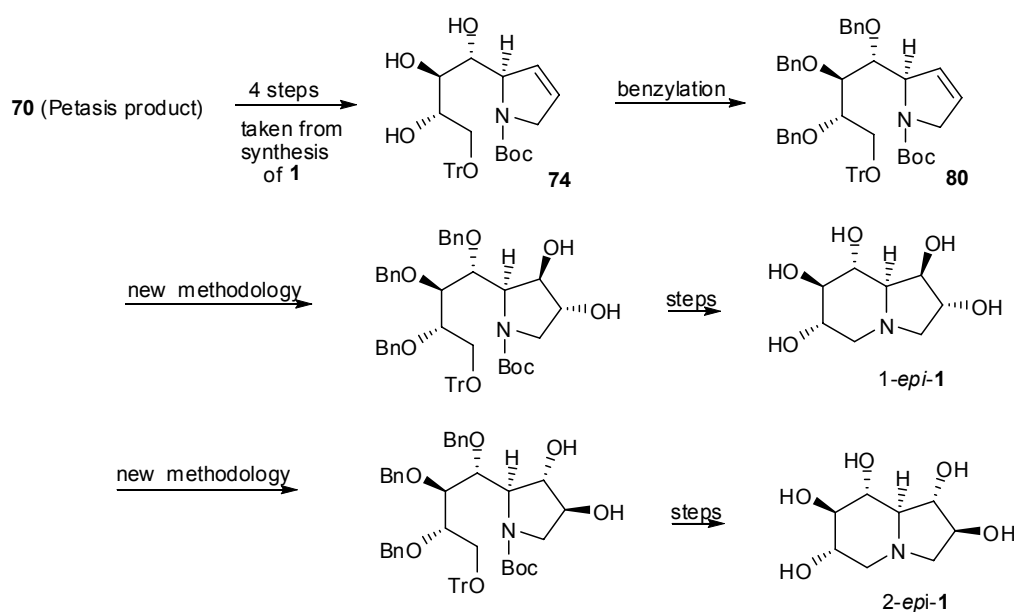


Figure 4.1. Synthetic targets 1-*epi*-1 and 2-*epi*-1.

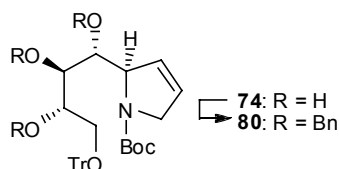
As much as possible, it was thought that the syntheses of 1-*epi*-1 and 2-*epi*-1 should incorporate the strategy used to synthesize *ent*-1 and **1**. The synthetic plan is outlined in Scheme 4.1 and it shows that the four steps required to access 2,5-dihydropyrrole **74** are from the earlier synthesis of **1**. New synthetic methodologies were required to install oxygen functionalities in the appropriate configurations at the C-1 and C-2 positions of the pyrrolidine ring. Prior to this, it was necessary to *O*-Bn protect the three secondary hydroxyl groups in **74**.



Scheme 4.1. Synthetic plan for 1-*epi*-1 and 2-*epi*-1, based on the previous synthesis of **1**.

4.1. Preparation of substrate **80**.

Tri-*O*-benzylation of triol **74** occurred without event, using the standard *O*-Bn protection conditions described previously (Scheme 4.2).

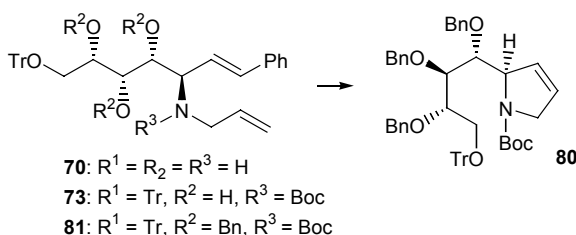


Reagents and conditions:

BnBr, NaH, cat. *n*Bu₄NI, THF, rt, 18 h, 97 %

Scheme 4.2. Synthesis of substrate **80**.

Access to **80** was also possible through the utilization of material left over from a previously discontinued synthesis, namely diene **81** (Scheme 4.3). The diene **81** was prepared in an analogous manner to its enantiomer **49**, starting from **70**, and its structure clearly represented just one RCM reaction away from **80**. In the event, the RCM reaction of **81** proceeded smoothly, giving the desired product **80** in good yield (Scheme 4.3).

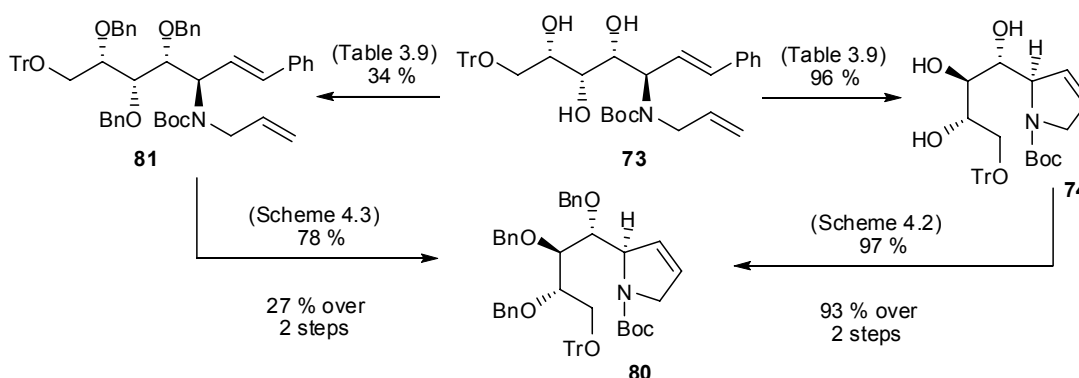


Reagents and conditions:

Grubbs' I cat., DCM, reflux, 1 d, 78 %.

Scheme 4.3. Alternative synthesis of substrate **80**.

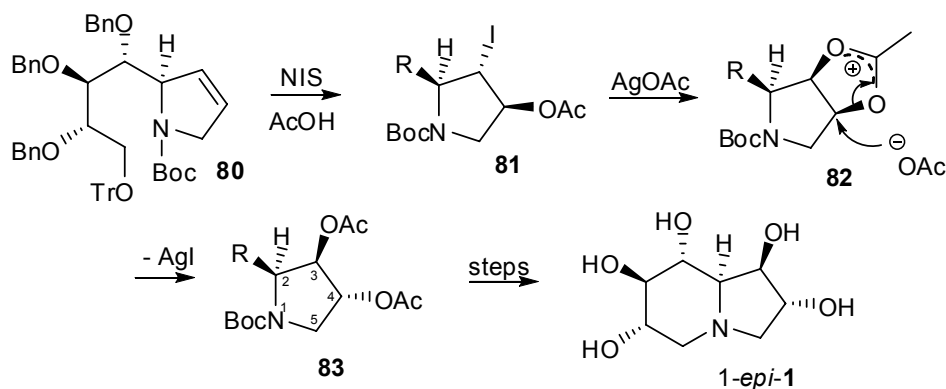
A comparison of the two synthetic routes from the diene **73** to the olefin **80**, shows that conducting a RCM reaction before *O*-benzylation was far more productive than performing these reactions in the reverse order (Scheme 4.4). Nonetheless, consolidating the otherwise redundant **83** was a quick and efficient way to access more of **80**.



Scheme 4.4. Summary of the two syntheses of **80**.

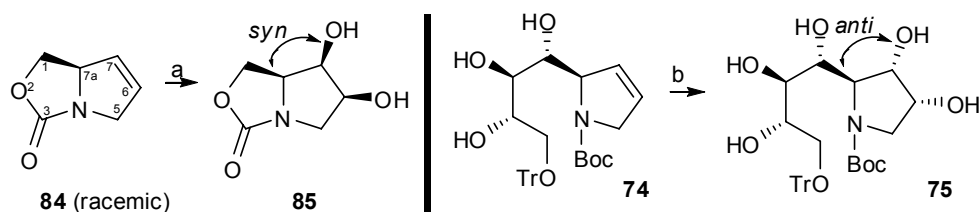
4.2. Synthetic strategies for 1-*epi*-1

Naturally, it would be very convenient if the *cis*-dihydroxylation of olefin **80** in Scheme 3.19 could simply be substituted by a one-pot *trans*-dihydroxylation reaction, as described in Scheme 4.1. Prevost developed a one-pot method of forming a *trans*-diol from an olefin, *via* the *in situ* generation of an α -iodoacetate, followed by reaction with a silver(I) salt.¹⁴¹ If applied to our substrate **80**, the reaction would theoretically follow a path shown in Scheme 4.5, and provide access to the di-*O*-Ac protected derivative **83**. Unfortunately, when the Prevost reaction was applied to a similar substrate in our laboratory, it achieved little success. We therefore turned our attention to other, more promising methodologies.



Scheme 4.5. A potential way of accessing *trans*-(3 β ,4 α)-diol **83** using the Prevost reaction.

A different synthetic strategy came from a serendipitous finding by a co-worker. In 2003, Nicole Gates observed *syn*-selectivity in a *cis*-dihydroxylation reaction of an oxazolidinone protected 2,5-dihydropyrrole **84**, which was the opposite selectivity found for the same reaction performed on our corresponding *N*-Boc protected 2,5-dihydropyrrole **74** (Scheme 4.6).^{142,143}



Reagents and conditions: (a) 5 mol % $K_2OsO_4 \cdot 2H_2O$, 2.1 eq. NMO, $C(O)Me_2$, H_2O (b) see Table 3.9

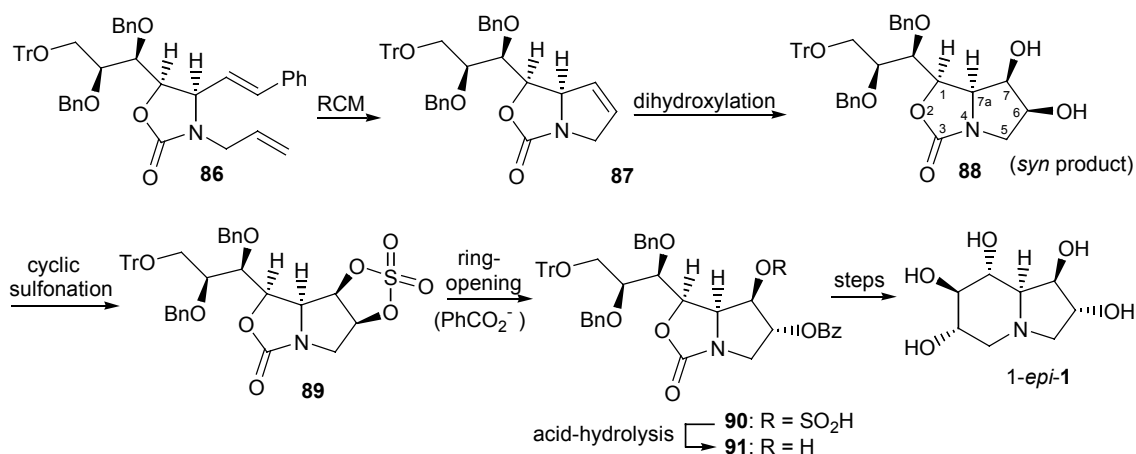
Scheme 4.6. Dihydroxylation of substituted 2,5-dihydropyrroles; comparison of diastereoselectivity according to nitrogen protection.

One explanation for the reversal of facial selectivity with the oxazolone substrate **84** is that the *pseudo*-axial protons H-7 α and H-5 β sterically shield electrophilic attack to the *exo*-face (Figure 4.2a).¹⁴³ Another explanation was put forward by Parsons *et al.*, who observed similar unexpected selectivity for dihydroxylations and epoxidations of **84**. By calculating the π -bond HOMO of **84** *via ab initio* experiments, more electron density was found on the *endo* face of the π bond, which they accounted for the high *endo* diastereoselectivity observed in their synthetic experiments (Figure 4.2b).¹⁴⁴

Please see print copy for Figure 4.2

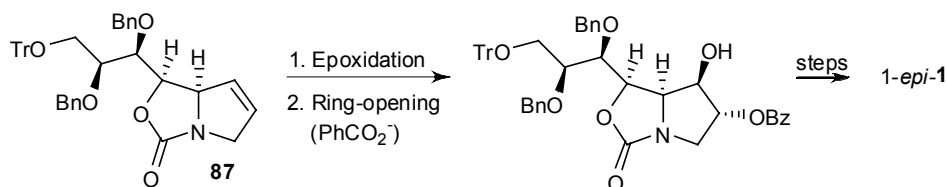
Figure 4.2. (a) AM1 representation of oxazolone **84** (b) 6-31G* representation of the HOMO of oxazolone **84** (Taken from Murray *et al.*¹⁴⁴).

Regardless of the reasons, this was a very interesting result as we already had experience with accessing oxazolidinones and oxazinanones (Section 3.5), even though they were unwanted side-products at the time. By subjecting our oxazolidinone **86** to RCM, we envisaged that a subsequent *cis*-dihydroxylation reaction of oxazolone **87** would give the 6 β ,7 β -diol **88**, in alignment with Gates' result (Scheme 4.7). We then envisaged converting the diol **88** into the protected *trans* 6 α ,7 β -diol **91** *via* Sharpless cyclic sulfate chemistry.¹⁴⁵ This procedure has been utilized successfully in our laboratory and operates by converting a *cis*-diol into a cyclic sulfite, followed by oxidation to a cyclic sulfate. Ring-opening of the cyclic sulfate with an oxygen nucleophile like benzoate, followed by acid hydrolysis of the resulting sulfate ester, would establish the *trans* 6 β ,7 α protected diol **91** (Scheme 4.7). With further elaboration, 1-*epi*-**1** would be obtained.



Scheme 4.7. Synthetic plan for 1-*epi*-1 using cyclic sulfate methodology.

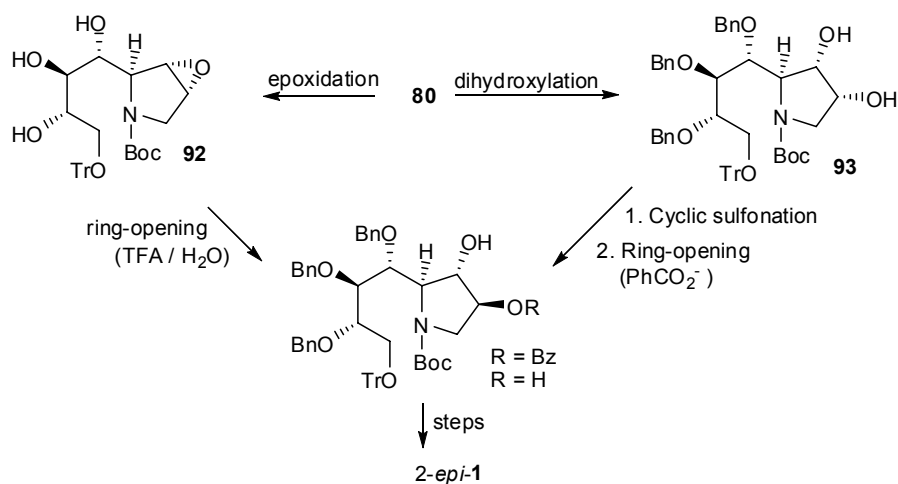
Another common method of generating a *trans*-diol from a cyclic olefin is to epoxidize then ring-open the resulting epoxide with an oxygen nucleophile. Epoxidation of **87** would result in a 6 β ,7 β epoxide, which would theoretically be regioselectively ring-opened by an oxygen nucleophile under acidic conditions, and further elaborated to also give 1-*epi*-1 (Scheme 4.8).



Scheme 4.8. Synthetic plan for 1-*epi*-1 using epoxide methodology.

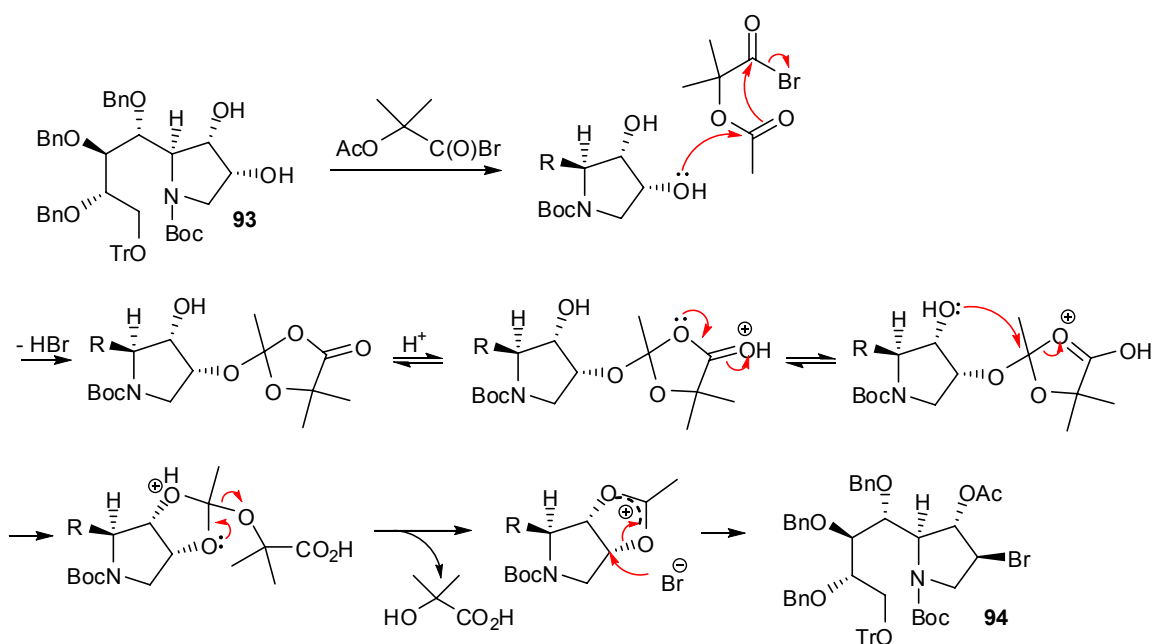
4.3. Synthetic strategies for 2-*epi*-1

Our plans for the synthesis of 2-*epi*-1 included the above cyclic sulfate and epoxide methodologies. However, the substrate would be changed from the oxazolone **87** to the 2,5-dihydropyrrole **80**, enabling either a dihydroxylation or epoxidation reaction to proceed with the desired *anti* stereoselectivity (Scheme 4.9).



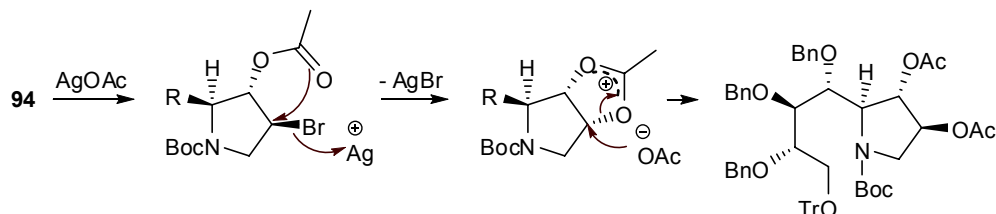
Scheme 4.9. Synthetic plan for 2-*epi*-1 using cyclic sulfonation or epoxidation methodologies.

One other synthetic strategy we had in mind involved the use of a 2-acetoxy-isobutyryl halide reagent. This method was discovered by Mattocks^{146,147} and was later re-examined and expanded upon by Moffatt *et al.*¹⁴⁸ It proceeds by converting a *cis*-diol into a *trans*-haloacetate. Scheme 4.10 outlines the mechanism when applied to diol **93**. Interestingly, the nucleophilic attack of a secondary hydroxyl group occurs at the acetoxy carbonyl rather than the typically more activated acid bromide carbonyl carbon. It is believed that the steric influence of the isobutyryl group causes this effect.



Scheme 4.10. Mechanism of the Mattocks reaction when applied to diol **93**.

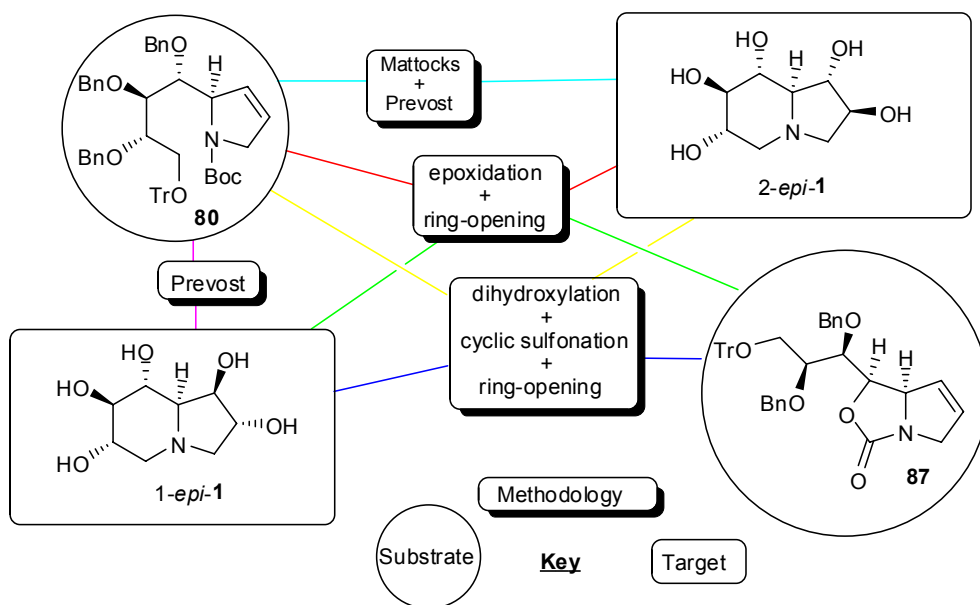
If successful, the isolated *trans*-bromoacetate **94** would then be subjected to the Prevost reaction outlined above, which would have the net effect of substituting the bromine atom for an acetoxy group with overall retention of stereochemistry at C-4 (Scheme 4.11).



Scheme 4.11. Application of Prevost chemistry to the α -bromoacetate **94**.

4.4. Choosing a synthesis from several options

To gain a clearer picture of all the options for the syntheses of 1-*epi*-**1** and 2-*epi*-**1**, a scheme was drawn up to include both the 2,5-dihydropyrrole **80** and oxazolidinone **87** substrates, together with methodologies and targets (Scheme 4.12). When choosing which synthesis to pursue, our decision started with methodology. Cyclic sulfate methodology was selected simply because it had the most utilization in our laboratory, on similar substrates to **82** and **80**. We chose **80** as the substrate because it was more efficient to access in good quantities. According to the strategy scheme, the combination of **80** and cyclic sulfate methodology gave 2-*epi*-**1** as the target. Efforts then commenced towards its synthesis.



Scheme 4.12. Strategies available for the synthesis of 1-*epi*-**1** and 2-*epi*-**1**.

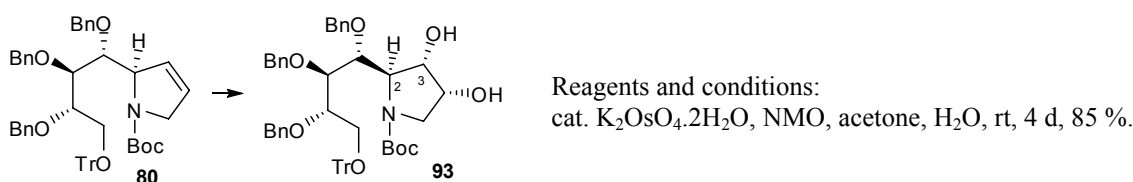
4.5. Formation of cyclic sulfate

In 2003, co-worker Minyan Tang reported the synthesis of 7-*epi*-australine **5** from an oxazolidinone diol **95** (Scheme 4.13).²⁵ She successfully inverted the stereochemistry at C-1 in **95**, *via* ring-opening of cyclic sulfate **96** with cesium benzoate. In this case, the C-3 benzyloxymethyl group in **95** controlled the regioselectivity of the ring-opening.

Please see print copy for Scheme 4.13

Scheme 4.13. Example of using cyclic sulfate chemistry to convert a diol moiety from *cis* to *trans*.²⁵

Before commencing this synthetic methodology on **91**, compound **80** required *cis*-dihydroxylation. In the event, *cis*-dihydroxylation of olefin **80** gave the diol **93** in 85 % yield (Scheme 4.14), with no isomeric products discernable by TLC analysis. The resultant stereochemistry of diol **93** was indeterminable by NOESY NMR analysis due to the presence of rotamers and broadened peaks. It was assumed that the diol moiety in **93** was in a 3 α ,4 α configuration, based on result of the dihydroxylation of 2,5-dihydropyrrole **58** in Section 3.7.



Scheme 4.14. Synthesis of cyclic sulfonation starting material **93**.

Initially, the sulfonation of **93** seemed to have proceeded well in producing the cyclic sulfite **98**. After 1 h, TLC analysis of the reaction mixture showed complete consumption of the starting material. It also showed two new spots of similar *R_f*, moderately less polar than the starting material. These spots were assumed to be representative of the two desired diastereomeric cyclic sulfite products (Figure 4.3).

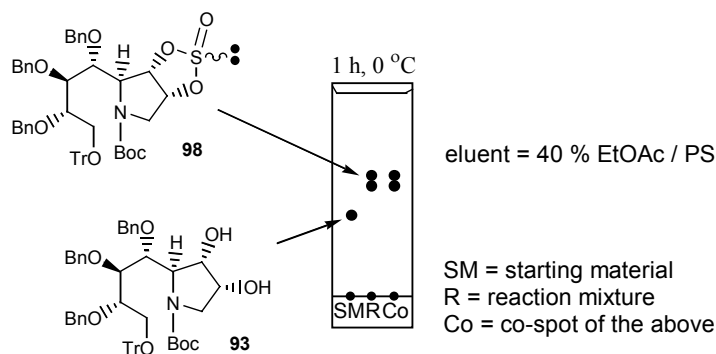
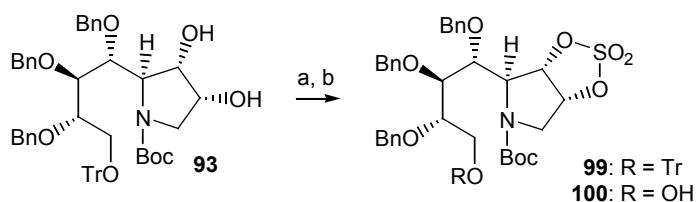


Figure 4.3. TLC analysis of reaction to produce cyclic sulfite **98**.

Following work-up, the crude product was subjected to oxidation using catalytic RuO_4 , formed *in situ* from RuCl_3 and NaIO_4 . Purification of the product by FCC produced two fractions, the first contained the desired cyclic sulfate **99** plus a significant amount of TrOH , in 50 % yield (Scheme 4.15). ^1H NMR analysis of the second fraction showed it to be a detritylated derivative of **99**. The primary alcohol **100** was isolated in 22 % yield and our explanation at the time was that the order of reagent addition was wrong. Thus, adding SOCl_2 before Et_3N probably had the effect of producing HCl in the reaction mixture, in the elapsed time before base was added. However, when the reaction was repeated with the base added before SOCl_2 , the same phenomenon occurred. This time **99** was isolated in 38 % yield, again with substantial TrOH contamination, while **100** was isolated in 38 % yield.

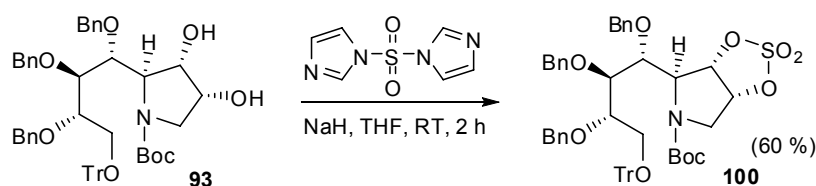


Reagents and conditions: (a) SOCl_2 , Et_3N , DCM, 0 °C 1 h, (b) $\text{RuCl}_3 \cdot 3\text{H}_2\text{O}$, NaIO_4 , 2:2:3 $\text{CCl}_4/\text{CH}_3\text{CN}/\text{H}_2\text{O}$, rt, 1 h. Yields: **99** 50 % with TrOH impurity; **100** 22%.

Scheme 4.15. Results of the formation of cyclic sulfate **99** from diol **93**.

An alternate method of preparing cyclic sulfates from *cis*-diols, without generating a cyclic sulfite, is to use a SO_2X_2 (X = leaving group) reagent. Such a method has extensive precedence in the literature, but with limited yields. The ring-strain energy ($\sim 5\text{--}6$ kcal / mol) of 1,2-cyclic sulfates is most often cited as the reason for the very poor yields in attempted direct preparations from the diol and SO_2Cl_2 or related SO_2X_2 species.¹⁴⁵ Nonetheless, given the problem of applying the Sharpless cyclic sulfate methodology to **93**, little was to be lost by attempting the direct route.

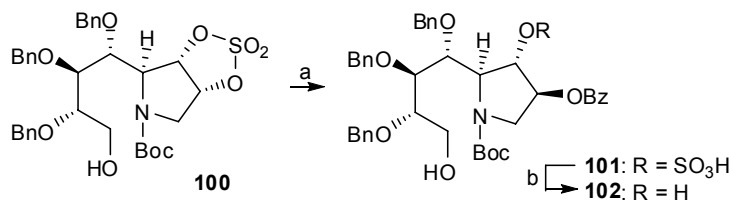
We selected 1,1'-sulfonyldiimidazole as the SO_2X_2 reagent for the reason that the two leaving groups in this reagent effectively produce 2 moles of base per mole of reagent, ensuring neutral conditions in the reaction. In the event, the reaction of **93** with 1,1'-sulfonyldiimidazole was capricious. The first small-scale (90 mg) reaction resulted in a 60 % yield of **99** (Scheme 4.16) but a subsequent larger scale (800 mg) reaction resulted in a 10 % yield of **99**. Further attempts of this reaction were also very low yielding. Instead of spending more time optimizing the synthesis of **99**, we decided to proceed with the next step using the alcohol **100**.



Scheme 4.16. Direct cyclic sulfonation using 1,1'-sulfonyldiimidazole.

4.6. Ring-opening of cyclic sulfate

Ring-opening of **100** was conducted using benzoate as a nucleophile and dry THF as the solvent. After 18 h of stirring at rt, conversion of starting material was slow and the reaction was heated to 100 °C and stirred for a further 18 h, resulting in the complete consumption of starting material. The crude sulfate ester **101** was subjected to acid hydrolysis using identical conditions to that outlined in Scheme 4.13, giving alcohol **102** as a single regioisomer in 30 % yield over two steps (Scheme 4.17). Although the structure of **102** was not unequivocally determined, we assume that this compound would result from $\text{S}_{\text{N}}2$ -like attack at the least hindered carbon of cyclic sulfate **100**. Other products of significant mass were not recovered. The low yield could be due to a double elimination reaction in the cyclic sulfate **100** or the products **101** or **102**, to give a pyrrole.



Reagents and conditions: (a) PhCO_2H , Cs_2CO_3 , THF, rt, 18 h, rt, 100 °C, 18 h
(b) H_2SO_4 (conc.), THF, H_2O , rt, 18 h, 30 % over 2 steps.

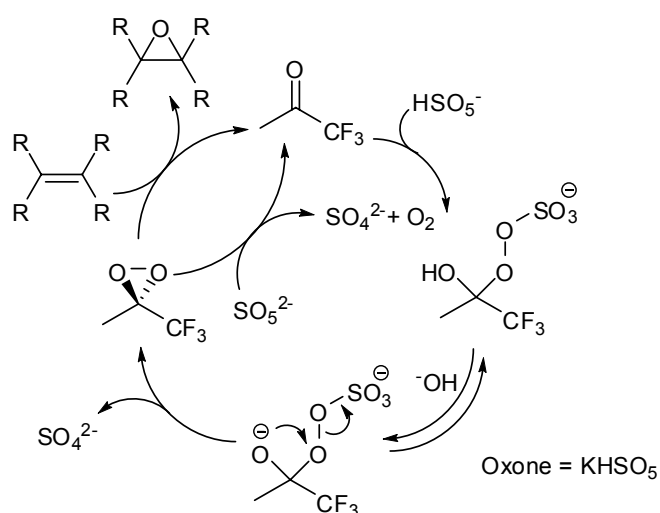
Scheme 4.17. Results of the ring-opening of cyclic sulfate **100**.

4.7. Epoxidation

With limited success being found in the cyclic sulfate methodology, our attention turned to the epoxidation methodology outlined in Scheme 4.9. Various reagents exist for the epoxidation of olefins with the most common being *meta*-chloroperoxybenzoic acid (*m*CPBA). However, in the hands of a co-worker, this method failed to work on a substrate similar to **80**, and was therefore not attempted.

An alternative method that has demonstrated a high degree of success in our laboratory involves the use of Oxone[®] and catalytic trifluoroacetone. This type of epoxidation is a two-step procedure in which Oxone[®] reacts with trifluoroacetone to generate methyltrifluoromethyl dioxirane *in situ*, which reacts with an olefin substrate, to produce an epoxide and regenerate the parent ketone (Scheme 4.18).¹⁴⁹ Hence, the reaction is catalytic in the parent ketone, making it possible to utilize expensive chiral ketones to afford enantioselective and diastereoselective epoxidations. Shi,^{150,151} and Denmark¹⁵² have independently exploited this potential by developing their own elaborate catalysts to couple with cheaper stoichiometric Oxone[®].

As discussed in Section 4.5, dihydroxylation of **80** produced diol **93** with 100 % diastereoselectivity, due to the steric influence exerted by the C-2 polyhydroxylated side-chain. In a similar manner, we envisaged that the epoxidation of **80** would be stereoselectively controlled by the C-2 side-chain, hence trifluoroacetone would be preferred over the abovementioned chiral catalysts.



Scheme 4.18. Mechanism of Oxone[®] mediated epoxidation of an olefin.

Trost *et al.* employed a strategy of oxone epoxidation on a substituted 2,5-dihydropyrrole, followed by aqueous TFA ring-opening, in the synthesis of (+) – broussonetine G (Scheme 4.19).¹⁵³ These reactions would form the basis of our next two synthetic steps.

Please see print copy for Scheme 4.19

Scheme 4.19. Literature example of the synthesis of a *trans* diol from a 2,5-dihydropyrrole.¹⁵³

In the event, epoxidation of **80** using oxone and trifluoroacetone produced consistently high yields of the epoxide **92** (Table 4.1). ¹H NMR analysis of the crude product showed that it did not require further purification. Only one product could be detected in both the ¹H NMR and TLC analyses. Although a 2D NOESY NMR experiment was conducted on a sample of **92**, the nOe cross-peaks were complicated by the presence of rotamers, to the extent that the C-2,3-stereochemistry of **92** was inconclusive. At the time, we assumed that compound **92** was the C-2,3-*anti* isomer based on the precedent of the *cis*-dihydroxylation reaction of 2,5-dihydropyrrole **58**, in which the resultant diol **59** was produced with complete C-2,3-*anti* stereoselectivity (see

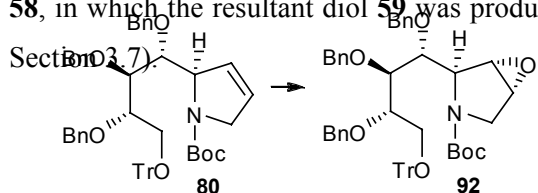


Table 4.1. Results of the epoxidation of **80**.

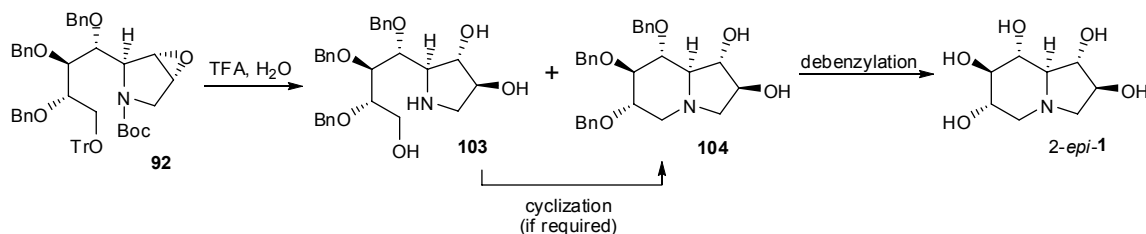
entry	scale	temp. / time	yield
1	330 mg	0 °C, 3 h	100 %
2	200 mg	rt, 4 h	93 %
3	2.8 g	0 °C, 2 h	100 %

Reagents: 5 equiv. Oxone, 8 equiv. NaHCO₃, 1 mL/mmol CF₃C(O)CH₃, 5 mL/mmol Na₂EDTA (4 × 10⁻⁴ M), MeCN.

4.8. Attempted epoxide ring-opening

The aqueous TFA mediated ring-opening of epoxide **92** was expected to occur by the protonation of the epoxide oxygen atom with TFA, followed by the S_N2 attack of water to give a *trans*-diol. In addition, the acidic conditions were expected to result in the cleavage of the *O*-Tr and *N*-Boc protecting groups. Furthermore, it was also hoped that the unusual cyclization event that occurred during the TFA deprotection of *O*-Tr and *N*-Boc groups in compound **60** (Section

3.9), would also occur in this reaction. To summarise, if all the transformations went as planned, the reaction of **92** with aqueous TFA would result in indolizidine **104**, with just one de-*O*-benzylation step required to access the final target 2-*epi*-**1** (Scheme 4.20).



Scheme 4.20. Proposed synthetic pathway from epoxide **92** to final product 2-*epi*-**1**.

In the event, TFA (20 equiv.) was added to a mixture of **92** (740 mg) in a 1:1 ratio of water to THF (2 mL per mmol of **92**). The reaction was complete after 3 h at 60 °C and purification of the crude product resulted in the isolation of three products, one major (180 mg) and two minor (85 mg and 90 mg). The ^1H NMR spectra of the minor products were complicated and not representative of any expected product. At the time, efforts toward the elucidation of these minor products were not deemed worthwhile.

A cursory inspection of the ^1H NMR spectrum of the major product showed it to be pure and likely to be representative of compound **104**. There was a loss of the *tert*-butyl resonance at 1.40 ppm and a reduction in the aromatic proton integration, associated with the loss of the trityl group (Figure 4.4).

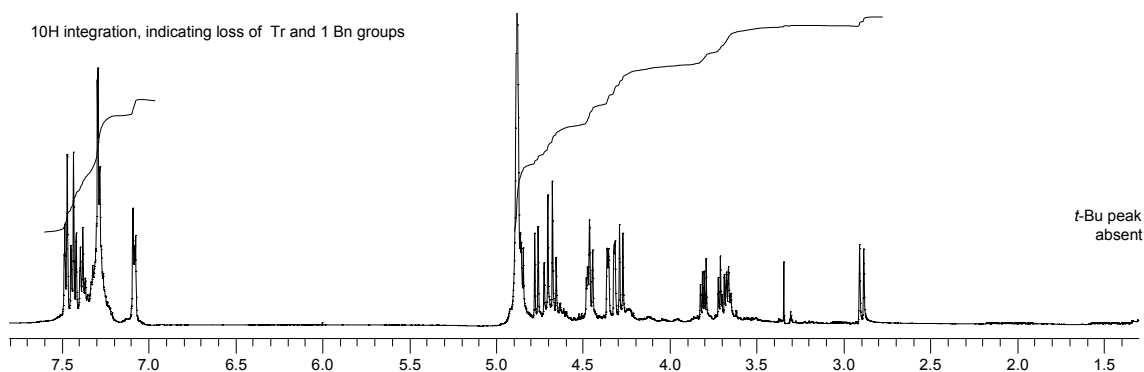


Figure 4.4. ^1H NMR (500 MHz, CD_3OD) spectrum of the major product.

A more detailed analysis of the NMR data provided some surprising observations. Firstly, there were two ^{13}C NMR methylene resonances (verified by a DEPT experiment) present in the spectroscopic region where OCH_2Ph ^{13}C nuclei typically resonate, instead of the expected three (Figure 4.5). Secondly, there was an absence of ^{13}C NMR resonances in the region where C-3 and C-4 methine carbons resonated in the analogous diol compounds of **93**

and **75** (Figures 4.5 and 4.6). Thirdly, there was an unusually downfield methine carbon resonance at 86.4 ppm, consistent with a carbon attached to either two oxygens or an oxygen and a nitrogen atom (Figure 4.5).

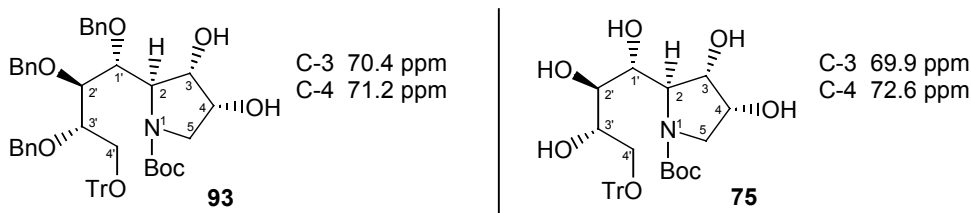
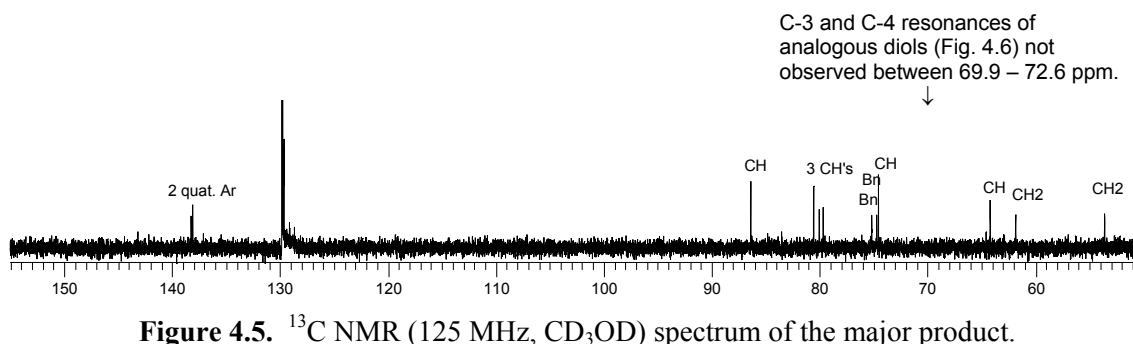


Figure 4.6. ^{13}C NMR chemical shifts (CDCl_3 , 75 MHz) of C-3 and C-4 carbinol carbons in the previously synthesized diols **93** and **75**.

Mass spectroscopic analysis of the major product gave a molecular ion of m/z 385 Da. Two possible compounds having such a molecular weight and loosely fitting the above NMR data were epoxide **105** and indolizidine **106** (Figure 4.7). However, these structures became obsolete for several reasons. Firstly, both compounds seemed unlikely to have a methine carbon capable of resonating at or close to 87 ppm in a ^{13}C NMR spectrum. Secondly, it was plainly counter-intuitive to suggest that an epoxide would not be opened under these acidic conditions, certainly not after a benzyl group had been lost. Thirdly, the indolizidine **106** would surely be soluble in chloroform, something that our product was not.

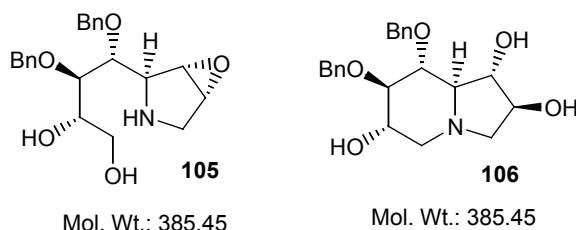
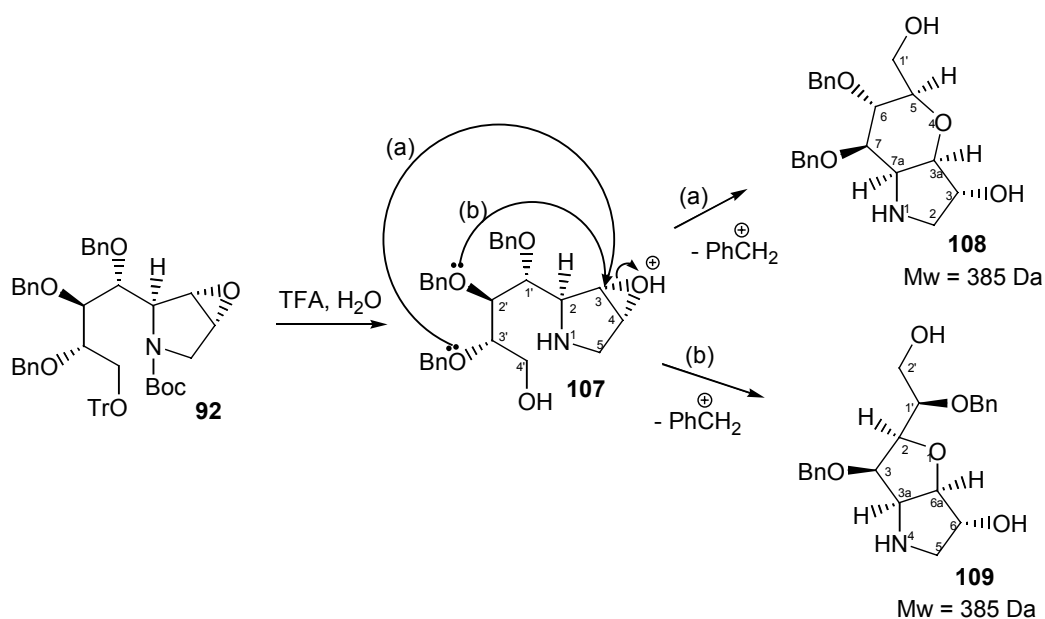


Figure 4.7. Possible structures for the major product of the epoxide ring-opening reaction.

After exploring alternate mechanisms in the reaction of **92** with TFA and water, it was proposed that one of the benzyl ether oxygen atoms could have participated in an S_N2 attack of the protonated epoxide **107** to form either a octahydropyrano[3,2-*b*]pyrrol-3-ol **108** or a hexahydro-2*H*-furo[3,2-*b*]pyrrol-6-ol **109** (Scheme 4.21). Such a process would liberate a benzyl cation, fulfilling the requirement of regioselective mono-*O*-debenzylation in the product.

Further analysis of the NMR data provided some identification to the structure of the product. Methylene protons vicinal to a nitrogen atom were identified based on their ^{13}C NMR chemical shifts in comparison to preceding compounds. A similar approach resulted in methylene protons vicinal to a primary alcohol group being identified. In a gCOSY experiment, these latter protons were found to couple with a methine proton resonating further upfield at 3.68 ppm. This observation ruled out **108** as the product because it was implausible for the H-5 proton in **108**, being vicinal to the pyranyl oxygen atom, to resonate at such an upfield frequency. Conversely, the methine proton resonating at 3.68 ppm could be assigned to H-1' in **109** because the corresponding proton in the starting material, H-3' in compound **92**, resonated at 3.96 ppm.

The above H-1' proton was found to couple to a methine proton with 'dt' multiplicity at 4.45 ppm. Although it would be more likely to see 'd' multiplicity for this proton, the possibility of long-range coupling cannot be ruled out, especially when one of the *J* values was a low 1.8 Hz. The chemical shift of H-2 is not unreasonable either, when compared to a similar proton (H-2, 4.92 ppm) in an analogous literature compound **110** (Figure 4.8).



Scheme 4.21. Alternate mechanisms of the epoxide ring-opening reaction.

A tentative assignment of all protons in **109** was completed and is shown in Figure 4.8. ^{13}C NMR assignments were made according to their associated coupling with protons in the gHSQC spectrum and Figure 4.9 shows the putatively assigned ^{13}C NMR spectrum. Literature compound **110** served as a useful guide in corroborating these assignments.¹⁵⁴ However, some significant inconsistencies remain with our assignments, including the fact that H-2 in **110** was α to two oxygen atoms, while in **109**, H-2 was α to one oxygen atom. Also, the resonance assigned to C-6a in the ^{13}C NMR spectrum seems too downfield while the C-2 resonance is unusually upfield. It should be noted that some of the 2D NMR data for **109** contained poorly resolved cross-peaks and was of limited help and in addition, there was no ^{13}C NMR data reported for the literature compound **110**. Therefore, we were not confident that structure **109** was the major product. However, based on a molecular weight of 385 Da, the major product was isolated in 51 % yield.

Please see print copy for Figure 4.8

Figure 4.8. ^1H NMR comparison of product **109** and an analogous literature compound **110**.¹⁵⁴

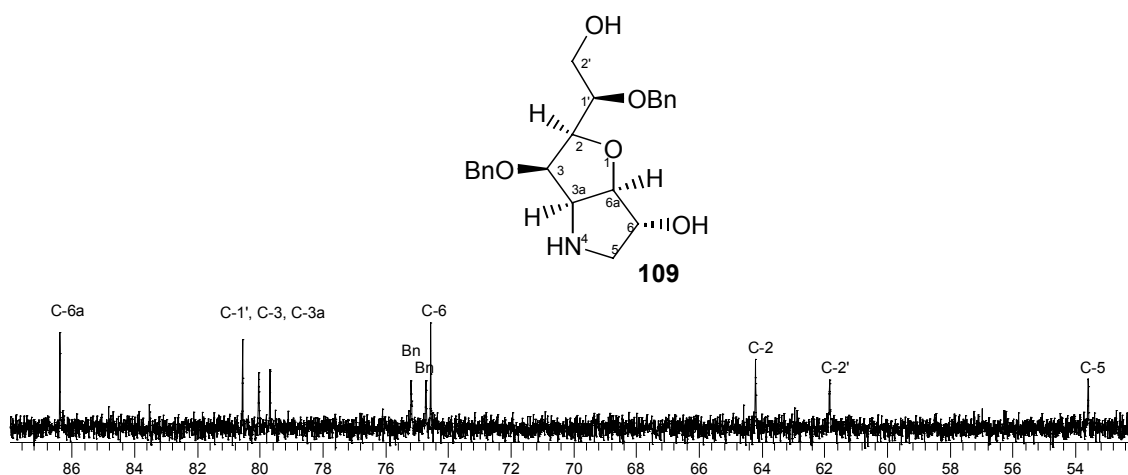


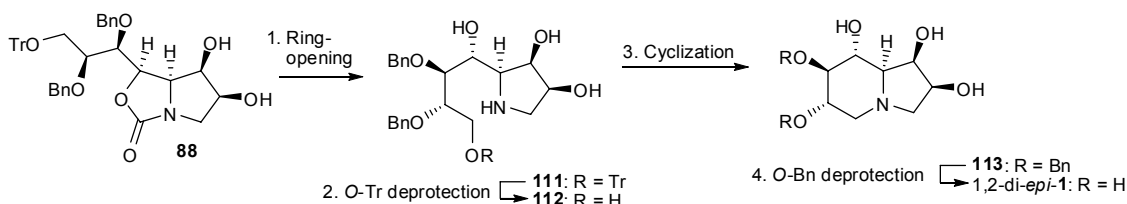
Figure 4.9. Assigned ^{13}C NMR spectrum (75 MHz, CDCl_3) of the major product.

After trying two different methods of generating a *trans*-diol, first with cyclic sulfate chemistry and second with epoxide chemistry, we decided to put this project aside and explore a synthesis of 1,2-di-*epi*-uniflorine A.

CHAPTER 5. Synthesis of putative 1,2-di-*epi*-1

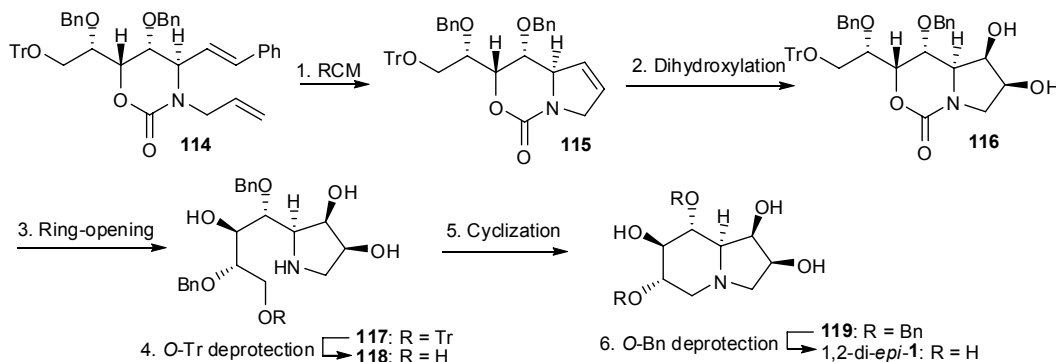
Although 1,2-di-*epi*-1 had already been synthesized by Fleet *et al.*,⁸³ it presented a good target to test the versatility of our new synthetic methodology. The successful synthesis of 1,2-di-*epi*-1 would be verified by comparison of its spectroscopic data with that in the literature.

For the synthesis of 1,2-di-*epi*-1, we considered an adaptation to the strategy for the synthesis of 1-*epi*-1, which involved the use of cyclic sulfate methodology with oxazalone **88** (see Scheme 4.7). Although compound **88** was not synthesized, it potentially represented an advanced intermediate in the proposed synthesis of 1,2-di-*epi*-1. The remaining steps required to access 1,2-di-*epi*-1 from **88** included oxazalone ring-opening, *O*-Tr deprotection, Appel cyclization and de-*O*-benzylation (Scheme 5.1).

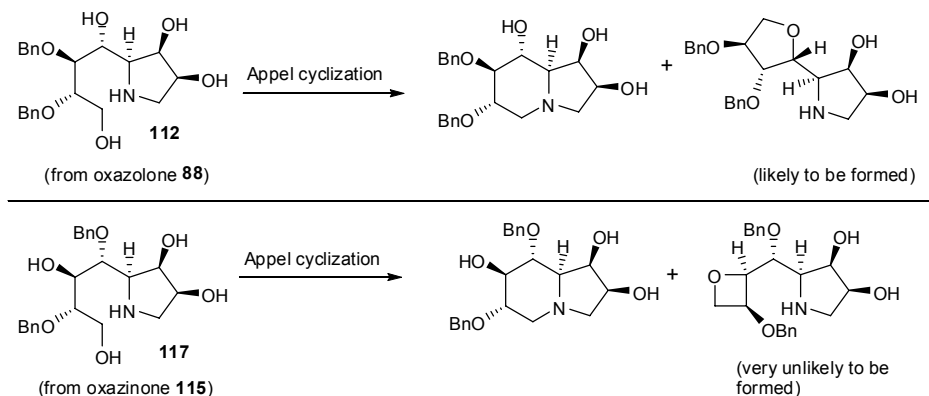


Scheme 5.1. Strategy for the synthesis of 1,2-di-*epi*-1 from oxazalone **88**.

Similarly, the above methodology could be applied to oxazinone **115**, which in turn could be accessed from the enantiomer of oxazinanone **57** (Scheme 5.2). The oxazinone methodology had a certain advantage over the oxazalone methodology. Chapter 2 demonstrated that subjecting the unprotected C-1 carbinol in **42** to cyclization conditions, resulted in this hydroxyl group reacting to form the unwanted furan **44** (see Section 2.5). The same event could happen in the cyclization of **112** but not in the case of **117** (Scheme 5.3). However, we chose to pursue the oxazalone approach also to compare the differences obtained from the oxazalone and oxazinone methodologies.

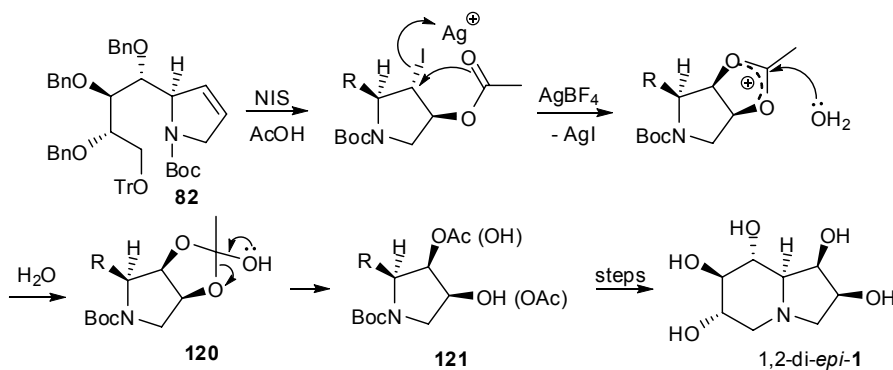


Scheme 5.2. A strategy for the synthesis of 1,2-di-*epi*-1 via an oxazinone **116** intermediate.



Scheme 5.3. Oxazinone **115** and oxazolone **88** approaches for the synthesis of 1,2-di-*epi*-1.

Also considered was a completely different methodology, derived from the silver salt chemistry developed by Prevost, and discussed in Section 4.2. Woodward *et al.* has also developed a method using a silver(I) salt, specifically AgBF_4 , in conjunction with water, to convert a *trans*-iodoacetate into a *cis*-hydroxyacetate.¹⁵⁵ The first half of the mechanism for this reaction is identical to that of the Prevost reaction (see Scheme 4.5). That is, the combination of NIS and acetic acid, reacting with an olefin, generates a *trans*-iodoacetate. In the case of olefin **82**, the initial iodium ion would probably be formed on the α -face, due to the steric influence of the C-2 R group (Scheme 5.4). The strong ionic bond formed between silver(I) and iodide drives the attack of the acetoxyl oxygen atom onto C-3, generating a resonance stabilized carbenium ion. Hereon, the mechanism is unique to Woodward. Instead of the Prevost method of having acetate perform an $\text{S}_{\text{N}}2$ attack at the least hindered sp^3 carbon (C-4 in Scheme 5.4), Woodward's reaction involves attack of water at the sp^2 carbenium ion, resulting in the retention of the *cis*-diol stereochemistry. Winstein *et al.* first observed this interesting effect of water on acetoxyl groups.¹⁵⁶ Collapse of the orthomonoacetate **120** to form a *cis*-hydroxy acetate **121** is not regiospecific, thus a mixture of regioisomers results. However, hydrolysis of this mixture would provide a single diol product.

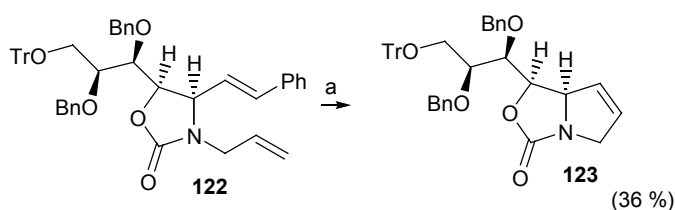


Scheme 5.4. Plan for the synthesis of 1,2-di-*epi*-1 using the Woodward reaction.

From the two methodologies presented above, we decided to proceed with the oxazolone/oxazinone approach, mainly because we had more experience with it. Also, we were dissuaded from using Woodward's reaction by numerous literature reports that cited problems including poor facial selectivity of *epi*-iodination in cyclic substrates,^{157,158} low reactivity of the halo acetate due to steric constraints,¹⁵⁹ and low yields.¹⁶⁰

5.1. RCM of oxazolidinone **122**

A trial RCM reaction of oxazolidinone **122** and 10 mol % of Grubbs' I catalyst was sluggish, with unconverted substrate remaining after 3 d at reflux in DCM. An additional 10 mol % of Grubbs' I catalyst was added to the reaction, but the TLC pattern remained the same. The ring-closed product **123** was isolated from the reaction, and was verified by ¹H NMR and ESI MS analyses. However, the yield for **123** was only 36 %. Strangely, there was no evidence of **122** following FCC of the crude product. Material corresponding to the most polar spot from TLC analysis was isolated and represented a significant mass recovery (31 %). Although not fully characterized, it represented a de-*O*-Tr RCM product.



Reagents and conditions: (a) 10-20 mol % Grubbs' I cat., DCM 0.01 M, reflux, 4d.

Scheme 5.5. Results for the RCM of oxazolidinone **122** with Grubbs' I catalyst.

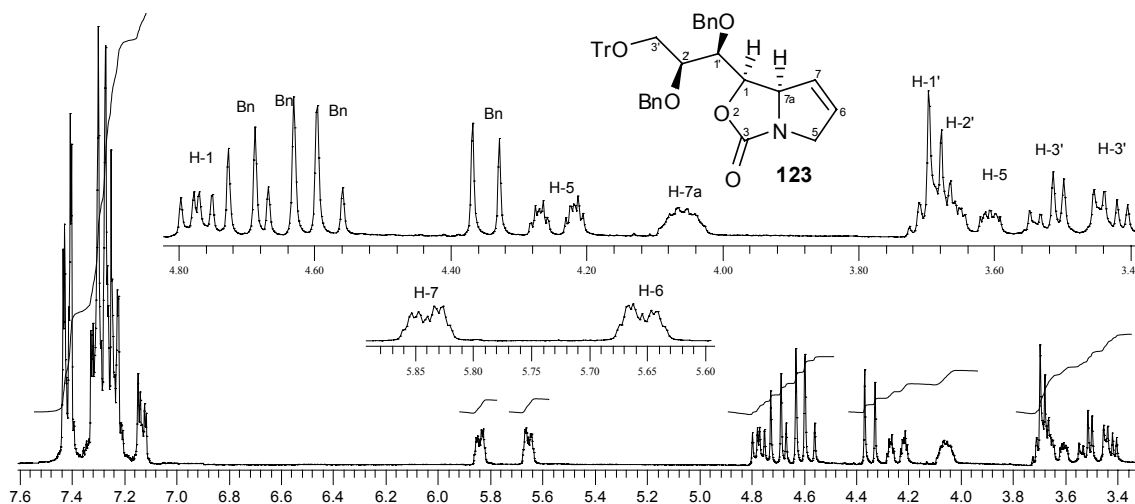
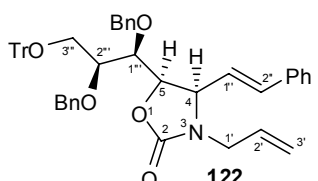
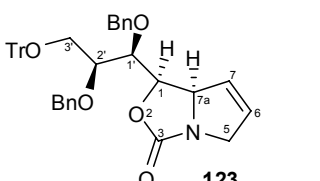


Figure 5.1. ¹H NMR spectrum of the oxazoline **123** (300 MHz, CDCl₃).

When comparing the ^1H NMR chemical shifts for the corresponding protons in the substrate and product, there was only one proton that changed significantly. The chemical shift for H-7a in **123** was 0.48 ppm downfield of the corresponding proton H-4 in **122** (Table 5.1).

Table 5.1. ^1H NMR chemical shifts of corresponding protons in **122** and **123**.

122	δ ^1H (ppm) ^a	123	δ ^1H (ppm) ^a
1'	4.10, 3.32	5	4.27, 3.63
4	3.58	7a	4.06
5	4.75	1	4.81
1''	3.96	1'	3.73-3.67
2''	3.75	2'	3.73-3.67
3''	3.43, 3.37	3'	3.56, 3.47

a: (300 MHz, CDCl_3)

The poor yield was not surprising given the difficulty co-worker Minyan Tang had in a Grubbs' I catalysed RCM reaction with a similar substrate. Tang *et al.* reported the poor conversion of an oxazolidinone to an oxazolone, using 5-10 mol % of Grubbs' I catalyst.²⁵ The yield was improved to 73 % by initially adding 25 mol % of Grubbs' I catalyst, followed by adding a further 25 mol % after 24 h, and stirring at reflux for a total of 48 h (Scheme 5.6).

Please see print copy for Scheme 5.6

Scheme 5.6. Literature example of RCM of an oxazolidinone with Grubbs' I catalyst.²⁵

Rather than optimize the reaction of **122** with Grubbs' I catalyst, we elected to experiment with Grubbs' II catalyst, given its reputation for enhanced activity. In the event, RCM of **122** with Grubbs' II catalyst resulted in higher yields of the ring-closed product **123**, in one instance a 90 % yield was obtained. Table 5.2 shows that the yields varied but were certainly much higher than the corresponding yield for the reaction with Grubbs' I catalyst. In addition, the reaction time was not optimized but was noticeably reduced compared to the

Grubbs' I reaction. One experiment used only 3.5 mol % of catalyst, due to an underestimate of the quantity of catalyst held in stock. The yield was 73 %, although a significant quantity of substrate (22 %) was recovered. This was something noticed in many of the reactions tried, even at 10 mol %, over time the catalyst appeared to become inactive, resulting in the incomplete conversion of the substrate. An explanation for this is discussed in Section 5.3.

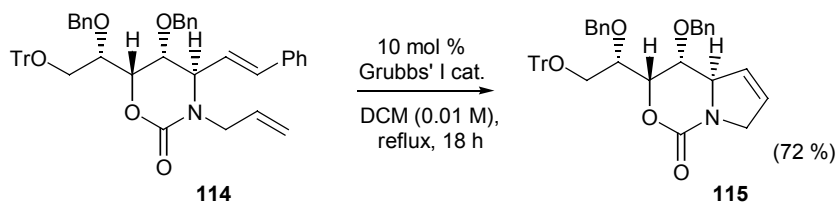
Table 5.2. Results for the RCM of **122** with Grubbs' II catalyst.

122 $\xrightarrow[\text{DCM (0.01M), reflux}]{\text{Grubbs' II cat.}}$ **123**

entry	cat. loading	time	yield of 123
1	10 mol %	24 h	90 %
2	10 mol %	18 h	63 %, (TLC analysis showed substrate present but it was not recovered)
3	3.5 mol %	18 h	73 %, (substrate recovered, 22%)

5.2. RCM of oxazinanone **114**

We anticipated that the RCM of oxazinanone **114** would be more efficient than that of the previous oxazolidinone **122** reaction because a less ring-strained 5,6-*cis*-fused bicyclic ring was being formed instead of a 5,5-*cis*-fused bicycle. Our hypothesis was validated after treatment of **114** with 10 mol % Grubbs' I catalyst in refluxing DCM over 18 h gave **115** in 72 % yield (Scheme 5.7).



Scheme 5.7. Result for the RCM of **114** with Grubbs' I catalyst.

5.3. Differences in Grubbs' I and II catalyst activities

The difference in efficiency of the Grubbs' I and II catalysts in the RCM of **122** and **114** reflect literature reports as there appeared to be a subtle interplay between thermodynamic and kinetic factors. Ring-strain energies may be a factor, and it would be expected that the energy required to form the oxazolone **123** is higher than that required to form the oxazinone **115**. However, the extent to which we can speculate on the thermodynamic properties of these RCM reactions is limited by the lack of temperature variation in our experiments. All reactions were carried out in DCM solution stirred at reflux temperature.

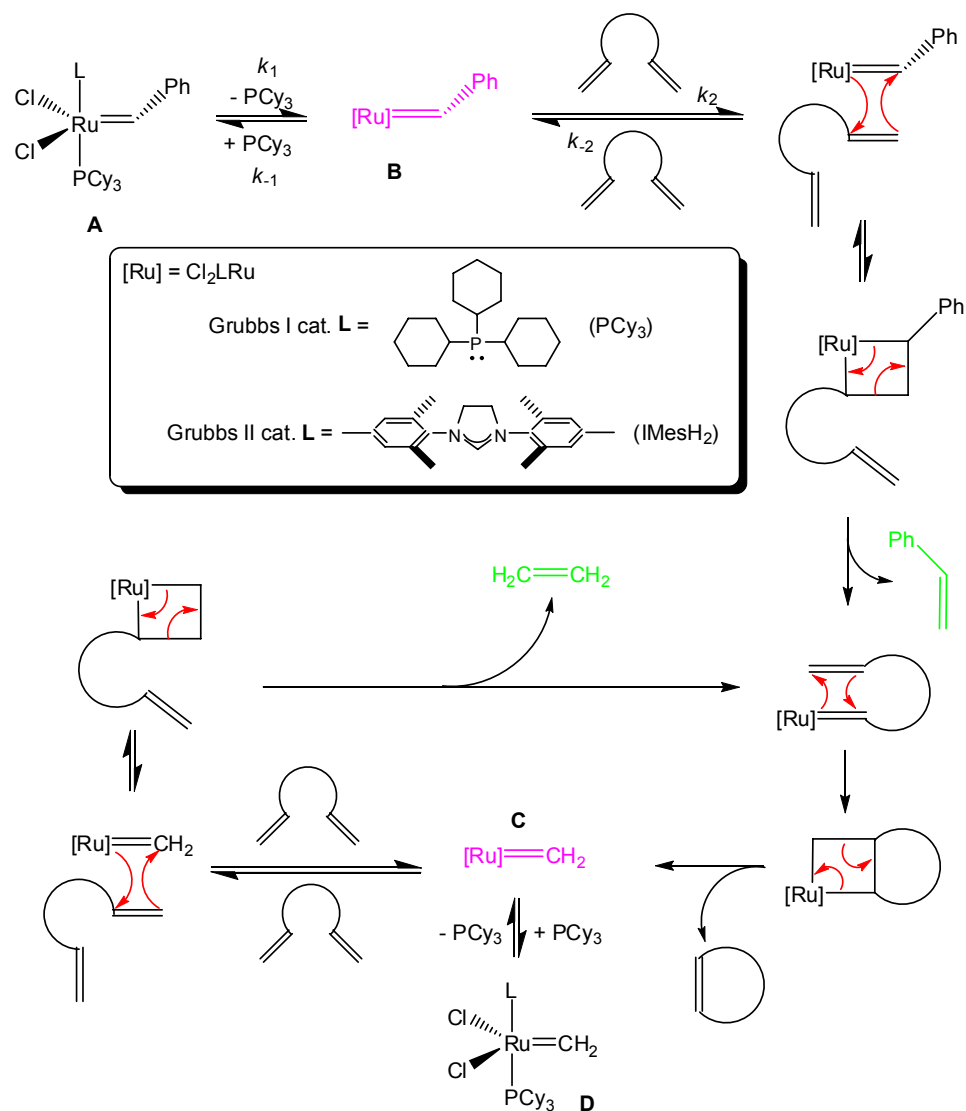
Due to the comprehensive work done by the Grubbs' group, the kinetics of Grubbs' I and II catalysts have been thoroughly investigated.¹⁶¹⁻¹⁶⁵ As such, a detailed study of the activity differences has been made on the basis of the rates of the formation of the discrete species included in the metathesis mechanism.

The mechanism begins with dissociation of the phosphine ligand, PCy₃, from **A** to give a 4-coordinate, 14-electron complex (species **B** in Scheme 5.8).¹⁶⁴ For Grubbs' I catalyst, species **B** is formed frequently (k_1 is large) but recoordination of free PCy₃ is competitive with substrate binding ($k_{-1}/k_2 \gg 1$).¹⁶⁴ Hence the active species performs few catalytic turnovers before being quenched with free PCy₃.

For Grubbs' II catalyst, the dissociation of PCy₃ occurs relatively inefficiently (k_1 is small).¹⁶⁴ However once PCy₃ comes off, coordination of olefinic substrate is facile compared to re-binding of PCy₃ ($k_{-1}/k_2 \sim 1$ and [olefin] is high).¹⁶⁴ Thus, the active species performs multiple catalytic turnovers before being quenched with free PCy₃.

Indeed the kinetic data for the two catalysts indicate that Grubbs' I catalyst initiates (k_1) 640-fold faster than Grubbs' II catalyst.¹⁶³ However, Grubbs' II catalyst has a 4 orders-of-magnitude higher turnover than Grubbs' I catalyst, giving it the greater overall activity.¹⁶³

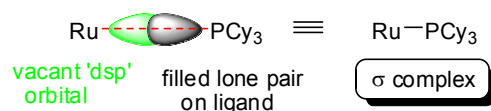
The differences in initiation and turnover for the two catalysts are caused to a large extent, by the electronic influence exerted from the L ligand. For Grubbs' II, this ligand is in the form of what is commonly referred to as *N*-heterocyclic carbene (NHC), in reference to a series of NHC variants Grubbs' and co-workers have produced. In Grubbs' I catalyst the L ligand is PCy₃, identical to that which dissociates upon initiation. NHCs are known to be excellent donor ligands relative to trialkylphosphines. Studies on Pd(0) – olefin complexes containing either NHC or phosphine ligands, indicate that the NHCs promote and stabilize metal-to-olefin back-bonding to a much greater extent than the phosphine ligands. This phenomenon is consistent with the observation made by Grubbs' *et al.* that the NHC complexes displayed increased affinities for π -acidic olefinic substrates relative to σ -donating PR₃.^{163,164}



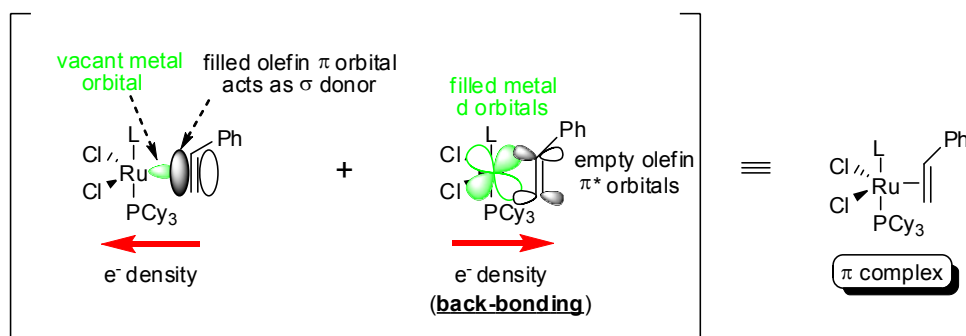
Scheme 5.8. Mechanism of the RCM reaction of a diene with either Grubbs' I or II catalyst.

5.3.1. Back-bonding

In transition-metal complexes, the majority of ligands contain a lone-pair of electrons in a filled sp^n type orbital, which can overlap with a vacant metal 'dsp' orbital, to form a σ -bond (Scheme 5.9).¹⁶⁶ This causes an increase of electron density on the metal atom. For an unsaturated ligand like an alkene, the ligand approaches the metal centre in a sideways fashion and overlaps the vacant metal orbital with its occupied π -orbital. Effectively, the filled π -orbital from the ligand acts as a σ -donor. However, there can also be a concomitant bonding operation from filled d-orbitals on the metal, to the empty π^* -orbital of the ligand. In this instance, the π^* orbital is a relatively low energy one, thereby reducing the energy differential between it and the metal orbital, allowing bonding to occur (Scheme 5.10).



Scheme 5.9. Formation of a σ -bond between a metal and ligand.



Scheme 5.10. Types of bonding involved in Grubbs' I and II catalysts.

Another factor affecting the activities of Grubbs' I and II catalysts is the metathesis inducing activity of the propagating catalytic species **C** (Scheme 5.8). In both catalysts, the original carbene ligand is benzyldiene, which gets converted to methyldiene in the propagating species **C**. Methyldiene complexes **C** (PCy_3) and **C** (IMesH_2) are extremely poor initiators for olefin metathesis at ambient temperatures.^{163,164} In particular, if **C** (IMesH_2) becomes trapped with free PCy_3 , it essentially becomes incapable of re-entering the catalytic cycle.^{163,164}

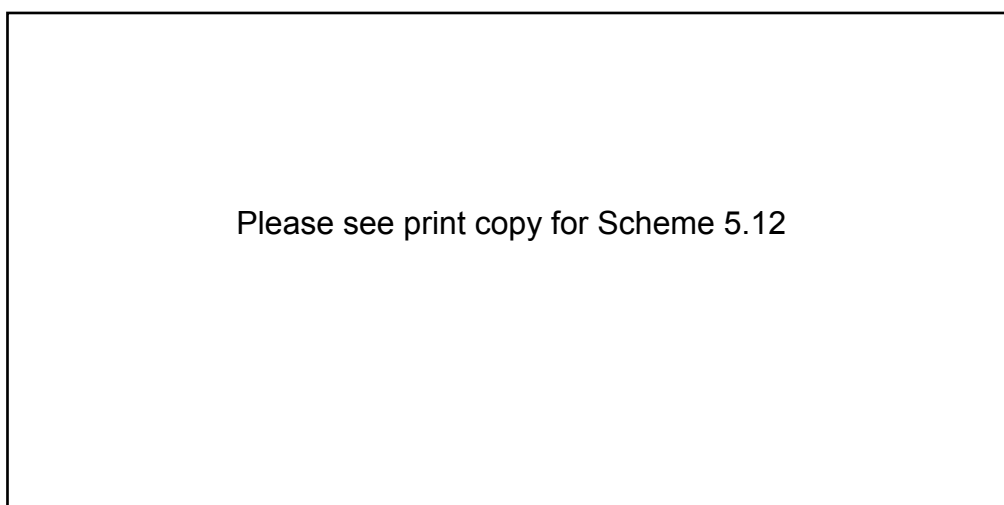
It has been demonstrated that the initiation kinetics of catalysts **A** (PCy_3) and **A** (IMesH_2) may also be linked to the decomposition rates of these complexes. The thermal decomposition of **A** (PCy_3) has been studied in detail and has been proposed to occur *via* phosphine dissociation followed by bimolecular coupling of two 4-coordinate ruthenium species (Scheme 5.11).¹⁶⁷

Please see print copy for Scheme 5.11

Scheme 5.11. Decomposition pathway for Grubbs' I catalyst.¹⁶⁷

The rate of decomposition is second order in species **E**, making it extremely sensitive to the concentration of **E** in solution, especially when the concentration of substrate is low. Conversely, Grubbs' II catalyst displays much greater thermal stability, probably due to reduced rates of phosphine dissociation.

Perhaps counter-intuitively, the methyldiene complexes **D** (PCy_3) and **D** (IMesH_2) decompose relatively rapidly despite displaying very slow rates of initiation. Unlike complex **B** (PCy_3), decomposition of **D** (IMesH_2) does not occur *via* the loss of a phosphine. Its decomposition has been demonstrated to be first order and has been proposed to proceed *via* a rather elaborate intramolecular C-H activation of its coordinated PCy_3 ligand (Scheme 5.12).¹⁶⁸

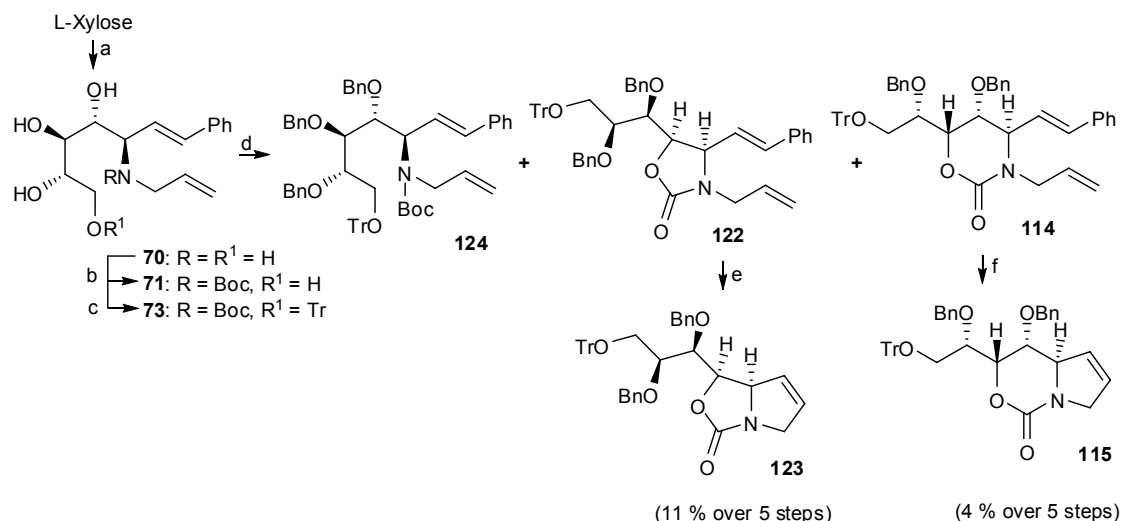


Scheme 5.12. Decomposition pathway for Grubbs' II catalyst.¹⁶⁸

To summarize, the two main factors differentiating Grubbs' I and II catalysts are that, although slower to initiate, Grubbs' II catalyst facilitates more catalytic cycles before free PCy_3 recoordinates to Ru; and Grubbs' II catalyst has a greater thermal stability.

5.4. Methods for improving access to oxazinone **115**

The overall yield to **115** from L-xylose was 4 % (Scheme 5.13). Clearly a different approach was required to access this compound in a more efficient manner. Two different methods were experimented with, one similar to the existing methodology in its use of a reactive *N*-Troc protecting group; and another that was a more direct route, using triphosgene.



Scheme 5.13. Results for the synthesis of **123** and **115** using *N*-Boc methodology.

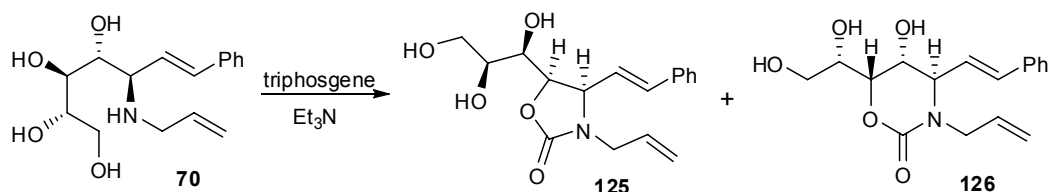
5.4.1. Triphosgene method

Phosgene has been widely employed in the acylation of amines. However, handling this compound is notoriously dangerous. Eckert *et al.* first reported the use of triphosgene as a much safer substitute for phosgene reactions.¹⁶⁹ Our laboratory had experience using triphosgene with Karl Lindsay converting a 1,2-amino alcohol to an oxazolidinone, in the synthesis of swainsonine (Scheme 5.14).²⁴

Please see print copy for Scheme 5.14

Scheme 5.14. Using triphosgene to form an oxazolidinone by Lindsay *et al.*²⁴

Based on this example, we decided to experiment with the delivery of an oxazolidinone or oxazinanone directly from the Petasis product **70**. Of course, the highly reactive nature of triphosgene in all likelihood meant that formation of the product would not be regio-specific (Scheme 5.15). Nonetheless, it was worth an investigation to see if the ratio of oxazinanone to oxazolidinone could be increased.



Scheme 5.15. Proposed synthesis of **125** and **126** from **70** using triphosgene.

In the event, reaction of **70** with triphosgene (0.33 equiv.) did not furnish any oxazinanone **126**. Oxazolidinone **125** was isolated in a modest 45 % yield, together with two other products of reduced polarity (Figure 5.2). MS analysis of these minor products indicated that both had a molecular weight of 345 Da, corresponding to 26 Da or one carbonyl unit minus two protons, greater than the mass of **125**. Hence, each of the two side-products contained a cyclic carbonate moiety, in addition to the oxazolidinone moiety.

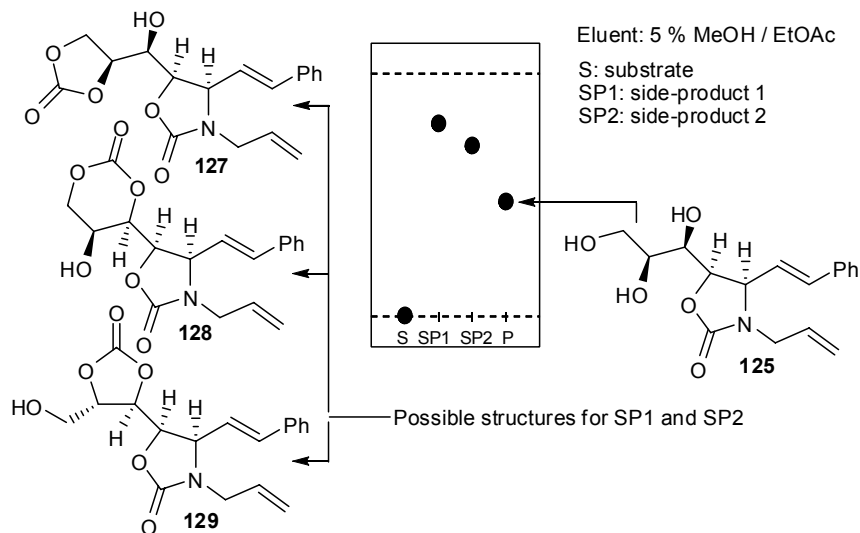


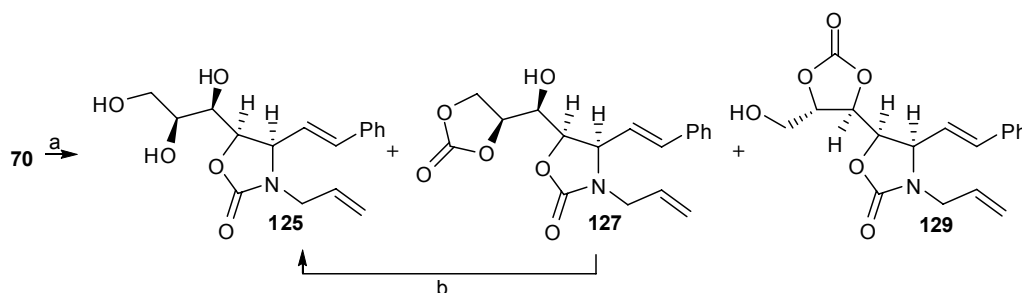
Figure 5.2. Desired oxazolidinone **125** and three other candidates for the two side-products.

With three hydroxyl groups free to participate in the formation of a cyclic carbonate, there were three possible products (Figure 5.2). It was intuitive to expect that the primary hydroxyl group in **125** would participate in both side-product formations, potentially yielding dioxolanyl-oxazolidinone **127** and dioxanyl-oxazolidinone **128**. However, one other possible isomer was the primary alcohol **129**, resulting from the reaction of the two secondary hydroxyl groups.

Distinguishing between the pair of dioxolanyl and dioxanyl candidates and primary alcohol **129** was swiftly achieved by comparing the ^{13}C NMR chemical shifts of the most downfield methylene carbon (Table 5.3). Specifically, the ^{13}C NMR chemical shift for C-1''' in **129** should have resonated in the region of 60-65 ppm, while C-5'''' in **127** and C-6''' in **128** should have resonated further downfield given they are both α to an oxycarbonyl group. Side-product 2 had its most upfield ^{13}C NMR methylene resonance at 60.8 ppm, confirming it to be the primary alcohol **129**, while side-product 1 had its most downfield ^{13}C NMR methylene resonance at 67.3 ppm.

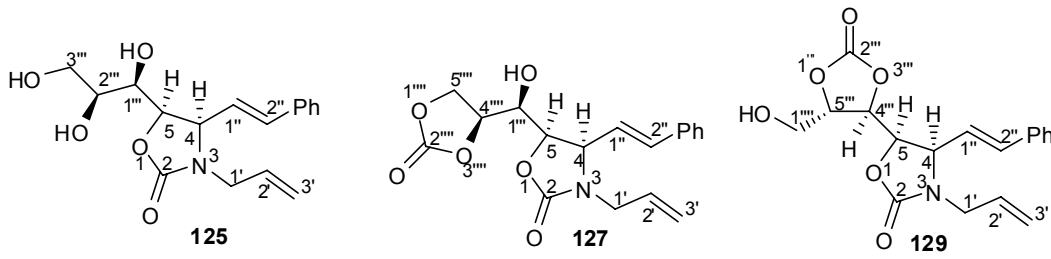
Identifying side-product 1 from the possible structures **127** and **128** was possible by analysing the ^1H - ^1H couplings in its COSY NMR spectrum. For this side-product to be compound **127**, a ^1H - ^1H coupling between the H-5'''' methylene protons and methine proton H-4'''' was required. In turn, H-4'''' should have had its attached ^{13}C nucleus resonating in the region of 78-83 ppm of the ^{13}C NMR spectrum. Secondly, a ^1H - ^1H coupling between the previously identified H-5 proton and H-1''', a CHOH proton, was necessary. Proton H-1''' itself should have had its attached ^{13}C nucleus resonating in the CHOH region of 70-75 ppm. Both of these criteria were met, indicating that the side-product was indeed dioxolanyl-oxazolidinone **127**.

The yields for the three products from the reaction of **70** with triphosgene were 45 % for oxazolidinone **125**, 11 % for the dioxolanyl-oxazolidinone **127** and 7 % for the primary alcohol **129**. More of **125** was obtained by subjecting **127** to base hydrolysis at rt (Scheme 5.16). The yield of this reaction was 70 %, increasing the overall yield of **125** to 53 %.



Reagents and conditions: (a) Triphosgene, Et_3N , THF, rt, 10 h, **125** (45 %); **127** (11 %),
(b) K_2CO_3 , MeOH, rt, 3 d, (70 %, 53 % total over steps a and b).

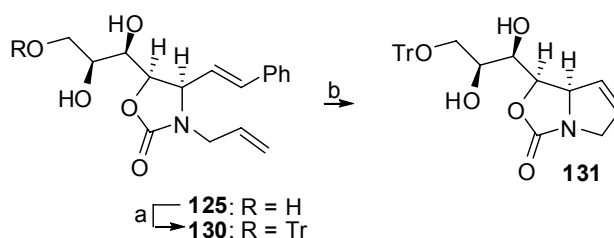
Scheme 5.16. Results for the synthesis of oxazolidinone **125** from Petasis product **70**.

Table 5.3. NMR chemical shifts for selected corresponding nuclei in **125**, **127** and **129**.


125^a		127^a		129^b	
nucleus	chemical shift (ppm)	nucleus	chemical shift (ppm)	nucleus	chemical shift (ppm)
C-2	159.8	C-2	162.1	C-2	156.3
		C-2''''	159.9	C-2''''	154.1
C-3''''	64.1	C-5''''	67.3	C-1''''	60.8
H-3''''	3.65, 3.57	H-5''''	4.48, 4.45	H-1''''	3.79, 3.64
C-2''''	73.3	C-4''''	78.0	C-5''''	78.4
H-2''''	3.73	H-4''''	4.88	H-5''''	4.71

a: in CD₃OD, ¹H NMR at 500 MHz, ¹³C NMR at 125 MHz
b: in CDCl₃, ¹H NMR at 300 MHz, ¹³C NMR at 75 MHz

O-Tritylation of the primary hydroxyl group in **125** resulted in a good yield (75 %) of **130**, using the standard conditions previously described in Section 3.4. The subsequent RCM step gave a moderate yield (66 %) of **131** but, as in the case of the RCM of **122**, the reaction failed to go to completion (Scheme 5.17).

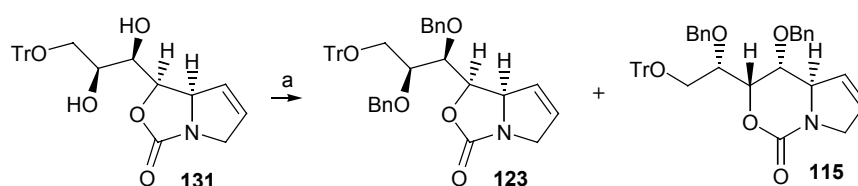


Reagents and conditions: (a) TrCl, pyridine, DCM, rt, 14 h, 75 %;
(b) Grubbs' II catalyst, DCM, reflux, 18 h, 66 %.

Scheme 5.17. Results for the *O*-Tritylation of **125** and RCM of **130**.

Subsequent di-*O*-benzylation of **131** produced an intriguing result. Based on the conditions outlined previously for *O*-benzylation, the reaction was conducted at 0 °C for 2 h then at rt for 14 h. TLC analysis of the crude product showed complete consumption of the substrate and the presence of seven new spots. The two major fractions were isolated by FCC and characterized in a straightforward manner by NMR and MS analysis. The slightly less

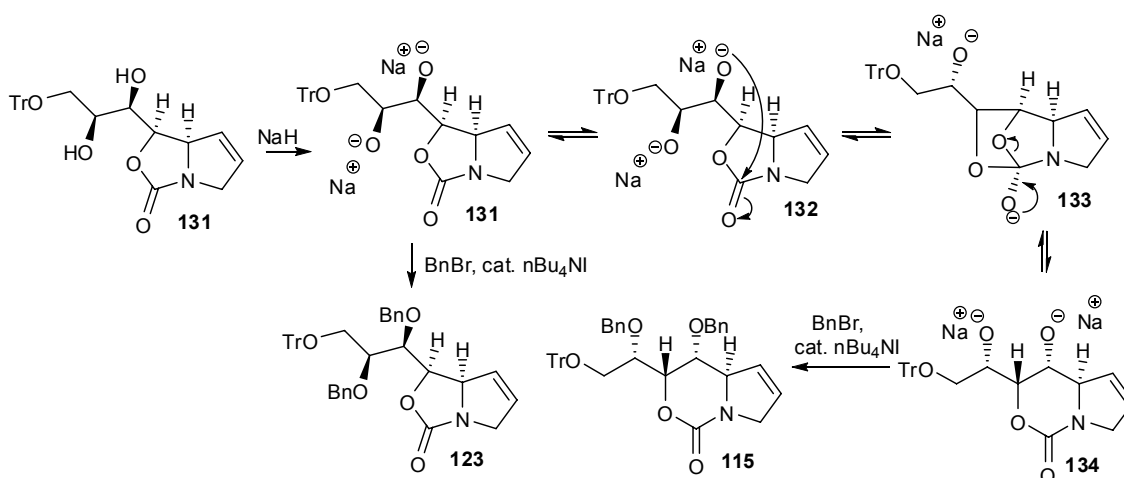
polar of the two major products was the desired oxazolone **123**, which was authenticated by comparing its ^1H NMR spectrum to that of the same compound previously synthesized in Section 5.1. In a similar manner, the other major product was determined to be the oxazinone **115**, by having an identical ^1H NMR spectrum to that of the same compound isolated in Section 5.2. Yields for **123** and **115** were 22 % and 26 %, respectively (Scheme 5.18). Contributing to the poor yield of **123** and **115** were at least five other minor products, which were not characterized.



Reagents and conditions: (a) NaH, BnBr, *n*Bu₄NI, THF, 0 °C, 2h, then rt, 14 h, **123** (22 %) and **115** (26 %).

Scheme 5.18. Results for the di-*O*-benzylation of **131**.

Generation of oxazinone **115** from this reaction was entirely unexpected, which prompted us to think in more detail about the reaction. Section 4.1 demonstrated that tri-*O*-benzylation of **74**, an analogous substrate with its *N*-Boc group conformationally restricted within a 2,5-dihydropyrrole ring, did not result in any production of an oxazolone or oxazinone (Scheme 4.2). Yet in the reaction above with an even more constrained substrate, the result included an attack of the C-1' hydroxyl group in **132** onto the carbonyl carbon (Scheme 5.19). Evidently, the isolation of the desired oxazolone **123** indicated that there was an equilibrium formed between the alkoxide species **132** and the alkoxide species **134**.

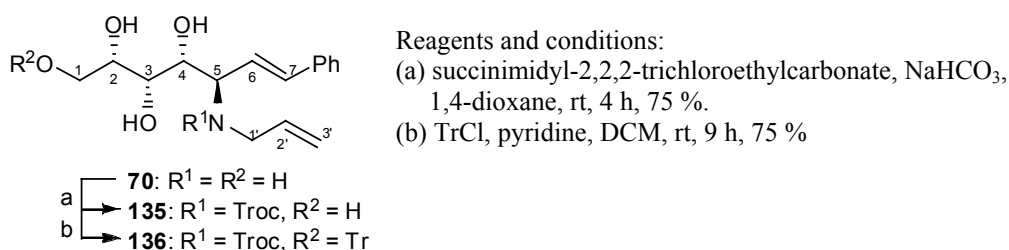


Scheme 5.19. Proposed mechanism for the formation of oxazinone **115** from oxazolone **123**.

5.4.2. The 'N-Troc' method

This approach was analogous to the earlier *N*-Boc methodology that generated oxazolidinone **56** and oxazinanone **57** (Scheme 3.8). We thought it would be interesting to observe the effect of changing the leaving group from *tert*-butoxide in the *N*-Boc group to something more labile. After considering several alternatives, we settled upon 2,2,2-trichloroethylcarbonate (Troc) as a new group to protect the nitrogen atom in **70**.

In the event, *N*-Troc protection of **70** using succinimidyl-2,2,2-trichloroethylcarbonate, gave **135** in 75 % yield (Scheme 5.20). However, in this particular instance the reaction was conducted on a large (14.25 g) scale. All other reactions were conducted on a much smaller scale (< 1 g) and the yields obtained ranged between 40 % and 50 %.



Scheme 5.20. Results for the *N*-Troc protection of **70** and *O*-Tr protection of **135**.

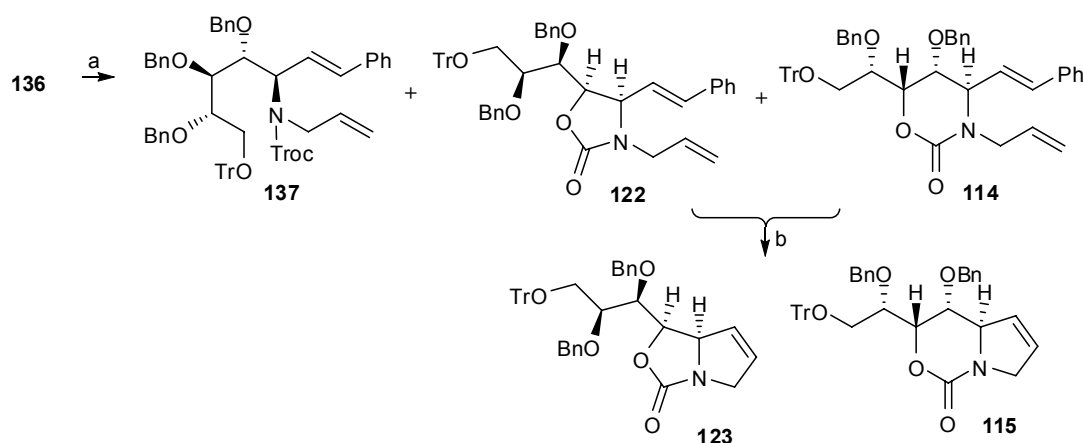
Characteristic ¹H NMR resonances of the methylene unit in the *N*-Troc moiety in **135** (and subsequent compounds) included two discrete protons exhibiting doublet multiplicity between 4.70 and 4.85 ppm. While in the ¹³C NMR spectra, characteristic resonances were found at 154 ppm and 95 ppm for the carbonyl and tri-chloro substituted quaternary carbons, respectively.

O-Trityl protection of the primary hydroxyl group in **135** proceeded smoothly, resulting in a 75 % yield of **136** (Scheme 5.20). Unlike the *O*-Tr protection of **47** in Section 3.4, the reactions conducted on **135** were in DCM with only 1.1 equiv. of pyridine. This was to avoid potential problems associated with the removal of large quantities of pyridine in the work-up of large-scale reactions. Similarly, the quantity of TrCl used was reduced to 1.05 equiv., instead of the 2.0 equiv. used in Section 3.4. The fact that the yield obtained under the new conditions was close to the yield obtained under the earlier conditions was particularly welcomed, as it reduced the expenditure of TrCl as well as improving the safe handling of the reaction.

The conditions for the *O*-benzylation of **136** were unchanged from those described in Section 3.5. However, the reaction was complete after 1 h at rt, much faster than the 18 h required for the *O*-benzylation of **48**. Predictably, the pattern of new spots in the TLC analysis mirrored that of the *O*-benzylation of **48** (see Figure 3.3). In Section 3.5, the separation of

oxazolidinone **56** and oxazinanone **57** required repeated purification due to their similar R_f values. In Sections 5.1 and 5.2, the isolation of oxazolone **123** and oxazinone **115** provided the knowledge that their individual R_f values had a significantly increased difference, over their oxazolidinone and oxazinanone precursors. Hence, we anticipated that it would be more efficient to separate a mixture of **122** and **114** from the tri-*O*-benzylated **137**, and then conduct a RCM reaction using Grubbs' II catalyst on the mixture of **122** and **114**.

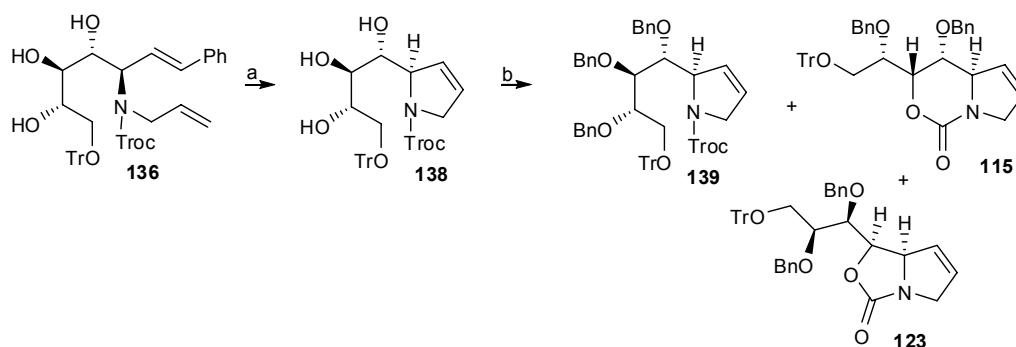
In the event, the RCM of the mixture of **122** and **114** proceeded smoothly, resulting in the complete conversion of starting material over 24 h, in DCM at reflux and with a Grubbs' II catalyst loading of 5 mol %. Given that the oxazolidinone and oxazinanone components of the starting material had the same molecular weight, a yield for the combined mass of oxazolone and oxazinone products could be obtained, and was calculated to be 84 %. Purification by FCC easily separated **123** and **115**. The combined yield over the *O*-benzylation and RCM steps was 39 % for oxazolone **123** and 31 % for oxazinone **115** (Scheme 5.21)



Reagents and conditions: (a) NaH, BnBr, *n*Bu₄NI, THF, rt, 1 h, **137** (not isolated); (b) Grubbs' II catalyst, DCM, reflux, 24 h, **123** (39 % over 2 steps) and **115** (31 % over 2 steps).

Scheme 5.21. Results of the *O*-Benzylation of **136**, and subsequent RCM of an isolated mixture of **122** and **114**.

To see if performing the last two reactions in the reverse order would provide a better yield of **123** and **115**, diene **136** was treated with Grubbs' I catalyst to give **138** (76 %) followed by *O*-benzylation to give **139** (not isolated), **123** (15 %) and **115** (14 %) (Scheme 5.22). The combined yields for these steps was 11 % for **123** and 14 % for **115**, significantly less than combined yields represented in Scheme 5.21. This was not a surprising result however, as Section 3.8 demonstrated that the *O*-benzylation of **59**, a substrate in which its *N*-Boc group was conformationally restricted within a 2,5-dihydropyrrole ring, resulted in a 0 % yield for **123** and **115**.



Reagents and conditions: (a) Grubbs' I catalyst, DCM, reflux, 12 h, 76 %; (b) NaH, BnBr, *n*Bu₄NI, THF, 0 °C, 2 h, **139** (not isolated) **123** 15 % (11 % over 2 steps) and **115** 18 % (14 % over 2 steps).

Scheme 5.22. Results of the RCM of **136** and subsequent *O*-Benzoylation of **138**.

5.4.3. Comparison of the different methods for accessing **123** and **115**

The purpose of trying the triphosgene and *N*-Troc approaches was to improve the overall yield for oxazinone **115**. For interest sake, the effect these approaches had for the overall yield of oxazolone **123** was also observed. Table 5.4 shows the decreased yield for **123** and the slightly improved yield for **115**, associated with the triphosgene method. Given that there was no oxazinanone obtained in the first step of this approach, it was remarkable that at the end of the synthesis, the yield of oxazinone **115** was greater than the yield of oxazolone **123**.

Clearly, within this study, the optimal approach for accessing **115**, as well as **123**, was *via* the *N*-Troc approach. Improving the efficiency for the synthesis of **115**, by 13 % over the original *N*-Boc method, facilitated a sufficient quantity to proceed with the remaining steps for the synthesis of 1,2-di-*epi*-**1**.

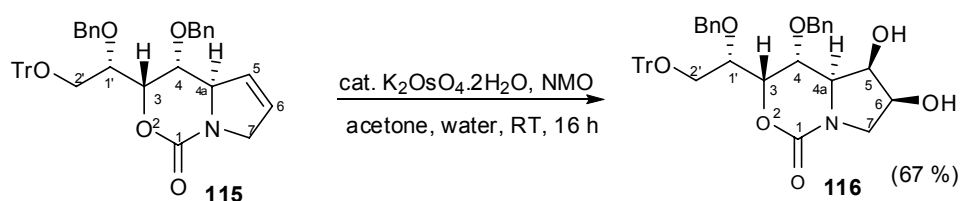
Table 5.4. Overall yields for **123** and **115** from **70** *via* different methodologies.

methodology	oxazolone 123	oxazinone 115
<i>N</i> -Boc	11 %	4 %
Triphosgene	6 %	7 %
<i>N</i> -Troc	21 %	17 %

5.5. Dihydroxylation of oxazinone **115**

According to Scheme 5.2 the next step in the synthesis of 1,2-di-*epi*-**1** was *cis*-dihydroxylation. Dihydroxylation of **115** occurred using a standard Upjohn procedure previously described (see Section 3.7). Perhaps the most interesting aspect about this reaction

was the reactivity of oxazinone **115** towards dihydroxylation when compared to the 2,5-dihydropyrrole **58** substrate in Section 3.7. In the latter case the reaction was slow, taking 3 d at rt to complete. The optimized time for the dihydroxylation of **115** was much quicker, taking 16 h at rt (Scheme 5.23). Gratifyingly, the reaction was completely diastereoselective in favour of the desired 4a,5-*syn* product. NOESY NMR analysis determined the stereochemistry of the C-5,6-diol moiety, solely on the basis of an observed nOe correlation between H-6 and H-4a. The other requisite correlation was between H-5 and H-7 α . However, this was difficult to confirm due to the 4H overlap of the resonances of H-2' α , H-2' β , H-4a and H-7 between 3.49 and 3.42 ppm in the ^1H NMR spectrum (300 MHz, CDCl_3). The effect of the dihydroxylation of **115** was to shift, in an upfield direction, the ^1H and ^{13}C NMR chemical shifts of the methine and methylene hydrocarbon units α to the nitrogen atom (Table 5.5).



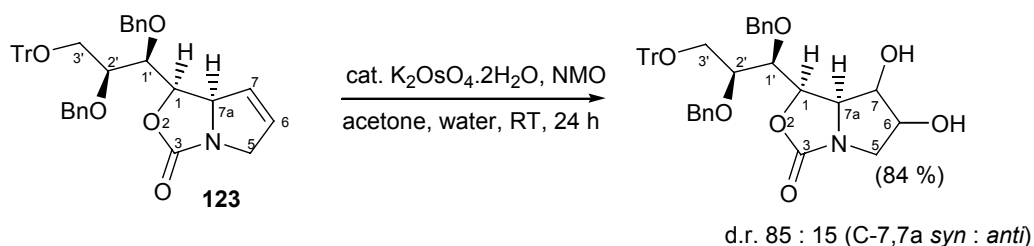
Scheme 5.23. Result of the *cis*-dihydroxylation of **115**.

Table 5.5. Selected NMR chemical shifts for corresponding nuclei in **115** and **116**.^a

Please see print copy for Table 5.5

5.6. Dihydroxylation of oxazolone **123**

The reactivity of oxazolone **123** in the *cis*-dihydroxylation reaction was slightly less compared to the oxazinone **115** substrate, with a complete reaction requiring 24 h (optimized) at rt with the same catalyst loading of 5 mol %. The yields were good, usually above 75 %, with a best yield of 84 % (Scheme 5.24). However the diastereoselectivity was reduced, with a reproducible diastereomeric ratio being obtained of 85 : 15 (C-7,7a *syn* : *anti*). These diastereomers were very difficult to separate on silica gel, requiring repeated FCC, and semi-preparative TLC operations, to isolate the individual diastereomers. Figure 5.3 shows a clear difference in the ^1H NMR resonances between the two diastereomers.



Scheme 5.24. Result of the *cis*-dihydroxylation of **123**.

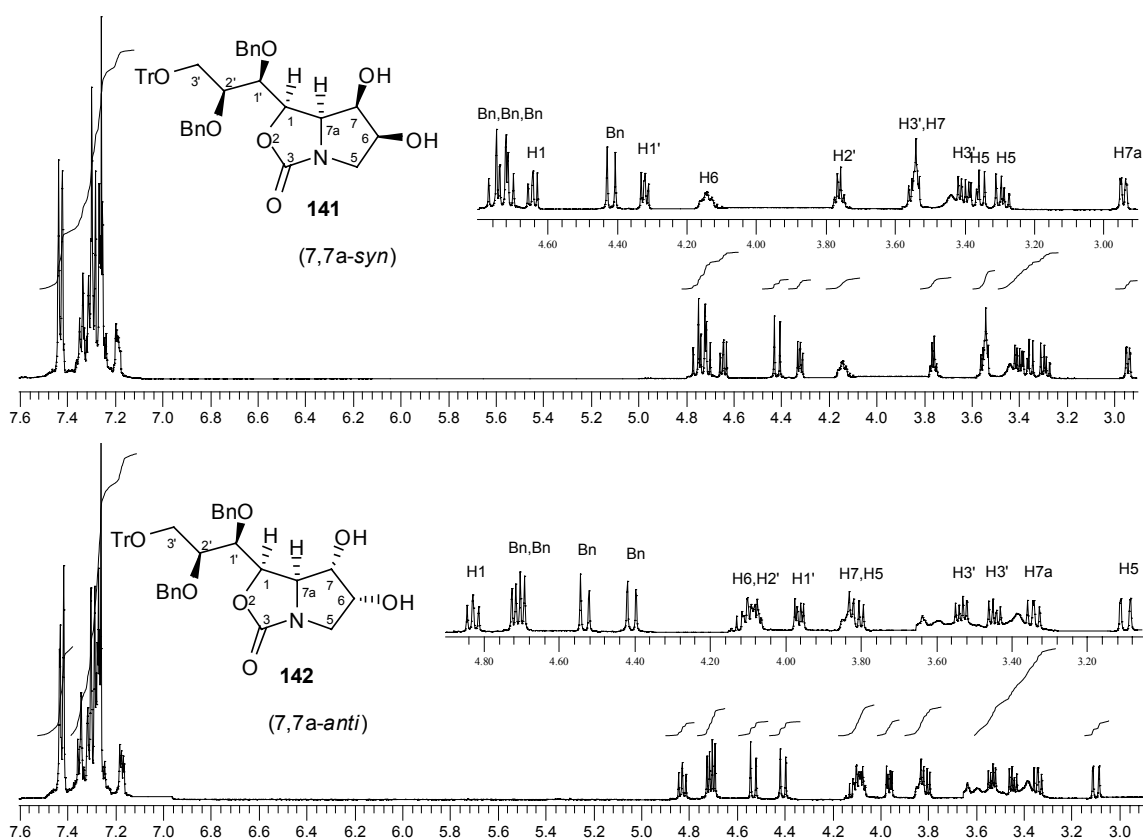


Figure 5.3. ^1H NMR spectra (500 MHz, CDCl_3) of diastereomers **141** and **142**.

Comparisons of the ^1H NMR chemical shifts for the conformationally restricted sp^3 units in the two diastereomers show that significant differences (> 0.3 ppm) occurred in H-7a, H-7 and in one of the H-5 protons (Table 5.6). Curiously, there was only a marginal difference (0.05 ppm) in the chemical shift for H-6, while significant differences in the ^{13}C NMR chemical shifts between **141** and **142** (> 2.0 ppm) occurred in C-5 and C-6. The C-6 chemical shift in **141** (74.1 ppm) was particularly unusual because all ^{13}C NMR chemical shifts for unprotected secondary hydroxyl groups hitherto have been observed in the region of 69.5-72.5 ppm.

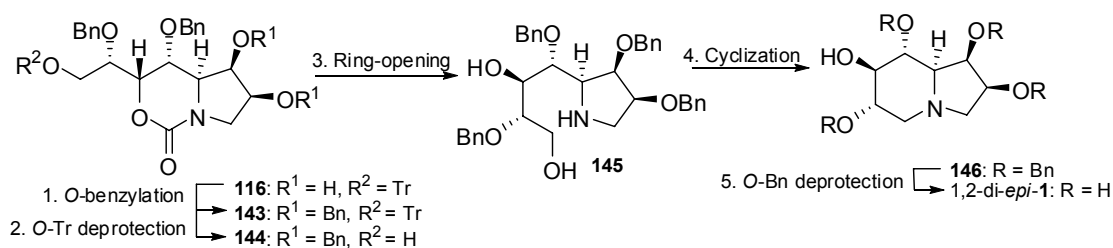
Table 5.6. Selected ^1H and ^{13}C NMR chemical shifts of corresponding nuclei in **141** and **142**.^a

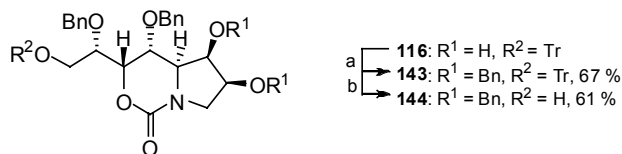
Please see print copy for Table 5.6

NOSY NMR analysis determined the stereochemistry of the resulting diol moieties in oxazolones **141** and **142**, in an analogous manner to the determination of the C-5,6 diol stereochemistry in oxazinone **116** (Section 5.5). At this time, further elaboration of diastereomers **141** and **142** was suspended (except for one trial reaction below), as our priority shifted to the elaboration of **116**.

5.7. *O*-Benzylation and *O*-Tr deprotection

Scheme 5.2 showed that the synthetic plan subsequent to the synthesis of oxazinone **116** was a ring-opening reaction to give compound **117**. This approach was changed to include a di-*O*-benzylation of **116**, followed by deprotection of the *O*-Tr group in **143**, and ring-opening of the oxazinone ring in **144** (Scheme 5.25). At the time, these changes reflected anticipated difficulties in the isolation of products arising from the original synthetic plan in Scheme 5.2. As such, they were all one-reaction trials; no optimization experiments were conducted. In the event, *O*-benzylation of **116** occurred in moderate yield (67 %), giving product **143** (Scheme 5.26). *O*-Tr deprotection of **143** was conducted under the previously used conditions of TFA and anisole in DCM at 0 °C, to give **144** in 61 % yield.

**Scheme 5.25.** Revised synthetic plan from oxazinone **146** to 1,2-di-*epi*-1.

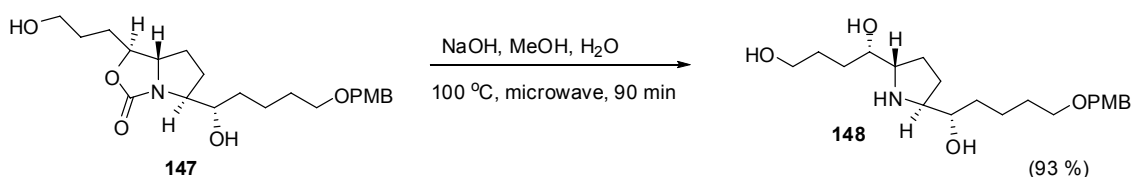


Reagents and conditions: (a) NaH, BnBr, nBu_4NI , THF, (b) TFA, anisole, DCM, 0 °C, 1 h

Scheme 5.26. Results of the *O*-Bn protection of **116** and *O*-Tr deprotection of **143**.

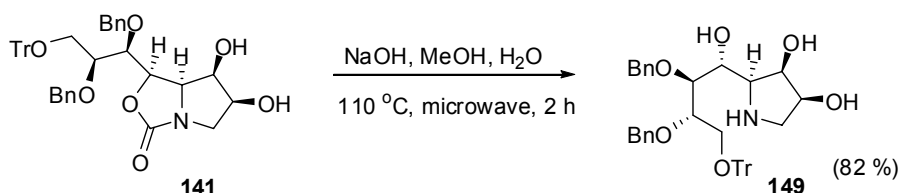
5.8. Hydrolysis of oxazinanone **144**

Previous attempts to hydrolyse oxazolones or oxazinones in our group, using NaOH / MeOH and conventional thermal heating, were slow and suffered poor yields. The access of microwave reactor technology to the laboratory in 2002 resulted in better yields and much faster reaction times. For instance, the hydrolysis of **147** by fellow student, Karl Lindsay, using the microwave reactor, gave amino alcohol **148** in excellent yield (Scheme 5.27).¹⁷⁰



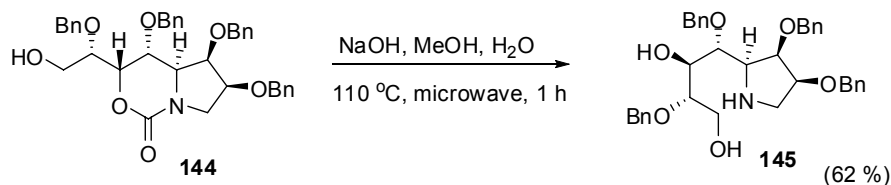
Scheme 5.27. Base hydrolysis of an oxazolinone under microwave conditions.

In gaining experience with this reaction, oxazolinone **141** was treated with NaOH (5 equiv.) in a mixture of MeOH and water (5:3) and stirred in the microwave reactor at 110 °C for 2 h. The product **149** was isolated in a good yield of 82 % (Scheme 5.28).



Scheme 5.28. Result of the microwave-assisted hydrolysis of **141**.

The same reaction conducted with oxazinone **144**, for 1 h, gave a lower yield of 62 % (Scheme 5.29). The time of reaction was reduced based on the assumption that 2 h was excessive. Optimization of these microwave-assisted reactions was limited by the fact that they could not be conveniently monitored by TLC analysis, coupled with a short supply of **144**.

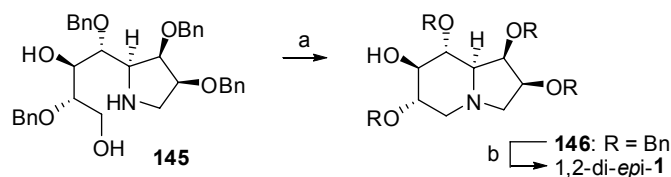


Scheme 5.29. Result of the microwave-assisted hydrolysis of **144**.

Uptake of microwave assisted organic synthesis (MAOS) technology was initially slow following the first reports due to the lack of temperature and pressure control, coupled with inferior knowledge of the basics of microwave dielectric heating.¹⁷¹ However, reports of MAOS in the literature have been growing rapidly in recent years, generally citing dramatically reduced reaction times (from hours and days to minutes), reduction of side-products, improved yields and improved reproducibility.¹⁷¹⁻¹⁷⁵ The reasons for these enhancements are still being debated. Essentially there is ongoing conjecture between an effect of the thermal heat generated by the microwaves and an effect that is specific for microwave heating. It is clear, however, that the energy of a microwave photon, at the operating frequency of microwave reactors (2.45 GHz), is too low (0.0016 eV) to break chemical bonds and is also lower than the energy of Brownian motion.¹⁷¹ Thus, microwaves themselves cannot induce chemical reactions.

5.9. Elaboration to the target

Appel cyclization of **145** was carried out under identical conditions to the cyclization of **61** (see Section 3.10) to give **146** in 85 % yield (Scheme 5.28). De-*O*-benzylation of **146** was achieved by palladium chloride catalyzed hydrogenolysis (see Section 3.11). The reaction was complete in 1 h and the crude product was purified by basic ion-exchange chromatography (Scheme 5.30) to give 1,2-di-*epi*-**1** in 62 % yield. The ¹H NMR spectrum of 1,2-di-*epi*-**1** is shown in Figure 5.4.



Reagents and conditions: (a) CBr₄, PPh₃, Et₃N, DCM, 0 °C, 2 h, 85 %;
(b) PdCl₂, H₂ (1 atm), MeOH, rt, 1 h, ion exchange, 62 %.

Scheme 5.30. Results of the Appel cyclization of **145** and *O*-Bn protection of **146**.

The NMR data of 1,2-di-*epi*-1 was consistent with the literature data (Table 5.6), both ^1H and ^{13}C NMR chemical shifts were in close alignment. However, the optical rotation value for 1,2-di-*epi*-1 (Table 5.6) did not accord very closely with the literature value, although it had the same sign. The difference may be due to the highly hygroscopic nature of this compound. The overall yield of 1,2-di-*epi*-1 from L-Xylose was 1 %.

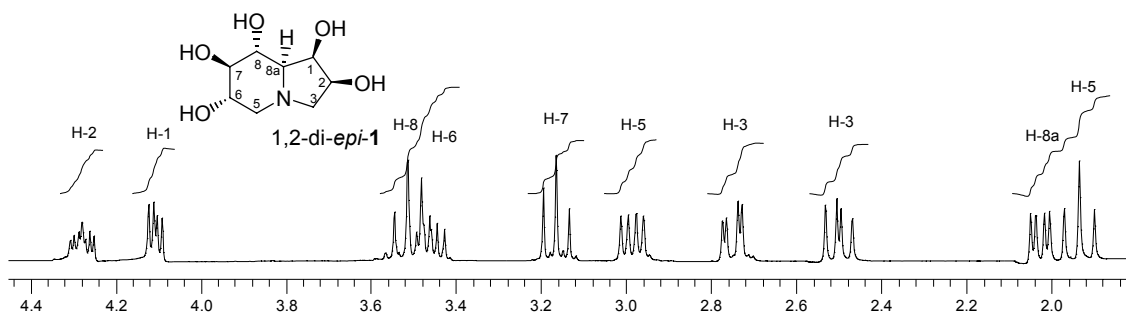


Figure 5.4. ^1H NMR spectrum (500 MHz, CDCl_3) of 1,2-di-*epi*-1.

Table 5.7. Comparison of the NMR data for 1,2-di-*epi*-1 and corresponding literature data.

nuclei	NMR chemical shifts (ppm)			J value	NMR coupling constants (Hz)		
	literature ^{83, a}	1,2-di- <i>epi</i> -1 ^b	$\Delta \delta$		literature ^{83, a}	1,2-di- <i>epi</i> -1 ^b	ΔJ
H-1	4.06	4.12	+ 0.06	J_{1-2}	5.8	5.8	0
H-2	4.24	4.29	+ 0.05	J_{1-8a}	3.8	3.8	0
H-3	2.71	2.76	+ 0.05	J_{2-3}	8.1	8.3	0.2
H-3	2.54	2.50	+ 0.04	J_{2-3}	2.6	2.8	0.2
H-5	2.95	3.00	+ 0.05	J_{8a-8}	9.8	9.5	0.3
H-5	1.91	1.95	+ 0.04	J_{8-7}	9.5	9.5	0
H-6	3.42	3.48	+ 0.06	J_{7-6}	9.2	9.3	0.1
H-7	3.12	3.18	+ 0.06	J_{6-5}	9.9	10.5	0.6
H-8	3.47	3.53	+ 0.06	J_{6-5}	5.3	5.5	0.2
H-8a	2.01	2.04	+ 0.03	J_{3-3}	11.0	10.8	0.2
				J_{5-5}	10.8	10.8	0
C-1	69.3	69.7	+ 0.4	optical rotation			
C-2	69.8	70.2	+ 0.4				
C-3	60.0	59.9	- 0.1	literature		1,2-di- <i>epi</i> -1	
C-5	55.8	55.7	- 0.1	$[\alpha]_D^{23} + 66.5$		$[\alpha]_D^{23} + 21$	
C-6	70.3	70.4	+ 0.1	(c 1.33, H_2O)		(c 1.5, H_2O)	
C-7	79.3	79.3	0				
C-8	70.9	69.3	- 0.6				
C-8a	70.4	70.7	+ 0.3				

a: ^1H NMR (D_2O , frequency not specified); ^{13}C NMR (D_2O , frequency not specified)

b: ^1H NMR (500 MHz, D_2O); ^{13}C NMR (75 MHz, D_2O)

CHAPTER 6. Glycosidase inhibitor testing

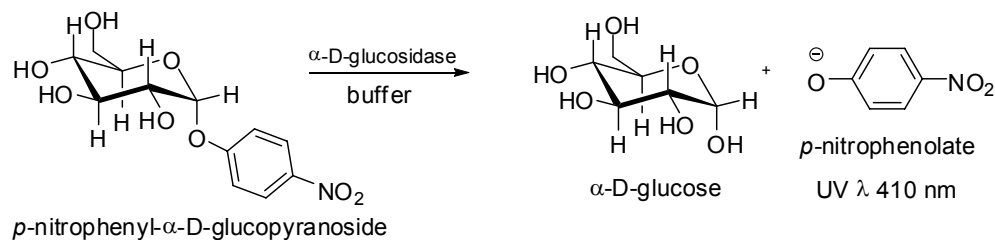
Enantiomers *ent*-**1** and **1** were tested in our lab by Leena Burgess as inhibitors of almond emulsion β -D-glucosidase, baker's yeast α -D-glucosidase, bovine liver β -D-galactosidase, green coffee bean α -D-galactosidase, jack bean α -D-mannosidase and bovine kidney α -L-fucosidase. As a negative control, castanospermine was tested for inhibition of baker's yeast α -D-glucosidase, for which it has been demonstrated to have no activity.¹⁷⁶ Castanospermine was also used, as a positive control, for inhibition of almond emulsion β -D-glucosidase. Its IC_{50} value for this enzyme has been reported to be 53 μ M.¹⁷⁶ Matsumura *et al.* reported that the natural product uniflorine A was active against rat intestinal α -maltase and α -sucrase, with IC_{50} values of 12.0 μ M and 3.1 μ M, respectively.²³ We were not able to test *ent*-**1** or **1** on these α -D-glucosidase enzymes for cost and availability reasons.

Each enzymatic assay was performed for 30 min at the correct temperature and pH for the individual enzyme, in the presence of the appropriate *p*-nitrophenyl glycoside substrate (Table 6.1). In terms of concentrations, the assays contained 25 mM buffer, 5 mM *p*-nitrophenyl glycoside, and varying amounts of inhibitor and an enzyme loading to give a final optical density of 0.4-0.8. The final volume of each assay was 0.5 mL. After 30 min incubation at the correct temperature each assay was diluted to a volume of 10 mL with the addition of 9.5 mL of 0.4 M glycine buffer and its absorbance at 410 nm was recorded.

Table 6.1. Types of buffer, substrate and temperature for each enzymatic assay.

enzyme	buffer	substrate	temperature °C
β -D-glucosidase	pH 5 sodium acetate	<i>p</i> -nitrophenyl β -D-glucopyranoside	37
α -D-glucosidase	pH 6.8 phosphate	<i>p</i> -nitrophenyl α -D-glucopyranoside	37
β -D-galactosidase	pH 7.3 phosphate	<i>p</i> -nitrophenyl β -D-galactopyranoside	37
α -D-galactosidase	pH 6.5 phosphate	<i>p</i> -nitrophenyl α -D-galactopyranoside	25
α -D-mannosidase	pH 4.5 sodium acetate	<i>p</i> -nitrophenyl α -D-mannopyranoside	25
α -L-fucosidase	pH 6.0 phosphate	<i>p</i> -nitrophenyl α -L-fucopyranoside	25

The quantity of *p*-nitrophenolate produced in each assay was measured by UV/vis spectrophotometry in order to determine the effect of varying concentrations of inhibitor. Theoretically, one molecule of *p*-nitrophenol is liberated for each enzymatic cleavage of the sugar substrate. Upon treatment with glycine buffer (pH 10.4), *p*-nitrophenol is converted to its corresponding *p*-nitrophenolate anion, which has a known extinction coefficient at 410 nm (Scheme 6.1).



Scheme 6.1. Mechanism of the glycosidase inhibitory activity assay.

Assays were performed in the concentration range in which a linear relationship existed between absorbance and *p*-nitrophenolate concentration, so that a 50% decrease in absorbance would indicate the IC_{50} of the inhibitor. A suitable concentration range for this was determined by producing a series of standard solutions with concentrations that ranged from 0-100 μ M. These solutions were basified by glycine buffer (pH 10.4) and the absorbance of each was measured at 410 nm on a UV/vis spectrophotometer. Tests were performed in triplicate and resulted in a calculated extinction coefficient of $16458 \text{ M}^{-1} \cdot \text{cm}^{-1}$ (literature value $17700 \text{ M}^{-1} \cdot \text{cm}^{-1}$ ¹⁷⁷) (Figure 6.1). A linear relationship was maintained up to a *p*-nitrophenolate concentration of 75 μ M, therefore all enzymatic assays were conducted so that the final concentration of *p*-nitrophenolate did not exceed this value.

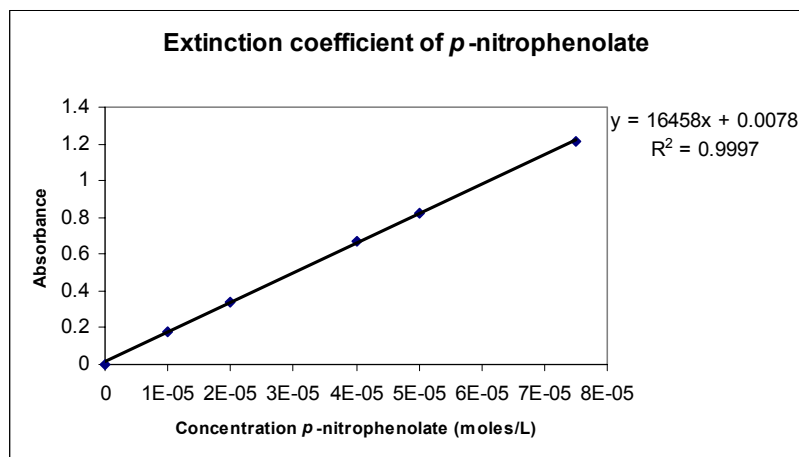


Figure 6.1. Determination of the extinction coefficient of *p*-nitrophenolate.

Assays on *ent-1* and **1** were conducted in duplicate and the average IC₅₀ of each is presented in Table 6.2. *Ent-1* displayed modest (200 μ M) activity for jack bean α -D-mannosidase but no activity (IC₅₀ > 1 mM) for the other glycosidases. Conversely, **1** was not active for any of the glycosidases at 1 mM. Castanospermine produced an IC₅₀ of 120 μ M, roughly double the literature value, which indicated that the IC₅₀ values of *ent-1* and **1** for all tested enzymes might be higher than they should be. However, castanospermine did not inhibit baker's yeast α -D-glucosidase, thereby providing some validation of this testing methodology.

Table 6.2. IC₅₀ values of *ent-1*, **1**, and castanospermine.

enzyme	inhibitor IC ₅₀ (μ M)		
	<i>ent-1</i>	1	castanospermine
α -glucosidase	•	•	•
β -glucosidase	•	•	120 (lit. value 53 ¹⁷⁸)
α -galactosidase	•	•	
β -galactosidase	•	•	
α -mannosidase	200	•	
α -fucosidase	•	•	

• Represents an IC₅₀ value greater than 1 mM.

Glycosidase testing of 1,2-di-*epi-1* was performed at a much later date from the previously tested *ent-1* and **1**. Consequently, the leftover enzyme supply was unsuitable for testing. Since α -mannosidase was the only enzyme that responded with inhibition to either *ent-1* or **1**, it was selected as the sole enzyme to test against compound 1,2-di-*epi-1*. This test employed a slightly different procedure that was based on the method of Tulsiani *et al.*¹⁷⁹ Quantities of the added components in this testing procedure are displayed in Table 6.3.

Table 6.3. Components in the α -D-mannosidase assay of putative 1,2-di-*epi-1*.

conc. of 1,2-di- <i>epi-1</i> (μ M)	vol. of 3.935x10 ⁻³ M α -D-mannosidase solution (μ L)	vol. of H ₂ O (μ L)	vol. of NaOAc buffer (μ L)	vol. of <i>p</i> -nitrophenyl α -D-mannopyranoside (μ L)
0	0	900	500	500
50	34.08	865.92	500	500
100	68.15	831.85	500	500
200	136.30	763.70	500	500
500	340.76	559.24	500	500
1000	681.52	218.48	500	500

The assay was performed in a UV/vis cuvette at 410 nm, employing the kinetics function of the UV/vis spectrophotometer. Buffer, 1,2-di-*epi*-**1**, and water were mixed together in the cuvette and loaded into the spectrophotometer. The enzymatic reaction was initiated by the addition of the enzyme, followed by rapid mixing. Reaction progress was monitored for one minute before taking a measurement of the initial rate. This procedure was repeated for each concentration of inhibitor. Activity is theoretically observed by a reduction in rate upon an increase of the inhibitor concentration. Furthermore, the IC₅₀ of an active inhibitor is the concentration where the rate of reaction is 50 % of the rate without the inhibitor.

Swainsonine, a known inhibitor of α -D-mannosidase with an IC₅₀ value of 2.0 μ M, was tested as a positive control.¹⁷⁹ Using our testing procedure, swainsonine produced an IC₅₀ of 2.0 μ M, indicating the reliability of the assay, while 1,2-di-*epi*-**1** recorded no activity at a concentration of 1 mM (Table 6.4).

Table 6.4. IC₅₀ of 1,2-di-*epi*-**1** and swainsonine.

enzyme	inhibitor IC ₅₀ (μ M)	
	1,2-di- <i>epi</i> - 1	swainsonine
α -D-mannosidase	> 1 mM.	2 (lit. ¹⁷⁹ value 2)

Although swainsonine is a good inhibitor of jack bean α -D-mannosidase, it is a marginally better inhibitor of lysosomal α -D-mannosidase (IC₅₀ 0.2 μ M) and Golgi mannosidase II (IC₅₀ 0.2 μ M). Thus, the glycosidase inhibition of the tested compounds was somewhat broadly defined by its response to these simple tests. In addition, the limited number of compounds tested prohibited an in-depth structure activity relationship (SAR) analysis. Nevertheless, these assays established a solid grounding upon which to base further investigations.

CHAPTER 7. Determining the correct structures of uniflorine A and B

In 2004 we published our synthesis of **1** and reported the structural misassignment of uniflorine A.¹⁸⁰ To date, the only other published synthesis of **1** was in reported in 2006 by Dhavale *et al.*¹⁸¹ Gratifyingly, their spectroscopic and analytical data for **1** was found to be in total agreement with ours. In 2005, Mariano *et al.* published a synthesis of 1-*epi*-**1**.¹⁸² The NMR data for this compound, either in its neutral form or as a hydrochloride salt, was not consistent with the NMR data that Matsumura *et al.*²³ reported for uniflorine A. Mariano also reported the synthesis of 1,2-di-*epi*-**1**¹⁸² in which its spectroscopic data was consistent with Fleet and co-workers' first preparation of this compound,⁸³ and our own synthesis in Chapter 5.

At this time, we began to suspect that uniflorine A was not actually an indolizidine alkaloid. We reviewed the literature for published NMR data of pentahydroxy alkaloids that did not contain an indolizidine framework but had a chemical formula of C₈H₁₅NO₅. Prominent examples of such structures were casuarine **150** and its diastereomers (Figure 7.1 and Table 7.1). Casuarine, a pyrrolizidine alkaloid with a C-3 CH₂OH group, is a natural product whose structure was elucidated by single-crystal X-ray structural analysis. Syntheses of several casuarine epimers have been reported (Figure 7.1). To date, casuarine **150** and 3-*epi*-casuarine **151** are the only known casuarine diastereomers that have been isolated as natural products.

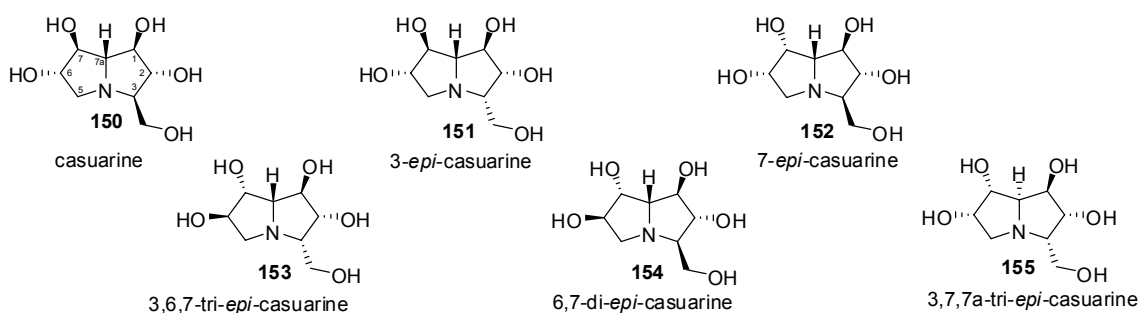


Figure 7.1. Casuarine diastereomers that have appeared in the literature.

Table 7.1. Literature sources of casuarine **150** diastereomers and related data.

Casuarine isomer	Natural product	Synthesis	X-ray structure
casuarine	Nash <i>et al.</i> ⁴⁴	Denmark <i>et al.</i> ^{183,184} , Izquierdo <i>et al.</i> ¹⁸⁵	Nash <i>et al.</i> ⁴⁴
7- <i>epi</i> -	•	Bell <i>et al.</i> ¹⁸⁶	•
6,7-di- <i>epi</i> -	•	Bell <i>et al.</i> ¹⁸⁶ ; Izquierdo <i>et al.</i> ¹⁸⁵	•
3,6,7-tri- <i>epi</i> -	•	Bell <i>et al.</i> ¹⁸⁶ ; Izquierdo <i>et al.</i> ¹⁸⁷	•
3- <i>epi</i> -	Van Ameijde <i>et al.</i> ¹⁸⁸	Van Ameijde <i>et al.</i> ¹⁸⁸ , Izquierdo <i>et al.</i> ¹⁸⁷	Newton <i>et al.</i> ¹⁸⁹
3,7,7a-tri- <i>epi</i> -	•	•	Punzo <i>et al.</i> ¹⁹⁰

• hitherto not published in the literature

When casuarine was first isolated from the bark of *Casuarina equisetifolia*, an equal quantity of its 6- α -glucopyranosyl derivative was also isolated (Figure 7.2).⁴⁴ Later, the same molecule was isolated from *Eugenia jambolana*.⁴⁵ This species of plant belongs to the same family as *Eugenia uniflora*, from whose leaves were isolated uniflorine A, uniflorine B and the known piperidine alkaloid **3** (Figure 7.2).

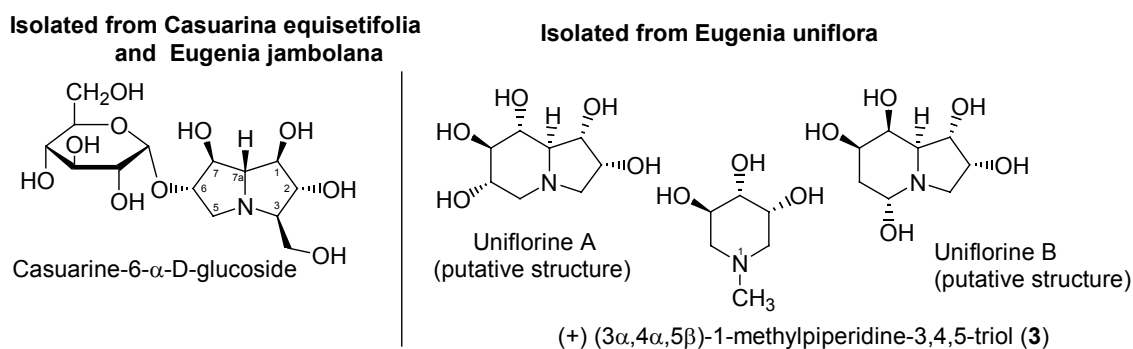


Figure 7.2 (a) Casuarine glycoside isolated from *Casuarina equisetifolia*, and *Eugenia jambolana*; (b) Natural products isolated from *Eugenia uniflora*.

A significant finding occurred during our comparison of the NMR data for casuarine and the above natural products isolated from *Eugenia uniflora*. Specifically, the NMR data for casuarine absolutely matched that of uniflorine B (Table 7.2), with the exception that the ^{13}C NMR shifts for uniflorine B were consistently 3.0-3.3 ppm downfield of the corresponding ^{13}C NMR resonances for casuarine. Alternative referencing between the two samples could account for this consistent discrepancy. Both samples were run on a 500 MHz NMR spectrometer (^{13}C NMR experiments were conducted at 125 MHz) in D_2O . Casuarine's ^{13}C NMR spectrum was referenced to acetone at δ 29.80 ppm while the uniflorine B sample was apparently referenced to a TMS internal standard. The $^3J_{\text{HH}}$ values for the two samples were in very close accord as were the ^1H NMR chemical shifts. The optical rotations of both were almost identical.

Table 7.2. NMR and optical rotation data for casuarine and uniflorine B.

nucleus	chemical shifts			coupling constants (Hz)	
	casuarine ⁴⁴	uniflorine B ²³		casuarine ⁴⁴	uniflorine B ²³
H-1	4.16	4.17	$J_{H-1, H-2}$	8.0	8.1
H-2	3.80	3.79	$J_{H-1, H7a}$	8.0	8.1
H-3	3.04	3.04	$J_{H-2, H-3}$	8.0	multiplet
H-5 α	2.91	2.92	$J_{H-3, H-8}$	3.8	3.7
H-5 β	3.27	3.26	$J_{H-3, H-8'}$	6.6	6.8
H-6	4.21	4.22	$J_{H-8, H-8a}$	11.9	11.3
H-7	4.19	4.19	$J_{H-5\alpha, H-6}$	4.0	3.9
H-7a	3.07	3.06	$J_{H-5\beta, H-6}$	4.7	4.5
H-8	3.77	3.78	$J_{H-6, H-7}$	*	4.5
H-8'	3.61	3.61	$J_{H-7, H-7a}$	3.5	3.2
	casuarine ⁴⁴	uniflorine B ²³	$\Delta \delta$ (ppm)	optical rotation	
C-1	77.8	80.9	3.1	casuarine ⁴⁴	$[\alpha]_D^{24} + 16.9$
C-2	76.6	79.8	3.2		(<i>c</i> 0.8, H ₂ O)
C-3	70.0	73.0	3.0		
C-5	58.0	61.1	3.1	uniflorine B ²³	$[\alpha]_D + 16.3$
C-6	77.4	70.6	3.2		(<i>c</i> 1.1, H ₂ O)
C-7	78.8	81.9	3.1		
C-7a	72.1	75.2	3.1		
C-8	62.2	65.5	3.3		

* could not be determined due to peak overlap

Following the revelation that uniflorine B was actually casuarine, we began to suspect that uniflorine A was an isomer of casuarine. When the NMR data for uniflorine A was correlated to our proposed pyrrolizidine structure (Table 7.3), a comparison with the NMR data for known synthetic casuarine diastereomers furnished a reasonably close spectroscopic alignment between uniflorine A and 7-*epi*- and 6,7-di-*epi*-casuarine (Figure 7.3.).

Several of the chemical shifts were not particularly close (Table 7.4). However, one must be very cautious when comparing ¹H NMR chemical shifts between polyhydroxylated pyrrolizidine structures. A remarkable feature of 3-*epi*-casuarine is how different its ¹H NMR spectrum is to that for casuarine, given that it is epimeric at only one position (Figure 7.4).¹⁸⁸ Inversion at just one stereocentre can therefore lead to substantial conformational changes of the bicyclic pyrrolizidine ring system and hence significant changes in chemical shifts.

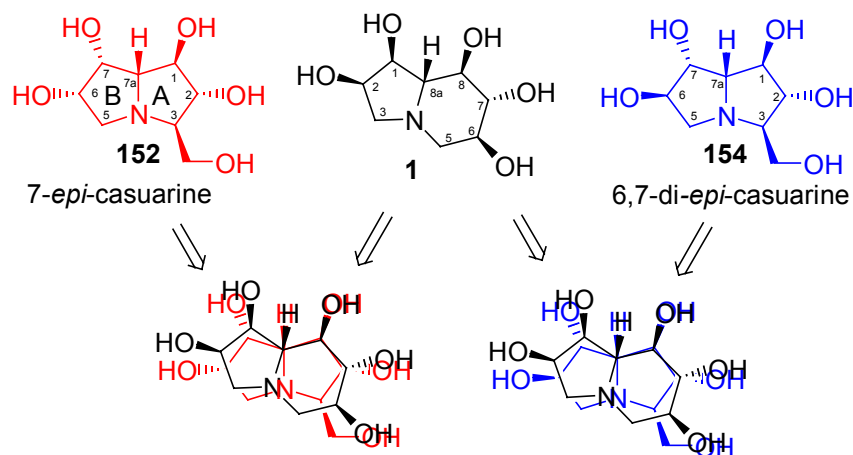


Figure 7.3. Overlap of **1** with **152** and **154**.

Table 7.3. Corresponding carbon nuclei in overlapping pyrrolizidine and indolizidine structures.

Pyrrolizidine	Indolizidine
C-1	C-8
C-2	C-7
C-3	C-6
C-5	C-3
C-6	C-2
C-7	C-1
C-7a	C-8a
C-8	C-5

Table 7.4. The ^1H NMR chemical shifts for **152**, **154** and uniflorine A.

	152 (D_2O^*) ¹⁸⁶	154 (D_2O^*) ¹⁸⁶	uniflorine A (500 MHz, D_2O) ²³	
nucleus	δ (ppm)	δ (ppm)	δ (ppm)	nucleus
H-1	4.29	4.23	3.94	H-8
H-2	3.75	3.86	3.81	H-7
H-3	2.73	2.67	2.76	H-6
H-5 α	2.54	2.85	2.98	H-3 β
H-5 β	3.18	3.00	3.04	H-3 α
H-6	4.15	4.15	3.81	H-2
H-7	4.07	4.08	3.94	H-1
H-7a	3.16	3.36	3.14	H-8a
H-8	3.50	3.55	3.61	H-5 α
H-8'	3.70	3.73	3.76	H-5 β

* Spectrometer frequency was not specified

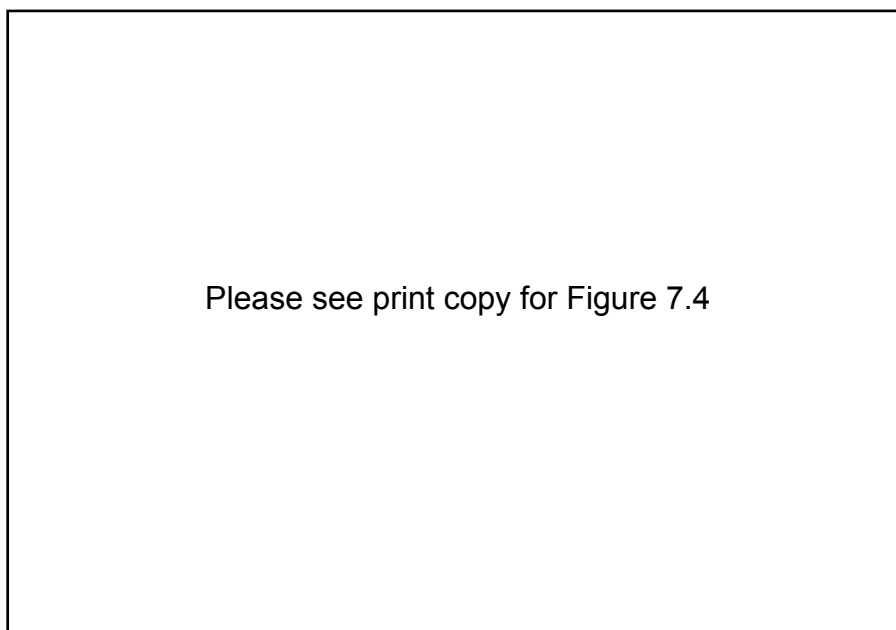


Figure 7.4. ^1H NMR spectra of D_2O at $30\text{ }^\circ\text{C}$ of (a) casuarine **150**, pH 8.3, and (b) 3-*epi*-casuarine **151**, pH 9.3. Spectra taken from Fleet *et al.*¹⁸⁸

A more reliable method of correlating proton assignments between polyhydroxylated pyrrolizidine diastereomers is to compare coupling constants. A study by Wormald *et al.* has demonstrated success in using this method to assign both the relative configurations of ring protons and the conformation of the pyrrolizidine framework, in alexine diastereomers.⁸²

A comparison of the coupling constants for protons in **152**, **154** and uniflorine A, revealed a strong correlation between several nuclei, according to the numbering system of correlated nuclei listed in Table 7.3. Specifically, the originally assigned J_{8-8a} value for uniflorine A was consistent with the J_{1-7a} values of **152** and **154**. Similarly, the originally assigned J_{7-8} value of uniflorine A was consistent with the J_{1-2} value of **152** and **154**, while the originally assigned J_{6-7} value of uniflorine A was also consistent with the J_{2-3} value of **152** and **154**. These high $^3J_{\text{HH}}$ values (7.9-9.6 Hz) describe a *trans*-diaxial configuration between the contiguous protons (Table 7.5). On this basis, it was proposed that the correct uniflorine A structure includes the C-7a - C-1 – C-2 – C-3 configuration (or the ‘A’ ring) of casuarine, 7-*epi*-casuarine and 6,7-di-*epi*-casuarine.

Table 7.5. $^3J_{\text{HH}}$ values for the A-ring protons of **152**, **154** and uniflorine A.

	casuarine ⁴⁴	(152) ¹⁸⁶	(154) ¹⁸⁶	uniflorine A ²³
J_{7a-1}	8.0	7.6	7.4	7.7 (J_{8-8a})
J_{1-2}	8.0	7.9	7.9	7.7 (J_{7-8})
J_{2-3}	8.8	9.6	9.6	9.0 (J_{6-7})

Analysis of the coupling constants for the known casuarine diastereomers that are epimeric at C-3, all show a departure from the diaxial configuration of the A ring protons (Table 7.6). Indeed the low to moderate $^3J_{\text{HH}}$ values (1.3-4.4 Hz) indicate either a *trans*_{ax-eq} or a *cis* configuration of the A ring protons. This evidence rules out the possibility of uniflorine A possessing an A ring that includes an epimeric C-3 CH₂OH group, and therefore provides further support for the proposed A ring configuration of uniflorine A.

Table 7.6. A-ring $^3J_{\text{HH}}$ values for casuarine diastereomers that are epimeric at C-3.

	3- <i>epi</i> -casuarine (151) ¹⁸⁸	3,6,7-tri- <i>epi</i> -casuarine (155) ¹⁸⁶	3,7,7a-tri- <i>epi</i> -casuarine (155)*
J_{7a-1}	1.6	3.9	4.4
J_{1-2}	1.4	3.6	1.3
J_{2-3}	3.3	4.4	3.3

* yet to be published, obtained directly from Prof. George Fleet.

Having established, with a reasonable degree of certainty, the A-ring configuration of uniflorine A, it was left for us to assign the configuration of the B-ring. Analysis of the coupling constants for the B-ring protons in **152** and **154** revealed inconsistencies with the corresponding data for uniflorine A (Table 7.7). The $^3J_{\text{HH}}$ values for the methylene protons (5 α , 5 β) aligned with uniflorine A more closely for **154**, but its J_{6-7} value was totally inconsistent with the corresponding J_{1-2} value for uniflorine A.

Table 7.7. B-ring $^3J_{\text{HH}}$ values for **152**, **154** and uniflorine A.

	152 ¹⁸⁶	154 ¹⁸⁶	uniflorine A ²³
$J_{5\alpha-6}$	9.7	3.8	5.1 ($J_{3\beta-6}$)
$J_{5\beta-6}$	6.4	4.2	5.1 ($J_{3\alpha-6}$)
J_{6-7}	3.8	2.2	4.5 (J_{1-2})
J_{7-7a}	4.2	4.5	4.5 (J_{1-8a})

Analysis of ¹³C NMR chemical shifts for **152** and **154** also provided some inconsistencies with the corresponding data for uniflorine A (Table 7.8). For instance, the C-1 chemical shifts in **152** and **154** were significant less (7.3-11.6 ppm) than the corresponding C-8 chemical shift for uniflorine A.

Table 7.8. ^{13}C NMR chemical shifts for **152**, **154** and uniflorine A.

152	$\delta (\text{D}_2\text{O}^*)^{186}$	154	$\delta (\text{D}_2\text{O}^*)^{186}$	uniflorine A	$\delta (125 \text{ MHz, D}_2\text{O})^{23}$
C-1	73.9	C-1	69.6	C-8	81.2
C-2	78.6	C-2	71.5	C-7	79.9
C-3	71.7	C-3	73.6	C-6	72.5
C-5	56.8	C-5	59.0	C-3	60.0
C-6	75.5	C-6	74.6	C-2	74.2
C-7	70.6	C-7	78.2	C-1	79.9
C-7a	69.1	C-7a	79.5	C-8a	73.6
C-8	63.2	C-8	63.3	C-5	65.3

* NMR spectrometer frequency was not specified

Perhaps not surprisingly then, the optical rotation data for **152** and **154** was also a poor fit for uniflorine A (Table 7.9).

Table 7.9. Optical rotation data for **152**, **154**, and uniflorine A.

Optical rotation	
152	$[\alpha]_{\text{D}}^{22} - 20.1 (c\ 0.65, \text{H}_2\text{O})^{186}$
154	$[\alpha]_{\text{D}}^{22} + 8.4 (c\ 0.89, \text{H}_2\text{O})^{186}$
uniflorine A	$[\alpha]_{\text{D}} - 4.4 (c\ 1.2, \text{H}_2\text{O})^{23}$

To summarize the above spectroscopic analyses, we determined that uniflorine A contains the A-ring present in **152** and **154**, but does not contain the B-ring of either **152** or **154**. Therefore, by a process of elimination, 6-*epi*-casuarine is the only isomer of casuarine remaining that could possibly represent uniflorine A.

The original paper that reported the uniflorine natural products included nOe analyses. Figure 7.5 illustrates the three observed nOe correlations used to assign the structure for uniflorine A. According to the diagram, the H-7 and H-5 α are on the same side of the molecule, which in the casuarine framework correlates to a through space coupling between H-2 and H-8. This confirms the proposition that uniflorine A contains the A-ring configuration of casuarine, given the aforementioned *trans* diaxial coupling constants observed between the contiguous H-7, H-8 and H-8a in uniflorine A. The second observed nOe in the uniflorine A sample was between H-6 and H-3. According to the corresponding casuarine structure, this nOe exists between H-3 and H-5 α , which neither confirms nor denies 6-*epi*-casuarine as the true structure for uniflorine A. However, the third and last nOe observed for uniflorine A provided telling evidence. This observation was observed between H-8 and H-1, which according to the

casuarine structure, is between H-1 and H-7. This indicates that H-1 and H-7 are on the same side of the molecule, which rules out the possibility of uniflorine A being 7-*epi*- or 6,7-di-*epi*-casuarine, and points to 6-*epi*-casuarine as the only possibility for the true structure of uniflorine A. However, it should be noted that no mention was made of an observed nOe between H-1 and H-2 for uniflorine A (H-6 and H-7 in casuarine), which would have otherwise confirmed the structure of 6-*epi*-casuarine. An attempt to acquire the original NMR spectra for uniflorine A was unsuccessful, insofar as the corresponding author did not respond to our email request.

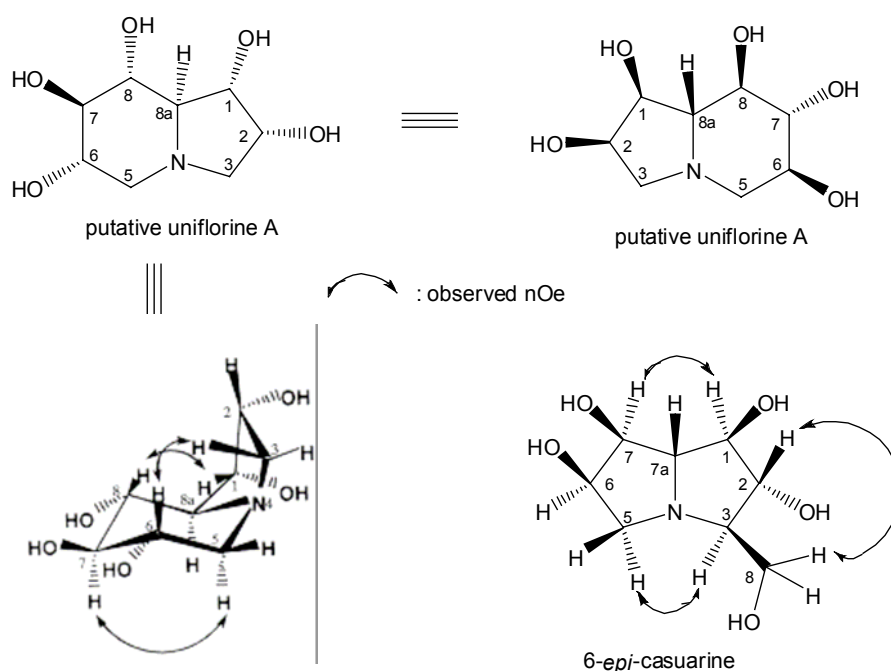


Figure 7.5. nOe Analysis of the proposed conformation of putative uniflorine A; comparison to 6-*epi*-casuarine.

While 6-*epi*-casuarine remains our best estimate as to the true structure for uniflorine A, ultimately we can only be somewhat equivocal about this proposition. The opportunity now exists for the synthetic chemist to synthesize this compound and check its spectroscopic data for a match with uniflorine A. At the time of writing, Prof. George Fleet had indicated to us, his groups' intention to publish the synthesis of a several more casuarine epimers in the near future. Although he did not specifically indicate that 6-*epi*-casuarine was one of these, it maybe sooner rather than later that we discover the true identity of uniflorine A. If it eventuates that 6-*epi*-casuarine is not the true structure for uniflorine A, then probably only one course of action would remain to solve the structure. It would require another quantity of leaves from *Eugenia uniflora* to be sampled from the exact location where the original sample was taken, and to repeat the natural product extraction. In the event that material is extracted, every attempt

should be made to grow crystals from either its neutral form, or from a protected product that is more amenable to recrystallization, such as a pentaacetate. Fleet *et al.* have already demonstrated their ability to grow single crystals from 3-*epi*-casuarine monohydrate and 3,7,7a-tri-*epi*-casuarine pentaacetate.^{189,190}

CONCLUSIONS

The initial aims of this project were to synthesize structure **1**, the proposed structure for the natural product uniflorine A and, in the event that compound **1** was synthesized, to compare its spectroscopic data with the corresponding data for uniflorine A and thereby verify structure **1** as a valid structure for uniflorine A.

A model study for the synthesis of **1** was reported in Chapter 2, which included the key Petasis reaction between D-Xylose **35a**, allylamine **37** and *trans*-2-phenylvinylboronic acid **36**; and the RCM reaction of diene **39**. The yields of these two steps were 76 % for the per-acetylated Petasis product **39** and 94 % for the ring-closing metathesis product **40**. Remarkably, compound **39** was obtained with complete 1,2-*anti* stereoselectivity as evidenced by single crystal X-ray analysis of the subsequent RCM product **40**. The model study also highlighted the inadequacy of not using orthogonal protecting groups to protect the amine and alcohol functionalities of the Petasis product. This was demonstrated in the attempted Mitsunobu cyclization reaction of amino alcohol **42** that, after subsequent per-acetylation, resulted in the only isolated product being the unwanted furan **45**.

In Chapter 3, the syntheses of *ent*-**1** and **1** were reported, which were identical except that the synthesis of *ent*-**1** used D-Xylose in the first step whereas the latter synthesis of **1** used its enantiomer in the first step. These syntheses utilized orthogonal protecting groups, with the amine functionality of the Petasis product **38** being protected by the Boc group, while the alcohol functionalities were protected as *O*-Benzyl ethers. This strategy enabled the selective deprotection of the *N*-Boc and primary *O*-Bn groups in compound **60** to give the penta-*O*-Bn protected amino alcohol **61** as the desired substrate for subsequent Appel cyclization (Section 3.9). As an unexpected bonus, this selective TFA mediated deprotection reaction also produced the indolizidine **62**, thereby making the Appel cyclization step partially redundant. Two mechanisms for the unusual TFA mediated cyclization of **60** were proposed in Section 3.9.

The timing of when to *O*-Bn protect proved to be particularly important. Section 3.5 demonstrated that when *O*-Bn protection was conducted on the diene **48**, substantial quantities of oxazolidinone **56** and oxazinanone **57** were produced, together with the desired tri-*O*-Bn product **49**. However, when *O*-Bn protection was performed at later stage in the synthesis of **1**, specifically on compound **59**, no oxazinone or oxazolone products were formed (Section 3.8).

The structure of our synthetic **1** was unequivocally established by a single-crystal X-ray crystallographic study of its pentaacetate derivative. However, the ¹H and ¹³C NMR data for synthetic **1** did not match with those reported for uniflorine A; the latter showed many more downfield peaks in the ¹H NMR, perhaps consistent with the amine salt. The ¹H NMR of the

hydrochloride salt of synthetic **1**, however, did not match the literature spectroscopic data either. We therefore concluded that the structure assigned to uniflorine A was not correct. We also found that the coupling constant $J_{1,8a}$ of 4.5 Hz for uniflorine A, was more consistent with the relative *syn*-H-8a, H-1 configuration, suggesting that uniflorine A, if it was an indolizidine alkaloid, had the same H-1 configuration as castanospermine.

In Chapter 4 the synthesis of 2-*epi*-**1** was attempted using two different methodologies employed on a common 2,5-dihydropyrrole **80** substrate. The first consisted of a *cis*-dihydroxylation of 2,5-dihydropyrrole **80**, which gave the diol **93** in an excellent 85 % yield. This was followed by the conversion of diol **93** into the cyclic sulfate **99** and subsequent ring-opening by benzoate to afford the benzoate-protected *trans*-3,4-diol **102**. These reactions resulted in moderately low yields and further elaboration of the ring-opened product **102** was not pursued. The second methodology involved the epoxidation of 2,5-dihydropyrrole **80** to give the epoxide **92** in excellent yields of 93 -100 %. Ring-opening of **92** with TFA and water afforded a product that could not be unequivocally identified, albeit in a moderate yield of 51 %. Attempts to access 2-*epi*-**1** from this sequence of reactions were also abandoned in favour of exploring of synthesis of 1,2-di-*epi*-**1**.

In Chapter 5, the diastereoselective synthesis of the C-1, C-2 di-epimer of **1** was achieved. This synthesis employed a novel pyrrolo[1,2-*c*]oxazin-1-one precursor **115** to allow for the reversal of π -facial diastereoselectivity in an osmium(VIII)-catalysed *syn*-dihydroxylation (DH) reaction. The NMR spectroscopic data of 1,2-di-*epi*-**1** also did not match that of uniflorine A.

Testing of *ent*-**1**, **1**, and 1,2-di-*epi*-**1** in Chapter 6 for activity against a series of α -glucosidases showed that only *ent*-**1** displayed inhibition, selectivity for α -mannosidase (IC₅₀ 200 μ M).

Finally, in Chapter 7, a comparison of the NMR data of uniflorine A and uniflorine B with that of casuarine and the known synthetic 1,2,6,7-tetrahydroxy-3-hydroxymethylpyrrolizidine isomers showed that uniflorine B is the known alkaloid casuarine. We also found that uniflorine A is a 1,2,6,7-tetrahydroxy-3-hydroxymethylpyrrolizidine with the same relative C-7-C-7a-C-1-C-2-C-3 configuration as casuarine. Although, we cannot unequivocally prove the structure of uniflorine A, without access to the original material and spectroscopic data, we proposed that uniflorine A is 6-*epi*-casuarine.

Chapter 9: Experimental

9.1.1 General reaction conditions

In general, all reactions unless otherwise stated were performed in oven dried, single-necked round bottom flasks. Progress of reactions was monitored by thin-layer chromatography (TLC) analysis. Solvents were purchased in Analytical Reagent (AR) grade. Where applicable, solvents were dried in the following manner:

THF was stored over KOH pellets until needed, then distilled over sodium wire under nitrogen, using benzophenone as an indicator.

DCM was heated at reflux for at least 30 min over CaH_2 , then distilled and stored over kiln dried ($200\text{ }^\circ\text{C}$) 4 Å molecular sieves.

Anhydrous MeOH was purchased from Aldrich.

Prepared starting materials were dried thoroughly under high vacuum. All reaction yields were obtained only after this drying process.

Where ‘evaporation’ is specified, this refers to the evaporation of solvent under reduced pressure using a rotary evaporator. Where ‘dried’ is specified, this refers to the drying of organic extract over MgSO_4 , unless otherwise indicated, followed by filtration.

9.1.2 Chromatography

TLC analyses were performed on aluminium backed Merck F₂₅₄ sorbet silica gel. Compounds were detected under a 254 nm ultraviolet lamp, or by staining with an acidified, aqueous solution of ammonium molybdate and cerium(IV) sulfate, followed by development with a 1400 Watt heat gun. One litre of the molybdate dip contained water (950 mL), concentrated H_2SO_4 (50 mL), $(\text{NH}_4)_6\text{MoO}_{24}$ (50 g) and $\text{Ce}(\text{SO}_4)_2$ (2 g).

Purification of compounds by flash column chromatography (FCC) was achieved using Merck flash silica gel (40 – 63 μm) and the technique reported by Still *et al.*¹⁹¹

Acidic ion-exchange chromatography was performed using DOWEX 50WX4-50 acidic cation exchange resin. Refer to Chapter 3.2 for further details. Basic ion-exchange chromatography was performed using Amberlyst A-26(OH) resin.

9.1.3 Melting points

Melting points were obtained using a Gallenkamp MF-370 capillary tube melting point apparatus and are uncorrected.

9.1.4 Polarimetry

Optical rotations were measured using a 1 cm or 5 cm cell, in a Jasco DIP-370 digital polarimeter. Five to ten measurements were taken and the average was used to calculate the specific rotation.

9.1.5 Mass spectrometry

Low-resolution mass spectra were obtained either on a Shimadzu GC mass spectrometer (EI and CI) or a Waters LCZ single quadropole (ESI). High-resolution mass spectra were obtained either on a VG Autospec mass spectrometer (EI and CI) or a Waters QTOF (ESI). HRMS (exact masses) were used in lieu of elemental analysis and ^1H and ^{13}C NMR spectroscopy were used as criteria for purity.

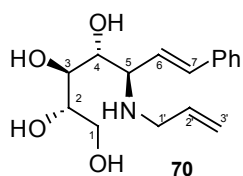
9.1.6 Nuclear magnetic resonance spectroscopy

^1H and ^{13}C NMR spectra were recorded on Varian Unity-300 (300 MHz ^1H , 75 MHz ^{13}C) or on a Varian INOVA-500 (500 MHz ^1H , 125 MHz ^{13}C) spectrometer in deuteriochloroform (CDCl_3), unless otherwise specified. NMR assignments were based on COSY, DEPT, HSQC and HMBC experiments. NMR solvents used in the experimental and their associated referencing data are displayed in Table 9.1. Unless otherwise stated, the applied NMR frequency was 300 MHz for ^1H NMR experiments and 75 MHz for ^{13}C NMR experiments, with samples dissolved in deuteriochloroform.

Solvent	^1H NMR		^{13}C NMR
	Internal standard	Other	Other
CDCl_3	TMS, s, 0.00 ppm	residual CHCl_3 , s, 7.26 ppm	CDCl_3 77.0 ppm
CD_3OD	TMS, s, 0.00 ppm,	residual MeOH, s, 3.34 ppm	CD_3OD , 49.0 ppm
D_2O	H_2O , s, 4.67 ppm	residual H_2O , s, 4.67 ppm	~ 5 % CH_3CN spike, 1.47 ppm

General method for the Petasis (Borono-Mannich) reaction

(6E)-5-(Allylamino)-5,6,7-trideoxy-7-phenyl-D-gluco-hept-6-enitol (**70**)



To a mixture of L-xylose (5 g, 33.3 mmol) and *trans*-2-phenylvinyl boronic acid (4.928 g, 33.3 mmol) was added absolute ethanol (65 mL) and allylamine (2.5 mL, 33.3 mmol). The mixture was stirred at RT for 16 h, followed by the evaporation of all volatiles. The residue was dissolved in 1 M HCl, applied to a column of DOWEX resin (H⁺ form) and washed with distilled H₂O (800 mL). The product was eluted with 7 M NH₄OH (500 mL) and 14 M NH₄OH (500 mL). The fractions containing the product were combined and concentrated to a brown foamy solid (7.147 g, 73 %).

$[\alpha]_D^{25} + 27$ (c 0.06, MeOH).

MS (CI +ve) m/z 294 (M + H⁺, 100 %).

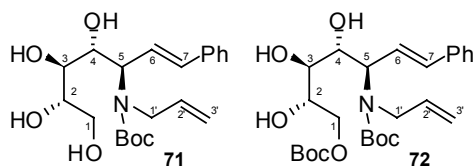
HRMS (CI +ve) calculated for C₁₆H₂₄NO₄ (M + H⁺) 294.1705, found 294.1713.

¹H NMR (CD₃OD) δ 7.44-7.29 (m, 5H, Ar), 6.56 (d, 1H, J 16.2 Hz, H-7), 6.17 (dd, 1H, J 9.2, 16.1 Hz, H-6), 5.92 (dddd, 1H, J 5.7, 6.6, 9.9, 17.0 Hz, H-2'), 5.20 (dq, 1H, J 1.5, 17.1 Hz, H-3'), 5.12 (dq, 1H, J 1.4, 9.9 Hz, H-3'), 3.85 (t, 1H, J 4.8 Hz, H-4), 3.76 (ddd, 1H, J 3.0, 5.1, 6.3 Hz, H-2), 3.69 (dd, 1H, J 3.2, 5.1 Hz, H-3), 3.62 (d, 1H, J 5.1 Hz, H-1), 3.61 (d, 1H, J 6.2 Hz, H-1), 3.50 (dd, 1H, J 4.8, 9.0 Hz, H-5), 3.34 (ddt, 1H, J 1.5, 5.6, 13.8 Hz, H-1'), 3.17 (ddt, 1H, J 1.5, 6.6, 13.5 Hz, H-1').

¹³C NMR (CD₃OD) δ 137.9 (q Ar), 136.3 (C-7), 135.8 (C-6), 129.5, 128.7, 127.4 (Ar), 117.9 (C-2'), 74.4 (CH), 73.1 (CH), 72.8 (CH), 64.4 (C-1), 63.4 (C-5), 50.0 (C-1').

General method for *N*-Boc protection

(6E)-5-[Allyl(*N*-*tert*-butylcarbonyl)amino]-5,6,7-trideoxy-7-phenyl-D-gluco-hept-6-enitol (**71**); (6E)-5-[Allyl(*N*-*tert*-butylcarbonyl)amino]-1-*O*-(*tert*-butoxycarbonyl)-5,6,7-trideoxy-7-phenyl-D-gluco-hept-6-enitol (**72**)



To a solution of **70** (3.8 g, 12.97 mmol) in dry THF (20 mL) was added dry Et₃N (2.0 mL, 14.37 mmol) and di-*tert*-butyl-dicarbonate (3.110 g, 14.27 mmol).

The reaction was stirred at rt for 24 h, followed by the evaporation of all volatiles. The residue was purified by FCC (60 - 100 % EtOAc / petrol) to give **71** (2.6 g, 51 %) as a brown oil, and **72** (1.28 g, 20 %) as a brown oil. Compound **72** was hydrolysed to **71** using the following method. To a solution of **72** (414 mg, 0.84 mmol) in MeOH (10 mL) was added K₂CO₃ (580 mg, 4.2 mmol). After stirring at rt for 3d, the mixture was evaporated and then dissolved in EtOAc and washed with water. The water layer was

extracted with EtOAc and the combined EtOAc extracts were washed with brine, dried and evaporated. The residue was purified by FCC (100 % EtOAc) to give **71** (210 mg, 64 %) as a brown oil.

71: $[\alpha]_D^{25}$ - 50 (*c* 3.0, CHCl₃).

MS (CI +ve) *m/z* 394 (*M* + *H*⁺, 30 %), 102 (Boc + *H*⁺, 100 %).

HRMS (CI +ve) calculated for C₂₁H₃₂NO₆ (*M* + *H*⁺) 394.2230, found 394.2229.

¹H NMR δ 7.37-7.17 (m, 5H, Ar), 6.56 (d, 1H, *J* 15.9 Hz, H-7), 6.40 (dd, 1H, *J* 6.6, 15.9 Hz, H-6), 5.76 (m, 1H, H-2'), 5.13 - 5.05 (m, 2H, H-3', H-3'), 4.42 (m, 1H, H-5), 4.38 (m, 1H, OH), 4.31 (m, 1H, OH), 4.14 (m, 1H, OH), 4.00 (m, 1H, H-4), 3.87 (m, 1H, H-2), 3.78 - 3.69 (m, 4H, H-1, H-1, H-1', H-1'), 3.57 (m, 1H, H-3), 1.44 (s, 9H, *t*-Bu).

¹³C NMR δ 156.4 (C=O), 136.6 (q Ar), 134.7 (C-2'), 134.4 (C-7), 128.4, 127.6, 126.4 (Ar), 125.1 (C-6), 116.9 (C-3'), 80.8 (q C, Boc), 73.0 (C-2), 72.4 (C-4), 70.2 (C-3), 63.8 (C-1), 60.2 (C-5), 48.9 (C-1'), 28.3 (CH₃).

72: MS (CI +ve) *m/z* 494 (*M* + *H*⁺, 40 %), 102 (Boc + *H*⁺, 100 %).

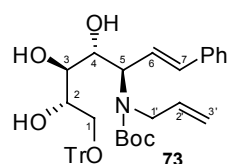
HRMS (CI +ve) calculated for C₂₆H₃₉NO₈ (*M* + *H*⁺) 494.2753, found 494.2752.

¹H NMR δ 7.40-7.22 (m, 5H, Ar), 6.60 (d, 1H, *J* 16.2 Hz, H-7), 6.41 (dd, 1H, *J* 7.2, 15.9 Hz, H-6), 5.80 (m, 1H, H-2'), 5.17-5.11 (m, 2H, H-3', H-3'), 4.42 (m, 1H, H-5), 4.23 (dd, 1H, *J* 5.1, 11.4 Hz, H-1), 4.16 (dd, 1H, *J* 6.0, 11.4 Hz, H-1), 4.05 (m, 1H, H-2), 3.98 (m, 1H, H-4), 3.81 (m, 2H, H-1', H-1'), 3.62 (m, 1H, H-3), 3.44 (m, 1H, OH), 3.29 (m, 1H, OH).

¹³C NMR δ 156.5 (C=O), 153.4 (C=O), 136.4 (q Ar), 134.7 (C-2', C-7), 128.4, 127.6, 126.4 (Ar), 124.6 (C-6), 117.0 (C-3'), 82.0 (q C, Boc), 80.8 (q C, Boc), 73.0 (C-4), 70.9 (C-2), 69.0 (C-3), 67.3 (C-1), 60.4 (C-5), 48.8 (C-1'), 28.2 (CH₃), 27.5 (CH₃).

General method for *O*-Trityl protection

(6*E*)-5-[Allyl(*N*-*tert*-butylcarbonyl)amino]-1-*O*-triphenylmethyl-5,6,7-trideoxy-7-phenyl-D-gluco-hept-6-enitol (**73**)



To a solution of **71** (2.6 g, 6.616 mmol) in dry pyridine (20 mL) was added TrCl (2.767 g, 9.924 mmol). The mixture was stirred for 18 h at rt, diluted with water (50 mL) and extracted with Et₂O (2 × 50 mL). The combined Et₂O extracts were washed with sat. aq. CuSO₄ (3 × 80 mL) and brine (80 mL), then dried and evaporated. The residue was purified by FCC (20 - 40 % EtOAc / petrol) to give **73** as a white foamy solid (2.66 g, 68 %).

$[\alpha]_D^{26}$ - 24 (*c* 1.5, CHCl₃).

MS (ESI +ve) *m/z* 658 (*M* + Na⁺, 43 %), 243 (Tr, 100 %).

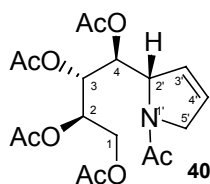
HRMS (ESI +ve) calculated for C₄₀H₄₅NO₆Na (*M* + Na⁺) 658.3145, found 658.3144.

^1H NMR δ 7.46-7.19 (m, 20H, Ar), 6.57 (d, 1H, J 15.9 Hz, H-7), 6.36 (dd, 1H, J 6.9, 15.9 Hz, H-6), 5.75 (m, 1H, H-2'), 5.10 - 5.01 (m, 2H, H-3'), 4.48 (m, 1H, H-5), 3.93 (m, 1H, H-2), 3.91-3.79 (m, 2H, H-4, H-3), 3.76 (m, 2H, H-1'), 3.37 (dd, 1H, J 2.7, 9.3 Hz, H-1), 3.19 (m, 1H, H-1), 1.43 (s, 9H, *t*-Bu).

^{13}C NMR δ 156.4 (C=O), 143.7, 136.5 (q Ar), 134.8 (C-2'), 134.5 (C-7), 128.6, 128.5, 127.8, 127.5, 127.0, 126.5 (Ar), 124.9 (C-6), 116.9 (C-3'), 86.9 (q C, Tr), 80.9 (q C, Boc), 73.2 (C-4), 72.2 (C-2), 69.3 (C-3), 64.0 (C-1), 60.4 (C-5), 48.8 (C-1'), 28.3 (CH_3).

General method for Ring-closing Metathesis

(2*R*,3*R*,4*S*)-3,4-Bis(acetyloxy)-4-[(2*S*)-1-acetyl-2,5-dihydro-1*H*-pyrrol-2-yl]butane-1,2-diyl diacetate (**40**)



To a solution of **39** (2.7 g, 5.41 mmol) in dry DCM (650 mL) was added Grubb's I catalyst (445 mg, 0.54 mmol). The mixture was stirred at reflux under N_2 for 18 h, then cooled to rt and evaporated to dryness. The residue was purified by FCC (80 % EtOAc / petrol) to give **40** (2.024 g, 94 %) as a light brown oil. Crystallization of the product was initiated by dissolving the residue in a minimum volume of boiling EtOAc. The flask was stoppered with a rubber septum and a needle was inserted to facilitate slow evaporation of the solvent. The flask was left in the dark for 3 d, resulting in the formation of a single large translucent crystal (6 mm) and several smaller crystals.

m.p. 128 °C

$[\alpha]_D^{23}$ - 67 (c 3.0, CHCl_3)

MS (CI +ve) m/z 400 ($\text{M} + \text{H}^+$, 100 %).

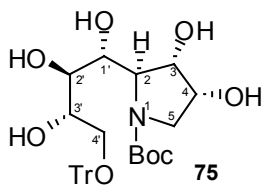
HRMS (CI +ve) calculated for $\text{C}_{18}\text{H}_{26}\text{NO}_9$ 400.1601 ($\text{M} + \text{H}^+$), found 400.1601.

^1H NMR δ 5.94 (ddd, 1H, J 2.1, 3.9, 6.3 Hz, H-4'), 5.75 (m, 2H, H-3' and H-4), 5.42 (dd, 1H, J 4.8, 6.3 Hz, H-3), 5.36 (m, 1H, H-2), 4.87 (m, 1H, H-2'), 4.34 (dd, 1H, J 4.5, 12.0 Hz, H-1), 4.16 (ddd, 1H, J 2.1, 4.2, 14.4 Hz, H-5'), 4.06 (m, 1H, H-5'), 3.99 (dd, 1H, J 6.6, 12.0 Hz, H-1), 2.18, 2.10, 2.06, 2.014, 2.01 (s, 1H, CH_3).

^{13}C NMR δ 170.1, 170.0, 169.4, 169.36, 168.8 (C=O), 127.5 (C-4'), 125.0 (C-3'), 70.51 (C-3, C-4), 68.8 (C-2), 64.3 (C-2'), 61.7 (C-1), 53.9 (C-5'), 22.2, 20.8, 20.6, 20.53, 20.53 (CH_3).

General method for *cis*-dihydroxylation

tert-Butyl(2*R*,3*S*,4*R*)-3,4-dihydroxy-2-[(1*R*,2*R*,3*S*)-1,2,3-trihydroxy-4-triphenylmethoxybutyl] pyrrolidine-1-carboxylate (**75**)



To a solution of **74** (1.56 g, 2.932 mmol) in acetone (15 mL) and water (15 mL) was added potassium osmate.dihydrate (54 mg, 0.147 mmol) and 4-morpholine-*N*-oxide (721 mg, 6.158 mmol). The reaction was stirred for 30 h at rt and evaporated to give a black oil which was purified by FCC (80 - 100 % EtOAc / petrol) to give **75** as a white foamy solid (1.46 g, 88 %).

$[\alpha]_D^{25} + 20$ (*c* 4.6, CHCl₃).

MS (ESI +ve) *m/z* 588 (*M* + Na⁺, 26 %), 243 (*Tr*, 100 %).

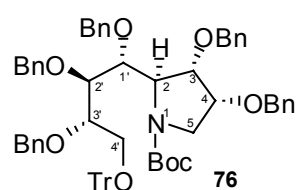
HRMS (ESI +ve) calculated for C₃₂H₃₉NO₈Na (*M* + Na⁺) 588.2541, found 588.2545.

¹H NMR δ 7.40-7.38 (m, 15H, Ar), 4.24 (m, 1H, H-4), 4.11 (m, 1H, H-3), 3.85 (m, 1H, H-2'), 3.78 (m, 1H, H-3'), 3.74 (m, 1H, H-1'), 3.37 (m, 1H, H-2), 3.35 (m, 2H, H-4', H-4'), 3.30 (m, 1H, H-5), 3.08 (m, 1H, H-5), 1.39 (s, 9H, *t*-Bu).

¹³C NMR δ 157.3 (C=O), 143.7 (q Ar), 128.6, 127.8, 127.0 (Ar), 86.5 (q C, *Tr*), 81.0 (q C, Boc), 73.3 (C-2), 72.6 (C-4), 72.5 (C-2'), 69.9 (C-3), 69.0 (C-3'), 65.1 (C-1'), 63.9 (C-5), 51.2 (C-4'), 28.3 (CH₃).

General method for *O*-Benzyl protection

tert-Butyl(2*S*,3*S*,4*R*)-3,4-bis(benzyloxy)-2-[(1*R*,2*R*,3*S*)-1,2,3-tris(benzyloxy)-4-triphenylmethoxybutyl] pyrrolidine-1-carboxylate (**76**)



To a solution of **75** (2.25 g, 3.989 mmol) in dry THF (20 mL) at 0 °C was added NaH (1.053 g, 21.94 mmol, 50 % in mineral oil). After H₂ evolution had ceased (10 min), BnBr (4.75 mL, 39.89 mmol) and *n*-BuNI (147 mg, 0.399 mmol) were added. The mixture was

brought to 50 °C and stirred for 18 h, then cooled to rt and treated with MeOH (5 mL) and Et₃N (3 mL) and stirred for 10 min. After evaporating all volatiles, the residue was dissolved in Et₂O and filtered through celite, followed by further washings of the solids with Et₂O. The solvent was evaporated and the residue was purified by FCC (5 - 30 % EtOAc / petrol) to give **76** as a brown oil (3.08 g, 76 %).

$[\alpha]_D^{23} + 14$ (*c* 3.5, CHCl₃).

MS (ESI +ve) *m/z* 1038 (*M* + Na⁺, 85 %), 1016 (*M* + H⁺, 33 %).

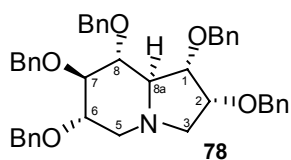
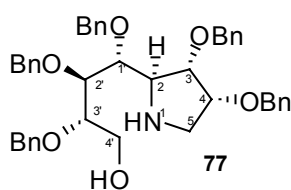
HRMS (ESI +ve) calculated for C₆₇H₇₀NO₈ (*M* + H⁺) 1016.5101, found 1016.5113.

¹H NMR (500 MHz) δ 7.44-6.69 (m, 40H, Ar), 4.80 - 4.40 (m, 10H, Bn), 4.40 - 3.26 (m, 10H, H-2, H-3, H-4, H-5, H-5, H-1', H-2', H-3', H-4', H-4'), 1.43 (s, 9H, *t*-Bu).

^{13}C NMR (125 MHz) δ (Major rotamer) 154.3 (C=O), 143.9, 138.7, 138.6, 138.3, 138.0, 137.8 (q Ar), 128.8, 128.7, 128.2, 128.14, 128.10, 128.0, 127.9, 127.8, 127.4, 127.3, 127.2, 126.8 (Ar), 86.9 (q C, Tr), 80.0 (q C, Boc), 79.9, 79.1, 78.0, 77.4, 76.9, 75.7, 75.1 (CH), 74.6, 73.7, 73.0 72.5, 71.7 (Bn), 64.0 (C-2), 63.8 (C-4'), 48.7 (C-5).

General Method for the removal of *O*-Trityl and or *N*-Boc protecting groups

(2*S*,3*S*,4*R*)-4-[(2*R*,3*S*,4*R*)-3,4-Dibenzyloxypyrrolidin-2-yl]-2,3,4-tribenzyloxybutan-1-ol (77); (1*S*,2*R*,6*S*,7*R*,8*R*,8*aR*)-1,2,6,7,8-pentabenzyloxyoctahydroindolizine (78)



To a solution of **76** (774 mg, 0.763 mmol) in dry DCM (7 mL) at 0 °C, was added anisole (0.83 mL, 7.626 mmol) and TFA (5.87 mL, 76.26 mmol). After stirring for 2 h at 0 °C, the mixture was evaporated to dryness, then dissolved in DCM (15 mL) and washed with sat. aq. Na_2CO_3 (20 mL). The aqueous layer was extracted with DCM (2 x 15 mL) and the combined DCM extracts were dried and evaporated. The residue was purified by FCC (40 - 100 % EtOAc / petrol and 20 % MeOH / EtOAc) to give cyclized compound **78** (270 mg, 54 %) and as a white solid and amino alcohol **77** (190 mg, 37 %) as a brown oil.

77: $[\alpha]_{\text{D}}^{22}$ - 21 (*c* 1.34, CHCl_3).

MS (CI +ve) m/z 674 ($\text{M} + 1^+$, 2 %), 566 ($\text{M} - \text{OBn}$, 3 %), 91 (Bn, 100 %).

HRMS (ESI +ve) calculated for $\text{C}_{43}\text{H}_{48}\text{NO}_6$ ($\text{M} + \text{H}^+$) 674.3481, found 674.3504.

^1H NMR δ 7.33-7.21 (m, 25H, Ar), 4.82 (d, 1H, *J* 11.4 Hz, Bn), 4.72 (d, 1H, *J* 11.4 Hz, Bn), 4.68 (d, 1H, *J* 11.1 Hz, Bn), 4.64 (d, 1H, *J* 11.7 Hz, Bn), 4.60 (d, 1H, *J* 11.1 Hz, Bn), 4.57 (d, 1H, *J* 11.4 Hz, Bn), 4.54 (d, 2H, *J* 12.0 Hz, Bn), 4.46 (d, 1H, *J* 12.0, Bn), 4.41 (d, 1H, *J* 11.4 Hz, Bn), 4.02 (dd, 1H, *J* 5.1, 5.7 Hz, H-3), 3.87 (m, 1H, H-4), 3.81 (m, 1H, H-1'), 3.78 (m, 1H, H-3'), 3.72 (m, 1H, H-4'), 3.68 (m, 1H, H-2'), 3.66 (m, 1H, H-2'), 3.66 (m, 1H, H-4'), 3.39 (dd, 1H, *J* 4.8, 5.4 Hz, H-2), 2.98 (dd, 1H, *J* 4.5, 12.0 Hz, H-5), 2.90 (dd, 1H, *J* 4.5, 12.0 Hz, H-5).

^{13}C NMR δ 138.6, 138.2, 138.11, 138.06, 138.0 (q Ar), 128.3, 128.25, 128.23, 128.0, 127.9, 127.8, 127.7, 127.64, 127.60, 127.4 (Ar), 80.6 (C-3'), 80.2 (C-1'), 79.7 (C-3), 78.6 (C-2'), 77.6 (C-4), 74.8, 74.3, 72.1, 71.9, 71.4 (Bn), 62.1 (C-2), 61.2 (C-4'), 48.9 (C-5).

78: $[\alpha]_{\text{D}}^{22}$ - 11 (*c* 0.7, CHCl_3).

MS (CI +ve) m/z 656 ($\text{M} + \text{H}^+$, 5 %), 107 (OBn, 100 %).

HRMS (ESI +ve) calculated for $\text{C}_{43}\text{H}_{46}\text{NO}_5$ ($\text{M} + \text{H}^+$) 656.3375, found 656.3367.

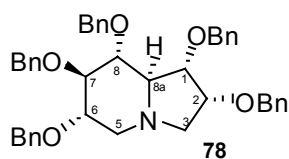
^1H NMR δ 7.33-7.20 (m, 25H, Ar), 4.93 (d, 1H, *J* 10.8 Hz, Bn), 4.89 (d, 1H, *J* 11.7 Hz, Bn), 4.81 (d, 1H, *J* 10.8 Hz, Bn), 4.72 (d, 1H, *J* 11.1 Hz, Bn), 4.66 - 4.51 (m, 6H, Bn), 3.99 (q, 1H, *J* 7.2 Hz, H-2), 3.80 (dd, 1H, *J* 5.7, 6.9 Hz, H-1), 3.63 (m, 1H, H-6), 3.57 (m, 1H, H-7), 3.35 (dd,

1H, *J* 8.4, 9.3 Hz, H-8), 3.19 (m, 1H, H-3), 3.15 (m, 1H, H-5), 2.56 (m, 1H, H-8a), 2.51 (m, 1H, H-3), 2.20 (t, 1H, *J* 10.2 Hz, H-5).

¹³C NMR δ 138.7, 138.5, 138.3, 138.2, 138.0 (q Ar), 128.4, 128.3, 128.2, 128.1, 128.0, 127.8, 127.7, 127.6, 127.5, 127.4, 127.3 (Ar), 87.1 (C-7), 81.6 (C-8), 80.2 (C-1), 79.0 (C-6), 76.0 (C-2), 75.7, 74.3, 72.8, 72.2, 72.0 (Bn), 70.3 (C-8a), 57.1 (C-3), 53.5 (C-5).

General method for Appel cyclization

(1*S*,2*R*,6*S*,7*R*,8*R*,8*aR*)-1,2,6,7,8-pentabenzyloxyoctahydroindolizine (**78**)



To a solution of amino alcohol **77** (55 mg, 81.72 μ mol) in dry DCM (1 mL) at 0 °C was added Et₃N (0.45 mL, 3.27 mmol), PPh₃ (54 mg, 0.204 mmol) and CBr₄ (68 mg, 0.204 mmol). The mixture was stirred for 30 min at 0 °C and poured into water (20 mL). The water

layer was extracted with DCM (2 \times 20 mL). The combined DCM extracts were washed with brine, dried and evaporated. The residue was purified by FCC (30 % EtOAc / petrol) to give **78** as a white solid film (45 mg, 84 %).

$[\alpha]_D^{22}$ - 11 (c 0.7, CHCl₃).

MS (CI +ve) *m/z* 656 (M + H⁺, 5 %), 107 (OBn, 100 %).

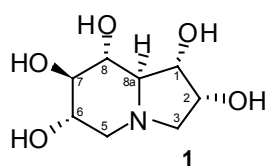
HRMS (ESI +ve) calculated for C₄₃H₄₆NO₅ (M + H⁺) 656.3375, found 656.3367.

¹H NMR δ 7.33-7.20 (m, 25H, Ar), 4.93 (d, 1H, *J* 10.8 Hz, Bn), 4.89 (d, 1H, *J* 11.7 Hz, Bn), 4.81 (d, 1H, *J* 10.8 Hz, Bn), 4.72 (d, 1H, *J* 11.1 Hz, Bn), 4.66-4.51 (m, 6H, Bn), 3.99 (q, 1H, *J* 7.2 Hz, H-2), 3.80 (dd, 1H, *J* 5.7, 6.9 Hz, H-1), 3.63 (m, 1H, H-6), 3.57 (m, 1H, H-7), 3.35 (dd, 1H, *J* 8.4, 9.3 Hz, H-8), 3.19 (m, 1H, H-3), 3.15 (m, 1H, H-5), 2.56 (m, 1H, H-8a), 2.51 (m, 1H, H-3), 2.20 (t, 1H, *J* 10.2 Hz, H-5).

¹³C NMR δ 138.7, 138.5, 138.3, 138.2, 138.0 (q Ar), 128.4, 128.3, 128.2, 128.1, 128.0, 127.8, 127.7, 127.6, 127.5, 127.4, 127.3 (Ar), 87.1 (C-7), 81.6 (C-8), 80.2 (C-1), 79.0 (C-6), 76.0 (C-2), 75.7, 74.3, 72.8, 72.2, 72.0 (Bn), 70.3 (C-8a), 57.1 (C-3), 53.5 (C-5).

General method for *O*-Benzyl deprotection

(1*S*,2*R*,6*S*,7*R*,8*R*,8*aR*)-Octahydroindolizine-1,2,6,7,8-pentol (**1**)



To a solution of **78** (460 mg, 0.702 mmol) in EtOAc (4 mL) and MeOH (3 mL) was added PdCl₂ (187 mg, 1.053 mmol). The mixture was stirred at rt under H₂ (> 1 atm) for 18 h. The mixture was filtered through celite and the solids were washed with MeOH. The combined

filtrates were evaporated and the residue was dissolved in H₂O and applied to a column of Amberlyst (OH⁻) A-26 resin. Elution with H₂O followed by evaporation resulted in a cloudy

white residue that was recrystallized from boiling EtOH with a few drops of H₂O to give **1** (90 mg, 63 %) as transparent micro-crystals.

m.p. 170-172 °C.

$[\alpha]^{25}_{\text{D}} - 10$ (*c* 0.67, MeOH). $[\alpha]^{25}_{\text{D}} - 6$ (*c* 5.0, H₂O).

MS (CI +ve) *m/z* 206 (M + H⁺, 100 %), 188 (M – OH, 50 %).

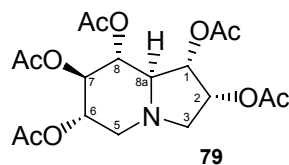
HRMS (CI +ve) calculated for C₈H₁₅NO₅ 205.0950, found 205.0947.

¹H NMR (500 MHz, D₂O) δ 4.11 (q, 1H, $J_{1,2} = J_{2,3\alpha} = J_{2,3\beta} = 7.0$ Hz, H-2), 3.82 (t, 1H, $J_{1,2} = J_{1,8a} = 7.5$ Hz, H-1), 3.46 (ddd, 1H, $J_{5\beta,6} = 5.5$ Hz, $J_{6,7} = 9.0$ Hz, $J_{5\alpha,6} = 11.0$ Hz, H-6), 3.26 (dd, 1H, $J_{2,3\alpha} = 6.5$, $J_{3\alpha,3\beta} = 10.5$ Hz, H-3 α), 3.25 (t, 1H, $J_{7,8} = J_{8,8a} = 9.0$ Hz, H-8), 3.20 (t, 1H, $J_{6,7} = J_{7,8} = 9.0$ Hz, H-7), 3.01 (dd, 1H, $J_{5\beta,6} = 5.5$ Hz, $J_{5\alpha,5\beta} = 10.5$ Hz, H-5 β), 2.20 (dd, 1H, $J_{2,3\beta} = 6.5$ Hz, $J_{3\alpha,3\beta} = 10.5$ Hz, H-3 β), 2.09 (t, 1H, $J_{5\alpha,5\beta} = J_{5\alpha,6} = 10.8$ Hz, H-5 α), 2.08 (dd, 1H, $J_{1,8a} = 7.5$ Hz, $J_{8,8a} = 9.3$ Hz, H-8a).

¹³C NMR (75 MHz, D₂O) δ 79.1 (C-7), 74.1 (C-8), 73.9 (C-1), 70.5 (C-8a), 70.4 (C-6), 68.6 (C-2), 59.2 (C-3), 55.4 (C-5).

General method for *O*-Acetylation

(1*S*,2*R*,6*S*,7*R*,8*R*,8a*R*)-Octahydroindolizine-1,2,6,7,8-pentyl pentaacetate (**79**)



To a solution of **1** (38 mg, 0.185 mmol) in dry pyridine (0.75 mL, 9.268 mmol) was added Ac₂O (0.87 mL, 9.268 mmol) and DMAP (*ca.* 2 crystals). The mixture was stirred at rt for 4 h followed by the evaporation of all volatiles. The oily residue was purified by FCC

(40 - 60 % EtOAc / petrol and 100 % EtOAc) and recrystallized (boiling petrol with a few drops of EtOAc) to give the pentaacetate **79** (68 mg, 88%) as colourless crystals.

m.p. 142 °C

$[\alpha]^{21}_{\text{D}} - 15$ (*c* 1.36, CHCl₃)

MS (CI +ve) *m/z* 416 (M + H⁺, 87 %), 356 (M - OAc, 100 %).

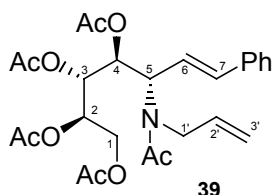
HRMS (ESI +ve) calculated for C₁₈H₂₆NO₁₀ (M + H⁺) 416.1557, found 416.1573.

¹H NMR (500 MHz) δ 5.25 (q, 1H, $J_{1,2} = J_{2,3\alpha} = J_{2,3\beta} = 6.3$ Hz, H-2), 5.11 (t, 1H, $J_{6,7} = J_{7,8} = 9.3$ Hz, H-7), 5.02 (t, 1H, $J_{1,2} = J_{1,8a} = 7.3$ Hz, H-1), 4.97 (dd, 1H, $J_{5\beta,6} = 5.8$ Hz, $J_{5\alpha,6} = 9.8$ Hz, H-6), 4.96 (t, 1H, $J_{7,8} = J_{8,8a} = 9.3$ Hz, H-8), 3.57 (dd, 1H, $J_{2,3\beta} = 6.8$ Hz, $J_{3\alpha,3\beta} = 10.3$ Hz, H-3 β), 3.28 (dd, 1H, $J_{5\beta,6} = 5.5$ Hz, $J_{5\alpha,5\beta} = 10.5$ Hz, H-5 β), 2.60 (t, 1H, $J_{1,8a} = J_{8,8a} = 8.5$ Hz, H-8a), 2.42 (dd, 1H, $J_{2,3\alpha} = 5.0$ Hz, $J_{3\alpha,3\beta} = 10.0$ Hz, H-3 α), 2.27 (t, 1H, $J_{5\alpha,5\beta} = J_{5\alpha,6} = 10.3$ Hz, H-5 α), 2.04, 2.028, 2.025, 2.02, 2.01 (s, 3H, Ac).

¹³C NMR (75 MHz) δ 170.3, 169.9, 169.8, 169.6, 168.9 (C=O), 73.9 (C-7), 73.7 (C-1), 72.0 (C-8), 69.9 (C-6), 69.3 (C-2), 65.7 (C-8a), 57.3 (C-3), 52.0 (C-5), 20.74, 20.67, 20.60, 20.2 (CH₃).

Chapter 2 Experimental

(6*E*)-2,3,4-Tri-*O*-acetyl-5-[allyl(*N*-acetyl)amino]-5,6,7-trideoxy-7-phenyl-*L*-gluco-hept-6-enitol (**39**)



To a solution of D-xylose (2.0 g, 13.3 mmol) in absolute EtOH (40 mL) was added *trans*-2-phenylvinylboronic acid (1.97 g, 13.3 mmol) and allylamine (1 mL, 13.3 mmol). The mixture was stirred for 18 h at rt and evaporated to give a brown foamy solid. The residue was dissolved in dry pyridine (52.6 mL, 650 mmol), followed by the addition of Ac₂O (61.3 mL, 650 mmol) and DMAP (162 mg, 1.33 mmol). The mixture was stirred at rt for 3 d then evaporated to dryness. The residue was purified by FCC (50 % EtOAc / petrol to 100 % EtOAc) to give **39** (5.068 g, 76 %) as a brown oil.

$[\alpha]_D^{26} + 36$ (*c* 2.0, CHCl₃).

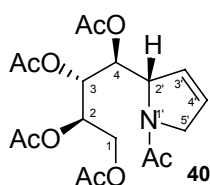
MS (CI +ve) *m/z* 504 (*M* + H⁺, 100 %), 444 (*M* - OAc, 75 %).

HRMS (CI +ve) calc for C₂₆H₃₄NO₉ (*M* + H⁺) 504.2199, found 504.2199.

¹H NMR δ 7.36-7.26 (m, 5H, Ar), 6.67 (d, 1H, *J* 15.6 Hz, H-7), 6.21 (dd, 1H, *J* 9.5, 15.8 Hz, H-6), 5.77 (dddd, 1H, *J* 5.4, 5.4, 10.8, 16.5 Hz, H-2'), 5.65 (dd, 1H, *J* 3.9, 7.5 Hz, H-4), 5.33 (dd, 1H, *J* 3.8, 6.8 Hz, H-3), 5.23 (ddd, 1H, *J* 3.6, 5.7, 6.6 Hz, H-2), 5.19 (m, 1H, H-3'), 5.14 (ddd, 1H, *J* 1.5, 2.7, 8.1 Hz, H-3'), 5.08 (dd, 1H, *J* 7.8, 9.3 Hz, H-5), 4.35 (dd, 1H, *J* 3.9, 12.3 Hz, H-1'), 4.01 (dd, 1H, *J* 5.9, 12.2 Hz, H-1'), 3.92 (m, 2H, H-1, H-1), 2.11, 2.10, 2.04 × 2, 2.03 (s, 3H, CH₃).

¹³C NMR δ 171.3, 170.2, 170.0, 169.97, 169.9 (C=O), 136.4 (C-7), 136.0 (q Ar), 134.0 (C-2'), 128.5, 128.1, 126.5 (Ar), 122.4 (C-6), 117.4 (C-3'), 70.9 (C-4), 69.5 (C-2), 68.7 (C-3), 61.9 (C-1'), 57.0 (C-5), 48.9 (C-1), 22.1, 21.1, 20.9 × 2, 20.7 (CH₃).

(2*R*,3*R*,4*S*)-3,4-Bis(acetyloxy)-4-[(2*S*)-1-acetyl-2,5-dihydro-1*H*-pyrrol-2-yl]butane-1,2-diyl diacetate (**40**)



To a solution of **39** (2.7 g, 5.41 mmol) in dry DCM (650 mL) was added Grubb's I catalyst (445 mg, 0.54 mmol). The mixture was stirred at reflux under N₂ for 18 h, then cooled to rt and evaporated to dryness. The residue was purified by FCC (80 % EtOAc / petrol) to give **40** (2.024 g, 94 %) as a light brown oil. Crystallization of the product was initiated by dissolving

the residue in a minimum volume of boiling EtOAc. The flask was stoppered with a rubber septum and a needle was inserted to facilitate slow evaporation of the solvent. The flask was left in the dark for 3 d, resulting in the formation of a single large translucent crystal (6 mm) and several smaller crystals.

m.p. 128 °C

$[\alpha]_D^{23}$ - 67 (*c* 3.0, CHCl₃)

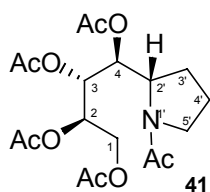
MS (CI +ve) *m/z* 400 (*M* + H⁺, 100 %).

HRMS (CI +ve) calculated for C₁₈H₂₆NO₉ 400.1601 (*M* + H⁺), found 400.1601.

¹H NMR δ 5.94 (ddd, 1H, *J* 2.1, 3.9, 6.3 Hz, H-4'), 5.75 (m, 2H, H-3' and H-4), 5.42 (dd, 1H, *J* 4.8, 6.3 Hz, H-3), 5.36 (m, 1H, H-2), 4.87 (m, 1H, H-2'), 4.34 (dd, 1H, *J* 4.5, 12.0 Hz, H-1), 4.16 (ddd, 1H, *J* 2.1, 4.2, 14.4 Hz, H-5'), 4.06 (m, 1H, H-5'), 3.99 (dd, 1H, *J* 6.6, 12.0 Hz, H-1), 2.18, 2.10, 2.06, 2.014, 2.01 (s, 1H, CH₃).

¹³C NMR δ 170.1, 170.0, 169.4, 169.36, 168.8 (C=O), 127.5 (C-4'), 125.0 (C-3'), 70.51 (C-3, C-4), 68.8 (C-2), 64.3 (C-2'), 61.7 (C-1), 53.9 (C-5'), 22.2, 20.8, 20.6, 20.53, 20.53 (CH₃).

(2*R*,3*R*,4*S*)-3,4-Bis(acetyloxy)-4-[(2*S*)-1-acetyl-pyrrolidin-2-yl]butane-1,2-diyl diacetate (41)



To a solution of **40** (1.145 g, 2.863 mmol) in THF (60 mL) was added 10 % palladium over activated carbon (115 mg). The mixture was stirred at rt for 16 h under a H₂ balloon. The mixture was filtered through celite and the remaining solids were washed with EtOAc (200 mL), followed by evaporation to give **41** (1.125 g, 98 %) as a brown oil. ¹H NMR analysis

showed that no further purification was required. Crystallization of the product was initiated by dissolving the residue in a minimum volume of boiling EtOAc. The flask was stoppered with a rubber septum and a needle was inserted to facilitate slow evaporation of the solvent. The flask was left overnight, furnishing a batch of white crystals (420 mg) from which NMR, optical rotation and m.p. data were derived.

m.p. 117 °C

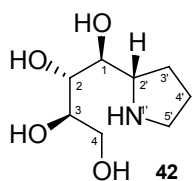
$[\alpha]_D^{23}$ - 27 (*c* 3.9, CHCl₃)

MS (CI +ve) *m/z* 402 (*M* + H⁺, 100 %), 342 (*M* - OAc, 20 %).

HRMS (CI +ve) calculated for C₁₈H₂₈NO₉ 402.1765, (*M* + H⁺) found 400.1765.

¹H NMR δ 5.78 (dd, 1H, *J* 2.1, 4.5 Hz, H-3), 5.32 (m, 1H, H-2), 5.29 (m, 1H, H-4), 4.30 (dd, 1H, *J* 4.5, 11.7 Hz, H-1), 4.15 (m, 1H, H-2'), 3.98 (dd, 1H, *J* 6.6, 11.7 Hz, H-1), 3.43 (m, 1H, H-5'), 3.30 (m, 1H, H-5'), 2.21, 2.08 (s, 3H, CH₃), 2.05 (m, 2H, H-4'), 2.04 × 2, 2.00 (s, 3H, CH₃), 1.92 (m, 2H, H-3').

¹³C NMR δ 170.0, 169.9, 169.3, 169.0, 168.98 (C=O), 70.6 (C-3), 70.4 (C-4), 68.3 (C-2), 61.5 (C-1), 56.1 (C-2'), 47.5 (C-5'), 24.8 (C-3'), 24.5 (C-4'), 22.5, 20.6, 20.58, 20.4, 20.36 (CH₃).

(1*S*,2*R*,3*R*)-1-[(2*S*)-Pyrrolidin-2-yl]butane-1,2,3,4-tetrol (42)

To a solution of **41** (1.113 g, 2.769 mmol) in Et₂O (6 mL) was added HCl (25 mL, 10 % v/v). The mixture was stirred in a sealed tube at 110 °C for 16 h. After cooling, the mixture was diluted with water (10 mL) and washed with Et₂O (2 × 15 mL). The aqueous layer was evaporated and the residue was dissolved in a minimum volume of HCl (1M), and applied to a column of DOWEX resin (H⁺ form). The column was washed with distilled H₂O (80 mL) and the product was eluted with 7 M NH₄OH (100 mL) and 14 M NH₄OH (100 mL). The fractions containing the product were combined and concentrated to give **42** (545 mg, 86 %) as a brown oil.

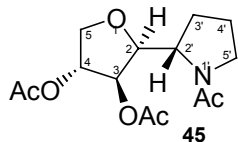
$[\alpha]_D^{26} + 10$ (*c* 0.8, MeOH)

MS (CI +ve) *m/z* 192 (*M* + 1⁺, 100 %).

HRMS (CI +ve) calculated for C₈H₁₈NO₄ 191.1236, found 191.1232

¹H NMR (D₂O) δ 3.67 (m, 1H, H-3), 3.64-3.45 (m, 4H, H-1, H-2, H-4, H-4), 3.17 (q, 1H, *J* 6.9 Hz, H-2'), 2.86-2.71 (m, 2H, H-5', H-5'), 1.81 (m, 1H, H-3'), 1.72-1.62 (m, 2H, H-4', H-4'), 1.50 (m, 1H, H-3').

¹³C NMR (75 MHz, D₂O) δ 73.2 (C-3 or C-4), 72.6 (C-3 or C-4), 71.6 (C-2), 62.7 (C-4), 59.6 (C-2'), 45.9 (C-5'), 27.2 (C-3'), 24.9 (C-4').

(2*S*,3*R*,4*R*)-2-[(2*S*)-1-Acetylpyrrolidin-2-yl]tetrahydrofuran-3,4-diyl diacetate (45)

DEAD (270 μL, 1.72 mmol) was added dropwise to stirred mixture of **42** (275 mg, 1.42 mmol), PPh₃ (451 mg, 1.72 mmol) and dry pyridine (8 mL) at 0 °C. The mixture was stirred at 0 °C for 4 h then diluted with H₂O (25 mL) and washed with DCM (3 × 25 mL). The aqueous layer was

evaporated and the residue was dissolved in dry pyridine (6 mL), followed by the addition of Ac₂O (3.2 mL) and DMAP (14 mg). The mixture was stirred at rt for 18 h, then diluted with H₂O (20 mL) and extracted with DCM (4 × 20 mL). The combined DCM extracts were dried and evaporated and the residue was purified by FCC (70 % EtOAc / petrol) and semi-preparative TLC (70 % EtOAc / petrol) to give **45** (76 mg, 18 % over two steps) as a brown oil.

MS (CI +ve) *m/z* 300 (*M* + H⁺, 100 %), 258 (*M* - Ac, 90 %).

HRMS (CI +ve) calculated for C₁₄H₂₂NO₆ 300.1447, (*M* + H⁺) found 300.1442.

¹H NMR δ 5.30 (dd, 1H, *J* 1.1, 3.5 Hz, H-2), 5.04 (ddd, 1H, *J* 1.1, 2.5, 5.0 Hz, H-4), 4.39-4.31 (m, 2H, H-2', H-3), 4.23 (dd, 1H, *J* 5.1, 10.5 Hz, H-5), 3.66 (dd, 1H, *J* 2.6, 10.7 Hz, H-5), 3.52-3.37 (m, 2H, H-5', H-5'), 2.25-2.16 (m, 1H, H-3'), 2.13-2.09 (m, 1H, H-4'), 2.10, 2.07, 2.06 (s, 3H, CH₃), 2.06-2.03 (m, 1H, H-4'), 1.92-1.82 (m, 1H, H-3').

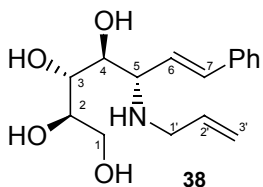
¹³C NMR δ 169.7, 169.4, 169.3 (C=O), 79.9 (C-3), 77.4 (C-4), 76.6 (C-2), 71.9 (C-5), 55.4 (C-2'), 47.9 (C-5'), 26.3 (C-3'), 24.9 (C-4'), 23.1, 21.0, 20.9 (CH₃).

Chapter 3 Experimental

(6*E*)-5-(Allylamino)-5,6,7-trideoxy-7-phenyl-D-*gluco*-hept-6-enitol (70)

See page 119.

(6*E*)-5-(Allylamino)-5,6,7-trideoxy-7-phenyl-L-*gluco*-hept-6-enitol (38)



Compound **38** (3.675 g, 94 %) was synthesized by the General method for the Petasis reaction, except that D-xylose (2.0 g, 13.3 mmol) was substituted for L-xylose as a starting material.

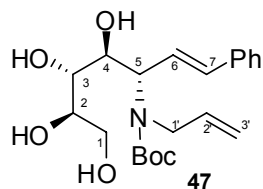
$[\alpha]_D^{25}$ - 17 (*c* 0.3, MeOH).

^1H and ^{13}C NMR data matched the corresponding data of compound **70**.

(6*E*)-5-[Allyl-*N*-(*tert*-butylcarbonyl)amino]-5,6,7-trideoxy-7-phenyl-D-*gluco*-hept-6-enitol (71)

See pages 119-120.

(6*E*)-5-[Allyl-*N*-(*tert*-butylcarbonyl)amino]-5,6,7-trideoxy-7-phenyl-L-*gluco*-hept-6-enitol (47)



Compound **47** (445 mg, 67 %) was synthesized by the General method for *N*-Boc protection from **39** (498 mg, 1.70 mmol), except that CH_3CN / DMF (10 mL, 9:1) was used as the solvent. Some *N*-Boc-*O*-Boc product was also isolated (151 mg, 18 %) and was hydrolysed to **47** (58 %), using the hydrolysis method outlined within the General method for *N*-Boc protection.

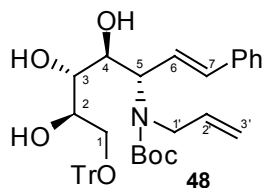
$[\alpha]_D^{25}$ + 29 (*c* 2.3, CHCl_3).

^1H and ^{13}C NMR data matched the corresponding data of compound **71**.

(6*E*)-5-[Allyl-*N*-(*tert*-butylcarbonyl)amino]-1-*O*-triphenylmethyl-5,6,7-trideoxy-7-phenyl-D-*gluco*-hept-6-enitol (73)

See page 120.

(6E)-5-[Allyl-N-(tert-butylcarbonyl)amino]-1-O-triphenylmethyl-5,6,7-trideoxy-7-phenyl-L-gluco-hept-6-enitol (48)

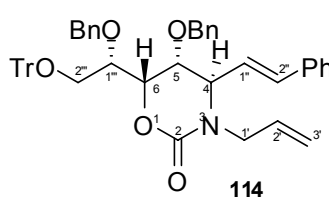
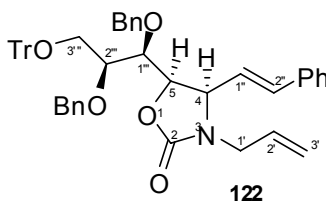
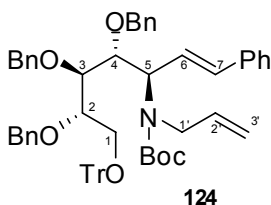


Compound **48** (400 mg, 84 %) was synthesized from **47** (295 mg, 0.75 mmol) by the General method for *O*-Tr protection.

$[\alpha]_D^{25} + 20$ (*c* 1.0, CHCl₃).

¹H and ¹³C NMR data matched the corresponding data of **73**.

(6E)-5-[Allyl-N-(tert-butylcarbonyl)amino]-2,3,4-tri-O-benzyl-1-triphenylmethyl-5,6,7-trideoxy-7-phenyl-D-gluco-hept-6-enitol (124); (4R,5R)-3-allyl-4[(E)-2-phenylvinyl]-5-[(1S,2S)-1, 2-bis(benzyloxy)-3-triphenylmethyloxypentyl]-1,3-oxazolidin-2-one (122); (4R,5R,6S)-3-allyl-4[(E)-2-phenylvinyl]-5-(benzyloxy)-6-[(1S)-1-(benzyloxy)-2-triphenylmethyloxyethyl]-1,3-oxazin-2-one (114)



To a solution of **73** (650 mg, 1.024 mmol) in dry THF (6 mL) was added BnBr (0.73 mL, 6.142 mmol) and *n*-BuNI (38 mg, 0.102 mmol). The mixture was cooled to 0 °C before the addition of NaH (164 mg, 3.409 mmol, 50 % dispersion in mineral oil), followed by stirring for 10 min. The mixture was brought to rt and stirred for 18 h then quenched with MeOH (1 mL). After stirring for 10 min, the mixture was poured into water and extracted with Et₂O (2 × 20 mL). The combined Et₂O extracts were washed with brine, dried and evaporated. The residue was purified by FCC (10 % EtOAc / petrol) to give three products **124** (323 mg, 35 %), **122** (326 mg, 43 %) and **114** (106 mg, 14 %).

124: $[\alpha]_D^{26} + 7$ (*c* 2.7, CHCl₃).

MS (ESI +ve) *m/z* 928 (M + Na⁺, 40 %), 243 (Ph₃C⁺, 100 %).

HRMS (ESI +ve) calculated for C₆₁H₆₄NO₆ 906.4733, found 906.4721.

¹H NMR δ 7.41-7.10 (m, 30H, Ar), 6.51 (m, 2H, H-6, H-7), 5.70 (m, 1H, H-2'), 4.94 (m, 1H, H-3'), 4.90 (m, 1H, H-3'), 4.74 (m, 2H, Bn), 4.56 (m, 2H, Bn), 4.50 (m, 3H, Bn, H-5), 4.15 (m, 1H, H-2 or H-4), 3.98 (m, 1H, H-2 or H-4), 3.78 (m, 1H, H-3), 3.73 (m, 1H, H-1'), 3.45-3.30 (m, 2H, H-1, H-1).

¹³C NMR δ 155.1 (C=O), 143.9, 138.7, 138.3, 137.0 (q Ar), 135.7 (C-2'), 134.8 (C-7), 128.7, 128.5, 128.2, 128.1, 128.0, 127.8, 127.7, 127.6, 127.4, 127.3, 127.2, 126.8, 126.5 (Ar), 125.0 (C-6), 115.4 (C-3'), 86.7 (q C, Tr), 80.8 (q C, Boc), 80.0 (C-2 or C-4), 78.5 (C-3 and C-2 or C-4), 74.1, 73.5, 73.5 (Bn), 63.4 (C-1), 59.7 (C-5), 48.8 (C-1').

122: $[\alpha]_D^{26} + 52$ (c 3.2, CHCl_3).

MS (ESI +ve) m/z 764 ($\text{M} + \text{Na}^+$, 90 %), 243 (Ph_3C^+ , 100 %).

HRMS (ESI +ve) calculated for $\text{C}_{50}\text{H}_{47}\text{NO}_5\text{Na}$ ($\text{M} + \text{Na}^+$) 764.3351, found 764.3352.

^1H NMR δ 7.40-7.14 (m, 30H, ArH), 6.02-5.91 (m, 2H, H-1'', H-2''), 5.66 (dddd, 1H, J 4.5, 7.2, 10.2, 17.4 Hz, H-2'), 5.19 (dd, 1H, J 0.9, 10.2 Hz, H-3'), 5.09 (dd, 1H, J 0.9, 17.3 Hz, H-3'), 4.82 (d, 1H, J 11.1 Hz, Bn), 4.75 (t, 1H, J 7.5 Hz, Bn), 4.64 (d, 1H, J 12.3 Hz, Bn), 4.63 (d, 1H, J 11.1 Hz, Bn), 4.17 (d, 1H, J 12.0 Hz, Bn), 4.10 (ddt, 1H, J 1.8, 4.0, 15.9 Hz, H-1'), 3.96 (dd, 1H, J 3.3, 4.5 Hz, H-1'''), 3.75 (ddd, 1H, J 3.3, 5.3, 6.2 Hz, H-2'''), 3.58 (ddd, 1H, J 3.5, 5.9, 7.5 Hz, H-4), 3.43 (dd, 1H, J 6.0, 9.6 Hz, H-3'''), 3.37 (dd, 1H, J 5.3, 9.5 Hz, H-3'''), 3.32 (ddt, 1H, J 0.9, 7.5, 15.6 Hz, H-1').

^{13}C NMR δ 157.2 (C-2), 143.5, 138.0, 137.8 (q Ar), 137.2 (C-2''), 134.9 (Ar), 132.3 (C-2'), 129.1, 128.7, 128.6, 128.4, 128.2, 128.1, 127.9, 127.7, 127.4, 127.0, 126.5 (Ar), 121.4 (C-1''), 118.1 (C-3'), 87.0 (q C, Tr), 77.8 (C-5), 77.0 (C-1'''), 74.8 (C-2'''), 74.7, 71.1 (Bn), 61.1 (C-3'''), 59.8 (C-4), 44.1 (C-1').

114: $[\alpha]_D^{26} + 37$ (c 1.2, CHCl_3).

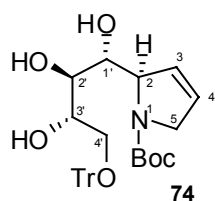
MS (ESI +ve) m/z 764 ($\text{M} + \text{Na}^+$, 70 %), 243 (Ph_3C^+ , 100 %).

HRMS (ESI +ve) calculated for $\text{C}_{50}\text{H}_{47}\text{NO}_5\text{Na}$ ($\text{M} + \text{Na}^+$) 764.3351, found 764.3349.

^1H NMR δ 7.49-6.98 (m, 30H, Ar), 6.54 (dd, 1H, J 1.5, 15.9 Hz, H-2''), 5.93 (dd, 1H, J 6.3, 15.9 Hz, H-1''), 5.77 (dddd, 1H, J 3.9, 7.8, 10.2, 17.7 Hz, H-2'), 5.17 (dq, 1H, J 1.5, 17.4 Hz, H-3'), 5.12 (dq, 1H, J 1.5, 10.2 Hz, H-3'), 4.93 (dd, 1H, J 1.5, 7.8 Hz, H-6), 4.84 (d, 1H, J 11.4 Hz, Bn), 4.70 (d, 1H, J 11.4 Hz, Bn), 4.56 (ddt, 1H, J 1.7, 3.8, 15.5 Hz, H-1'), 4.24 (d, 1H, J 11.1 Hz, Bn), 4.08 (dt, 1H, J 1.7, 6.3 Hz, H-4), 3.90 (ddd, 1H, J 1.8, 2.7, 7.8 Hz, H-1'''), 3.70 (dd, 1H, J 1.8, 10.5 Hz, H-2'''), 3.57 (d, 1H, J 10.8 Hz, Bn), 3.45 (t, 1H, J 1.8 Hz, H-5), 3.34 (ddt, 1H, J 1.1, 7.8, 15.5 Hz, H-1'), 2.92 (dd, 1H, J 2.9, 10.7 Hz, H-2''').

^{13}C NMR δ 152.8 (C-2), 143.2, 138.4, 136.8, 135.3 (q Ar), 133.7 (C-2''), 132.5 (C-2'), 128.7, 128.5, 128.3, 128.2, 127.8, 127.5, 127.4, 127.0, 126.6 (Ar), 124.8 (C-1''), 117.7 (C-3'), 86.2 (q C, Tr), 78.9 (C-1'''), 76.6 (C-6), 73.6 (Bn), 72.8 (C-5), 71.2 (Bn), 61.8 (C-2'''), 57.5 (C-4), 49.6 (C-1').

***tert*-Butyl(2*R*)-2-[(1*R*,2*R*,3*S*)-1,2,3-trihydroxy-4-triphenylmethoxybutyl]-2,5-dihydro-1*H*-pyrrole-1-carboxylate (74)**



Compound **74** (605 mg, 86 %) was synthesized from **73** (840 mg, 1.323 mmol), using the General method for ring-closing metathesis (Grubbs' I), except that the crude product was purified by FCC (40 - 60 % EtOAc / petrol) to give **74** as a white foamy solid.

$[\alpha]^{25}_{\text{D}} + 74$ (c 0.72, CHCl_3).

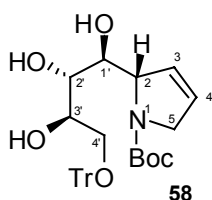
MS (ESI +ve) m/z 554 ($\text{M} + \text{Na}^+$, 60 %), 243 (Tr^+ , 100 %).

HRMS (ESI +ve) calculated for $\text{C}_{32}\text{H}_{37}\text{NO}_6\text{Na}$ ($\text{M} + \text{Na}^+$) 554.2519, found 554.2524.

^1H NMR δ 7.44-7.20 (m, 15H, Ar), 5.87 (dd, 1H, J 1.8, 6.4 Hz, H-4), 5.81 (d, 1H, J 6.6 Hz, H-3), 4.67 (m, 1H, H-2), 4.22 (dd, 1H, J 1.5, 15.9 Hz, H-5), 3.98 (dd, 1H, J 3.0, 15.6 Hz, H-5), 3.83 (m, 1H, H-3'), 3.80 (m, 1H, H-2'), 3.53 (m, 1H, H-1'), 3.33 (dd, 1H, J 4.8, 9.6 Hz, H-4'), 3.15 (dd, 1H, J 4.8, 9.6 Hz, H-4'), 1.47 (s, 9H, t -Bu).

^{13}C NMR δ 157.0 (C=O), 143.8 (q Ar), 128.6, 128.5, 127.8, 127.0 (Ar), 126.4 (C-3), 86.6 (q C, Tr), 80.8 (q C, Boc), 75.3 (C-1'), 72.5 (C-3'), 69.5 (C-2'), 67.2 (C-2), 64.3 (C-4'), 54.3 (C-5), 28.4 (CH_3).

***tert*-Butyl(2*S*)-2-[(1*S*,2*S*,3*R*)-1,2,3-trihydroxy-4-triphenylmethoxybutyl]-2,5-dihydro-1*H*-pyrrole-1-carboxylate (**58**)**

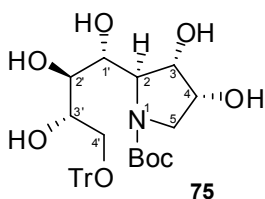


Compound **58** (845 mg, 96 %) was synthesized from **48** (1.055 g, 1.661 mmol) using the General method for ring-closing metathesis (Grubbs' I), except that the crude product was purified by FCC (40 - 60 % EtOAc / petrol) to give **58** as a white foamy solid.

$[\alpha]^{25}_{\text{D}} - 82$ (c 5.0, CHCl_3).

^1H and ^{13}C NMR data matched the corresponding data of **74**.

***tert*-Butyl(2*R*,3*S*,4*R*)-3,4-dihydroxy-2-[(1*R*,2*R*,3*S*)-1,2,3-trihydroxy-4-triphenylmethoxybutyl] pyrrolidine-1-carboxylate (**75**)**



Compound **75** (1.46 g, 88 %) was synthesized from **74** (1.56 g, 2.932 mmol) using the General method for cis-dihydroxylation.

$[\alpha]^{25}_{\text{D}} + 20$ (c 4.6, CHCl_3).

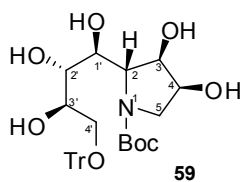
MS (ESI +ve) m/z 588 ($\text{M} + \text{Na}^+$, 26 %), 243 (Tr , 100 %).

HRMS (ESI +ve) calculated for $\text{C}_{32}\text{H}_{39}\text{NO}_8\text{Na}$ ($\text{M} + \text{Na}^+$) 588.2541, found 588.2545.

^1H NMR δ 7.40-7.38 (m, 15H, Ar), 4.24 (m, 1H, H-4), 4.11 (m, 1H, H-3), 3.85 (m, 1H, H-2'), 3.78 (m, 1H, H-3'), 3.74 (m, 1H, H-1'), 3.37 (m, 1H, H-2), 3.35 (m, 2H, H-4', H-4'), 3.30 (m, 1H, H-5), 3.08 (m, 1H, H-5), 1.39 (s, 9H, t -Bu).

^{13}C NMR δ 157.3 (C=O), 143.7 (q Ar), 128.6, 127.8, 127.0 (Ar), 86.5 (q C, Tr), 81.0 (q C, Boc), 73.3 (C-2), 72.6 (C-4), 72.5 (C-2'), 69.9 (C-3), 69.0 (C-3'), 65.1 (C-1'), 63.9 (C-5), 51.2 (C-4'), 28.3 (CH_3).

***tert*-Butyl(2*S*,3*R*,4*S*)-3,4-dihydroxy-2-[(1*S*,2*S*,3*R*)-1,2,3-trihydroxy-4-triphenylmethoxybutyl] pyrrolidine-1-carboxylate (**59**)**

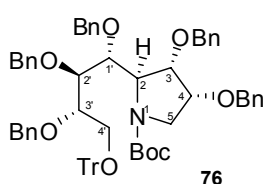


Compound **59** (1.20 g, 79 %) was synthesized from **58** (1.42 g, 2.679 mmol) by the General method for *cis*-dihydroxylation.

$[\alpha]_D^{23}$ - 20 (*c* 9.0, CHCl₃).

¹H and ¹³C NMR data matched the corresponding data of **75**.

***tert*-Butyl(2*S*,3*S*,4*R*)-3,4-bis(benzyloxy)-2-[(1*R*,2*R*,3*S*)-1,2,3-tris(benzyloxy)-4-triphenylmethoxybutyl]-pyrrolidine-1-carboxylate (**76**)**



Compound **76** (3.08 g, 76 %) was synthesized as a brown oil from **75** (2.25 g, 3.989 mmol) using the General method for *O*-Bn protection.

$[\alpha]_D^{23}$ + 14 (*c* 3.5, CHCl₃).

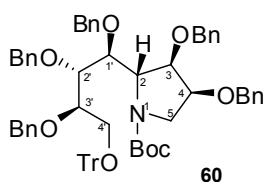
MS (ESI +ve) *m/z* 1038 (*M* + Na⁺, 85 %), 1016 (*M* + H⁺, 33 %).

HRMS (ESI +ve) calculated for C₆₇H₇₀NO₈ (*M* + H⁺) 1016.5101, found 1016.5113.

¹H NMR (500 MHz) δ 7.44-6.69 (m, 40H, Ar), 4.80 - 4.40 (m, 10H, Bn), 4.40 - 3.26 (m, 10H, H-2, H-3, H-4, H-5, H-5, H-1', H-2', H-3', H-4', H-4'), 1.43 (s, 9H, *t*-Bu).

¹³C NMR (125 MHz) δ (Major rotamer) 154.3 (C=O), 143.9, 138.7, 138.6, 138.3, 138.0, 137.8 (q Ar), 128.8, 128.7, 128.2, 128.14, 128.10, 128.0, 127.9, 127.8, 127.4, 127.3, 127.2, 126.8 (Ar), 86.9 (q C, Tr), 80.0 (q C, Boc), 79.9, 79.1, 78.0, 77.4, 76.9, 75.7, 75.1 (CH), 74.6, 73.7, 73.0 72.5, 71.7 (Bn), 64.0 (C-2), 63.8 (C-4'), 48.7 (C-5).

***tert*-Butyl(2*R*,3*R*,4*S*)-3,4-bis(benzyloxy)-2-[(1*S*,2*S*,3*R*)-1,2,3-tris(benzyloxy)-4-triphenylmethoxybutyl] pyrrolidine-1-carboxylate (**60**)**

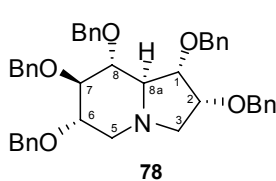
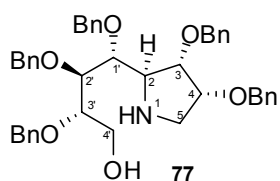


Compound **60** (2.049 g, 81 %) was synthesized as a light brown oil from **59** (1.40 g, 2.482 mmol) by the General method for *O*-Bn protection.

$[\alpha]_D^{27}$ - 12 (*c* 39.5, CHCl₃).

¹H and ¹³C NMR data matched the corresponding data of **76**.

(2*S*,3*S*,4*R*)-4-[(2*R*,3*S*,4*R*)-3,4-Dibenzyloxypyrrolidin-2-yl]-2,3,4-tribenzyloxybutan-1-ol (77**); (1*S*,2*R*,6*S*,7*R*,8*R*,8*aR*)-1,2,6,7,8-pentabenzyloxyoctahydroindolizine (**78**)**



Compounds **77** (190 mg, 37 %) and **78** (270 mg, 54 %) were synthesized from **76** (774 mg, 0.763 mmol) using the General method for the removal of *N*-Boc and *O*-Tr groups.

Amino alcohol **77** was isolated as a brown oil while cyclized product **78** was isolated as a white solid.

77: $[\alpha]_D^{22} - 21$ (*c* 1.34, CHCl₃).

MS (CI +ve) *m/z* 674 (*M* + 1⁺, 2 %), 566 (*M* - OBn, 3 %), 91 (Bn, 100 %).

HRMS (ESI +ve) calculated for C₄₃H₄₈NO₆ (*M* + H⁺) 674.3481, found 674.3504.

¹H NMR δ 7.33-7.21 (m, 25H, Ar), 4.82 (d, 1H, *J* 11.4 Hz, Bn), 4.72 (d, 1H, *J* 11.4 Hz, Bn), 4.68 (d, 1H, *J* 11.1 Hz, Bn), 4.64 (d, 1H, *J* 11.7 Hz, Bn), 4.60 (d, 1H, *J* 11.1 Hz, Bn), 4.57 (d, 1H, *J* 11.4 Hz, Bn), 4.54 (d, 2H, *J* 12.0 Hz, Bn), 4.46 (d, 1H, *J* 12.0 Hz, Bn), 4.41 (d, 1H, *J* 11.4 Hz, Bn), 4.02 (dd, 1H, *J* 5.1, 5.7 Hz, H-3), 3.87 (m, 1H, H-4), 3.81 (m, 1H, H-1'), 3.78 (m, 1H, H-3'), 3.72 (m, 1H, H-4'), 3.68 (m, 1H, H-2'), 3.66 (m, 1H, H-2'), 3.66 (m, 1H, H-4'), 3.39 (dd, 1H, *J* 4.8, 5.4 Hz, H-2), 2.98 (dd, 1H, *J* 4.5, 12.0 Hz, H-5), 2.90 (dd, 1H, *J* 4.5, 12.0 Hz, H-5).

¹³C NMR δ 138.6, 138.2, 138.11, 138.06, 138.0 (q Ar), 128.3, 128.25, 128.23, 128.0, 127.9, 127.8, 127.7, 127.64, 127.60, 127.4 (Ar), 80.6 (C-3'), 80.2 (C-1'), 79.7 (C-3), 78.6 (C-2'), 77.6 (C-4), 74.8, 74.3, 72.1, 71.9, 71.4 (Bn), 62.1 (C-2), 61.2 (C-4'), 48.9 (C-5).

78: $[\alpha]_D^{22} - 11$ (*c* 0.7, CHCl₃).

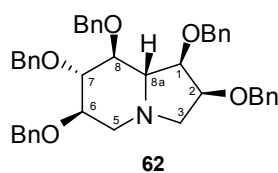
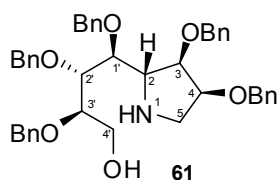
MS (CI +ve) *m/z* 656 (*M* + H⁺, 5 %), 107 (OBn, 100 %).

HRMS (ESI +ve) calculated for C₄₃H₄₆NO₅ (*M* + H⁺) 656.3375, found 656.3367.

¹H NMR δ 7.33-7.20 (m, 25H, Ar), 4.93 (d, 1H, *J* 10.8 Hz, Bn), 4.89 (d, 1H, *J* 11.7 Hz, Bn), 4.81 (d, 1H, *J* 10.8 Hz, Bn), 4.72 (d, 1H, *J* 11.1 Hz, Bn), 4.66 - 4.51 (m, 6H, Bn), 3.99 (app-q, 1H, *J* 7.2 Hz, H-2), 3.80 (dd, 1H, *J* 5.7, 6.9 Hz, H-1), 3.63 (m, 1H, H-6), 3.57 (m, 1H, H-7), 3.35 (dd, 1H, *J* 8.4, 9.3 Hz, H-8), 3.19 (m, 1H, H-3), 3.15 (m, 1H, H-5), 2.56 (m, 1H, H-8a), 2.51 (m, 1H, H-3), 2.20 (t, 1H, *J* 10.2 Hz, H-5).

¹³C NMR δ 138.7, 138.5, 138.3, 138.2, 138.0 (q Ar), 128.4, 128.3, 128.2, 128.1, 128.0, 127.8, 127.7, 127.6, 127.5, 127.4, 127.3 (Ar), 87.1 (C-7), 81.6 (C-8), 80.2 (C-1), 79.0 (C-6), 76.0 (C-2), 75.7, 74.3, 72.8, 72.2, 72.0 (Bn), 70.3 (C-8a), 57.1 (C-3), 53.5 (C-5).

(2*R*,3*R*,4*S*)-4-[(2*S*,3*R*,4*S*)-3,4-Dibenzyloxypyrrolidin-2-yl]-2,3,4-tribenzyloxybutan-1-ol (61); (1*R*,2*S*,6*R*,7*S*,8*S*,8a*S*)-1,2,6,7,8-pentabenzyloxyoctahydroindolizine (62)

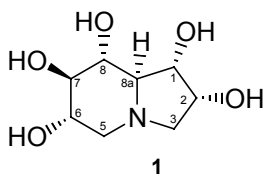


Compounds **61** (22 mg, 44 %) and **62** (16 mg, 34 %) were synthesized from **60** (75 mg, 73.89 μmol) using the General method for the removal of *N*-Boc and *O*-Tr groups.

61: $[\alpha]_D^{27} + 25$ (*c* 14.0, CHCl₃).

62: $[\alpha]_D^{26} + 2$ (*c* 12.2, CHCl₃).

¹H and ¹³C NMR data for **61** matched the corresponding data of **77**. ¹H and ¹³C NMR data for **62** matched the corresponding data of **78**.

(1*S*,2*R*,6*S*,7*R*,8*R*,8*aR*)-Octahydroindolizine-1,2,6,7,8-pentol (1)

Compound **1** (90 mg, 63 %) was synthesized as transparent micro-crystals from **78** (460 mg, 0.702 mmol) using the General method for *O*-Bn deprotection.

m.p. 170-172 °C.

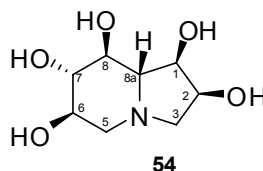
$[\alpha]_D^{25}$ - 10 (*c* 0.67, MeOH). $[\alpha]_D^{25}$ - 6 (*c* 5.0, H₂O).

MS (CI +ve) *m/z* 206 (*M* + H⁺, 100 %), 188 (*M* - OH, 50 %).

HRMS (CI +ve) calculated for C₈H₁₅NO₅ 205.0950, found 205.0947.

¹H NMR (500 MHz, D₂O) δ 4.11 (q, 1H, *J*_{1,2} = *J*_{2,3α} = *J*_{2,3β} = 7.0 Hz, H-2), 3.82 (t, 1H, *J*_{1,2} = *J*_{1,8a} = 7.5 Hz, H-1), 3.46 (ddd, 1H, *J*_{5β,6} = 5.5 Hz, *J*_{6,7} = 9.0 Hz, *J*_{5α,6} = 11.0 Hz, H-6), 3.26 (dd, 1H, *J*_{2,3α} = 6.5, *J*_{3α,3β} = 10.5 Hz, H-3α), 3.25 (t, 1H, *J*_{7,8} = *J*_{8,8a} = 9.0 Hz, H-8), 3.20 (t, 1H, *J*_{6,7} = *J*_{7,8} = 9.0 Hz, H-7), 3.01 (dd, 1H, *J*_{5β,6} = 5.5 Hz, *J*_{5α,5β} = 10.5 Hz, H-5β), 2.20 (dd, 1H, *J*_{2,3β} = 6.5 Hz, *J*_{3α,3β} = 10.5 Hz, H-3β), 2.09 (t, 1H, *J*_{5α,5β} = *J*_{5α,6} = 10.8 Hz, H-5α), 2.08 (dd, 1H, *J*_{1,8a} = 7.5 Hz, *J*_{8,8a} = 9.3 Hz, H-8a).

¹³C NMR (75 MHz, D₂O) δ 79.1 (C-7), 74.1 (C-8), 73.9 (C-1), 70.5 (C-8a), 70.4 (C-6), 68.6 (C-2), 59.2 (C-3), 55.4 (C-5).

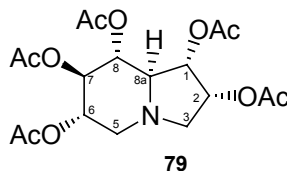
(1*R*,2*S*,6*R*,7*S*,8*S*,8*aS*)-Octahydroindolizine-1,2,6,7,8-pentol (*ent*-1)

Compound *ent*-**1** (74 mg, 83 %) was synthesized from **62** (285 mg, 0.435 mmol) using the General method for *O*-Bn deprotection.

m.p. 171 - 172 °C.

$[\alpha]_D^{24}$ + 4 (*c* 1.2, MeOH).

¹H and ¹³C NMR data match the corresponding data of **79**.

(1*S*,2*R*,6*S*,7*R*,8*R*,8*aR*)-Octahydroindolizine-1,2,6,7,8-pentyl pentaacetate (79)

Compound **79** (68 mg, 88%) was synthesized as colourless crystals from **1** (38 mg, 0.185 mmol) using the General method for *O*-Ac protection.

m.p. 142 °C

$[\alpha]_D^{21}$ - 15 (*c* 1.36, CHCl₃)

MS (CI +ve) *m/z* 416 (*M* + H⁺, 87 %), 356 (*M* - OAc, 100 %).

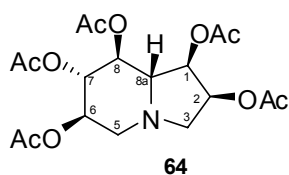
HRMS (ESI +ve) calculated for C₁₈H₂₆NO₁₀ (*M* + H⁺) 416.1557, found 416.1573.

¹H NMR (500 MHz) δ 5.25 (q, 1H, *J*_{1,2} = *J*_{2,3α} = *J*_{2,3β} = 6.3 Hz, H-2), 5.11 (t, 1H, *J*_{6,7} = *J*_{7,8} = 9.3 Hz, H-7), 5.02 (t, 1H, *J*_{1,2} = *J*_{1,8a} = 7.3 Hz, H-1), 4.97 (dd, 1H, *J*_{5β,6} = 5.8 Hz, *J*_{5α,6} = 9.8 Hz, H-6), 4.96 (t, 1H, *J*_{7,8} = *J*_{8,8a} = 9.3 Hz, H-8), 3.57 (dd, 1H, *J*_{2,3β} = 6.8 Hz, *J*_{3α,3β} = 10.3 Hz, H-3β), 3.28 (dd, 1H, *J*_{5β,6} = 5.5 Hz, *J*_{5α,5β} = 10.5 Hz, H-5β), 2.60 (t, 1H, *J*_{1,8a} = *J*_{8,8a} = 8.5 Hz, H-

8a), 2.42 (dd, 1H, $J_{2,3\alpha} = 5.0$ Hz, $J_{3\alpha,3\beta} = 10.0$ Hz, H-3 α), 2.27 (t, 1H, $J_{5\alpha,5\beta} = J_{5\alpha,6} = 10.3$ Hz, H-5 α), 2.04, 2.028, 2.025, 2.02, 2.01 (s, 3H, Ac).

^{13}C NMR (75 MHz) δ 170.3, 169.9, 169.8, 169.6, 168.9 (C=O), 73.9 (C-7), 73.7 (C-1), 72.0 (C-8), 69.9 (C-6), 69.3 (C-2), 65.7 (C-8a), 57.3 (C-3), 52.0 (C-5), 20.74, 20.67, 20.60, 20.2 (CH₃).

(1*R*,2*S*,6*R*,7*S*,8*S*,8a*S*)-Octahydroindolizine-1,2,6,7,8-pentyl pentaacetate (64**)**



Compound **64** (15 mg, 53 %) was synthesized from **54** (14 mg, 68.29 μmol) by the General method for *O*-Ac protection.

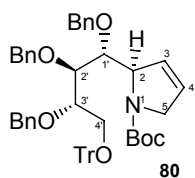
m.p. 146 °C

$[\alpha]_{\text{D}}^{25} + 26$ (c 1.5, CHCl₃).

^1H and ^{13}C NMR data matched the corresponding data of **80**.

Chapter 4 Experimental

tert-Butyl (2*R*)-2-[(1*R*,2*R*,3*S*)-1,2,3-*tris* (benzyloxy)-4-triphenylmethyloxybutyl]-2,5-dihydro-1*H*-pyrrole-1-carboxylate (**80**)



Compound **80** (3.38 g, 97 %) was synthesized from triol **74** (2.3 g, 4.33 mmol) using the General method for *O*-Benzyl protection, except that the reaction was maintained at rt for 18 h. The crude product was purified by FCC (10 % EtOAc / petrol) to give **80** as a yellow oil.

Compound **80** (0.785 g, 78 %) was also synthesized from diene **81** (1.09 g, 1.204 mmol) using the General method for Ring-closing metathesis (Grubbs' I). The crude product was purified by FCC (5 % EtOAc, petrol).

$[\alpha]_D^{29} + 73$ (*c* 4.6, CHCl₃).

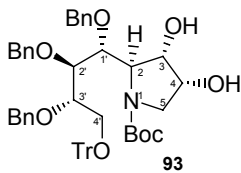
MS (ESI +ve) *m/z* 824 (*M* + Na⁺, 100 %).

HRMS (ESI +ve) calculated for C₅₃H₅₅NO₆Na 824.3926, found 824.3925.

¹H NMR δ 7.46-7.05 (m, 30H, Ar), 5.84-5.80 (m, 1H, H-4), 5.76-5.74 (m, 1H, H-3), 4.84 (d, 1H, *J* 11.4 Hz, Bn), 4.73 (d, 1H, *J* 11.4 Hz, Bn), 4.66 (d, 1H, *J* 11.4 Hz, Bn), 4.59 (d, 1H, *J* 11.4 Hz, Bn), 4.49-4.46 (m, 1H, H-2), 4.33 (d, 1H, *J* 11.0 Hz, Bn), 4.21 (d, 1H, *J* 11.0 Hz, Bn), 4.09 (dq, 1H, *J* 1.8, 15.3 Hz, H-5), 4.01-3.97 (m, 1H, H-1'), 3.96-3.91 (m, 2H, H-3', H-5), 3.66 (t, 1H, *J* 5.4 Hz, H-2'), 3.47 (dd, 1H, *J* 3.9 Hz, 10.2 Hz, H-4'), 3.39 (dd, 1H, *J* 5.3, 10.4 Hz, H-4'), 1.45 (s, 3H, *t*-Bu).

¹³C NMR δ 153.9 (C=O), 144.0, 138.7, 138.5, 138.2 (q Ar), 128.2, 128.1, 128.0, 127.9, 127.8, 127.7, 127.6, 127.5, 127.4, 127.3, 127.2 (Ar), 126.9 (C-4), 126.5 (C-3), 86.9 (q C, Tr), 80.9 (C-2'), 80.3 (C-1'), 79.7 (q C, Boc), 79.3 (C-3'), 74.8, 74.6, 73.4 (Bn), 67.0 (C-2), 63.8 (C-4'), 53.5 (C-5), 28.4 (*t*-Bu).

tert-Butyl (2*R*,3*S*,4*R*)-3,4-dihydroxy-2-[(1*R*,2*S*,3*S*)-1,2,3-*tris*-(benzyloxy)-4-triphenylmethyloxybutyl]pyrrolidine-1-carboxylate (**93**)



Compound **93** (1.15 g, 74 %) was synthesized from olefin **80** (1.5 g, 1.873 mmol) using the General method for *cis*-dihydroxylation except that the reaction went for 3 d. The crude product was purified by FCC (40 % EtOAc / petrol) to give **93** as a light brown foamy solid.

$[\alpha]_D^{25} + 17$ (*c* 1.0, CHCl₃).

MS (ESI +ve) *m/z* 858 (*M* + Na⁺, 25 %), 243 (Tr⁺, 100 %).

HRMS (ESI +ve) calculated for C₅₃H₅₇NO₈Na (*M* + Na⁺) 858.3981, found 858.3991.

¹H NMR δ 7.46-7.05 (m, 30H, Ar), 4.86 (d, 1H, *J* 11.4 Hz, Bn), 4.70 (d, 1H, *J* 11.4 Hz, Bn), 4.62 (d, 1H, *J* 11.4 Hz, Bn), 4.53 (d, 1H, *J* 11.4 Hz, Bn), 4.38 (d, 1H, *J* 10.8 Hz, Bn), 4.21-4.26

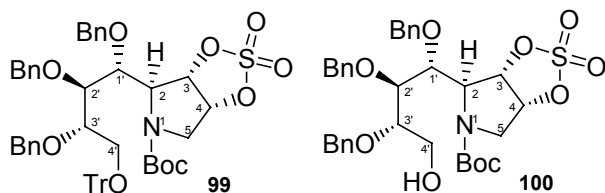
(m, 3H, Bn, H-1', H-4), 4.12-4.04 (m, 2H, H-3, H-3'), 3.83 (t, 1H, H-2'), 3.72 (m, 1H, H-2), 3.62-3.54 (m, 2H, H-4' and H-4'), 3.43-3.40 (m, 1H, H-5), 3.22-3.19 (m, 1H, H-5), 1.43 (s, 9H, *t*-Bu).

^{13}C NMR δ 154.5 (C=O), 143.9, 138.5, 137.9, 137.8 (q Ar), 128.8, 128.4, 128.3, 128.2, 128.1, 128.0, 127.9, 127.8, 127.7, 127.6, 127.4, 126.9 (Ar), 87.0 (q C, Tr), 81.2 (C-2'), 79.3 (q C, Boc), 79.0 (C-3'), 78.0 (C-1'), 75.2, 74.0, 73.7 (Bn), 71.2 (C-4), 70.4 (C-3), 65.1 (C-2), 64.5 (C-4'), 51.7 (C-5), 28.4 (*t*-Bu).

***tert*-Butyl (3*aS*,4*S*,6*aR*)-4-[(1*R*,2*S*,3*S*)-1,2,3-tris-(benzyloxy)-4-triphenylmethyloxybutyl] tetrahydro-5*H*-[1,3,2] dioxathiol[4,5-*c*] pyrrole-5-carboxylate 2,2-dioxide (**99**); *tert*-Butyl (3*aS*,4*S*,6*aR*)-4-[(1*R*,2*S*,3*S*)-1,2,3-tris-(benzyloxy)-4-hydroxybutyl] tetrahydro-5*H*-[1,3,2] dioxathiol[4,5-*c*] pyrrole-5-carboxylate 2,2-dioxide (**100**)**

Two methods were used to synthesize **99**, both using diol **93** as the substrate. The first method was a one-pot two-step procedure involving the production of a cyclic sulfite, followed by oxidation to cyclic sulfate **99**. The second method used involved a direct conversion of **93** to **99** using sulfonyl-diimidazole.

Method 1:



To a chilled (0 °C) solution of diol **93** (0.12 g, 0.144 mmol) in dry DCM (1 mL) was added SOCl_2 (0.013 mL, 0.172 mmol) and Et_3N (0.046 mL, 0.331 mmol). After

1 h of stirring at 0 °C, the reaction was quenched with water (10 mL) and the product was extracted with DCM (2 \times 20 mL). The combined DCM extracts were dried and evaporated to give a dark brown oil (400 mg). This residue was dissolved in a mixture of CCl_4 (1.5 mL), CH_3CN (1 mL) and water (1 mL). RuCl_3 (1.9 mg, 7.19 μmol) and NaIO_4 (58 mg, 0.273 mmol) were added and the mixture was stirred at rt for 18 h. The reaction mixture was diluted with Et_2O (20 mL) and filtered through a pad of celite. The filtrate was washed with water, sat. aq. NaHCO_3 , brine, then dried and evaporated. The crude product was purified by FCC (30 % EtOAc) to give cyclic sulfate **99** (65 mg, 50 %, contaminated substantially with TrOH that co-eluted with **99**) and the deprotected primary alcohol **100** (21 mg, 22%).

99:

$[\alpha]$ not determined due to the TrOH impurity

MS (ESI +ve) m/z 920 ($\text{M} + \text{Na}^+$, 50 %), 243 (Tr^+ , 100 %)

HRMS (ESI +ve) calculated for $\text{C}_{53}\text{H}_{55}\text{NO}_{10}\text{SNa}$ 920.3444, found 920.3439.

^1H NMR (500 MHz) δ 7.42-6.93 (m, 30H, Ar), 5.44 (d, 1H, J 5.0 Hz, H-3), 5.07 (m, 1H, H-4), 4.76 (d, 1H, J 11.5 Hz, Bn), 4.69 (d, 1H, J 11.0 Hz, Bn), 4.57 (d, 1H, J 12.0 Hz, Bn), 4.50 (d,

1H, *J* 11.5 Hz, Bn), 4.45 (d, 1H, *J* 11.5 Hz, Bn), 4.41 (br s, 1H, H-2), 4.18 (d, 1H, *J* 11.0 Hz, Bn), 4.13 (m, 1H, H-2'), 4.04 (br d, 1H, *J* 6.5 Hz, H-1'), 3.89-3.86 (m, 1H, H-3'), 3.73-3.68 (m, 1H, H-5), 3.59-3.55 (m, 1H, H-4'), 3.46 (dd, 1H, *J* 4.0, 10.5 Hz, H-4'), 3.39 (dd, 1H, *J* 6.3, 13.3 Hz, H-5), 1.44 (s, 9H, *t*-Bu).

¹³C NMR (125 MHz) δ 152.8 (C=O), 143.9, 138.2, 137.6, 137.4 (q Ar), 128.7, 128.5, 128.3, 127.9, 127.89, 127.8, 127.7, 127.5, 127.2, 127.0 (Ar), 87.1 (q C, Tr), 84.4 (C-3), 83.5 (C-4), 80.8 (q C, Boc), 79.6 (C-1'), 79.3 (C-2'), 77.7 (C-3'), 75.4, 74.2, 73.7 (Bn), 64.4 (C-2), 63.3 (C-4'), 51.3 (C-5), 28.3 (*t*-Bu).

100: $[\alpha]_D^{23} + 33$ (*c* 0.4, CHCl₃).

MS (ESI +ve) *m/z* 678 (M + Na⁺, 30 %), 243 (Tr⁺, 100 %)

HRMS (ESI +ve) calculated for C₃₄H₄₁NO₁₀SNa 678.2348, found 678.2349.

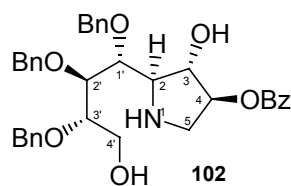
¹H NMR (500 MHz) δ 7.35-7.15 (m, 15H, Ar), 5.40 (d, 1H, *J* 6.0 Hz, H-3), 5.15 (m, 1H, H-4), 4.84 (d, 1H, *J* 11.5 Hz, Bn), 4.80 (m, 1H, H-2), 4.67 (d, 1H, *J* 11.5 Hz, Bn), 4.60 (d, 1H, *J* 11.5 Hz, Bn), 4.59 (d, 1H, *J* 11.5 Hz, Bn), 4.58 (s, 1H, Bn), 4.36 (d, 1H, *J* 11.0 Hz, Bn), 4.16 (d, 1H, *J* 8.5 Hz, H-1'), 3.95-3.89 (m, 2H, H-4', H-2'), 3.79-3.74 (m, 2H, H-4', H-5), 3.61 (dd, 1H, *J* 4.3, 8.3 Hz, H-3'), 3.48 (dd, 1H, *J* 6.8, 13.3 Hz, H-5), 1.48 (s, 9H, *t*-Bu).

¹³C NMR (125 MHz) δ 151.9 (C=O), 142.0, 137.5, 137.3 (q Ar), 128.7, 128.6, 128.4, 128.3, 128.2, 127.9, 127.7, 127.6 (Ar), 84.3 (C-3), 83.6 (C-4), 81.2 (C-1'), 80.5 (C-2'), 77.2 (C-3'), 76.2, 74.1, 73.2 (Bn), 63.8 (C-2), 60.9 (C-4'), 51.6 (C-5), 28.3 (*t*-Bu).

Method 2:

To a solution of diol **93** (0.09 g, 0.1 mmol) in dry THF (1 mL) was added NaH (43 mg, 0.43 mmol, 30 % in mineral oil). After stirring for 10 min, 1,1'-sulfonyldiimidazole (23 mg, 0.12 mmol) was added and the mixture was stirred for 1 h at rt. The mixture was filtered through a pad a celite and washed with Et₂O. The organic filtrate was washed with brine, dried and evaporated. The residue was purified by FCC (40 % EtOAc / petrol) to give **99** (57 mg, 60 %) as a yellow oil and recovered **93** (38 mg, 40 %).

tert-Butyl-(2*R*,3*S*,4*S*)-3-hydroxy-4-[(phenylacetyl)oxy]-2-[(1*R*,2*S*,3*S*)-1,2,3-tris(benzyloxy)-4-hydroxybutyl]pyrrolidine-1-carboxylate (**102**)



To a solution of cyclic sulfate **100** (120 mg, 0.183 mmol) in dry THF (2 mL) was added benzoic acid (60 mg, 0.495 mmol) and cesium carbonate (150 mg, 0.458 mmol). The mixture was stirred under N₂ for 18 h at 100 °C in a sealed tube. After cooling to rt, all volatiles were evaporated and the residue was dissolved in THF (2 mL), followed by the addition of water (5 drops) and conc. H₂SO₄ (3 drops). The mixture was stirred for 18 h at rt, then

evaporated to dryness. The residue was dissolved in DCM and washed with sat. aq. NaHCO₃. The aqueous layer was separated and extracted with DCM (2 × 20 mL) and the combined DCM portions were washed with brine, dried and evaporated. The crude product was purified by FCC (40 % EtOAc / petrol) to give **102** (50 mg, 30 %) as a clear oil.

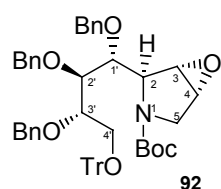
MS (ESI +ve) m/z 620 ($M + Na^+$, 50 %).

HRMS (ESI +ve) calculated for C₃₆H₃₉NO₇Na ($M + Na^+$) 620.2623, found 620.2630.

¹H NMR (500 MHz) δ 8.00 (m, 2H, *o*-Bz), 7.58 (t, 1H, *p*-Bz), 7.43 (m, 2H, *m*-Bz), 7.35-7.24 (m, 15H, Ar), 5.05 (m, 1H, H-4), 4.86 (d, 1H, J 11.0 Hz, Bn), 4.76 (d, 1H, J 11.5 Hz, Bn), 4.70 (d, 1H, J 11.5 Hz, Bn), 4.66 (d, 1H, J 11.5 Hz, Bn), 4.64 (d, 1H, J 11.5 Hz, Bn), 4.63 (d, 1H, J 12.0 Hz, Bn), 4.28 (dd, 1H, J 2.5, 6.0 Hz, H-1'), 3.98 (dd, 1H, J 5.0, 7.0 Hz, H-3), 3.88 (m, 1H, H-2'), 3.85 (dd, 1H, J 5.0, 11.0 Hz, H-4'), 3.80 (dd, 1H, J 4.3, 8.8 Hz, H-3'), 3.76 (dd, 1H, J 4.0, 11.0 Hz, H-4'), 3.20 (dd, 1H, J 6.0, 13.0 Hz, H-5), 3.08 (dd, 1H, J 2.5, 13.0 Hz, H-5), 3.03 (t, 1H, J 5.5 Hz, H-2).

¹³C NMR (125 MHz) δ 163.5 (C=O), 138.2, 137.9, 133.2, 129.7 (q Ar), 128.53, 128.48, 128.45, 128.42, 128.4, 128.3, 127.99, 127.96, 127.72, 127.67 (Ar), 84.0 (C-4), 80.6 (C-2), 79.8 (C-3), 79.1 (C-1'), 78.3 (C-3'), 74.74, 74.67, 72.5 (Bn), 66.1 (C-2), 61.3 (C-4'), 50.5 (C-5).

***tert*-Butyl (1*S*,2*S*,5*R*)-2-[(1*R*,2*S*,3*S*)-1,2,3-*tris*-(benzyloxy)-4-triphenylmethoxybutyl]-6-oxa-3-azabicyclo[3.1.0]hexane-3-carboxylate (**92**)**



To a solution of the olefin **80** (500 mg, 0.624 mmol) in MeCN was added Na₂EDTA (3.1 mL, 4 × 10⁻⁴ M, 5 mL / mmol) and CF₃C(O)CH₃ (0.62 mL, 1 mL / mmol). The mixture was chilled to 0 °C before the portionwise addition of a mixture of NaHCO₃ (420 mg, 4.99 mmol) and oxone (1.92 g,

3.12 mmol) over 30 min. After stirring for 1 h at 0 °C, the mixture was poured into water and extracted with Et₂O (2 × 40 mL). The combined ether extracts were washed with brine, dried and evaporated to give **92** as a yellow oil (650 mg, 100 %) that did not require further purification.

$[\alpha]_D^{26} + 41$ (c 2.5, CHCl₃).

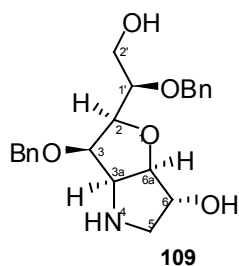
MS (ESI +ve) m/z 840 ($M + Na^+$, 22 %), 598 ($M + Na^+ - Tr$ (243), 100 %).

HRMS (ESI +ve) calculated for C₄₃H₄₈NO₆ ($M + H^+$) 674.3481, found 674.3504.

¹H NMR (500 MHz) δ 7.45-7.01 (m, 30H, Ar), 4.84 (d, 1H, J 12.0 Hz, Bn), 4.72 (d, 1H, J 11.5 Hz, Bn), 4.65 (s, 1H, Bn), 4.59 (d, 1H, J 11.0 Hz, Bn), 4.36 (d, 1H, J 11.5 Hz, Bn), 4.26 (d, 1H, J 11.5 Hz, Bn), 4.14 (dd, 1H, J 1.5, 5.5 Hz, H-1'), 3.96 (m, 1H, H-3'), 3.87-3.85 (m, 1H, H-3'), 3.81 (dd, 1H, J 5.5, 9.0 Hz, H-3), 3.76-3.74 (m, 1H, H-4), 3.62 (d, 1H, J 13.0 Hz, H-5), 3.51 (m, 1H, H-4'), 3.44 (m, 1H, H-2), 3.36 (dd, 1H, J 6.3, 10.3 Hz, H-4'), 3.13 (dd, 1H, J 1.5, 12.5 Hz, H-5), 1.42 (s, 9H, *t*-Bu).

^{13}C NMR δ 154.0 (C=O), 143.9 (q Ar, Tr), 138.5, 138.0, 137.8 (q Ar), 128.8, 128.6, 128.3, 128.2, 127.8, 127.7, 127.6, 127.5, 127.4, 127.3, 127.0, 126.9 (Ar), 86.9 (q C, Tr), 80.2 (q C, Boc), 80.1 (C-2'), 80.0 (C-4), 79.5 (C-1'), 78.8 (C-3), 78.7 (C-3'), 74.8, 74.3, 73.4 (Bn), 63.8 (C-4'), 63.5 (C-2), 47.8 (C-5), 28.4 (*t*-Bu).

(2*S*,3*R*,3*aS*,6*R*,6*aR*)-2-[(1*R*)-1-benzyloxy-2-hydroxyethyl]-3-benzyloxyhexahydro-2*H*-furo[3,2-*b*]pyrrol-6-ol (109)



To a solution of epoxide **92** (740 mg, 0.91 mmol) in THF (3 mL) was added a solution of TFA (1.4 mL, 18.1 mmol) in H_2O (3 mL). The mixture was stirred at 60 °C for 3 h, then poured into sat. aq. NaHCO_3 and extracted with EtOAc. The combined EtOAc extracts were washed with brine, dried and evaporated. The crude product was purified by FCC to give **109** (180 mg, 51 %) as a yellow oil.

$[\alpha]_D^{26} + 27$ (*c* 3.2, MeOH)

MS (ESI +ve) m/z 386 ($\text{M} + \text{H}^+$).

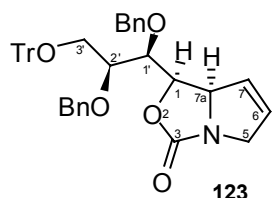
HRMS (ESI +ve) calculated for $\text{C}_{22}\text{H}_{28}\text{NO}_5$ ($\text{M} + \text{H}^+$) 386.1967, found 386.1962.

^1H NMR (500 MHz, CD_3OD) δ 7.48-7.07 (m, 10H, Ar), 4.86 (ddd, 1H, J 1.5, 7.0, 8.3 Hz, H-3), 4.77 (d, 1H, J 10.0 Hz, Bn), 4.71 (d, 1H, J 10.5 Hz, Bn), 4.67 (d, 1H, J 11.0 Hz, Bn), 4.47 (dd, 1H, J 3.3, 5.3 Hz, H-3a), 4.45 (dt, 1H, J 1.8, 8.5 Hz, H-2), 4.36 (dt, 1H, J 1.3, 4.5 Hz, H-6), 4.32 (dd, 1H, J 1.5, 3.5 Hz, H-6a), 4.28 (d, 1H, J 10.0 Hz, Bn), 3.81 (dd, 1H, J 6.0, 11.0 Hz, H-2'), 3.70 (dd, 1H, J 6.5, 11.0 Hz, H-2'), 3.66 (ddd, 1H, J 2.0, 2.0, 6.3 Hz, H-1'), 3.36 (dd, 1H, J 4.3, 12.3 Hz, H-5), 2.89 (d, 1H, J 12.5 Hz, H-5).

^{13}C NMR (125 MHz, CD_3OD) δ 138.3, 138.1 (q Ar), 129.8, 129.77, 129.75, 129.66, 129.2, 128.5 (Ar), 86.4 (C-6a), 80.6, 80.1, 79.7 (C-1', C-3, C-3a), 75.2, 74.7 (Bn), 74.6 (C-6), 64.2 (C-2), 61.8 (C-2'), 53.6 (C-5).

Chapter 5 Experimental

(1*R*,7*aR*)-1-[(1*R*,2*S*)-1,2-bis(benzyloxy)-3-triphenylmethyloxypropyl]-5,7*a*-dihydro-1*H*-pyrrolo[1,2-*c*][1,3]oxazol-3-one (**123**)



To a solution of diene **122** (460 mg, 0.621 mmol) in dry DCM (62 mL) was added Grubbs' II catalyst (53 mg, 62.08 μ mol). The solution was stirred at reflux for 24 h, followed by the evaporation of all volatiles.

The crude product was purified by FCC (30 % EtOAc / petrol) to give **123** (355 mg, 90%) as a foamy white solid.

$[\alpha]_D^{25} + 13$ (*c* 4.5, CHCl₃).

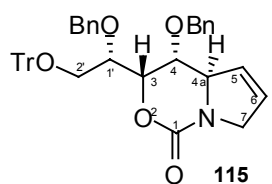
MS (ESI +ve) *m/z* 660 (*M* + Na⁺, 43 %).

HRMS (ESI +ve) calculated for C₄₂H₃₉NO₅Na (*M* + Na⁺) 660.2726, found 660.2712.

¹H NMR δ 7.47-7.15 (m, 25H, Ar), 5.86 (dq, 1H, *J* 2.0, 5.9 Hz, H-7), 5.69 (dq, 1H, *J* 2.0, 5.9 Hz, H-6), 4.81 (dd, 1H, *J* 5.7, 8.1 Hz, H-1), 4.74 (d, 1H, *J* 12.0 Hz, Bn), 4.68 (d, 1H, *J* 11.1 Hz, Bn), 4.61 (d, 1H, *J* 11.1 Hz, Bn), 4.39 (d, 1H, *J* 11.1 Hz, Bn), 4.27 (ddt, 1H, *J* 2.1, 3.6, 15.5 Hz, H-5), 4.09-4.03 (m, 1H, H-7a), 3.73-3.67 (m, 2H, H-1', H-2'), 3.63 (dddd, 1H, *J* 1.5, 2.7, 4.8, 15.6 Hz, H-5), 3.56 (dd, 1H, *J* 4.8, 10.2, H-3'), 3.47 (dd, 1H, *J* 4.8, 10.2 Hz, H-3').

¹³C NMR δ 162.2 (C-3), 144.0, 138.2, 138.1 (q Ar), 131.7 (C-7), 128.53, 128.49, 128.5, 128.1, 128.0, 127.9, 127.6, 127.3, 127.2, (Ar), 125.8 (C-6), 87.4 (q C, Tr), 79.0 (C-1), 78.3, 77.1 (C-1' or C-2'), 74.6, 72.6 (Bn), 67.0 (C-7a), 62.5 (C-3'), 54.7 (C-5).

(3*S*,4*R*,4*aR*)-3-[(1*S*)-1-(benzyloxy)-2-triphenylmethyloxyethyl]-4-(benzyloxy)-3,4,4*a*,7-tetrahydropyrrolo[1,2-*c*][1,3]oxazin-1-one (**115**)



Compound **115** (80 mg, 72 %) was synthesized from diene **114** (130 mg, 0.175 mmol) using the General method for ring-closing metathesis (Grubbs' I). The crude product was purified by FCC (30 % EtOAc / petrol) to give **115** as a brown oil.

$[\alpha]_D^{25} + 80$ (*c* 7.8, CHCl₃).

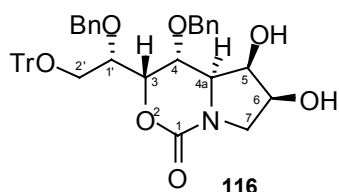
MS (ESI +ve) *m/z* 660 (*M* + Na⁺, 45 %), 243 (Tr⁺, 100 %).

HRMS (ESI +ve) calculated for C₄₂H₃₉NO₅ 637.2828, found 637.2811.

¹H NMR (500 MHz) δ 7.44-7.16 (m, 25H, Ar), 5.82 (s, 2H, H-5, H-6), 4.603 (dd, 1H, *J* 1.3, 6.3 Hz, H-3), 4.601 (d, 1H, *J* 11.5 Hz, Bn), 4.59 (d, 1H, *J* 11.8 Hz, Bn), 4.56 (d, 1H, *J* 11.8 Hz, Bn), 4.52 (dd, 1H, *J* 1.2, 9.5 Hz, H-4a), 4.45 (d, 1H, *J* 11.8 Hz, Bn), 4.39 (dd, 1H, *J* 4.8, 15.3 Hz, H-7), 4.01 (dd, 1H, *J* 5.3, 15.5 Hz, H-7), 3.86 (ddd, 1H, *J* 1.5, 6.3, 7.3 Hz, H-1'), 3.60 (dd, 1H, *J* 6.0, 10.0 Hz, H-4), 3.54 (dd, 1H, *J* 6.0, 10.0 Hz, H-2'), 3.51 (dd, 1H, *J* 7.0, 10.0 Hz, H-2').

^{13}C NMR δ 151.7 (C-1), 143.8, 138.0, 136.9 (q Ar), 128.59 (C-5 or C-6), 128.55, 128.2, 128.1 (Ar), 127.8 (C-5 or C-6), 127.7, 127.6, 127.4, 127.3, 127.1, 127.0 (Ar), 87.4 (q C, Tr), 75.2 (C-1'), 75.0 (C-3), 73.9 (C-4), 72.7, 72.2 (Bn), 62.8 (C-2'), 62.7 (C-4a), 55.1 (C-7).

(3*S*,4*R*,4*aR*,5*R*,6*S*)-4-benzyloxy-3-[(1*S*)-1-(benzyloxy)-2-triphenylmethyloxyethyl]-5,6-dihydroxy-hexahydropyrrolo[1,2-*c*][1,3]oxazin-1-one (116)



Compound **116** (2.4 g, 67 %) was synthesized from olefin **115** (3.43 g, 5.38 mmol) using the General method for *cis*-dihydroxylation, except that the reaction went for 16 h at rt. The crude product was purified by FCC (60 % EtOAc / petrol) to give **116** as a brown foamy solid.

$[\alpha]_D^{24} + 75$ (*c* 2.8, CHCl_3).

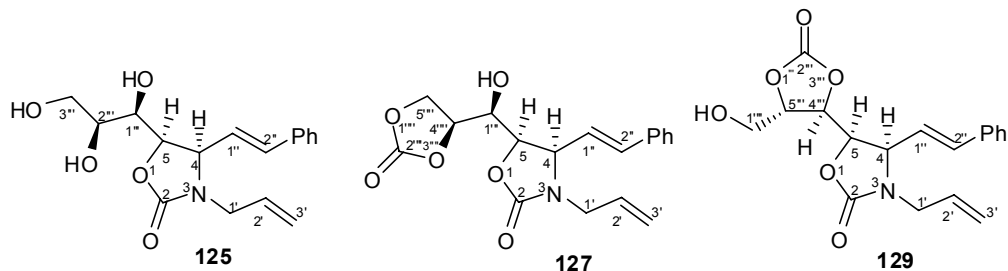
MS (ESI +ve) m/z 672 ($\text{M} + \text{H}^+$, 100 %).

HRMS (ESI +ve) calculated for $\text{C}_{42}\text{H}_{42}\text{NO}_7$ ($\text{M} + \text{H}^+$) 672.2961, found 672.2941.

^1H NMR (500 MHz) δ 7.45-7.17 (m, 25H, Ar), 4.70 (d, 1H, J 11.5 Hz, Bn), 4.581 (d, 1H, Bn), 4.579 (dd, 1H, J 1.5, 6.0 Hz, H-3), 4.51 (d, 1H, J 12.0 Hz, Bn), 4.33 (d, 1H, J 11.5 Hz, Bn), 4.06 (dd, 1H, J 5.8, 9.3 Hz, H-4), 3.97 (dt, 1H, J 3.9, 8.1 Hz, H-6), 3.88 (q, 1H, J 3.5 Hz, H-5), 3.84 (dt, 1H, J 1.5, 6.3 Hz, H-1'), 3.54 (dd, 1H, J 6.0, 10.0 Hz, H-2'), 3.52-3.48 (m, 3H, H-2', H-7, H-4a), 3.22 (dd, 1H, J 8.3, 11.3 Hz, H-7).

^{13}C NMR δ 152.5 (C-1), 143.8, 138.1, 137.5 (q Ar), 128.6, 128.5, 128.2, 128.1, 127.84, 127.77, 127.5, 127.1, 126.9 (Ar), 87.3 (q C, Tr), 75.7 (C-1'), 75.5 (C-3), 72.5 (Bn), 72.4 (Bn), 70.9 (C-5), 69.9 (C-6), 67.6 (C-4), 62.7 (C-2'), 60.3 (C-4a), 50.3 (C-7).

(4*R*,5*R*)-3-allyl-5-[(1*R*,2*S*)-1,2,3-trihydroxypropyl]-4-[(*E*)-2-phenylvinyl]-1,3-oxazolidin-2-one (125); (4*R*,5*R*)-3-allyl-5-{(*S*)-hydroxy[(4*S*)-2-oxo-1,3-dioxolan-4-yl]methyl}-4-[(*E*)-2-phenylvinyl]-1,3-oxazolidin-2-one (127); (4*R*,5*R*)-3-allyl-5-[(4*S*,5*S*)-5-(hydroxymethyl)-2-oxo-1,3-dioxolan-4-yl]-4-[(*E*)-2-phenylvinyl]-1,3-oxazolidin-2-one (129)



To a solution of amino alcohol **70** (2.48 g, 8.46 mmol) in dry THF (200 mL) was added Et_3N (2.94 mL, 21.2 mmol) and triphosgene (833 mg, 2.82 mmol). The mixture was stirred at rt for 30 h and evaporated to dryness. The residue was suspended in water (100 mL) and extracted with DCM (100 mL \times 3). The combined DCM extracts were dried and evaporated to give a

yellow solid. The residue was purified by FCC (80 - 100 % EtOAc / petrol and 5 % MeOH / EtOAc) to give three products **125** (1.22 g, 45 %) **127** (330 mg, 11 %), and **129** (210 mg, 7 %).

125: $[\alpha]_D^{27} - 10$ (c 4.5, MeOH).

m.p. 141 °C.

MS (ESI +ve) m/z 320 ($M + H^+$, 100 %).

HRMS (ESI +ve) calculated for $C_{17}H_{22}NO_5$ ($M + H^+$) 320.1245, found 320.1196.

1H NMR (500 MHz, CD_3OD) δ 7.46-7.26 (m, 5H, Ar), 6.70 (d, 1H, J 16.0 Hz, H-2''), 6.38 (dd, 1H, J 9.5, 16.0 Hz, H-1''), 5.79 (dddd, 1H, J 5.0, 6.5, 10.0, 17.0 Hz, H-2'), 5.22 (dq, 1H, J 2.0, 17.0 Hz, H-3'), 5.20 (dq, 1H, J 2.0, 10.0 Hz, H-3'), 4.83 (dd, 1H, J 4.0, 8.5 Hz, H-5), 4.61 (t, 1H, J 9.0 Hz, H-4), 4.01 (ddt, 1H, J 1.7, 4.7, 15.7 Hz, H-1'), 3.83 (t, 1H, J 4.3 Hz, H-1''), 3.73 (ddd, 1H, J 4.6, 4.8, 6.0 Hz, H-2'''), 3.65 (dd, 1H, J 5.3, 11.3 Hz, H-3'''), 3.60 (ddt, 1H, J 1.3, 6.7, 15.7 Hz, H-1'), 3.57 (dd, 1H, J 6.3, 11.3 Hz, H-3''').

^{13}C NMR (125 MHz, CD_3OD) δ 159.8 (C-2), 138.6 (C-2''), 137.3 (q Ar), 133.4 (C-2'), 129.7, 129.5, 127.9 (Ar), 124.2 (C-1''), 118.3 (C-3'), 78.9 (C-5), 73.3 (C-2'''), 71.0 (C-1'''), 64.1 (C-3'''), 62.6 (C-4), 45.5 (C-1').

127: $[\alpha]_D^{25} + 18$ (c 2.0, MeOH).

m.p. 146 °C.

MS (ESI +ve) m/z 346 ($M + H^+$, 100 %).

HRMS (ESI +ve) calculated for $C_{18}H_{20}NO_6$ ($M + H^+$) 346.1416, found 346.1454.

1H NMR (500 MHz, CD_3OD) δ 7.48-7.24 (m, 5H, Ar), 6.76 (d, 1H, J 15.8 Hz, H-2''), 6.36 (dd, 1H, J 9.5, 15.8 Hz, H-1''), 5.80 (dddd, 1H, J 4.8, 6.8, 10.1, 16.8 Hz, H-2'), 5.22 (dq, 1H, J 1.5, 17.0 Hz, H-3'), 5.21 (dq, 1H, J 1.5, 10.0 Hz, H-3'), 4.88 (1H, ddd, J 3.7, 6.4, 8.3 Hz, H-4'''), 4.75 (dd, 1H, J 4.2, 8.5 Hz, H-5), 4.64 (dd, 1H, J 9.0, 15.0 Hz, H-4), 4.48 (dd, 1H, J 8.4, 16.0 Hz, H-5'''), 4.45 (dd, 1H, J 8.4, 16.0 Hz, H-5'''), 4.02 (ddt, 1H, J 1.8, 5.1, 16.2 Hz, H-1'), 3.92 (t, 1H, J 3.9 Hz, H-1''), 3.61 (ddt, 1H, J 1.2, 6.6, 16.1 Hz, H-1').

^{13}C NMR (125 MHz, CD_3OD) δ 159.1, 156.9 (C=O), 138.9 (C-2''), 136.8 (q Ar), 132.5 (Ar, C-2'), 129.4, 127.8, 127.0 (Ar), 123.3 (C-1''), 118.2 (C-3'), 78.1 (C-4'''' or C-5), 77.9 (C-4'''' or C-5), 69.9 (C-1'), 67.3 (C-5'''), 62.1 (C-4), 45.3 (C-1''').

129: MS (ESI +ve) m/z 346 ($M + H^+$, 100 %).

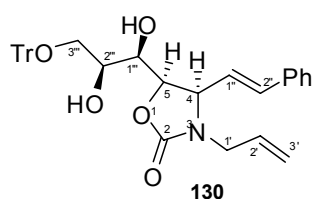
HRMS (ESI +ve) calculated for $C_{18}H_{20}NO_6$ ($M + H^+$) 346.1416, found 346.1450.

1H NMR δ 7.43-7.26 (m, 5H, Ar), 6.70 (d, 1H, J 15.6 Hz, H-2''), 6.20 (dd, 1H, J 9.0, 15.9 Hz, H-1''), 5.71 (dddd, 1H, J 5.1, 6.9, 10.2, 17.4 Hz, H-2'), 5.21 (dq, 1H, J 1.3, 10.2 Hz, H-3'), 5.17 (dq, 1H, J 1.3, 17.1 Hz, H-3'), 4.75 (dd, 1H, J 1.2, 5.4 Hz, H-4'''), 4.73 (dd, 1H, J 0.9, 9.3 Hz, H-5), 4.71 (q 1H, J 3.0 Hz, H-5'''), 4.65 (t, 1H, J 9.2 Hz, H-4), 4.02 (ddt, 1H, J 1.7, 4.8, 15.9

Hz, H-1'), 3.79 (dd, 1H, J 3.6, 12.6 Hz, H-1'''), 3.64 (dd, 1H, J 3.3, 12.6 Hz, H-1'''), 3.54 (ddt, 1H, J 1.2, 7.3, 15.8 Hz, H-1').

^{13}C NMR δ 156.3, 154.1 (C=O), 138.4 (C-2''), 134.9 (q Ar), 131.1 (C-2'), 128.7, 128.6, 126.8 (Ar), 121.6 (C-1''), 118.6 (C-3'), 78.4 (C-5'''), 75.8 (C-5 or C-4'''), 75.2 (C-5 or C-4'''), 60.8 (C-1'''), 60.3 (C-4), 44.4 (C-1').

(4*R*,5*R*)-3-allyl-5-[(1*R*,2*S*)-1,2-dihydroxy-3-triphenylmethoxypropyl]-4-[(*E*)-2-phenylvinyl]-1,3-oxazolidin-2-one (130)



To a solution of primary alcohol **125** (2.42 g 7.586 mmol) in dry pyridine (40 mL) was added TrCl (3.17 g, 11.379 mmol). The mixture was stirred for 20 h at rt, then quenched with water (60 mL) and extracted with Et₂O (80 mL \times 3). The combined ether portions were washed with sat. aq. CuSO₄ (90 mL \times 3) and brine (90 mL), dried and evaporated. The crude product was purified by FCC (40 % EtOAc / petrol) to give **130** (3.68 g, 75 %) as a white foamy solid.

$[\alpha]_D^{27}$ - 18 (c 4.4, CHCl₃).

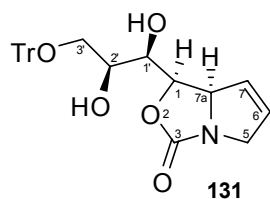
MS (ESI +ve) m/z 579 ($M + \text{NH}_4^+$, 100 %).

HRMS (ESI +ve) calculated for C₃₆H₃₅NO₅Na ($M + \text{Na}^+$) 584.2413, found 584.2419.

^1H NMR (500 MHz) δ 7.39-7.19 (m, 20H, Ar), 6.61 (d, 1H, J 15.5 Hz, H-2''), 6.32 (dd, 1H, J 9.5, 16.0 Hz, H-1''), 5.74 (dddd, 1H, J 4.7, 7.2, 10.1, 17.1 Hz, H-2'), 5.21 (dq, 1H, J 1.4, 10.3 Hz, H-3'), 5.18 (dq, 1H, J 1.5, 17.3 Hz, H-3'), 4.55 (dd, 1H, J 3.8, 8.8 Hz, H-5), 4.46 (t, 1H, J 9.3 Hz, H-4), 4.11 (ddt, 1H, J 1.8, 4.8, 15.8 Hz, H-1'), 3.96 (dd, 1H, J 4.0, 8.0 Hz, H-1'''), 3.90 (dt, 1H, J 4.7, 9.5 Hz, H-2'''), 3.54 (ddt, 1H, J 1.1, 7.0, 15.5 Hz, H-1'), 3.31 (dd, 1H, J 5.5, 9.5 Hz, H-3'''), 3.18 (dd, 1H, J 5.5, 10.0 Hz, H-3''').

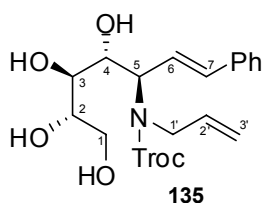
^{13}C NMR (125 MHz) δ 157.2 (C-2), 143.7 (q Ar), 137.6 (C-2''), 135.6 (q Ar), 132.1 (C-2'), 129.0, 128.9, 128.8, 128.1, 127.4, 127.1 (Ar), 123.0 (C-1''), 118.7 (C-3'), 87.2 (q C, Tr), 77.3 (C-5), 71.0 (C-2'''), 69.9 (C-1'''), 64.4 (C-3'''), 61.1 (C-4), 44.8 (C-1').

(1*R*,7*aR*)-1-[(1*R*,2*S*)-1,2-dihydroxy-3-triphenylmethoxypropyl]-5,7*a*-dihydro-1*H*-pyrrolo[1,2-*c*][1,3]oxazol-3-one (131)



To a solution of diene **130** (2.4 g, 4.28 mmol) in dry DCM (200 mL) was added Grubbs' II catalyst (182 mg, 0.214 mmol). The mixture was stirred at reflux for 18 h then evaporated to dryness. The crude product was purified by FCC (40 % EtOAc / petrol) to give **131** (1.3 g, 66 %) as brown foamy solid. This compound was not fully characterized but converted directly to the previously described compounds **115** and **123**.

(6E)-5-{Allyl[(2,2,2-trichloroethoxy)carbonyl]amino}-5,6,7-trideoxy-7-phenyl-D-gluco-hept-6-enitol (135**)**



To a solution of **70** (4.94 g, 16.9 mmol) in 1,4-dioxane (50 mL) was added NaHCO_3 solution (34 mL, 2M), and succinimidy-2,2,2-trichloroethyl carbonate (4.90 g, 16.9 mmol). The mixture was stirred at rt for 5 h then diluted with water (100 mL) and extracted with EtOAc (2×100 mL). The combined EtOAc extracts were washed with HCl (2×100 mL) and brine (100 mL) before being dried and evaporated, giving a clear oil. The residue was purified by FCC (100 % EtOAc) to give **135** as a clear oil (5.75 g, 75 %).

$[\alpha]_D^{22} - 35$ (c 2.0, CHCl_3).

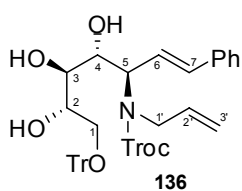
MS (ESI +ve) m/z 490 ($M + \text{Na}^+$, 60 %), 243 (Tr, 100 %).

HRMS (ESI +ve) calculated for $\text{C}_{19}\text{H}_{24}\text{Cl}_3\text{NO}_6\text{Na}$ ($M + \text{Na}^+$) 490.0567, found 490.0566.

^1H NMR δ 7.39-7.22 (m, 5H, Ar), 6.62 (d, 1H, J 16.2 Hz, H-7), 6.45 (dd, 1H, J 7.8, 15.9 Hz, H-6), 5.86 (dddd, 1H, J 2.7, 7.1, 10.2, 17.0 Hz, H-2'), 5.22 (d, 1H, J 17.4 Hz, H-3'), 5.16 (d, 1H, J 10.2 Hz, H-3'), 4.83 (d, 1H, J 12.0 Hz, CH_2CCl_3), 4.74 (d, 1H, J 12.0 Hz, CH_2CCl_3), 4.42 (t, 1H, J 7.7 Hz, H-5), 4.13 (m, 1H, H-4), 4.00 (m, 2H, H-1', H-1'), 3.86 (q, 1H, J 4.2 Hz, H-2), 3.72 (m, 2H, H-1, H-1), 3.65 (m, 1H, H-3).

^{13}C NMR δ 154.8 (C=O), 136.3 (q Ar), 135.1 (C-7), 133.7 (C-2'), 128.5, 127.9, 126.5 (Ar), 124.1 (C-6), 118.1 (C-3'), 95.3 (CCl_3), 75.0 (CH_2CCl_3), 73.2 (C-2), 72.2 (C-4), 70.0 (C-3), 63.9 (C-1), 61.6 (C-5), 49.7 (C-1').

(6E)-5-{Allyl[(2,2,2-trichloroethoxy)carbonyl]amino}-1-O-triphenylmethyl-5,6,7-trideoxy-7-phenyl-D-gluco-hept-6-enitol (136**)**



To a solution of primary alcohol **135** (15.0 g, 32.1 mmol) in dry DCM (150 mL) was added dry pyridine (2.85 mL, 35.3 mmol) and TrCl (9.04 g, 32.4 mmol). The mixture was stirred at rt for 9 h, then poured into water and extracted with DCM. The combined DCM portions were washed with brine, dried and evaporated. The crude product was purified

by FCC (40 % EtOAc / petrol) to give **136** (17.15 g, 75 %) as a clear oil.

$[\alpha]_D^{25} - 8$ (c 1.0, CHCl_3).

MS (ESI +ve) m/z 732 ($M + \text{Na}^+$, 100 %).

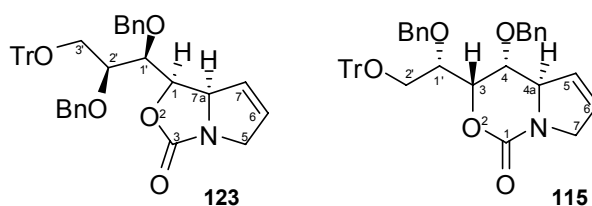
HRMS (ESI +ve) calculated for $\text{C}_{38}\text{H}_{38}\text{Cl}_3\text{NO}_6\text{Na}$ ($M + \text{Na}^+$) 732.1662, found 732.1631.

^1H NMR (Major rotamer *inter alia*) δ 7.44-7.21 (m, 20H, Ar), 6.59 (d, 1H, J 16.2 Hz, H-7), 6.44 (dd, 1H, J 7.5, 15.8 Hz, H-6), 5.83 (dddd, 1H, J 6.2, 6.2, 10.8, 16.5 Hz, H-2'), 5.17 (d, 1H, J 17.1 Hz, H-3'), 5.10 (d, 1H, J 10.5 Hz, H-3'), 4.77 (d, 1H, J 11.7 Hz, CH_2CCl_3), 4.70 (d, 1H, J 11.7 Hz, CH_2CCl_3), 4.37 (t, 1H, J 7.8 Hz, H-5), 4.07 (m, 1H, H-4), 3.96 (m, 2H, H-1', H-1'),

3.91 (m, 1H, H-2), 3.71 (m, 1H, H-3), 3.34 (dd, 1H, J 4.8, 9.6 Hz, H-1), 3.24 (dd, 1H, J 5.7, 9.6 Hz, H-1).

^{13}C NMR δ 154.9 (C=O), 143.6 (q Ar), 136.2 (C-7), 135.0 (C-2'), 133.7 (q Ar), 128.6, 127.9, 127.1, 126.6 (Ar), 123.9 (C-6), 118.1 (C-3'), 95.3 (CCL_3), 86.9 (q C, Tr), 75.1 (CH_2CCl_3), 73.0 (C-4), 72.4 (C-2), 69.5 (C-3), 64.6 (C-1), 62.1 (C-5), 50.0 (C-1').

(1*R*,7*aR*)-1-[(1*R*,2*S*)-1,2-bis(benzyloxy)-3-triphenylmethyloxypropyl]-5,7*a*-dihydro-1*H*-pyrrolo[1,2-*c*][1,3]oxazol-3-one (123); (3*S*, 4*R*, 4*aR*)-3-[(1*S*)-1-(benzyloxy)-2-triphenylmethyloxyethyl]-4-(benzyloxy)-3,4,4*a*,7-tetrahydropyrrolo[1,2-*c*][1,3]oxazin-1-one (115)

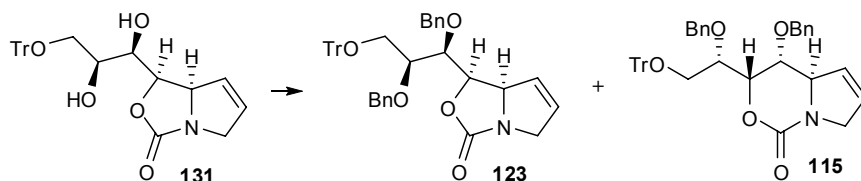


Three different approaches were used to access **123** and **115**. The first method (Method 1) was by the treatment of oxazolidinone **131** with standard *O*-benzyl protection conditions.

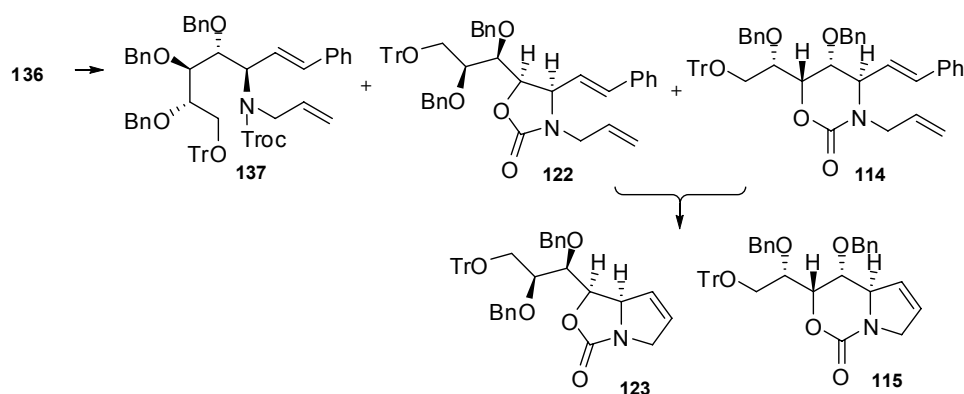
The second method (Method 2) was a two-step one that initially involved the treatment of *N*-Troc protected triol **136** with standard *O*-benzylation conditions, to produce oxazolidinone **122** and oxazinanone **114**. Some tri-*O*-Bn-*N*-Troc protected product **137** was also produced (in limited yield) but was not fully characterized. The oxazolidinone and oxazinanone isomers were not isolated individually but were exposed as a mixture to RCM (Grubbs' II) conditions, and then isolated as individual oxazolone **123** and oxazinone **115** compounds.

The third method (Method 3) contained the same two reactions as Method 2 but in the reverse order.

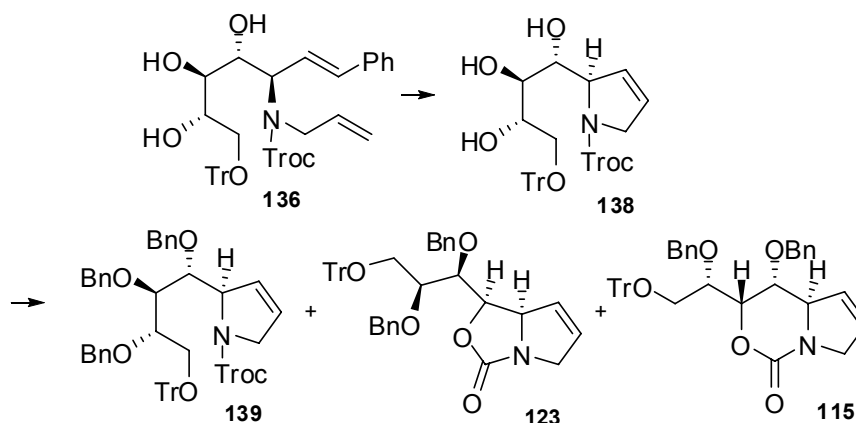
In each method, the spectroscopic data for **123** and **115** were consistent with the data for the identical compounds, which were synthesized earlier in Chapter 5 Experimental, using a RCM reaction.

Method 1:

Compounds **123** (300 mg, 22 %) and **115** (356 mg, 26 %) were synthesized from diol **131** (970 mg, 2.118 mmol) using the General method for *O*-benzyl protection except that the concentration of **131** in dry THF was 1.0 M (2 mL). Also, the reaction was stirred at 0 °C for 2 h and then at rt for 14 h. The products were purified by FCC (10 % EtOAc / petrol) and were both isolated as foamy white solids.

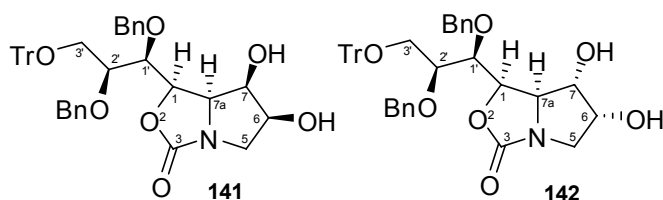
Method 2:

To a solution of triol **136** (14.0 g, 19.74 mmol) in dry THF (200 mL) was added *n*-Bu₄NI (730 mg, 1.974 mmol) and BnBr (14.10 mL, 118.48 mmol). The mixture was stirred at rt for 10 min then cooled to 0 °C before the addition of NaH (7.3 g, 78.98 mmol, 30 % dispersion in mineral oil). The mixture was then raised to rt and stirred for 1 h before the addition of MeOH (2 mL). After stirring for 10 min, the mixture was filtered through celite followed by the washing of the solids with DCM. The products were extracted with DCM (3 × 200 mL) and the combined DCM extracts were washed with brine, dried and evaporated. Oxazolidinone **122** and oxazinone **114** were separated as a mixture of compounds (12.0 g) from tri-*O*-benzylated **137** (which was not isolated) by FCC (25 % EtOAc / petrol). The combined oxazolidinone / oxazinone mixture was dried under high vacuum and dissolved in dry DCM (900 mL). To this solution was added Grubbs' II catalyst (687 mg, 0.81 mmol) and the mixture was stirred at reflux for 24 h, then cooled to rt and evaporated. The residue was purified by FCC (40 % EtOAc) to give oxazolone **123** (4.85 g 39 %) and oxazinone **115** (3.85 g, 31 %) as oils.

Method 3:

To a solution of diene **136** (3.15 g, 4.44 mmol) in dry DCM (200 mL) was added Grubbs' I catalyst (366 mg, 0.44 mmol). The mixture was stirred at reflux for 12 h and then evaporated to dryness. The residue was purified by FCC (40 % EtOAc / petrol) to give **138** (2.05 g, 76 %). This compound was then treated with standard *O*-benzylation conditions (see General method for *O*-benzylation). The crude product mixture from this reaction was purified by FCC (40 % EtOAc / petrol) to give oxazolone **123** (320 mg, 15 %) and oxazinone **115** (375 mg, 18 %). Compound **139** was not isolated.

(1*R*,6*S*,7*R*,7*aR*)-1-[(1*S*,2*S*)-1,2-dibenzyloxy-3-triphenylmethyloxypropyl]tetrahydro-1*H*-pyrrolo[1,2-*c*][1,3]oxazol-3-one (141); (1*R*,6*R*,7*S*,7*aR*)-1-[(1*S*,2*S*)-1,2-dibenzyloxy-3-triphenylmethyloxypropyl]tetrahydro-1*H*-pyrrolo[1,2-*c*][1,3]oxazol-3-one (142)



To a solution of olefin **123** (1.403 g, 2.203 mmol) in acetone (13 mL) and water (9 mL) was added potassium osmate.dihydrate (57 mg, 0.154 mmol) and 4-morpholine-*N*-oxide (516 mg, 4.405 mmol). The mixture was stirred at rt for 48 h followed by the evaporation of all volatiles. The residue was purified by FCC (70 % EtOAc / petrol) to give a mixture of diastereomers **141** and **142** as a foamy white solid (1.242 g, 84 %, dr 85 (**141**) : 15 (**142**)). These isomers were separated by column chromatography (1 cm × 30 cm) using 2 % MeOH / DCM as eluent.

141: $[\alpha]_{\text{D}}^{27} + 43$ (*c* 3.5, CHCl₃).

MS (ESI +ve) *m/z* 694 (*M* + Na⁺, 100 %).

HRMS (ESI +ve) calculated for C₄₂H₄₂NO₇ (*M* + H⁺) 672.2961, found 672.3005.

¹H NMR (500 MHz) δ 7.44-7.18 (m, 25H, Ar), 4.76 (d, 1H, *J* 11.0 Hz, Bn), 4.73 (d, 1H, *J* 12.0 Hz, Bn), 4.71 (d, 1H, *J* 11.0 Hz, Bn), 4.64 (dd, 1H, *J* 6.0, 7.5 Hz, H-1), 4.41 (d, 1H, *J* 12.0 Hz, Bn), 4.32 (dd, 1H, *J* 4.5, 6.0 Hz, H-7a), 4.14 (ddd, 1H, *J* 4.0, 8.0, 8.0 Hz, H-6), 3.76 (dd, 1H, *J* 4.8, 9.3 Hz, H-7), 3.55 (dd, 1H, *J* 4.5, 10.5 Hz, H-3'), 3.54 (dd, 1H, *J* 1.8, 3.8 Hz, H-2'), 3.29

(dd, 1H, J 7.5, 11.5 Hz, H-5), 3.36 (dd, 1H, J 8.0, 11.5 Hz, H-5), 3.40 (dd, 1H, J 5.5, 10.0 Hz, H-3'), 2.94 (dd, 1H, J 2.0, 7.0 Hz, H-1'), 2.57 (br s, 1H, OH).

^{13}C NMR δ 162.1 (C-3), 144.0, 138.0, 137.2 (q Ar), 129.0, 128.9, 128.83, 128.79, 128.6, 128.35, 128.30, 128.2, 127.5 (Ar), 87.4 (q C, Tr), 77.4 (C-7a), 76.6 (C-6), 75.1 (Bn), 74.1 (C-1), 72.3 (Bn), 70.8 (C-2), 64.6 (C-1'), 62.6 (C-3'), 50.6 (C-5).

142: $[\alpha]_{\text{D}}^{24} + 24$ (c 1.2, CHCl_3).

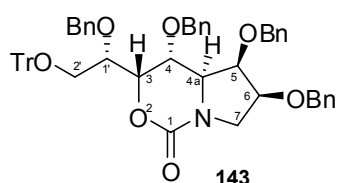
MS (ESI +ve) m/z 694 ($\text{M} + \text{Na}^+$, 100 %).

HRMS (ESI +ve) calculated for $\text{C}_{42}\text{H}_{42}\text{NO}_7$ ($\text{M} + \text{H}^+$) 672.2961, found 672.3020.

^1H NMR (500 MHz, CDCl_3) δ 7.44–7.14 (m, 25H, Ar), 4.83 (dd, 1H, J 7.0, 8.0 Hz, H-1), 4.71 (d, 1H, J 11.5 Hz, Bn), 4.70 (d, 1H, J 11.5 Hz, Bn), 4.53 (d, 1H, J 11.0 Hz, Bn), 4.41 (d, 1H, J 12.0 Hz, Bn), 4.09 (ddd, 1H, J 1.4, 5.6, 14.1 Hz, H-6), 4.08 (dd, 1H, J 5.0, 8.5 Hz, H-7), 3.96 (dd, 1H, J 3.5, 8.0 Hz, H-7a), 3.84 (dd, 1H, J 5.4, 9.0 Hz, H-2'), 3.81 (dd, 1H, J 5.5, 13.0 Hz, H-5), 3.53 (dd, 1H, J 5.0, 10.0 Hz, H-3'), 3.44 (dd, 1H, J 5.5, 10.0 Hz, H-3'), 3.41 (dd, 1H, J 7.0, 9.0 Hz, H-1'), 3.08 (dd, 1H, J 1.8, 12.8 Hz, H-5), 2.49 (br s, 1H, OH).

^{13}C NMR δ 161.0 (C-3), 143.7, 137.8, 137.2 (q Ar), 128.8, 128.7, 128.62, 128.58, 128.4, 128.3, 128.1, 128.0, 127.9, 127.8, 127.2 (Ar), 87.7 (q C, Tr), 77.2 (C-7a), 76.8 (C-6), 76.2 (C-1), 74.7 (Bn), 72.5 (Bn), 71.4 (C-7), 70.0 (C-2'), 63.5 (C-1'), 62.2 (C-3'), 52.7 (C-5).

(3*S*,4*R*,4*aR*,5*R*,6*S*)-4,5,6-tris(benzyloxy)-3-[(1*S*)-1-(benzyloxy)-2-triphenylmethoxyethyl]-hexahydropyrrolo[1,2-*c*][1,3]oxazin-1-one (143)



Compound **143** (1.9 g, 67 %) was synthesized from **116** (2.24 g, 3.34 mmol) using the General method for *O*-benzyl protection.

The crude product was purified by FCC (30 % EtOAc / petrol) to give **143** as a yellow oil.

$[\alpha]_{\text{D}}^{24} + 64$ (c 2.77, CHCl_3).

MS (ESI +ve) m/z 874 ($\text{M} + \text{Na}^+$, 100 %).

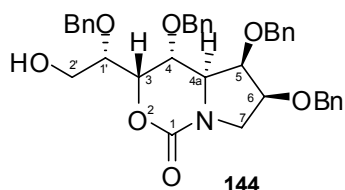
HRMS (ESI +ve) calculated for $\text{C}_{42}\text{H}_{42}\text{NO}_7$ ($\text{M} + \text{Na}^+$) 874.3719, found 874.3720.

^1H NMR δ 7.42–7.08 (m, 35H, ArH), 4.96 (d, 1H, J 11.4 Hz, Bn), 4.65 (d, 1H, J 11.7 Hz, Bn), 4.56 (dt, J 1.2, 6.0 Hz, H-3), 4.50 (d, 1H, J 12.0 Hz, Bn), 4.48 (s, 2H, Bn \times 2), 4.44 (d, 1H, J 11.7 Hz, Bn), 4.37 (d, 1H, J 11.4 Hz, Bn), 4.21 (d, 1H, J 11.7 Hz, Bn), 4.14 (ddd, 1H, J 1.2, 5.9, 9.6 Hz, H-4), 3.94 (dt, 1H, J 1.0, 3.0 Hz, H-5), 3.77 (dt, 1H, J 1.2, 3.5 Hz, H-1'), 3.65 (ddd, 1H, J 3.0, 6.8, 10.2 Hz, H-6), 3.54 (dd, 1H, J 7.5, 10.0 Hz, H-7), 3.51 (m, 4H, H-2', H-2', H-4a, H-7).

^{13}C NMR δ 151.7 (C-1), 143.9, 138.23, 138.18, 137.4, 137.2 (q Ar), 128.6, 128.5, 128.45, 128.3, 128.2, 128.1, 128.0, 127.9, 127.8, 127.74, 127.67, 127.4, 127.3, 127.1, 126.6 (Ar), 87.5

(q C, Tr), 78.0 (C-6), 76.0 (C-5), 75.6 (C-1'), 74.6 (C-3), 73.4, 72.4, 72.2, 72.1 (Bn), 67.7 (C-4), 62.7 (C-2'), 59.4 (C-4a), 48.0 (C-7).

(3*S*,4*R*,4*aR*,5*R*,6*S*)-4,5,6-tris(benzyloxy)-3-[(1*S*)-1-(benzyloxy)-2-hydroxyethyl]-hexahydropyrrolo[1,2-*c*][1,3]oxazin-1-one (144)



To a solution of **143** (1.88 g, 2.21 mmol) in dry DCM (20 mL) was added anisole (2.41 mL, 22.1 mmol) and the mixture was cooled to 0 °C before the addition of TFA (1.7 mL, 22.1 mmol).

The mixture was stirred for 1 h at 0 °C then poured into sat. aq. Na₂CO₃ and extracted with DCM (2 × 50 mL). The combined DCM extracts were washed with brine, dried and evaporated. The residue was purified by FCC (60 % EtOAc / petrol) to give **144** (820 mg, 61 %) as a yellow oil.

[α]_D²⁵ + 120 (*c* 1.5, CHCl₃).

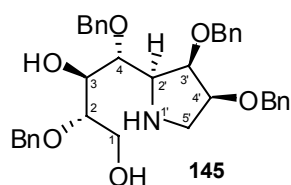
MS (ESI +ve) *m/z* 633 (M + Na⁺, 100 %).

HRMS (ESI +ve) calculated for C₃₇H₃₉NO₇ (M + Na⁺) 633.2702, found 633.2690.

¹H NMR δ 7.38-7.26 (m, 16H, Ar H), 7.21-7.17 (m, 4H, Ar H), 4.97 (d, 1H, *J* 11.4 Hz, Bn), 4.79 (d, 1H, *J* 12.0 Hz, Bn), 4.58 (dd, 1H, *J* 2.0, 5.6 Hz, Bn), 4.53 (d, 1H, *J* 11.1 Hz, Bn), 4.52 (d, 1H, *J* 11.7 Hz, Bn), 4.51 (s, 2H, Bn × 2), 4.49 (d, 1H, *J* 12.3 Hz, Bn), 4.40 (d, 1H, *J* 11.1 Hz, Bn), 4.17 (dd, 1H, *J* 5.7, 9.3 Hz, H-4), 4.01 (t, 1H, *J* 3.0 Hz, H-5), 3.92 (ddd, 1H, *J* 1.5, 5.4, 7.1 Hz, H-1'), 3.84 (ddd, 1H, *J* 1.2, 5.7, 10.2 Hz, H-2'), 3.79 (m, 1H, H-2'), 3.74 (dd, 1H, *J* 3.2, 7.8 Hz, H-6), 3.61 (dd, 1H, *J* 2.9, 9.5 Hz, H-4a), 3.58 (dd, 1H, *J* 7.8, 10.2 Hz, H-7), 3.50 (t, 1H, *J* 9.9 Hz, H-7).

¹³C NMR δ 152.4 (C-1), 138.1, 138.0, 137.3, 137.0 (q Ar), 128.5, 128.3, 128.2, 128.1, 128.0, 127.9, 127.8, 127.7, 127.4, 126.8 (Ar), 77.8 (C-6), 77.6 (C-1'), 77.3 (C-5), 75.7 (C-3), 73.4, 72.5, 72.2, 72.1 (Bn), 67.7 (C-4), 60.6 (C-2'), 59.4 (C-4a), 48.0 (C-7).

(2*S*,3*S*,4*R*)-4-[(2*S*,3*R*,4*S*)-3,4-Dibenzyloxypyrrolidin-2-yl]-2,4-dibenzyloxybutane-1,3-diol (145)



To a solution of **144** (30 mg, 49.18 μmol) in MeOH (1 mL) was added NaOH (20 mg, 0.5 mmol) and H₂O (0.5 mL). The mixture was stirred and irradiated with microwaves in a CEM microwave reactor for 1 h at 110 °C using a maximum applied power of 500 W.

After cooling, the mixture was poured into water and the product was extracted with EtOAc (2 × 5 mL). The combined EtOAc extracts were washed with brine, dried (Na₂SO₄) and evaporated. The residue was purified by FCC (100 % EtOAc and 10 % MeOH / EtOAc) to give **145** as a clear oil (18 mg, 62 %).

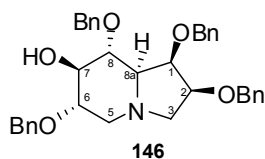
$[\alpha]_D^{21} + 75$ (*c* 0.85, CHCl₃).

MS (ESI +ve) *m/z* 584 (*M* + H⁺, 100 %).

HRMS (ESI +ve) calculated for C₃₇H₄₂NO₆ 584.3012 (*M* + H⁺), found 584.3023.

¹H NMR (500 MHz) δ 7.35-7.14 (m, 20H, Ar), 5.02 (d, 1H, *J* 11.5 Hz, Bn), 4.75 (d, 1H, *J* 10.5 Hz, Bn), 4.52 (s, 2H, Bn \times 2), 4.50 (d, 1H, *J* 11.5 Hz, Bn), 4.43 (d, 1H, *J* 10.5 Hz, Bn), 4.42 (s, 2H, Bn \times 2), 4.11 (t, 1H, *J* 3.3 Hz, H-3), 4.08 (t, 1H, *J* 4.0 Hz, H-3'), 4.02 (dd, 1H, *J* 3.5, 9.5 Hz, H-4), 3.96 (m, 1H, H-1), 3.73-3.66 (m, 3H, H-1, H-2, H-4'), 3.57 (dd, 1H, *J* 4.8, 9.3 Hz, H-2'), 2.90 (dd, 1H, *J* 9.3, 10.8 Hz, H-5'), 2.77 (dd, 1H, *J* 6.8, 10.8 Hz, H-5').

¹³C NMR δ 138.7, 138.3, 138.04, 138.0 (q Ar), 128.43, 128.4, 128.3, 128.2, 128.1, 127.9, 127.7, 127.6, 127.5, 127.3 (Ar), 80.9 (C-2 or C-4'), 77.4 (C-3'), 76.9 (C-2 or C-4'), 74.6 (C-4), 73.3 (C-3), 73.2, 72.11, 72.10, 71.7 (Bn), 62.7 (C-1), 61.1 (C-2'), 46.4 (C-5').

(1R,2S,6S,7R,8R,8aR)-1,2,6,8-Tetrabenzoyloxyoctahydroindolizin-7-ol (146)

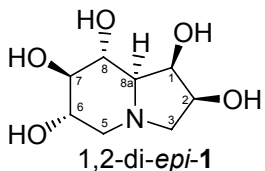
Compound **146** (240 mg, 85 %) was synthesized from primary alcohol **145** (290 mg, 0.497 mmol) using the General method for Appel cyclization, with the exception that the mixture was stirred for 2 h at 0 °C. The crude product was purified by FCC (50 % EtOAc / petrol) to give **146** as a brown oil.

MS (ESI +ve) m/z 566 ($M + H^+$, 100 %).

HRMS (ESI +ve) calculated for $C_{36}H_{40}NO_5$ ($M + H^+$) 566.2906, found 566.2922.

1H NMR δ 7.37-7.20 (m, 20H, Ar), 4.95 (d, 1H, J 11.1 Hz, Bn), 4.88 (d, 1H, J 11.4 Hz, Bn), 4.65 (d, 1H, J 11.7 Hz, Bn), 4.58 (d, 1H, J 12.0 Hz, Bn), 4.56 (d, 1H, J 11.7 Hz, Bn), 4.54 (d, 1H, J 12.0 Hz, Bn), 4.52 (d, 1H, J 11.1 Hz, Bn), 4.50 (d, 1H, J 12.0 Hz, Bn), 4.19 (dd, 1H, J 3.5, 5.3 Hz, H-1), 4.14 (ddd, 1H, J 3.6, 5.6, 8.0 Hz, H-2), 3.84 (t, 1H, J 9.2 Hz, H-8), 3.59 (m, 1H, H-6), 3.57 (m, 1H, H-7), 3.24 (dd, 1H, J 4.2, 10.2 Hz, H-5), 3.20 (dd, 1H, J 3.3, 9.9 Hz, H-3), 2.47 (dd, 1H, J 8.0, 10.1 Hz, H-3), 2.17 (dd, 1H, J 3.5, 9.2 Hz, H-8a), 1.94 (t, 1H, J 10.1 Hz, H-5).

^{13}C NMR δ 139.1, 138.4, 138.1, 138.0 (q Ar), 128.5, 128.32, 128.3, 128.2, 128.1, 127.9, 127.6, 127.5, 127.4, 127.3 (Ar), 79.2 (C-7), 78.5 (C-2), 78.2 (C-6), 77.4 (C-1), 77.0 (C-8), 74.2, 73.8, 72.4, 72.2 (Bn), 69.2 (C-8a), 57.3 (C-3), 53.4 (C-5).

(1R,2S,6S,7R,8R,8aR)-Octahydroindolizine-1,2,6,7,8-pentol (1,2-di-*epi*-1)

Compound **1,2-di-*epi*-1** (38 mg, 62 %) was synthesized from **146** (168 mg, 0.297 mmol) using the General method for *O*-benzyl deprotection, with the exception that **146** was dissolved solely in MeOH (3 mL). The crude product was dissolved in water and applied to a column of

Amberlyst (OH⁻) A-26 resin. Elution with water followed by evaporation resulted in a cloudy white residue that was recrystallized from boiling EtOH with a few drops of H₂O to give compound **1,2-di-*epi*-1** as colourless micro-crystals.

$[\alpha]_D^{23} + 21$ (c 1.5, H₂O).

MS (ESI +ve) m/z 206 ($M + H^+$, 100 %).

HRMS (ESI +ve) calculated for $C_8H_{16}NO_5$ ($M + H^+$) 206.1028, found 206.1036.

1H NMR (500 MHz, D₂O) δ 4.29 (ddd, 1H, $J_{2,3\beta} = 2.8$, $J_{1,2} = 5.8$, $J_{2,3\alpha} = 8.5$ Hz, H-2), 4.12 (dd, 1H, $J_{1,8a} = 3.8$, $J_{1,2} = 6.3$ Hz, H-1), 3.53 (t, 1H, $J_{7,8} = J_{8,8a} = 9.5$ Hz, H-8), 3.48 (ddd, 1H, $J_{5\alpha,6} = 5.5$, $J_{6,7} = 9.0$, $J_{5\beta,6} = 10.5$ Hz, H-6), 3.18 (t, 1H, $J_{6,7} = J_{7,8} = 9.3$ Hz, H-7), 3.00 (t, 1H, $J_{5\alpha,6} = 5.0$, $J_{5\alpha,5\beta} = 11.0$ Hz, H-5 α), 2.76 (dd, 1H, $J_{2,3\beta} = 2.8$, $J_{3\alpha,3\beta} = 10.8$ Hz, H-3 β), 2.50 (dd, 1H, $J_{2,3\alpha} = 8.3$, $J_{3\alpha,3\beta} = 10.8$ Hz, H-3 α), 2.04 (dd, 1H, $J_{1,8a} = 3.5$, $J_{8,8a} = 9.5$ Hz, H-8a), 1.95 (t, 1H, $J_{5\alpha,5\beta} = J_{5\beta,6} = 10.5$ Hz, H-5 β).

^{13}C NMR (D_2O) δ 79.3 (C-7), 70.7 (C-8a), 70.4 (C-6), 70.2 (C-2), 69.7 (C-1), 69.3 (C-8), 59.9 (C-3), 55.7 (C-5).

REFERENCES

1. Zenk, M. H.; Juenger, M. *Phytochemistry* **2007**, *68*, 2757-2772.
2. Serturmer, F. W. *Ann. Phys.* **1817**, *25*, 56-90.
3. Winterstein, E.; Trier, G. *Die Alkaloide*; Verlag Gebruder Borntrager: Berlin, 1910.
4. Roberts, M. F.; Wink, M. **1998**, *2*, 3, 14, 321-322.
5. King, A. G.; Meinwald, J. *Chem. Rev.* **1996**, *96*, 1105-1122.
6. Wikipedia. URL: <http://en.wikipedia.org/wiki/Coccinella.septempunctata>.
7. Wikipedia URL: <http://en.wikipedia.org/wiki/Phyllobates>.
8. Rotman, A. D. *Boletin de la Sociedad Argentina de Botanica* **1995**, *30*, 63-93.
9. Alonso, J. R. *Isis Ediciones S.R.L.* **1998**, 808-810.
10. Schmada-Hirschmann, G. *Ethnopharmacol.* **1988**, *22*, 73-79.
11. Amat, A. G.; Yajia, M. E. *Acta Farma. Bonaerense* **1991**, *10*, 153-159.
12. Bandoni, A. L.; Mendiando, M. E.; Rondina, R. V. D.; Coussio, J. D. *Lloydia* **1972**, *35*, 69-80.
13. Ratera, E. E.; Ratera, M. O. *Editorial Hemisferio Sur, Buenos Aires* **1980**, 128-129.
14. Alice, C. B.; Vargas, V. M. F.; Silva, G. A. A. B.; de Siqueira, N. C. S.; Schapoval, E. E. S.; Gleye, J.; Henriques, A. T. *J. Ethnopharmacol.* **1991**, *35*, 165-171.
15. Ferro, E.; Schinini, A.; Maldonado, M.; Rosner, J.; Hirschmann, G. S. *J. Ethnopharmacol.* **1988**, *24*, 321-325.
16. Rivera, D.; Obon, C. *J. Ethnopharmacol.* **1995**, *46*, 73-93.
17. Grainger, C. R. *Royal Soc. Health* **1996**, *116*, 107-109.
18. Agbedahunsi, J. M.; Aladesanmi, A. J. *Filoterapia* **1993**, *64*, 174-175.
19. Carr, G. D. URL: <http://www.botany.hawaii.edu>.
20. Schapoval, E. E.; Silveira, S. M.; Miranda, M. L.; Alice, C. B.; Henriques, A. T. *J. Ethnopharmacol.* **1994**, *44*, 137-142.
21. Theoduloz, C.; Franco, L.; E., F.; Schmeda-Hirschmann, G. *J. Ethnopharmacol.* **1988**, *24*, 179-183.
22. Gonzalez, J. J.; Sanabria, C.; Fructos, C.; Chiola, M.; de Garay, J. M. R. *J. C. Rev. Inst. Investig. Cienc. Salud* **1984**, *1*, 11-17.
23. Matsumura, T.; Kasai, M.; Hayashi, T.; Arisawa, M.; Momose, Y.; Arai, I.; Amagaya, S.; Komatsu, Y. *Pharm. Biol.* **2000**, *38*, 302-307.
24. Lindsay, K. B.; Pyne, S. G. *Aust. J. Chem.* **2004**, *57*, 669-672.
25. Tang, M.; Pyne, S. G. *J. Org. Chem.* **2003**, *68*, 7818-7824.
26. Tang, M.; Pyne, S. G. *Tetrahedron.* **2004**, *60*, 5759-5767.
27. Inouye, S.; Tsuruoka, T.; Niida, T. *J. Antibiot.* **1966**, *19*, 288.

28. Asano, N.; Nash, R. J.; Molyneux, R. J.; Fleet, G. W. J. *Tetrahedron: Asymmetry*. **2000**, *11*, 1645-1680.
29. Paulsen, H.; Sangster, I.; Heyns, K. *Chem. Ber.* **1967**, *100*, 802-815.
30. Inouye, S.; Tsuruoka, T.; Ito, T.; Niida, T. *Tetrahedron*. **1968**, *24*, 2125-2144.
31. Fellows, L. E.; Bell, E. A.; Lynn, D. G.; Pikiewicz, F.; Miura, I.; Nakanishi, K. *J. Chem. Soc., Chem. Commun.* **1979**, 977-978.
32. Kite, G. C.; Fellows, L. E.; Fleet, G. W. J.; Liu, P. S.; Scofield, A. M.; Smith, N. G. *Tetrahedron Lett.* **1988**, *29*, 6483-6485.
33. Molyneux, R. J.; Pan, Y. T.; Tropea, J. E.; Elbein, A. D.; Lawyer, C. H.; Hughes, D. J.; Fleet, G. W. J. *J. Nat. Prod.* **1993**, *56*, 1356-1364.
34. Ezure, Y.; Ojima, N.; Konno, K.; Miyazaki, K.; Sugiyama, M. *J. Antibiot.* **1988**, *41*, 1142-1144.
35. Ezure, Y.; Murao, S.; Miyazaki, K.; Kawamata, M. *Agric. Biol. Chem.* **1985**, *49*, 1119.
36. Koyama, M.; Sakamura, S. *Agric. Biol. Chem.* **1974**, *38*, 1111.
37. Molyneux, R. J.; Benson, M.; Wong, R. Y.; Tropea, J. H.; Elbein, A. D. *J. Nat. Prod.* **1988**, *51*, 1198-1206.
38. Kato, A.; Asano, N.; Kizu, H.; Matsui, K.; Watson, A. A.; Nash, R. J. *J. Nat. Prod.* **1997**, *60*, 312-314.
39. Asano, N.; Kato, A.; Miyauchi, M.; Kizu, H.; Tomimori, T.; Matsui, K.; Nash, R. J.; Molyneux, R. J. *Eur. J. Biochem.* **1997**, *248*, 296.
40. Welter, A.; Jadot, J.; Dardenne, G.; Marlier, M.; Casimir, J. *Phytochemistry*. **1976**, *15*, 747-749.
41. Nash, R. J.; Asano, N.; Watson, A. A. In *Alkaloids: Chemical and Biological Perspectives*; Pelletier, S. W., Ed.; Elsevier Science: Oxford, 1996. **1996**, *11*, 345-376.
42. Nash, R. J.; Bell, E. A.; Williams, J. M. *Phytochemistry*. **1985**, *24*, 1620-1622.
43. Nash, R. J.; Fellows, L. E.; Dring, J. V.; Fleet, G. W. J.; Derome, A. E.; Hamor, T. H.; Scofield, A. M.; Watkin, D. J. *Tetrahedron Lett.* **1988**, *29*, 2487-2490.
44. Nash, R. J.; Thomas, P. I.; Waigh, R. D.; Fleet, G. W.; Wormald, M. R.; Lilley, P. M. d. Q.; Watkin, D. J. *Tetrahedron Lett.* **1994**, *35*, 7849-7852.
45. Wormald, M. R.; Nash, R. J.; Watson, A. A.; Bhadoria, B. K.; Langford, R.; Sims, M.; Fleet, G. W. J. *Carbohydr. Lett.* **1996**, *2*, 169-174.
46. Kato, A.; Adachi, I.; Miyauchi, M.; Ikeda, K.; Komae, T.; Kizu, H.; Kameda, Y.; Watson, A. A.; Nash, R. J.; Wormald, M. R.; Fleet, G. W. J.; Asano, N. *Carbohydrate Res.* **1999**, *316*, 95-103.
47. Colegate, S. M.; Doring, P. R.; Huxtable, C. R. *Aust. J. Chem.* **1979**, *32*, 2257-2264.
48. Hohenshutz, L. D.; Bell, E. A.; Jewess, P. J.; Leworthy, D. P.; Pryce, R. J.; Arnold, E.; Clardy, J. *Phytochemistry*. **1981**, *20*, 811-814.

49. Molyneux, R. J.; James, L. F. *Science*. **1982**, *216*, 190-191.
50. Nash, R. J.; Fellows, L. E.; Dring, J. V.; Stirton, C. H.; Carter, D.; Hegarty, M. P.; Bell, E. A. *Phytochemistry*. **1988**, *27*, 1403-1404.
51. Pastuszak, I.; Molyneux, R. J.; James, L. F.; Elbein, A. D. *Biochemistry*. **1990**, *29*, 1886-1891.
52. Watson, A. A.; Fleet, G. W. J.; Asano, N.; Molyneux, R. J.; Nash, R. J. *Phytochemistry*. **2001**, *56*, 265-295.
53. Tepfer, D.; Goldmann, A.; Pamboukdjian, N.; Maille, M.; Lepingue, A.; Chevalier, D.; Denarie, J.; Rosenberg, C. J. *Bacteriol*. **1988**, *170*, 1153-1161.
54. Asano, N.; Kato, A.; Yokoyama, Y.; Miyauchi, M.; Yamamoto, M.; Kizu, H.; Matsui, K. *Carbohydrate Res*. **1996**, *284*, 169-178.
55. Kato, A.; Asano, N.; Kizu, H.; Matsui, K.; Suzuki, S.; Arisiwa, M. *Phytochemistry*. **1997**, *45*, 425-429.
56. Asano, N.; Tomioka, E.; Kizu, H.; Matsui, K. *Carbohydr. Res*. **1994**, *253*, 235-245.
57. Asano, N.; Oseki, K.; Tomioka, E.; Kizu, H.; Matsui, K. *Carbohydr. Res*. **1994**, *259*, 243-255.
58. Asano, N.; Kato, A.; Matsui, K.; Watson, A. A.; Nash, R. J.; Molyneux, R. J.; Hackett, L.; Topping, J.; Winchester, B. *Glycobiology*. **1997**, *7*, 1085-1088.
59. Liebig, J.; Wohler, F. *Ann. Pharmazie*. **1837**, *21*, 96.
60. Legler, G. *Adv. Carbohydr. Chem. Biochem*. **1990**, *48*, 319-384.
61. Sinnott, M. L. *Chem. Rev*. **1990**, *90*, 1171-1202.
62. Withers, S. G.; Namchuk, M.; Mosi, R. *Stutz AE (ed) Iminosugars as Glycosidase Inhibitors* **1999**, 188.
63. Asano, N.; Kizu, H.; Oseki, K.; Tomioka, E.; Matsui, K.; Okamoto, M.; Baba, M. *J. Med. Chem*. **1995**, *38*, 2349-2356.
64. Wrodnigg, T. M. *Monatshefte fuer Chemie*. **2002**, *133*, 393-426.
65. Dwek, R. A.; Butters, T. D.; Platt, F. M.; Zitzmann, N. *Nat. Rev. Drug Discov*. **2002**, *1*, 65-75.
66. Mitrakou, A.; Tountas, N.; Raptis, A. E.; Bauer, R. J.; Schulz, H.; Raptis, S. A. *Diabet. Med*. **1998**, *15*, 657-660.
67. Wohler, F. *Ann. Phys. Chem*. **1828**, *12*, 253.
68. Armstrong, R. W.; Beau, J. M.; Cheon, S. H.; Christ, W. J.; Fujioka, H.; Ham, W. H.; Hawkins, L. D.; Jin, H.; Kang, S. H.; Kishi, Y.; Martinelli, M. J.; McWhorter, W. W.; Mizuno, M.; Nakata, M.; Stutz, A. E.; Talamas, F. X.; Taniguchi, M.; Tino, J. A.; Ueda, K.; Uenishi, J.; White, J. B.; Yonaga, M. *J. Am. Chem. Soc*. **1989**, *111*, 7525-7530.
69. Armstrong, R. W.; Beau, J. M.; Cheon, S. H.; Christ, W. J.; Fujioka, H.; Ham, W. H.; Hawkins, L. D.; Jin, H.; Kang, S. H.; Kishi, Y.; Martinelli, M. J.; McWhorter, W. W.;

- Mizuno, M.; Nakata, M.; Stutz, A. E.; Talamas, F. X.; Taniguchi, M.; Tino, J. A.; Ueda, K.; Uenishi, J.; White, J. B.; Yonaga, M. *J. Am. Chem. Soc.* **1989**, *111*, 7530-7533.
70. Kishi, Y. *Chem. Scr.* **1987**, *27*, 573.
71. Kishi, Y. *Pure & Appl. Chem.* **1989**, *61*, 313-324.
72. Suh, E. M.; Kishi, Y. *J. Am. Chem. Soc.* **1994**, *116*, 11205-11206.
73. Weinreb, S. M. *Acc. Chem. Res.* **2003**, *36*, 59-65.
74. Heintzelman, G. R.; Fang, W.-K.; Keen, S. P.; Wallace, G. A.; Weinreb, S. M. *J. Am. Chem. Soc.* **2002**, *124*, 3939-3945.
75. Bernardelli, P.; Moradei, O. M.; Friedrich, D.; Yang, J.; Gallou, F.; Dyck, B. P.; Duskotch, R. W.; Lang, T.; Paquette, L. A. *J. Am. Chem. Soc.* **2001**, *123*, 9021-9032.
76. Overman, L. E.; Pennington, L. D. *Org. Lett.* **2000**, *2*, 2683-2686.
77. Cohen, F.; Overman, L. E. *J. Am. Chem. Soc.* **2001**, *123*, 10782-10783.
78. Li, J.; Burgett, A.; Esser, L.; Amezcua, C.; Harran, P. G. *Angew. Chem., Intl. Ed. Engl.* **2001**, *40*, 4770-4773.
79. Ritter, T.; Carreira, E. M. *Angew. Chem. Intl. Ed. Engl.* **2002**, *41*, 2489-2495.
80. Nash, R. J.; Fellows, L. E.; Dring, J. V.; Fleet, G. W. J.; Girdhar, A.; Ramsden, N. G.; Peach, J. M.; Hegarty, M. P.; Scofield, A. M. *Phytochemistry*. **1990**, *29*, 111-114.
81. Denmark, S. E.; Herbert, B. *J. Am. Chem. Soc.* **1998**, *120*, 7357-7358.
82. Wormald, M. R.; Nash, R. J.; Hrniciar, P.; White, J. D.; Molyneux, R. J.; Fleet, G. W. J. *Tetrahedron: Asymmetry*. **1998**, *9*, 2549-2558.
83. Bell, A. A.; Pickering, L.; Watson, A. A.; Nash, R. J.; Griffiths, R. C.; Jones, M. G.; Fleet, G. W. J. *Tetrahedron Lett.* **1996**, *37*, 8561-8564.
84. Denmark, S. E.; Herbert, B. *J. Org. Chem.* **2000**, *65*, 2887-2896.
85. Bell, A. A.; Nash, R. J.; Fleet, G. W. J. *Tetrahedron: Asymmetry*. **1996**, *7*, 595-606.
86. Petasis, N. A.; Zavialov, I. A. *J. Am. Chem. Soc.* **1998**, *120*, 11798-11799.
87. Mitsunobu, O. *Synthesis*. **1981**, 1-28.
88. Appel, R. *Angew. Chem.* **1975**, *87*, 863-874.
89. Van Rheenen, V.; Kelly, R. C.; Cha, D. Y. *Tetrahedron Lett.* **1976**, 1973-1976.
90. Kolb, H. C.; VanNieuwenhze, M. S.; Sharpless, K. B. *Chem. Rev.* **1994**, *94*, 2483-2547.
91. Casiraghi, G.; Ulgheri, F.; Spanu, P.; Rassu, G.; Pinna, L.; Gasparri Fava, G.; Belicchi Ferrari, M.; Pelosi, G. *J. Chem. Soc., Perkin Trans. 1: Organic and Bio-Organic Chemistry (1972-1999)*. **1993**, 2991-2997.
92. Hendry, D.; Hough, L.; Richardson, A. C. *Tetrahedron Lett.* **1987**, *28*, 4597-4600.
93. Hendry, D.; Hough, L.; Richardson, A. C. *Tetrahedron*. **1988**, *44*, 6143-6152.
94. Izquierdo, I.; Plaza, M. T.; Robles, R.; Rodriguez, C.; Ramirez, A.; Mota, A. J. *Eur. J. Org. Chem.* **1999**, 1269-2174.
95. Martin, S. F.; Chen, H. J.; Yang, C. P. *J. Org. Chem.* **1993**, *58*, 2867-2873.

96. Patil, N. T.; Tilekar, J. N.; Dhavale, D. D. *Tetrahedron Lett.* **2001**, *42*, 747-749.
97. Patil, N. T.; Tilekar, J. N.; Dhavale, D. D. *J. Org. Chem.* **2001**, *66*, 1065-1074.
98. St. Denis, Y.; Chan, T. H. *J. Org. Chem.* **1992**, *57*, 3078-3085.
99. Yoda, H.; Nakajima, T.; Takabe, K. *Synlett.* **1997**, 911-912.
100. Weber, H.; Khorana, H. G. *J. Mol. Biol.* **1972**, *72*, 219-249.
101. Dilbeck, G. A.; Field, L.; Gallo, A. A.; Gargiulo, R. J. *J. Org. Chem.* **1978**, *43*, 4593-4596.
102. Au, C. W. G.; Pyne, S. G. *J. Org. Chem.* **2006**, *71*, 7097-7099.
103. Johnson, F. *Chem. Rev.* **1968**, *68*, 375-413.
104. Hoffmann, R. W. *Chem. Rev.* **1989**, *89*, 1841-1860.
105. Mercury 1.4.1. Software download from the Cambridge Crystallographic Data Centre. URL: www.ccdc.cam.ac.uk/mercury/.
106. Zhdanov, R. I.; Zhenodarova, S. M. *Synthesis.* **1975**, 222-245.
107. Banfi, L.; Cascio, G.; Guanti, G.; Manghisi, E.; Narisano, E.; Riva, R. *Tetrahedron.* **1994**, *50*, 11967-11982.
108. Barton, D. H. R.; Gero, S. D.; Holliday, P.; Quiclet-Sire, B. *Tetrahedron.* **1996**, *52*, 8233-8244.
109. Berges, D. A.; Fan, J.; Liu, N.; Kent Dalley, N. *Tetrahedron.* **2001**, *57*, 9915-9924.
110. Chaudhary, S. K.; Hernandez, O. *Tetrahedron Lett.* **1979**, 95-98.
111. Krohn, K.; Heins, H. *Carbohydr. Res.* **1989**, *191*, 253-260.
112. Streith, J.; Rudyk, H.; Tschamber, T.; Tarnus, C.; Strehler, C.; Deredas, D.; Frankowski, A. *Eur. J. Org. Chem.* **1999**, 893-898.
113. Tschamber, T.; Siendt, H.; Boiron, A.; Gessier, F.; Deredas, D.; Frankowski, A.; Picasso, S.; Steiner, H.; Aubertin, A.-M.; Streith, J. *Eur. J. Org. Chem.* **2001**, 1335-1347.
114. Sigma-Aldrich. *Aldrich Technical Bulletin AL-142*. URL: www.sigmaaldrich.com/suite7/Brands/Aldrich/Technical_Bulletins/AL_142.
115. Ishizuka, T.; Kunieda, T. *Tetrahedron Lett.* **1987**, *28*, 4185-4188.
116. Saotome, C.; Kanie, Y.; Kanie, O.; Wong, C. H. *Biorg. Med. Chem.* **2000**, *8*, 2249-2261.
117. Kanai, K.; Sakamoto, I.; Ogawa, S.; Suami, T. *Bull. Chem. Soc. Jpn.* **1987**, *60*, 1529-1531.
118. Ikota, N. *Heterocycles.* **1993**, *36*, 2035-2050.
119. Deiters, A.; Martin, S. F. *Chem. Rev.* **2004**, *104*, 2199-2238.
120. Baker, S. R.; Cases, M.; Keenan, M.; Lewis, R. A.; Tan, P. *Tetrahedron Lett.* **2003**, *44*, 2995-2999.
121. Furstner, A.; Gastner, T.; Weintritt, H. *J. Org. Chem.* **1999**, *64*, 2361-2366.

122. Nicolaou, K. C.; He, Y.; Vourloumis, D.; Vallberg, H.; Yang, Z. *Angew. Chem. Int. Ed.* **1996**, *35*, 2399-2401.
123. Yang, Z.; He, Y.; Vourloumis, D.; Vallberg, H.; Nicolaou, K. C. *Angew. Chem. Int. Ed.* **1997**, *36*, 166-168.
124. Denmark, S. E.; Yang, S.-M. *Tetrahedron*. **2004**, *60*, 9695-9708.
125. Hoye, T. R.; Zhao, H. *Org. Lett.* **1999**, *1*, 1123-1125.
126. Criegee, R.; Marchand, B.; Wannowius, H. *Ann.* **1942**, *550*, 99-133.
127. Nelson, D. W.; Gypser, A.; Ho, P. T.; Kolb, H. C.; Kondo, T.; Kwong, H.-L.; McGrath, D. V.; Rubin, A. E.; Norrby, P.-O.; Gable, K. P.; Sharpless, K. B. *J. Am. Chem. Soc.* **1997**, *119*, 1840-1858.
128. Erdik, E.; Kahya, D.; Daskapan, T. *Synth. Commun.* **1998**, *28*, 1-7.
129. Birch, A. J.; Haas, M. A. *Journal of the Chemical Society [Section] C: Organic*. **1971**, 2465-2467.
130. Bodner, G. S.; Gladysz, J. A.; Nielsen, M. F.; Parker, V. D. *J. Am. Chem. Soc.* **1987**, *109*, 1757-1764.
131. Cohen, L.; Giering, W. P.; Kenedy, D.; Magatti, C. V.; Sanders, A. *J. Organomet. Chem.* **1974**, *65*, C57-C60.
132. Sanders, A.; Cohen, L.; Giering, W. P.; Kenedy, D.; Magatti, C. V. *J. Am. Chem. Soc.* **1973**, *95*, 5430-5431.
133. Faller, J. W.; Rosan, A. M. *J. Am. Chem. Soc.* **1977**, *99*, 4858-4859.
134. Fischer, E. O.; Fischer, R. D. *Angew. Chem.* **1960**, *72*, 919.
135. Green, M. L. H.; Nagy, P. L. I. *J. Organomet. Chem.* **1963**, *1*, 58-69.
136. Rosan, A.; Rosenblum, M.; Tancrede, J. *J. Am. Chem. Soc.* **1973**, *95*, 3062-3064.
137. Hoye, T. R.; Caruso, A. J.; Dellaria, J. F., Jr.; Kurth, M. J. *J. Am. Chem. Soc.* **1982**, *104*, 6704-6709.
138. Barton, D. H. R.; Magnus, P. D.; Streckert, G.; Zurr, D. *Journal of the Chemical Society [Section] D: Chemical Communications*. **1971**, 1109-1111.
139. Barton, D. H. R.; Magnus, P. D.; Smith, G.; Streckert, G.; Zurr, D. *J. Chem. Soc., Perkin Trans. 1: Organic and Bio-Organic Chemistry (1972-1999)*. **1972**, 542-552.
140. Naruse, M.; Aoyagi, S.; Kibayashi, C. *J. Org. Chem.* **1994**, *59*, 1358-1364.
141. Prevost, C. *Compt. rend.* **1933**, *196*, 1129-1131.
142. Davis, A. S.; Gates, N. J.; Lindsay, K. B.; Tang, M.; Pyne, S. G. *Synlett*. **2004**, 49-52.
143. Pyne, S. G.; Davis, A. S.; Gates, N. J.; Hartley, J. P.; Lindsay, K. B.; Machan, T.; Tang, M. *Synlett*. **2004**, 2670-2680.
144. Murray, A. J.; Parsons, P. J.; Greenwood, E. S.; Viseux, E. M. E. *Synlett*. **2004**, 1589-1591.
145. Gao, Y.; Sharpless, K. B. *J. Am. Chem. Soc.* **1988**, *110*, 7538-7539.

146. Mattocks, A. R.. *J. Chem. Soc.* **1964**, 1918-1930.
147. Mattocks, A. R.. *J. Chem. Soc.* **1964**, 4840-4845.
148. Greenberg, S.; Moffatt, J. G. *J. Am. Chem. Soc.* **1973**, *95*, 4016-4025.
149. Denmark, S. E.; Forbes, D. C.; Hays, D. S.; DePue, J. S.; Wilde, R. G. *J. Org. Chem.* **1995**, *60*, 1391-1407.
150. Shi, Y. *Acc. Chem. Res.* **2004**, *37*, 488-496.
151. Burke, C. P.; Shi, Y. *Angew. Chem. Int. Ed.* **2006**, *45*, 4475-4478.
152. Denmark, S. E.; Matsuhashi, H. *J. Org. Chem.* **2002**, *67*, 3479-3486; and references cited therein.
153. Trost, B. M.; Horne, D. B.; Woltering, M. J. *Angew. Chem. Int. Ed.* **2003**, *42*, 5987-5990.
154. Reymond, J. L.; Pinkerton, A. A.; Vogel, P. *J. Org. Chem.* **1991**, *56*, 2128-2135.
155. Woodward, R. B.; Brutcher, F. V., Jr. *J. Am. Chem. Soc.* **1958**, *80*, 209-211.
156. Winstein, S.; Buckles, R. E. *J. Am. Chem. Soc.* **1942**, *64*, 2787-2790.
157. Brimble, M. A.; Nairn, M. R. *J. Org. Chem.* **1996**, *61*, 4801-4805.
158. Whitesell, J. K.; Minton, M. A. *J. Am. Chem. Soc.* **1987**, *109*, 6403-6408.
159. Hamm, S.; Hennig, L.; Findeisen, M.; Muller, D.; Welzel, P. *Tetrahedron.* **2000**, *56*, 1345-1348.
160. Kamano, Y.; Pettit, G. R.; Tozawa, M.; Komeichi, Y.; Inoue, M. *J. Org. Chem.* **1975**, *40*, 2136-2138.
161. Trnka, T. M.; Grubbs, R. H. *Acc. Chem. Res.* **2001**, *34*, 18-29.
162. Dias, E. L.; Nguyen, S. T.; Grubbs, R. H. *J. Am. Chem. Soc.* **1997**, *119*, 3887-3897.
163. Sanford, M. S.; Love, J. A.; Grubbs, R. H. *J. Am. Chem. Soc.* **2001**, *123*, 6543-6554.
164. Sanford, M. S.; Ulman, M.; Grubbs, R. H. *J. Am. Chem. Soc.* **2001**, *123*, 749-750.
165. Grubbs, R. H. *Tetrahedron.* **2004**, *60*, 7117-7140.
166. Wothers, P. D.; Greeves, N.; Warren, S.; Clayden, J. P. *Organic Chemistry*; Oxford University Press, 2001.
167. Ulman, M.; Grubbs, R. H. *J. Org. Chem.* **1999**, *64*, 7202-7207.
168. Hong, S. H.; Day, M. W.; Grubbs, R. H. *J. Am. Chem. Soc.* **2004**, *126*, 7414-7415.
169. Eckert, H.; Forster, B. *Angew. Chem. Int. Ed. Engl.* **1987**, *26*, 894-895.
170. Lindsay, K. B.; Pyne, S. G. *Synlett.* **2004**, 779-782.
171. Kappe, C. O. *Angew. Chem. Int. Ed.* **2004**, *43*, 6250-6284.
172. Lidstrom, P.; Tierney, J.; Wathey, B.; Westman, J. *Tetrahedron.* **2001**, *57*, 9225-9283.
173. Wathey, B.; Tierney, J.; Lidstrom, P.; Westman, J. *Drug Discov. Today.* **2002**, *7*, 373-380.
174. Perreux, L.; Loupy, A. *Tetrahedron.* **2001**, *57*, 9199-9223.
175. Larhed, M.; Hallberg, A. *Drug Discov. Today.* **2001**, *6*, 406-416.

176. Saul, R.; Chambers, J. P.; Molyneux, R. J.; Elbein, A. D. *Arch. Biochem. Biophys.* **1983**, *221*, 593-597.
177. Shikita, M.; Fahey, J. W.; Golden, T. R.; Holtzclaw, W. D.; Talalay, P. *Biochem. J.* **1999**, *341* (Pt 3), 725-732.
178. Saul, R.; Chambers, J. P.; Molyneux, R. J.; Elbein, A. D. *Arch. Biochem. Biophys.* **1983**, *221*, 593-597.
179. Tulsiani, D. R. P.; Broquist, H. P.; Touster, O. *Arch. Biochem. Biophys.* **1985**, *236*, 427-434.
180. Davis, A. S.; Pyne, S. G.; Skelton, B. W.; White, A. H. *J. Org. Chem.* **2004**, *69*, 3139-3143.
181. Karanjule, N. S.; Markad, S. D.; Dhavale, D. D. *J. Org. Chem.* **2006**, *71*, 6273-6276.
182. Zhao, Z.; Song, L.; Mariano, P. S. *Tetrahedron.* **2005**, *61*, 8888-8894.
183. Denmark, S. E.; Hurd, A. R. *Org. Lett.* **1999**, *1*, 1311-1314.
184. Denmark, S. E.; Hurd, A. R. *J. Org. Chem.* **2000**, *65*, 2875-2886.
185. Izquierdo, I.; Plaza, M. T.; Tamayo, J. A. *Tetrahedron.* **2005**, *61*, 6527-6533.
186. Bell, A. A.; Pickering, L.; Watson, A. A.; Nash, R. J.; Pan, Y. T.; Elbein, A. D.; Fleet, G. W. J. *Tetrahedron Lett.* **1997**, *38*, 5869-5872.
187. Izquierdo, I.; Plaza, M. T.; Tamayo, J. A. *J. Carbohydr. Chem.* **2006**, *25*, 281-295.
188. Van Ameijde, J.; Horne, G.; Wormald, M. R.; Dwek, R. A.; Nash, R. J.; Jones, P. W.; Evinson, E. L.; Fleet, G. W. J. *Tetrahedron: Asymmetry.* **2006**, *17*, 2702-2712.
189. Newton, C.; van Ameijde, J.; Fleet, G. W. J.; Nash, R. J.; Watkin, D. J. *Acta Crystallogr. Sect. E: Struct. Rep. Online.* **2004**, *E60*, o1463-o1464.
190. Punzo, F.; Watkin, D. J.; Van Ameijde, J.; Horne, G.; Fleet, G. W. J.; Wormald, M. R.; Nash, R. J. *Acta Crystallogr. Sect. E: Struct. Rep. Online.* **2006**, *E62*, o928-o930.
191. Still, W. C.; Kahn, M.; Mitra, A. *J. Org. Chem.* **1978**, *43*, 2923-2925.